frontiers | Research Topics

Microbial fermentation for improved sensory properties and functionality of sustainable foods

Edited by
Sylvester Holt, Michela Verni and Carlo Giuseppe Rizzello

Published in
Frontiers in Microbiology

ISSN 1664-8714
ISBN 978-2-8325-4604-8
DOI 10.3389/978-2-8325-4604-8

About Frontiers

Frontiers is more than just an open access publisher of scholarly articles: it is a pioneering approach to the world of academia, radically improving the way scholarly research is managed. The grand vision of Frontiers is a world where all people have an equal opportunity to seek, share and generate knowledge. Frontiers provides immediate and permanent online open access to all its publications, but this alone is not enough to realize our grand goals.

Frontiers journal series

The Frontiers journal series is a multi-tier and interdisciplinary set of open-access, online journals, promising a paradigm shift from the current review, selection and dissemination processes in academic publishing. All Frontiers journals are driven by researchers for researchers; therefore, they constitute a service to the scholarly community. At the same time, the *Frontiers journal series* operates on a revolutionary invention, the tiered publishing system, initially addressing specific communities of scholars, and gradually climbing up to broader public understanding, thus serving the interests of the lay society, too.

Dedication to quality

Each Frontiers article is a landmark of the highest quality, thanks to genuinely collaborative interactions between authors and review editors, who include some of the world's best academicians. Research must be certified by peers before entering a stream of knowledge that may eventually reach the public - and shape society; therefore, Frontiers only applies the most rigorous and unbiased reviews. Frontiers revolutionizes research publishing by freely delivering the most outstanding research, evaluated with no bias from both the academic and social point of view. By applying the most advanced information technologies, Frontiers is catapulting scholarly publishing into a new generation.

What are Frontiers Research Topics?

Frontiers Research Topics are very popular trademarks of the *Frontiers journals series*: they are collections of at least ten articles, all centered on a particular subject. With their unique mix of varied contributions from Original Research to Review Articles, Frontiers Research Topics unify the most influential researchers, the latest key findings and historical advances in a hot research area.

Find out more on how to host your own Frontiers Research Topic or contribute to one as an author by contacting the Frontiers editorial office: frontiersin.org/about/contact

Microbial fermentation for improved sensory properties and functionality of sustainable foods

Topic editors

Sylvester Holt — University of Copenhagen, Denmark

Michela Verni — Sapienza University of Rome, Italy

Carlo Giuseppe Rizzello — Sapienza University of Rome, Italy

Citation

Holt, S., Verni, M., Rizzello, C. G., eds. (2024). *Microbial fermentation for improved sensory properties and functionality of sustainable foods*. Lausanne: Frontiers Media SA. doi: 10.3389/978-2-8325-4604-8

Table of contents

frontiers | Frontiers in Microbiology

TYPE Editorial
PUBLISHED 05 March 2024
DOI 10.3389/fmicb.2024.1387745

OPEN ACCESS

EDITED AND REVIEWED BY
Aldo Corsetti,
University of Teramo, Italy

*CORRESPONDENCE
Michela Verni
michela.verni@uniroma1.it
Sylvester Holt
sylvester.holt@food.ku.dk

RECEIVED 18 February 2024
ACCEPTED 23 February 2024
PUBLISHED 05 March 2024

CITATION
Verni M, Holt S and Rizzello CG (2024) Editorial: Microbial fermentation for improved sensory properties and functionality of sustainable foods.
Front. Microbiol. 15:1387745.
doi: 10.3389/fmicb.2024.1387745

Editorial: Microbial fermentation for improved sensory properties and functionality of sustainable foods

Michela Verni[1]*, Sylvester Holt[2]* and Carlo Giuseppe Rizzello[1]

[1]Department of Environmental Biology, Sapienza University of Rome, Rome, Italy, [2]Department of Biology, University of Copenhagen, Copenhagen, Denmark

KEYWORDS

fermentation, microbial fermentation, nutrition sustainable food, microbial flavor, yeasts, plant-based

Editorial on the Research Topic
Microbial fermentation for improved sensory properties and functionality of sustainable foods

Growing awareness of the health and climate crises has led consumers to reduce meat and alcohol consumption, and government organizations to act on it, driving academic and industry research toward plant-based foods. One of the major challenges in transitioning from animal- to plant-based diets is to replicate the unique sensory characteristics of animal-based foods. Therefore, there is a need for innovation in flavor, texture, and trigeminal sensations to meet the expectations of the growing consumer groups. In this framework, the main objective of this Research Topic was to explore our current understanding of flavor and functionally active microbes in the production of novel foods, with a focus on microbial secondary metabolites.

The volatile flavor compounds of food are closely related to the nature of the microorganisms responsible for fermentation, as ascertained by Wang et al. and Wu et al.. The latter focused on the correlation of dominant microorganisms and the main flavor substances of cigar tobacco leaves during fermentation, whereas the first examined the metabolic improvements in the polyphenolic profile of black tea fermented by *Eurotium crisantum*. The authors provided a comprehensive understanding of the molecular mechanisms affecting the taste and sensory traits of black tea and its related antioxidant potential during the fermentation process (Wang et al.).

While performing their core functions (ethanol production in fermented beverages and carbon dioxide generation in leavened baked goods), yeasts produce several secondary metabolites that contribute significantly to the flavor and aroma of foods and beverages. Higher alcohols and esters deriving from amino acid catabolism are the most abundant of these compounds. Owing to its highly efficient metabolism, *Saccharomyces cerevisiae* is the most preferred yeast species for industrial fermentations, and Li L. et al. reviewed the current literature on the cell-to-cell communication mechanisms in *S. cerevisiae*, studying how its quorum sensing system is essential in stress adaptation, food preservation, and the modulation of metabolites. In another study, indigenous *S. cerevisiae* strains were used to improve the organoleptic profile of Italian Grape Ale beers. Using a multidisciplinary approach, combining results from analyses of the chemical, volatile, and organoleptic

profiles of the beers, the authors underlined the relationships between yeast starter and the quality of the final products, thus highlighting the interaction between the strain used and the sensory output (Pietrafesa et al.).

Nevertheless, as opposed to the over-employed and overstudied *S. cerevisiae*, new non-conventional yeast species also offer a very promising route to food and beverage bio-flavoring. For example, while screening non-*Saccharomyces* yeasts for their metabolic performance and oenological properties, Li Y. et al. found that mixed inoculation of the non-*Saccharomyces* yeast strains with *S. cerevisiae* could regulate the volatile aroma characteristics of fermented *Rosa roxburghii* wine, enriching and enhancing its aroma flavor. Non-conventional yeasts are often the key to developing the aroma profile of spontaneous fermented traditional foods and beverages, as is the case of South-road Dark Tea, typical of a Chinese province. It was indeed observed that glycoside hydrolase genes in *Debaryomyces hansenii*, involved in polysaccharide and oligosaccharide degradation as well as catechin transformation, can improve the mellow mouthfeel of South-road Dark Tea (Zou et al.).

In addition to its impact on the sensory properties of food, fermentation can significantly improve the nutritional value of food by introducing new pathways that produce vitamins and micronutrients. This is particularly important for vulnerable groups who may have limited food choices. Fermentation can also increase food functionality by releasing or synthesizing bioactive compounds with functional potential, such as bacteriocins, or providing probiotics and postbiotics. For instance, the fermentation of soybean with *Enterococcus faecium* contributed to flavor development but also the inhibition of *Lysteria monocytogenes* through a bacteriocin produced during fermentation (Kim et al.). Jeon et al., instead, evaluated the prebiotic effect of red ginseng dietary fiber on a *Lactiplantibacillus plantarum* strain. Red ginseng dietary fiber supplementation promoted the probiotic properties of *L. plantarum*, including the production of short chain fatty acids, carbohydrate utilization, attachment to intestinal epithelial cells, and pathogen inhibition.

Improvements with proteins and microbial fermentation are currently in the process of making novel foods a global commercial success. For instance, recent progress in plant-based foods has focused on producing proteins that may lead to umami flavors and precursors that are transformed into savory compounds during the cooking process. The investigation of efficient and cost-effective alternative protein sources is also a topic of interest explored by Li G. et al.. The researchers focused on distillers' dried grains, a co-product of bioethanol production, which are rich in protein. They used an integrated approach that included analyzing the genome of *Paenibacillus pabuli*, assessing *in vitro* enzymatic activities, and conducting solid-state fermentation to assess the suitability of the strain to degrade non-starch polysaccharides.

In conclusion, this Research Topic explored the beneficial effects of microorganisms on food quality and safety, highlighting the correlation between microbial communities and flavor compounds. The reasonable application of beneficial microorganisms is essential for achieving the desired properties, leading to reliable food products and ensuring food quality, safety, and consistency. Although none of the papers published in this Research Topic focused on mimicking the sensory traits that identify animal-based foods, each one of them highlighted specific metabolic pathways that can help steer fermentation processes toward this goal. These pathways could be further explored in future research.

Author contributions

MV: Writing—original draft, Writing—review & editing. SH: Writing—original draft, Writing—review & editing. CR: Writing—original draft, Writing—review & editing.

Funding

The author(s) declare that no financial support was received for the research, authorship, and/or publication of this article.

Conflict of interest

The authors declare that the research was conducted in the absence of any commercial or financial relationships that could be construed as a potential conflict of interest.

The author(s) declared that they were an editorial board member of Frontiers, at the time of submission. This had no impact on the peer review process and the final decision.

Publisher's note

frontiers | Frontiers in Microbiology

TYPE Original Research
PUBLISHED 06 March 2023
DOI 10.3389/fmicb.2023.1139386

OPEN ACCESS

EDITED BY
Michela Verni,
University of Bari Aldo Moro, Italy

REVIEWED BY
Hasan Ufuk Celebioglu,
Bartın University, Türkiye
Jianming Zhang,
Zhejiang Academy of Agricultural Sciences, China

*CORRESPONDENCE
Young Hoon Jung
younghoonjung@knu.ac.kr
Minhye Shin
mhshin@inha.ac.kr

†These authors have contributed equally to this work and share first authorship

SPECIALTY SECTION
This article was submitted to Food Microbiology, a section of the journal Frontiers in Microbiology

RECEIVED 06 January 2023
ACCEPTED 20 February 2023
PUBLISHED 06 March 2023

CITATION
Jeon HJ, You S-H, Nam EH, Truong V-L, Bang J-H, Bae Y-J, Rarison RHG, Kim S-K, Jeong W-S, Jung YH and Shin M (2023) Red ginseng dietary fiber promotes probiotic properties of *Lactiplantibacillus plantarum* and alters bacterial metabolism. *Front. Microbiol.* 14:1139386. doi: 10.3389/fmicb.2023.1139386

Red ginseng dietary fiber promotes probiotic properties of *Lactiplantibacillus plantarum* and alters bacterial metabolism

Hyeon Ji Jeon[1†], Seung-Hwan You[2†], Eoun Ho Nam[3,4], Van-Long Truong[1], Ji-Hong Bang[1], Yeon-Ji Bae[1], Razanamanana H. G. Rarison[1], Sang-Kyu Kim[2], Woo-Sik Jeong[1], Young Hoon Jung[1*] and Minhye Shin[3,4*]

[1]Food and Bio-Industry Research Institute, School of Food Science and Biotechnology, College of Agriculture and Life Sciences, Kyungpook National University, Daegu, Republic of Korea, [2]Laboratory of Efficacy Research, Korea Ginseng Corporation, Daejeon, Republic of Korea, [3]Department of Microbiology, College of Medicine, Inha University, Incheon, Republic of Korea, [4]Department of Biomedical Sciences, Program in Biomedical Science and Engineering, Inha University, Incheon, Republic of Korea

Korean red ginseng has been widely used as an herbal medicine. Red ginseng dietary fiber (RGDF) is a residue of the processed ginseng product but still contains bioactive constituents that can be applied as prebiotics. In this study, we evaluated changes on fermentation profiles and probiotic properties of strains that belong to family *Lactobacillaceae* with RGDF supplementation. Metabolomic analyses were performed to understand specific mechanisms on the metabolic alteration by RGDF and to discover novel bioactive compounds secreted by the RGDF-supplemented probiotic strain. RGDF supplementation promoted short-chain fatty acid (SCFA) production, carbon source utilization, and gut epithelial adhesion of *Lactiplantibacillus plantarum* and inhibited attachment of enteropathogens. Intracellular and extracellular metabolome analyses revealed that RGDF induced metabolic alteration, especially associated with central carbon metabolism, and produced RGDF-specific metabolites secreted by *L. plantarum*, respectively. Specifically, *L. plantarum* showed decreases in intracellular metabolites of oleic acid, nicotinic acid, uracil, and glyceric acid, while extracellular secretion of several metabolites including oleic acid, 2-hydroxybutanoic acid, hexanol, and butyl acetate increased. RGDF supplementation had distinct effects on *L. plantarum* metabolism compared with fructooligosaccharide supplementation. These findings present potential applications of RGDF as prebiotics and bioactive compounds produced by RGDF-supplemented *L. plantarum* as novel postbiotic metabolites for human disease prevention and treatment.

KEYWORDS

red ginseng, dietary fiber, probiotics, prebiotics, metabolomics

Introduction

Ginseng is the root of plants in the genus *Panax* and has been widely used as an herbal medicine in Eastern Asia (So et al., 2018). It is typically characterized by the presence of ginsenosides, which are the main bioactive components with antioxidant, anti-proliferative, and neuroprotective properties (Tam et al., 2018). In recent years, the biological properties of ginseng have been extensively demonstrated; these include enhanced immune system performance and memory, and improved blood circulation (Geng et al., 2010; Cho et al., 2018; Su et al., 2022).

Korean red ginseng (*Panax ginseng* C.A. Meyer) is a processed product made by the repetitive steaming and drying of fresh ginseng to extend shelf life, reduce toxic effects, and enhance biological benefits (He et al., 2018). Red ginseng is traditionally consumed as a water extract containing a high concentration of ginsenosides. The residues are usually discarded, but they still contain bioactive constituents, such as unextracted ginsenosides, acidic polysaccharides, mineral elements, and dietary fiber (Yu et al., 2020). Many attempts to make the most use of these residues have included pharmaceutical, health functional foods, and cosmetics applications (Truong and Jeong, 2022).

Dietary fibers are carbohydrate polymers from plant-derived foods that are not digested by human enzymes or absorbed in the gut. Polymers contribute to human gut health by increasing stool weight and regularity, thickening the contents of the intestinal tract, and promoting growth of gut microbes (Makki et al., 2018). In particular, dietary fiber can be a good fermentable source for bacteria within the large intestine and influences the composition of bacterial communities as well as microbial metabolic activities producing fermentative end products, such as short-chain fatty acids (SCFAs). These prebiotic fermentable fibers promote metabolic interactions among bacterial communities that cross-feed probiotics and inhibit the proliferation of pathogens (Holscher, 2017).

Lactobacillaceae (including newly defined *Lactobacillus*-associated genera by taxonomic changes such as *Lactiplantibacillus* and *Limosilactobacillus*) and *Bifidobacteria* are the most well-known genera of probiotic organisms that normally reside in human gastrointestinal tracts. Probiotics are live microorganisms which benefit the host by producing useful physiologically bioactive compounds. These compounds have immunomodulatory, anti-carcinogenic, anti-aging, and antimicrobial effects in hosts. However, the use of these compounds is currently limited by a lack of knowledge of their molecular mechanisms, strain specific behaviors, and safety (Bourebaba et al., 2022). To address these limitations, recent studies have focused on elucidating microbial metabolism and discovering postbiotic molecules, which are defined as metabolic products secreted by probiotics in cell-free supernatants (Nataraj et al., 2020).

Metabolomics is the systematic study of unique chemical molecules, termed metabolites, generated by specific cellular processes (Jordan et al., 2009). Metabolomic data are used for phenotyping molecular interactions, identifying potential biomarkers, and discovering new therapeutic targets. In this study, we aimed to find an effective strategy for utilizing processed red ginseng residue as a prebiotic dietary fiber source and evaluated its prebiotic properties on the changes in growth, metabolism, and epithelial attachment ability of probiotic *Lactobacillaceae* strains. Comprehensive metabolomic analyses were performed to investigate the effects of red ginseng dietary fiber (RGDF) on bacterial metabolism and to discover novel bioactive compounds secreted by the RGDF-supplemented probiotic strain.

Materials and methods

Bacterial strains and media

Limosilactobacillus reuteri KCTC 3594 and *Lactiplantibacillus plantarum* KCTC 3108 were obtained from the Korean Collection for Type Cultures (KCTC, Jeongeup, Republic of Korea). The strains were pre-cultured in 50 ml of MRS broth (BD Difco, Franklin Lakes, NJ, USA) in 50 ml conical tubes and were incubated at 37°C without shaking (Biofree, Seoul, Republic of Korea) overnight. Cultures of the probiotic strains were then generated at 37°C in 50 ml of MRS broth supplemented with 0.5, 1, or 2% RGDF (Korea Ginseng Corporation, Daejeon, Republic of Korea). Composition of MRS broth is as follows: 10 g/L proteose peptone, 10 g/L beef extract, 5 g/L yeast extract, 20 g/L dextrose, 1 g/L polysorbate 80, 2 g/L ammonium citrate, 5 g/L sodium acetate, 0.1 g/L magnesium sulfate, 0.05 g/L manganese sulfate, and 2 g/L dipotassium phosphate.

Preparation of RGDF

The residue remaining after water extraction of red ginseng at 87°C for 24 h was provided by Korea Ginseng Corporation (Daejeon, Republic of Korea). RGDF was prepared from the residue by drying it at 115°C and pulverizing it to 50 mesh. The physicochemical characteristics of RGDF were analyzed as previously reported (Yu et al., 2022), and same RGDF material was used in this study.

Measurement of bacterial growth and cell mass

Colony forming units per ml of probiotic strains cultured in MRS broth or in MRS supplemented with 0.5, 1, or 2% of RGDF were measured by serial dilution at 0, 3, 6, 12, and 24 h. Dry cell weight of strains at 24 h was measured by collecting cell pellets by centrifugation at 4,000 rpm and 4°C for 15 min, washing the pellets three times with 10 ml of 1% (w/v) phosphate buffered saline, and drying in a dry oven (JS Research Inc., Natural Convection Oven, Gongju, Republic of Korea) at 70°C for 24 h. pH of the cultured media was measured using a pH meter (Ohaus, Parsippany, NJ, USA).

Analysis of SCFAs

The concentrations of formic, acetic, propionic, and butyric acids were measured by high-performance liquid chromatography

(HPLC) using the LC-6000 system (FUTECS, Daejeon, Republic of Korea). Each 1.5 ml of culture medium was collected by centrifugation (Eppendorf, Hamburg, Germany) at 13,000 rpm for 5 min at 4°C and filtered through a 0.45 μm nylon membrane filter. HPLC analysis was performed using an Aminex HPX-87X organic acid column (Bio-Rad, Hercules, CA, USA) with 0.005 M H_2SO_4 as the mobile phase, with a constant elution flow of 0.5 ml/min at 55°C.

Carbon source utilization analysis

An API kit (BioMérieux, Marcy l'Étoile, France) was used to compare the ability of probiotic strains to utilize the particular carbon source. Inoculation samples were prepared by collecting cultured strains from each medium that had a turbidity greater than a McFarland standard of 4. One hundred microliters of sample were inoculated into the API strip and incubated at 37°C for 4 h. After incubation, the reagents were added for reading, incubated for 10 min, and exposed to strong light at 1,000 W for 10 s to decolorize any excess reagent. Identification and interpretation were performed using the numerical profiles.

Analysis of bacterial attachment to intestinal epithelial cells

Caco-2 cell line was procured from the American Type Culture Collection (ATCC, Manassas, VA, USA) and cultured in Minimum Essential Medium (MEM) supplemented with 10% fetal bovine serum, 100 U/ml penicillin, and 100 μg/ml streptomycin at 37°C in a 5% CO_2 atmosphere. *Escherichia coli*, purchased from ATCC, were grown in Luria Broth (LB) overnight. *E. coli* and RGDF-pretreated probiotic strains were harvested by centrifugation at 5,000 rpm for 10 min, washed twice with sterile PBS, and re-suspended in serum and antibiotic-free MEM.

For adhesion assay, Caco-2 monolayer was inoculated with approximately 10^8 CFU/ml of *L. reuteri* or *L. plantarum* and incubated for 2 h in a 5% CO_2 incubator. After incubation, the monolayers were washed three times with sterile PBS to remove non-adherent bacteria. The Caco-2 cells with adherent bacteria were detached using trypsin-EDTA solution. Bacterial counts were performed by the colony counting method on MRS agar plates. Adhesion result was expressed as the percentage of the bacteria adhered divided by the initial count of bacteria added.

For competition assay, approximately 10^8 CFU/ml of each probiotic strain and *E. coli* was co-incubated with Caco-2 monolayer for 1 h in a 5% CO_2 incubator. Non-bounded bacteria were then washed three times with sterile PBS and the Caco-2 cells with adherent bacteria were detached using trypsin-EDTA solution. The number of viable adhering *E. coli* was determined using the colony counting method on LB agar plates. The competition index was expressed as the percentage inhibition of *E. coli* adhesion in the presence of each probiotic strain divided by the adhesion of bacteria in the absence of probiotic strains.

Metabolome analysis

GC-MS has advantages of a greater chromatographic resolution compared to LC-MS and large spectral libraries, although the chemical range of metabolome coverage is narrower than LC-MS (Aretz and Meierhofer, 2016). Recently, more researches have used LC-MS to detect more peaks, but most of the identified metabolites by LC-MS are considerably overlapped with GC-MS except for lipid molecules having large molecular weights. GC-MS has been the most commonly used technique for metabolite profiling because of its hard ionization method which is highly reproducible and easy for metabolite annotation, and it still has been widely applied for metabolite profiling and identification (Baiges-Gaya et al., 2023; Kurbatov et al., 2023; Neag et al., 2023).

For metabolome analysis, each intracellular and extracellular metabolites were measured in *L. plantarum* and *L. reuteri* grown in MRS medium with different supplementation of RGDF, fructooligosaccharides, or without addition. To extract intracellular and extracellular metabolites from the probiotic strains, each strain was cultured in 15 ml of medium until the mid-exponential phase determined by measuring its growth curve. Fifteen milliliters of each probiotic culture was centrifuged at 4,000 rpm for 15 min at 4°C. The supernatant was filtered through a 0.2 μm syringe filter composed of polyvinylidene fluoride for the extraction of extracellular metabolites. Aliquots (750 μL) of the filtered supernatants was mixed with 2.25 ml of 4°C methanol (GC-grade 100%; Sigma-Aldrich, St. Louis, MO, USA) and vortexed for 1 min. The mixtures were centrifuged at 13,000 rpm and 4°C for 10 min, and 0.1 ml of each supernatant was collected and completely dried using a Spin Driver Lite VC-36R (TAITEC Corporation, Koshigaya City, Saitama, Japan) at 2,000 rpm for 24 h.

To extract intracellular metabolites from the cell pellet, 1 ml of 0.9% cold NaCl (w/v) was added to the pellet and filtered through a 0.2 μm syringe filter. Then, it was transferred to a 15 ml conical tube and washed twice with 10 ml of 0.9% cold NaCl (w/v). The final washed pellet was mixed with 2 ml methanol, vortexed for 10 min, and sonicated for 1 min on ice. The material was mixed with 2 ml of chloroform, vortexed for 10 min, and sonicated for 1 min with ice. Water (1.8 ml) was added and vortexing and sonication were repeated. The final mixtures were centrifuged at 13,000 rpm and 4°C for 10 min, and 0.1 ml the upper supernatant layer of each was collected and completely dried using the aforementioned Spin Driver Lite VC-36R under same conditions to extract extracellular metabolites. Methoxymation and silylation were performed for the derivatization of intracellular and extracellular metabolites. For methoxymation, 10 μL containing 20,000 ppm methyl hydroxyl chloride amine in pyridine was mixed with each dried sample and incubated at 30°C for 90 min. Next, 45 μL of N-methyl-N-trimethylsilyl-trifluoroacetamide (Fluka, Buchs, Switzerland) and 30 μL of fluoranthene as internal standard were added, vortexed for silylation, and incubated at 37°C for 30 min. The derivatized sample was transferred to a gas chromatography (GC) vial with an insert.

Gas chromatography was performed using a Crystal 9000 chromatograph (Chromatotec, Val-de-Virvée, France) coupled with a Chromatotec-crystal mass spectrometer (photomultiplier detector) for the analysis of untargeted metabolites. One microliter of the derivatized sample was injected into a VF-5MS GC column (Agilent, Santa Clara, CA, USA). The oven temperature was initially

50°C for 2 min, then increased to 320°C at a rate of 5°C/min, and held at 320°C for 10 min. The helium carrier gas flowed at a rate of 1.5 ml/min.

Statistical analysis

For the deconvolution of the mass spectrometry (MS) data and identification of metabolites, MS-DIAL ver. 4.70 was used. All records of the Fiehn RI Library were used to identify metabolites by matching the MS peaks. Based on n-alkane mixture, the calculation of retention index was conducted using Kovats retention index formula:

$$\mathrm{RI} = 100 \times (\mathrm{n}) + 100 \times (m - n) \times \frac{tri - trn}{trm - trn}$$

where RI, retention index of a metabolite "i"; n, carbon number of the alkane which elutes before "i"; m, number of carbons of the alkane which elutes after "i"; tri, retention time of "i"; trn, retention time of the alkane which elutes before "i"; and trm, retention time of the alkane which elutes after "i". Retention index of each metabolite was compared with the value of standards registered in NIST 2020 Mass Spectral Library (NIST, Gaithersburg, MD, USA), and metabolites were identified based on the retention indices and mass fragmentation profiles.

Uni- and multi-variance analyses, principal component analysis (PCA), hierarchical clustering analysis, and metabolite set enrichment analysis (MSEA) were performed using MetaboAnalyst (Ver. 5.0). Network analysis, such as MetaMapp, was performed using Cytoscape software.

Results

RGDF supplementation promotes SCFA production and carbon source utilization in *L. plantarum*

Red ginseng contains ginsenosides that have important pharmacological roles in cancer, diabetes, and aging (Yuan et al., 2012; Yu et al., 2020; Hong et al., 2022). The by-products of the processing red ginseng still contain several types of bioactive components, such as acidic polysaccharides and dietary fiber, as well as the remaining ginsenosides (Park and Kim, 2006). RGDF is a byproduct composed of approximately 31% dietary fiber (314.3 mg/g) and 0.66% ginsenoside (6.63 mg/g of total ginsenosides) (Yu et al., 2022).

Since dietary fibers are well-known prebiotic ingredients for bacterial growth promotion and probiotic functionality, we first screened the effects of RGDF on metabolic profiles of probiotic strains, including *L. reuteri*, *L. plantarum*, *Lactobacillus acidophilus*, *Lacticaseibacillus casei,* and *Lactococcus lactis* (**Supplementary Table 1**). We selected two probiotic strains, *L. plantarum* and *L. reuteri*, which were most positively and negatively affected, respectively, by RGDF supplementation. Although RGDF supplementation slightly enhanced the growth of both probiotic *Lactobacillaceae* strains, the difference was not significant compared with control (**Figures 1A, B**). The pH change of cultured media also was not different between control and RGDF supplementation. To reveal possible associations between RGDF and probiotic functionality, we next measured the production of SCFAs and carbon source utilization profiles with RGDF. *L. plantarum* enhanced the production of SCFAs, specifically lactate and acetate, with RGDF supplementation in a dose-dependent manner. *L. reuteri* reduced the production of these metabolites (**Figures 1C, D**). RGDF also improved the carbon source utilization ability of *L. plantarum* but had no effect on *L. reuteri* (**Figure 1E**). Thus, RGDF supplementation can promote the production of beneficial metabolites (lactate and acetate) and carbon source utilization by *L. plantarum*.

RGDF supplementation promotes gut epithelial adhesion of *L. plantarum* and protects against enteropathogens

Dietary fibers help maintain intestinal homeostasis by promoting probiotics, limiting the growth and adhesion of pathogenic microbes, and stimulating fiber-derived SCFA production (Cai et al., 2020). RGDF supplementation significantly increased the adhesion of *L. plantarum* to gut epithelial cells compared to the control. The adhesion was most pronounced in the presence of 0.5% RGDF (**Figure 2A**). Adhesion of *L. plantarum* and *L. reuteri* to the gut epithelium was decreased by adding RGDF (**Figure 2B**). *L. reuteri* is a probiotic that has a well-documented adhesive ability (approximately 30% in the control) (Gao et al., 2016). This behavior was confirmed in the present study; a high percentage of adhesion in the control was evident compared with *L. plantarum* (approximately 2% in the control).

To evaluate the competitive inhibitory effects of RGDF-supplemented strains on binding of enteropathogenic bacteria to the host epithelium, *E. coli* and RGDF-pretreated probiotic strains were co-incubated with Caco-2 monolayer (**Figures 2C, D**). Supplementation with RGDF increasingly reduced the *E. coli* attachment in the presence of both *L. plantarum* and *L. reuteri*; greater differences were observed in *L. plantarum*. Similar to the epithelial adhesion of *L. reuteri*, the strain showed a higher basal level of competitiveness against pathogen attachment than *L. plantarum*. However, addition of RGDF significantly improved adhesion of the gut epithelium and protected against *E. coli* attachment of *L. plantarum*, which can broaden the applicability of the strain as a probiotic. It is noted that several factors would affect epithelial adhesion of the strains including presence of surface proteins, auto-aggregation and bacterial surface hydrophobicity. Bacterial adhesion is based on non-specific physical interactions and aggregation abilities that also form a barrier preventing colonization of pathogens (Kos et al., 2003). Dell'Anno et al. (2021), showed that both *L. plantarum* and *L. reuteri* showed auto-aggregation and epithelial adhesion. *L. plantarum* and *L. reuteri* had higher hydrophobicity and greater auto-aggregation, respectively, reflecting their different colonizing ability. The collective findings indicate that RGDF supplementation promoted gut epithelial adhesion and had a protective role against enteropathogens in the presence of *L. plantarum*.

10.3389/fmicb.2023.1139386

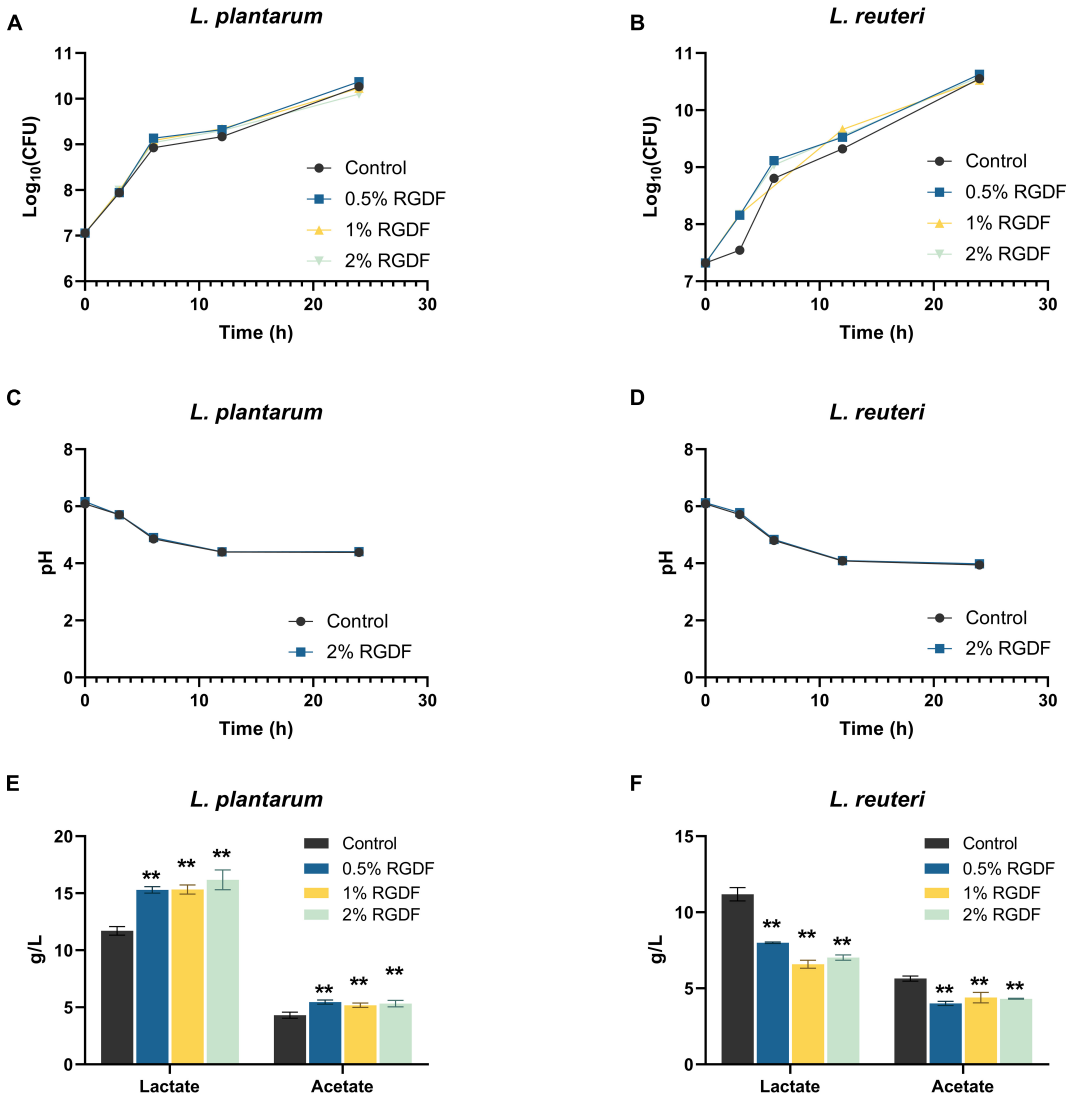

G

Carbon	*L. plantarum*				*L. reuteri*			
	Control	0.50%	1%	2%	Control	0.50%	1%	2%
RIB	+	+	+	+	+	+	+	+
ARA	+	+	+	+	+	+	+	+
MAN	+	+	+	+	-	-	-	-
SOR	+	+	+	+	-	-	-	-
LAC	+	+	+	+	+	+	+	+
TRE	+	+	+	+	-	-	-	-
INU	-	-	±	±	-	-	-	-
RAF	-	+	+	+	+	+	+	+
AMD	-	-	±	±	-	-	-	-
GLYG	-	-	-	-	-	-	-	-

FIGURE 1
Fermentation profiles of *L. plantarum* and *L. reuteri*. **(A,B)** Bacterial growth, **(C,D)** pH of cultured media, **(E,F)** lactate and acetate production, and **(G)** carbon source utilization. Differences were indicated at a significance level of 95% (*) and 99% (**), as determined by one-way ANOVA with Dunnett's *post-hoc* analysis. Error bars represent standard deviation (SD). RGDF, red ginseng dietary fiber; RIB, D-ribose; ARA, L-arabinose; MAN, D-mannitol; SOR, D-sorbitol; LAC, D-lactose; TRE, D-trehalose; INU, inulin; RAF, D-raffinose; AMD, starch; GLYG, glycogen; +, positive; –, negative.

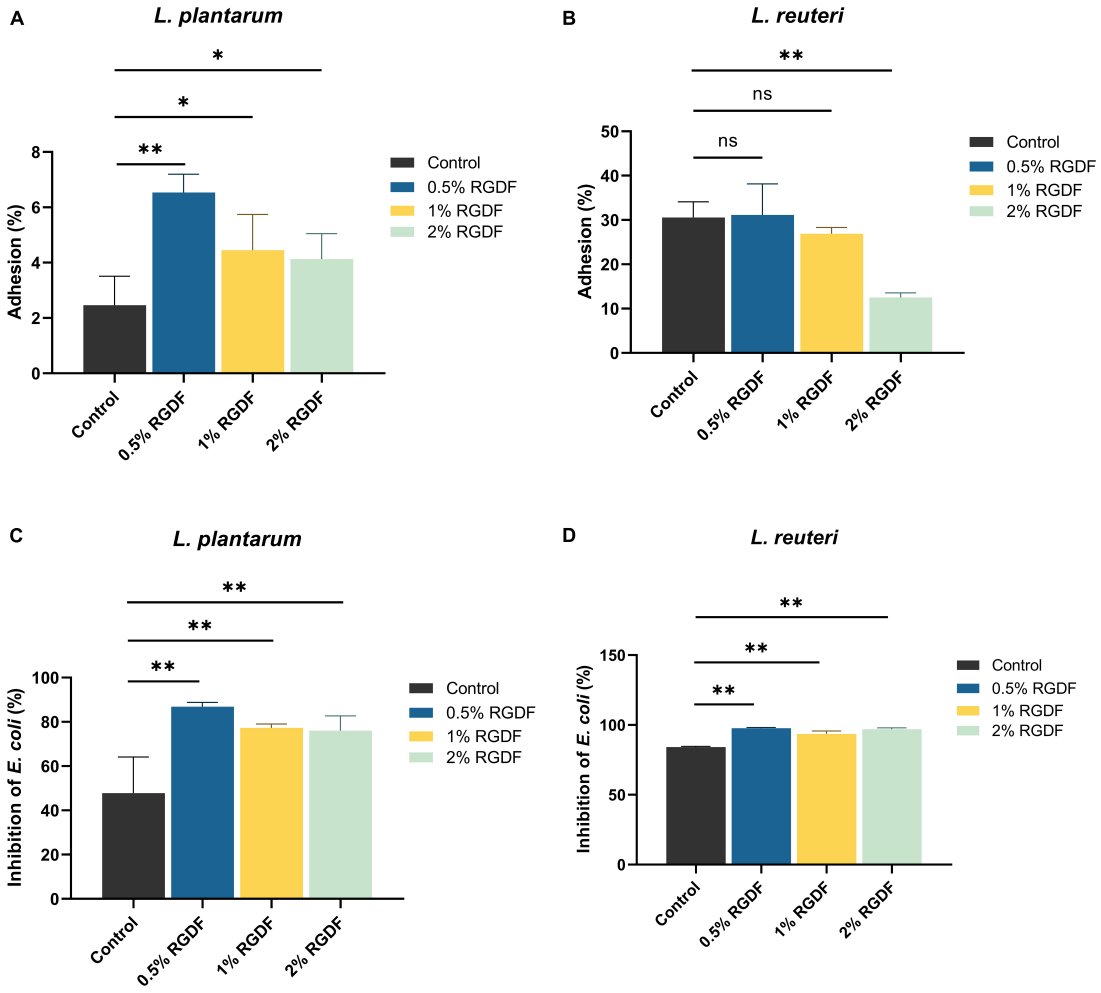

FIGURE 2
Gut epithelial adhesion **(A,B)** and inhibition of *E. coli* attachment **(C,D)** of *L. plantarum* and *L. reuteri*. Differences were indicated at a significance level of 95% (*) and 99% (**), as determined by one-way ANOVA with Dunnett's *post-hoc* analysis.

RGDF supplementation alters intracellular metabolic profiles of *L. plantarum*, but not *L. reuteri*

Although both *L. plantarum* and *L. reuteri* utilize dietary fibers as prebiotics, our results indicate that RGDF supplementation was effective in *L. plantarum*, but not in *L. reuteri*. To identify the effects of RGDF on bacterial metabolism, we first determined the intracellular metabolome changes between RGDF supplementation and control in *L. plantarum* and *L. reuteri*. Total 106 of metabolites were identified including sugars, amino acids, fatty acids, organic acids, and polyamines (**Supplementary Table 2**). PCA results clearly showed metabolic alterations with 0.5% (w/v) RGDF supplementation in *L. plantarum*, while the metabolic profile of *L. reuteri* with RGDF was not different (**Figure 3A**). Loading of PC1 and PC2 indicated that fumaric acid (−0.834 at PC1), uracil (−0.924 at PC1), picolinic acid (0.791 at PC1), and 2-hydroxybutanoic acid (0.763 at PC1) were important metabolites determining the metabolic differences between *L. plantarum* and *L. reuteri*.

MetaMapp, a network graph of metabolites based on biochemical pathways and chemical and mass spectral similarities, displayed significantly altered metabolites ($p < 0.05$) with RGDF compared to the control in *L. plantarum* (**Figure 3C**). MSEA also supported the results of significantly altered bacterial metabolism, especially sugar (galactose, starch, and sucrose) metabolism and unsaturated fatty acid biosynthesis (**Figure 3D**). Considering the significant increase in lactate and acetate production and carbohydrate utilization in *L. plantarum* with RGDF (**Figure 1**), we suggest that glycolytic metabolic flow and membrane flexibility, respectively, can be affected by RGDF supplementation.

In addition, we compared the effect of RGDF on the intensity of each metabolite with that of the control using a volcano plot (**Figure 3B**). The intensities of the four metabolites (oleic acid, nicotinic acid, uracil, and glyceric acid) decreased after RGDF supplementation in *L. plantarum* (**Figure 3E**). The relative abundance of these metabolites was also significantly reduced by RGDF, verifying that metabolic processes associated with the four metabolites were specifically altered by RGDF (**Supplementary Figure 1**). Together, these findings suggest that *L. plantarum*, but

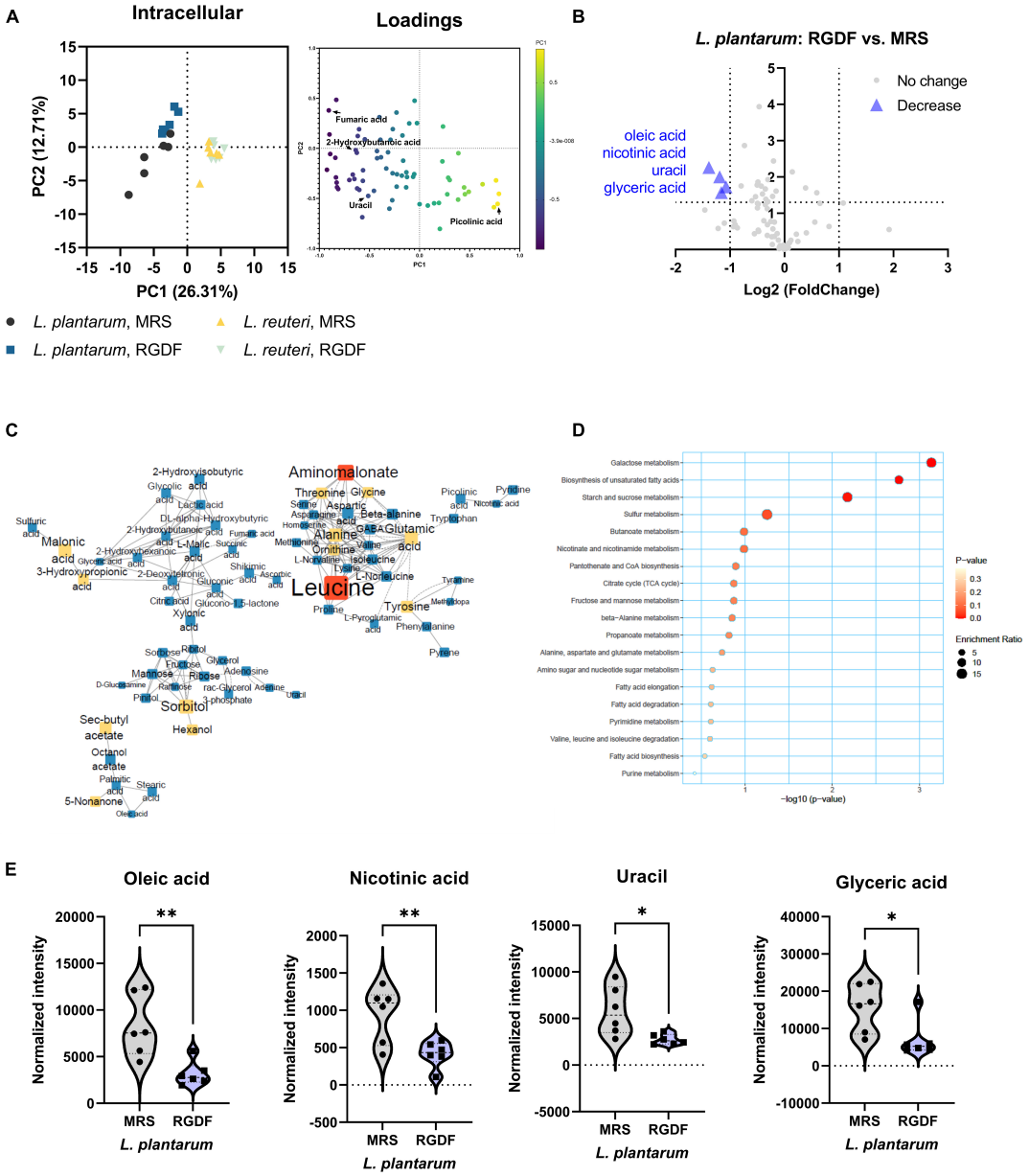

FIGURE 3
Intracellular metabolomic analysis of *L. plantarum* and *L. reuteri* cultured with 0.5% (w/v) RGDF compared to the control MRS broth. **(A)** Principle component analysis (PCA) score and loading plots. **(B)** Volcano plot of *L. plantarum*. Significantly decreased metabolites are indicated by blue triangles. **(C)** MetaMapp of *L. plantarum* culture with RGDF compared to the control MRS broth. Each node is a structurally identified metabolite. Blue nodes are decreased metabolites, and yellow nodes are unchanged metabolites. The size of nodes and labels reflect fold-changes and *p*-values by *t*-test, respectively. **(D)** MSEA of *L. plantarum*. **(E)** Normalized abundance of intracellular metabolites of *L. plantarum* cultured with 0.5% (w/v) RGDF compared to the control MRS broth. Data are expressed as violin plots of six determinations. Differences between metabolite abundances were all significant at a significance level of 95% (*) and 99% (**), as determined by the Student's *t*-test.

not *L. reuteri*, is specifically affected by RGDF supplementation via central carbon metabolism.

RGDF supplementation promotes biosynthesis of specific metabolites in *L. plantarum*

Postbiotics are nonviable bacterial metabolic products with biological activity in the host (Nataraj et al., 2020). These molecules have several advantages over probiotics with respect to safety and effectiveness, such as triggering only targeted responses by a defined mechanism, better accessibility of microbe-associated molecular patterns, and ease of production and storage (Nataraj et al., 2020). To systemically characterize postbiotic metabolites specifically produced by RGDF supplementation in *L. plantarum*, we further analyzed the extracellular metabolome in *L. plantarum* and *L. reuteri* grown with 0.5% RGDF, defined as the relative metabolite intensity in spent medium from bacterial culture to metabolite intensity in baseline medium (Jain et al., 2012). As

shown in the PCA results, exometabolome profiles were clearly separated between the bacterial strains, as well as between the RGDF supplement and control (**Figure 4A**).

Red ginseng dietary fiber-specific bacteria-derived metabolites were distinguished from the media components based on three criteria: (1) the averaged value of metabolite intensity in the spent medium subtracted from its intensity in the uncultured medium should be positive; (2) the statistical significance between RGDF and control should be under the level of 95% confidence; and (3) the absolute change in metabolite intensity with RGDF compared to the control should be >2. Based on these criteria, we identified four *L. plantarum* metabolites (oleic acid, 2-hydroxybutanoic acid, hexanol, and sec-butyl acetate) biosynthesized specifically in response to the RGDF supplement (**Figures 4B–E**). The collective findings indicate that RGDF supplementation promoted the biosynthesis of specific metabolites in *L. plantarum*. These metabolites included oleic acid, 2-hydroxybutanoic acid, hexanol, and butyl acetate.

RGDF supplementation has distinct effects on *L. plantarum* metabolism compared with fructooligosaccharide supplementation

Dietary fiber, a plant-derived component that cannot be completely digested by human enzymes, consists of non-starch polysaccharides, including cellulose and oligosaccharides (Veronese et al., 2018). Fructooligosaccharides (FOS) are dietary fibers composed of linear chains of fructose units linked by β-(2,1) bonds (Sabater-Molina et al., 2009). They naturally occur in plants, such as onion, chicory, and banana, and are increasingly used in food products because of their prebiotic effect, which stimulates the growth of probiotic gut microbiota (Sabater-Molina et al., 2009). To compare the effects of different type of dietary fibers on metabolic alteration in *L. plantarum*, we cultured *L. plantarum* on control MRS, MRS with 0.5% RGDF, and MRS with 0.5% FOS. Similar to the growth results of RGDF shown in **Figure 1**, supplementation with either RGDF or FOS did not have an effect on bacterial growth (**Supplementary Table 3**).

In contrast to the lack of observable differences in bacterial growth, the metabolome profile of *L. plantarum* supplemented with RGDF showed a transition between MRS and FOS in both intracellular and extracellular states (**Figures 5A, B**). Similar to the effect of RGDF shown in **Figures 3C, D**, FOS also decreased the abundance of specific metabolites in sugar and central carbon metabolism, while the abundance of leucine specifically increased with FOS supplementation compared to the control (**Figure 5C**). MSEA analysis indicated that the citrate cycle and its associated pathways, such as alanine, aspartate, and glutamate metabolism, as well as sugar metabolism, were altered by FOS treatment (**Figure 5D**). Comparison of the intracellular metabolite abundance of RGDF with FOS revealed that RGDF supplementation resulted in a decreased abundance of palmitic acid and stearic acid, while uracil, raffinose, ascorbic acid, and 2-hydroxybutanoic acid comparatively increased in RGDF (**Figures 5E, F**).

Next, we compared the extracellular metabolites differentially produced by FOS treatment to the control, applying the same criteria used for RGDF treatment (**Figure 6**). As expected, the culture supernatant of cells grown with FOS contained a significantly higher abundance of sugars and sugar derivatives than those grown with RGDF, including raffinose, D-glucosamine, and pinitol. Production of RGDF-specific metabolites, including oleic acid, 2-hydroxybutanoic acid, hexanol, and sec-butyl acetate, was not significantly induced by FOS, suggesting that the metabolism of these molecules is RGDF-specific. Thus, RGDF supplementation had distinct effects on *L. plantarum* metabolism compared with FOS supplementation.

Discussion

Dietary fibers and the associated phytochemicals in ginseng-derived products provide various functional and health benefits. In this study, we evaluated the effects of RGDF as a prebiotic constituent on the physiological and metabolic alterations of probiotics. With RGDF supplementation in the growth media, *L. plantarum* showed the highest production of SCFAs, specifically lactate and acetate, and the most increased carbohydrate-fermenting capability compared with other probiotic *Lactobacillaceae* species, especially *L. reuteri*. In addition, RGDF improved gut epithelial adhesion of *L. plantarum* and protected against enteropathogens. Analysis of the intracellular metabolome of *L. plantarum* indicated decreases in metabolites of sugars and unsaturated fatty acids, and significant decreases in the abundance of oleic acid, nicotinic acid, uracil, and glyceric acid. RGDF supplementation also promoted the secretion of specific metabolites, such as oleic acid, 2-hydroxybutanoic acid, hexanol, and butyl acetate, in *L. plantarum*. Comparison of the metabolic alteration by red ginseng-derived dietary fiber with a representative dietary fiber, FOS, showed distinguishable effects between the two different types of fibers in *L. plantarum*.

Although dietary fibers generally promote probiotic growth, their effects are strain specific. Our results consistently revealed that RGDF supplementation improved the probiotic properties of *L. plantarum*, but not of *L. reuteri*. *L. plantarum*, unlike most probiotic *Lactobacillaceae* species, exhibits ecological and metabolic flexibility and thus maintains a diverse functional genome that facilitates the flexibility to colonize a variety of environments (Fidanza et al., 2021). For example, *L. plantarum* strains exhibit acid tolerance by inducing alterations in the fatty acid composition of the bacterial membrane upon exposure to low-pH conditions (Huang et al., 2016). Genome analysis of 165 *L. plantarum* strains revealed the presence of a large number of carbohydrates metabolizing genes and two-component systems and signal transduction systems regulating physiological processes, facilitating the adaptability of the species in various environments compared to other lactic acid bacteria and even among probiotic *Lactobacillaceae* strains (Cui et al., 2021). In addition, *L. plantarum* produces bacteriocins termed plantaricins, which can effectively inhibit enteropathogenic bacteria, such as *E. coli*, under specific circumstances (Pal and Srivastava, 2014). These findings based on the diverse functional genetic characteristics support our results that *L. plantarum* greatly modulates and improves their metabolic functions, including acid production, carbohydrate utilization, and inhibition of pathogen growth in the presence of RGDF.

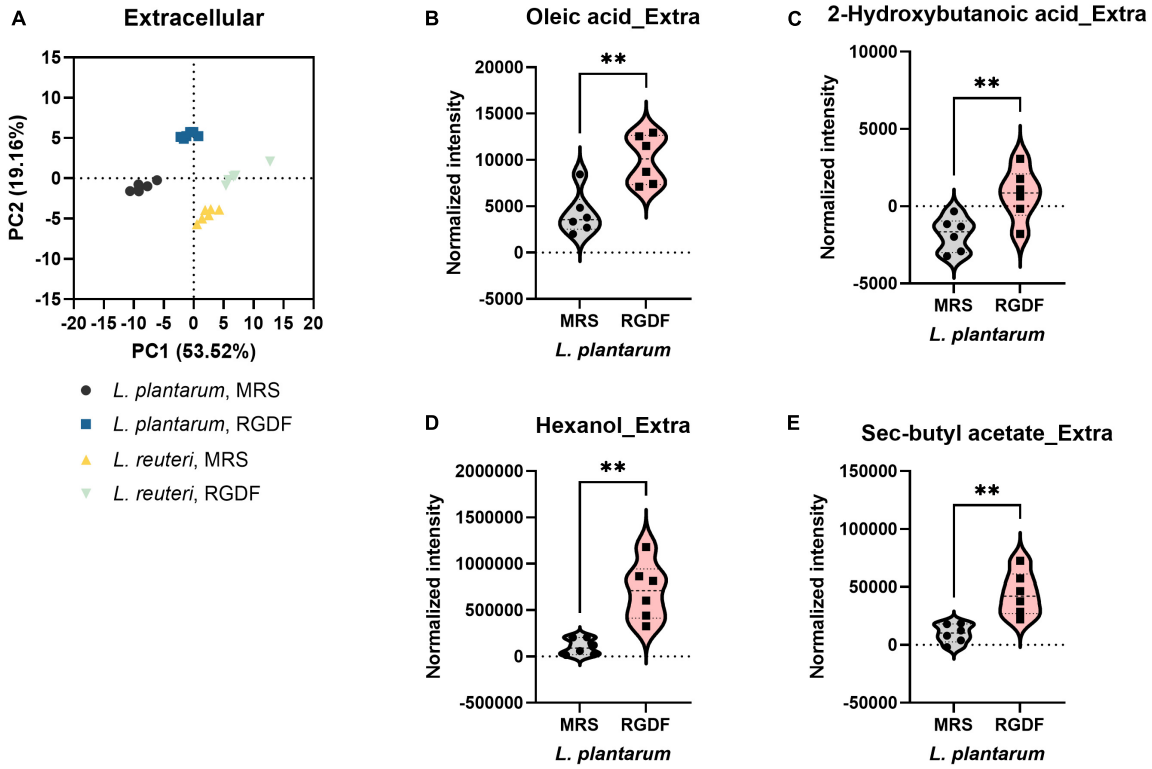

FIGURE 4
Extracellular metabolomic analysis of *L. plantarum* and *L. reuteri* cultured with 0.5% (w/v) RGDF compared to the control MRS broth. **(A)** Principle component analysis (PCA) score and loading plots. Normalized abundance of intracellular metabolites of *L. plantarum* **(B–E)** cultured with 0.5% (w/v) RGDF compared to the control MRS broth. Data are expressed as violin plots of six determinations. Differences between metabolite abundances were all significant at a significance level of 95% (*) and 99% (**), as determined by the Student's *t*-test.

To explain how RGDF promotes bacterial metabolic alterations in *L. plantarum*, but not in *L. reuteri*, and how the effects of RGDF are different from those of other dietary fibers, beyond the genetic flexibility of *L. plantarum*, we interpreted intracellular metabolic changes of *L. plantarum* and *L. reuteri* when supplied with RGDF and FOS. RGDF supplementation resulted in a significant decrease in the abundance of oleic acid, nicotinic acid, uracil, and glyceric acid. Oleic acid [*cis*-9-octadecenoic acid; 18:1(9c)] is the most common monounsaturated fatty acid in animals and vegetables. It is incorporated into the membranes of lactic acid bacteria grown in a medium, but is not synthesized (Johnsson et al., 1995). In *L. plantarum*, our metabolomic analysis indicated that the intracellular abundance of oleic acid decreased, while the extracellular abundance increased with RGDF supplementation. These findings suggest that oleic acid might be less incorporated from the medium, possibly by modified membrane rigidity by RGDF. Nicotinic acid, also known as niacin, is a form of vitamin B3 and is an essential human nutrient that can be supplied by plants and bacteria. Several cellular processes require the compound as a component of the coenzymes nicotinamide adenine dinucleotide (NAD) and NAD phosphate (NADP). In probiotic *Lactobacillaceae* spp., free nicotinic acid decrease with increasing cellular activity as it is largely incorporated in the form of cofactors (McIlwain et al., 1949). Nicotinic acid is also an important cofactor for lactate dehydrogenase, acting as the limiting factor for lactate production during fermentation, which might be associated with the reduced intracellular abundance and improved lactate production by RGDF (Colombié and Sablayrolles, 2004). Glyceric acid is a precursor of several phosphate derivatives that are important biochemical intermediates in glycolysis. 3-Phosphoglyceric acid is one derivative that is especially important for serine and cysteine biosynthesis. A recent study demonstrated that *L. plantarum* supplemented with 2% RGDF upregulates the expression of genes involved in serine (sdhA, sdhB, and sdaC) and cysteine metabolism (cysE) (Yu et al., 2022). Although further verification of the changes in specific metabolic and physiologic mechanisms is required, our results support the view that RGDF supplementation alters cellular and metabolic processes.

Lactobacilli are recognized for their ability to secrete many beneficial metabolites, such as SCFAs, indole-derivatives, and vitamins (Wang et al., 2018; Thompson et al., 2020; Sugimura et al., 2022). Our exometabolomic analysis revealed that 2-hydroxybutanoic acid, hexanol, and butyl acetate as metabolites that were secreted specifically in response to RGDF supplementation. These compounds are generally excreted as end products during propanoate biosynthesis and butanol metabolism. In mammalian tissues, 2-hydroxybutanoic acid, also known as α-hydroxybutyrate, is released as a byproduct when cystathionine is cleaved to cysteine for detoxification against oxidative stress. Although it has been used as a biomarker of type 2 diabetes and lactic acidosis, novel roles of 2-hydroxybutanoic acid have been suggested to protect against acetaminophen-induced liver injury and immune modulation against viral infection (Liu et al., 2018; Zheng et al., 2020; Shi et al., 2021). For example, the level

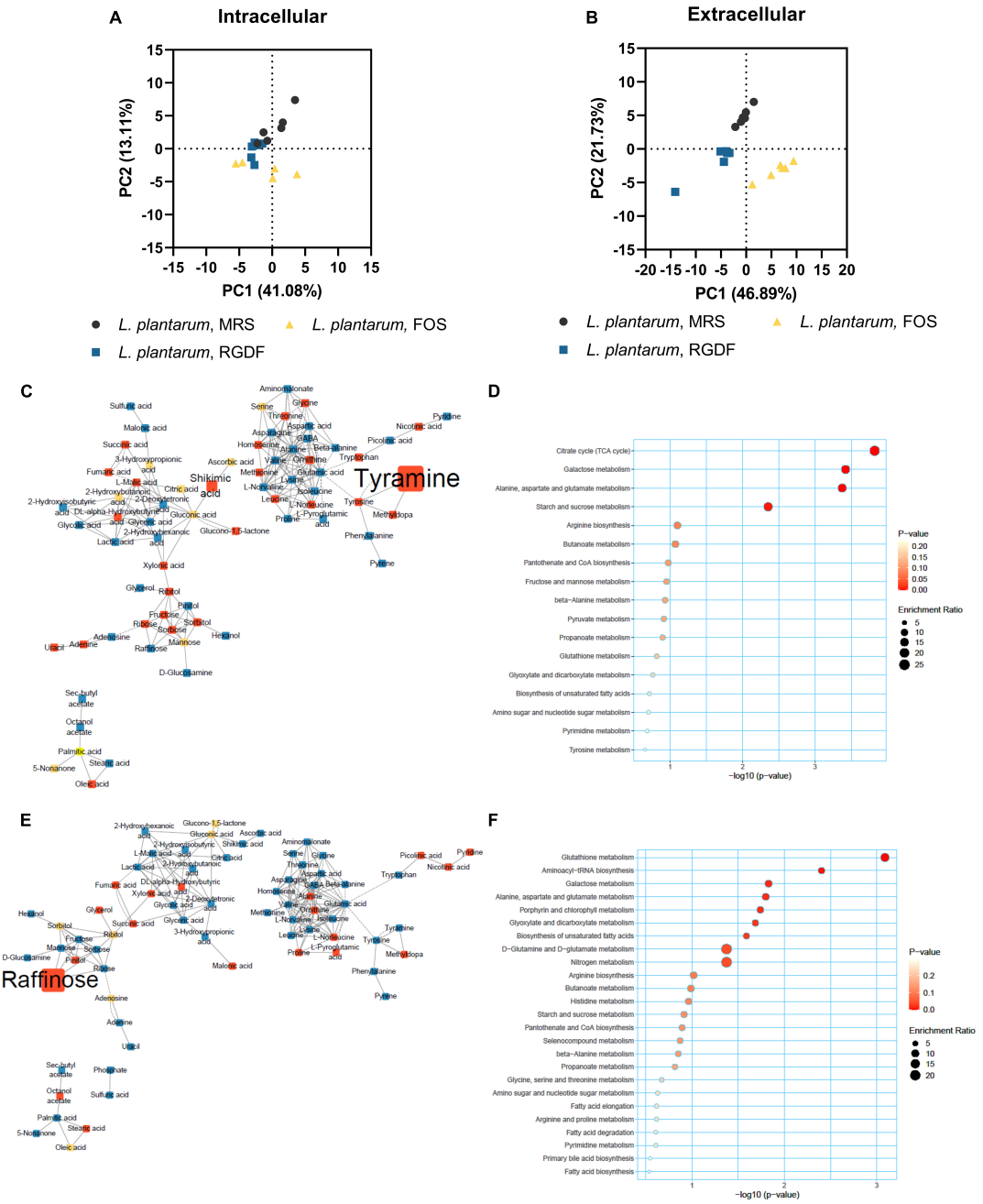

FIGURE 5
Metabolomic analysis of *L. plantarum* cultured with 0.5% (w/v) RGDF or 0.5% (w/v) FOS. Principle component analysis (PCA) score and loading plots of intracellular **(A)** and extracellular **(B)** metabolome. MetaMapp of *L. plantarum* cultured with FOS compared to the control MRS broth **(C)** and cultured with RGDF compared to FOS **(E)**. Each node is a structurally identified metabolite. Blue nodes are decreased metabolites, red nodes are increased metabolites, and yellow nodes are unchanged metabolites. The size of nodes and labels reflect fold-changes and *p*-values by *t*-test, respectively. MSEA of *L. plantarum* cultured with FOS compared to the control MRS broth **(D)** and cultured with RGDF compared to FOS **(F)**.

of serum 2-hydroxybutanoic acid was reportedly enriched in patients with viral infections that included human papilloma virus or SARS-CoV-2 compared to healthy controls (Liu et al., 2018; Shi et al., 2021). It could be a result of the activation of antioxidant responses and control of cellular redox balance. Hexanol is an organic alcohol used in the perfume industry; its odor is that of freshly mown grass with a hint of strawberries. Its health-related functions are unclear, but it reportedly modulates the function of the actomyosin motor (Komatsu et al., 2004). Similar to hexanol, butyl acetate possesses characteristic flavors and a sweet odor of bananas or apples (Holland et al., 2005). It also has antimicrobial activity against undesirable microorganisms in cosmetic products, such as *Staphylococcus aureus* and *E. coli* (Lens et al., 2016). The specific mechanism of the secretion of these metabolites following stimulation by RGDF supplementation and comparative studies with FOS, would provide some evidence that metabolite production is highly specific to RGDF, but not to carbohydrate polymer-based dietary fiber. Further

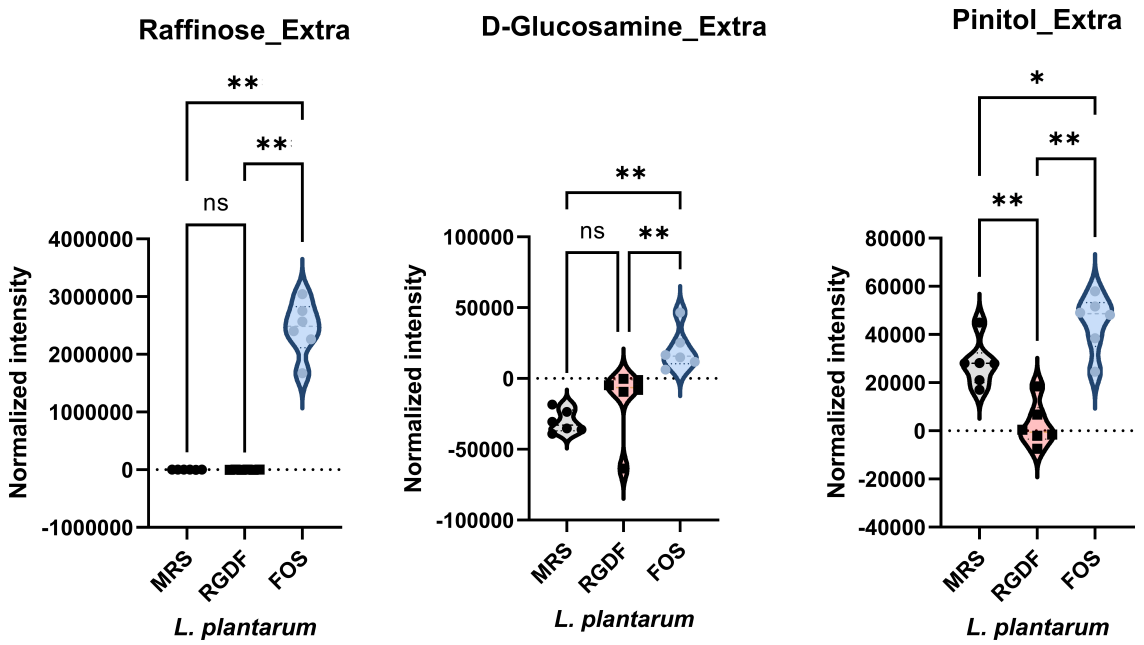

FIGURE 6
Normalized abundance of extracellular metabolites of *L. plantarum* cultured with 0.5% (w/v) RGDF or 0.5% (w/v) FOS. Data are expressed as violin plots of six determinations. Differences were indicated at a significance level of 95% (*) and 99% (**), as determined by one-way ANOVA with Tukey's *post-hoc* analysis.

genetic investigations are required to elucidate the underlying mechanism.

Conclusion

Red ginseng dietary fiber supplementation promoted probiotic properties of *L. plantarum*, including production of SCFAs (lactate and acetate), carbohydrate utilization, epithelial attachment, and pathogen inhibition. Comparative metabolomic analyses suggested RGDF-related modification of cellular and metabolic processes, including membrane biology and central carbon metabolism. In addition, the potential applications of bioactive compounds produced by RGDF-supplemented *L. plantarum* have been proposed as novel postbiotic metabolites.

Data availability statement

The raw data supporting the conclusions of this article will be made available by the authors, without undue reservation.

Author contributions

S-HY, YJ, and MS designed the study, and drafted and revised the manuscript. HJ, V-LT, J-HB, Y-JB, and RR performed the experiments, analyzed the data, and collected the samples and data interpretation. EN, S-KK, and W-SJ revised the manuscript and obtained the funding. All authors had read and approved the final manuscript.

Funding

This research was supported by the Basic Science Research Program (NRF-2022R1C1C1008574) through the National Research Foundation of Korea (NRF) to MS.

Conflict of interest

S-HY and S-KK were employed by Korea Ginseng Corporation.

The remaining authors declare that the research was conducted in the absence of any commercial or financial relationships that could be construed as a potential conflict of interest.

Publisher's note

All claims expressed in this article are solely those of the authors and do not necessarily represent those of their affiliated organizations, or those of the publisher, the editors and the reviewers. Any product that may be evaluated in this article, or claim that may be made by its manufacturer, is not guaranteed or endorsed by the publisher.

Supplementary material

The Supplementary Material for this article can be found online at: https://www.frontiersin.org/articles/10.3389/fmicb.2023.1139386/full#supplementary-material

References

Aretz, I., and Meierhofer, D. (2016). Advantages and pitfalls of mass spectrometry based metabolome profiling in systems biology. *Int. J. Mol. Sci.* 17:632. doi: 10.3390/ijms17050632

Baiges-Gaya, G., Iftimie, S., Castañé, H., Rodríguez-Tomàs, E., Jiménez-Franco, A., López-Azcona, A. F., et al. (2023). Combining semi-targeted metabolomics and machine learning to identify metabolic alterations in the serum and urine of hospitalized patients with COVID-19. *Biomolecules* 13:163. doi: 10.3390/biom13010163

Bourebaba, Y., Marycz, K., Mularczyk, M., and Bourebaba, L. (2022). Postbiotics as potential new therapeutic agents for metabolic disorders management. *Biomed. Pharmacother.* 153:113138. doi: 10.1016/j.biopha.2022.113138

Cai, Y., Folkerts, J., Folkerts, G., Maurer, M., and Braber, S. (2020). Microbiota-dependent and -independent effects of dietary fibre on human health. *Br. J. Pharmacol.* 177, 1363–1381. doi: 10.1111/bph.14871

Cho, I.-H., Kang, B.-W., Yun-Jae, P., Lee, H.-J., Park, S., and Lee, N. (2018). Ginseng berry extract increases nitric oxide level in vascular endothelial cells and improves cGMP expression and blood circulation in muscle cells. *J. Exerc. Nutr. Biochem.* 22, 6–13. doi: 10.20463/jenb.2018.0018

Colombié, S., and Sablayrolles, J.-M. (2004). Nicotinic acid controls lactate production by K1-LDH: A Saccharomyces cerevisiae strain expressing a bacterial LDH gene. *J. Ind. Microbiol. Biotechnol.* 31, 209–215. doi: 10.1007/s10295-004-0138-5

Cui, Y., Wang, M., Zheng, Y., Miao, K., and Qu, X. (2021). The carbohydrate metabolism of *Lactiplantibacillus plantarum*. *IJMS* 22: 13452. doi: 10.3390/ijms222413452

Dell'Anno, M., Giromini, C., Reggi, S., Cavalleri, M., Moscatelli, A., Onelli, E., et al. (2021). Evaluation of adhesive characteristics of *L. plantarum* and *L. reuteri* isolated from weaned piglets. *Microorganisms* 9:1587. doi: 10.3390/microorganisms9081587

Fidanza, M., Panigrahi, P., and Kollmann, T. R. (2021). *Lactiplantibacillus plantarum*–nomad and ideal probiotic. *Front. Microbiol.* 12:712236. doi: 10.3389/fmicb.2021.712236

Gao, K., Liu, L., Dou, X., Wang, C., Liu, J., Zhang, W., et al. (2016). Doses *Lactobacillus* reuteri depend on adhesive ability to modulate the intestinal immune response and metabolism in mice challenged with lipopolysaccharide. *Sci. Rep.* 6:28332. doi: 10.1038/srep28332

Geng, J., Dong, J., Ni, H., Lee, M. S., Wu, T., Jiang, K., et al. (2010). Ginseng for cognition. *Cochrane Database Syst. Rev.* 2010:CD007769. doi: 10.1002/14651858.CD007769.pub2

He, M., Huang, X., Liu, S., Guo, C., Xie, Y., Meijer, A. H., et al. (2018). The Difference between white and red ginseng: Variations in ginsenosides and immunomodulation. *Planta Med.* 84, 845–854. doi: 10.1055/a-0641-6240

Holland, D., Larkov, O., Bar-Ya'akov, I., Bar, E., Zax, A., Brandeis, E., et al. (2005). Developmental and varietal differences in volatile ester formation and acetyl-coA: Alcohol acetyl transferase activities in apple (*Malus domestica* Borkh.) fruit. *J. Agric. Food Chem.* 53, 7198–7203. doi: 10.1021/jf050519k

Holscher, H. D. (2017). Dietary fiber and prebiotics and the gastrointestinal microbiota. *Gut Microbes* 8, 172–184. doi: 10.1080/19490976.2017.1290756

Hong, J., Gwon, D., and Jang, C.-Y. (2022). Ginsenoside Rg1 suppresses cancer cell proliferation through perturbing mitotic progression. *J. Ginseng Res.* 46, 481–488. doi: 10.1016/j.jgr.2021.11.004

Huang, R., Pan, M., Wan, C., Shah, N. P., Tao, X., and Wei, H. (2016). Physiological and transcriptional responses and cross protection of *Lactobacillus plantarum* ZDY2013 under acid stress. *J. Dairy Sci.* 99, 1002–1010. doi: 10.3168/jds.2015-9993

Jain, M., Nilsson, R., Sharma, S., Madhusudhan, N., Kitami, T., Souza, A. L., et al. (2012). Metabolite profiling identifies a key role for glycine in rapid cancer cell proliferation. *Science* 336, 1040–1044. doi: 10.1126/science.1218595

Johnsson, T., Nikkila, P., Toivonen, L., Rosenqvist, H., and Laakso, S. (1995). Cellular fatty acid profiles of *Lactobacillus* and *Lactococcus* strains in relation to the oleic acid content of the cultivation medium. *Appl. Environ. Microbiol.* 61, 4497–4499. doi: 10.1128/aem.61.12.4497-4499.1995

Jordan, K. W., Nordenstam, J., Lauwers, G. Y., Rothenberger, D. A., Alavi, K., Garwood, M., et al. (2009). Metabolomic characterization of human rectal adenocarcinoma with intact tissue magnetic resonance spectroscopy. *Dis. Colon Rectum* 52, 520–525. doi: 10.1007/DCR.0b013e31819c9a2c

Komatsu, H., Shigeoka, T., Ohno, T., Kaseda, K., Kanno, T., Matsumoto, Y., et al. (2004). Modulation of actomyosin motor function by 1-hexanol. *J. Muscle Res. Cell Motil.* 25, 77–85. doi: 10.1023/B:JURE.0000021350.85334.2f

Kos, B., Šušković, J., Vuković, S., Šimpraga, M., Frece, J., and Matošić, S. (2003). Adhesion and aggregation ability of probiotic strain *Lactobacillus acidophilus* M92. *J. Appl. Microbiol.* 94, 981–987. doi: 10.1046/j.1365-2672.2003.01915.x

Kurbatov, I., Kiseleva, O., Arzumanian, V., Dolgalev, G., and Poverennaya, E. (2023). Some lessons learned on the impact of the storage conditions, syringe wash solvent, and the way of GC-MS injection on the reproducibility of metabolomic studies. *Metabolites* 13:75. doi: 10.3390/metabo13010075

Lens, C., Malet, G., and Cupferman, S. (2016). Antimicrobial activity of Butyl acetate, Ethyl acetate and Isopropyl alcohol on undesirable microorganisms in cosmetic products. *Int. J. Cosmet Sci.* 38, 476–480. doi: 10.1111/ics.12314

Liu, Y., Guo, J.-Z., Liu, Y., Wang, K., Ding, W., Wang, H., et al. (2018). Nuclear lactate dehydrogenase A senses ROS to produce α-hydroxybutyrate for HPV-induced cervical tumor growth. *Nat. Commun.* 9:4429. doi: 10.1038/s41467-018-06841-7

Makki, K., Deehan, E. C., Walter, J., and Bäckhed, F. (2018). The impact of dietary fiber on gut microbiota in host health and disease. *Cell Host Microbe* 23, 705–715. doi: 10.1016/j.chom.2018.05.012

McIlwain, H., Stanley, D. A., and Hughes, D. E. (1949). The behaviour of *Lactobacillus arabinosus* towards nicotinic acid and its derivatives. *Biochem. J.* 44, 153–158. doi: 10.1042/bj0440153

Nataraj, B. H., Ali, S. A., Behare, P. V., and Yadav, H. (2020). Postbiotics-parabiotics: The new horizons in microbial biotherapy and functional foods. *Microb. Cell Fact.* 19:168. doi: 10.1186/s12934-020-01426-w

Neag, E. J., Collao, V., and Bhattacharya, S. K. (2023). Analysis of cholesterol lipids using gas chromatography mass spectrometry. *Methods Mol. Biol.* 2625, 141–148. doi: 10.1007/978-1-0716-2966-6_13

Pal, G., and Srivastava, S. (2014). Inhibitory effect of plantaricin peptides (Pln E/F and J/K) against *Escherichia coli*. *World J. Microbiol. Biotechnol.* 30, 2829–2837. doi: 10.1007/s11274-014-1708-y

Park, S.-H., and Kim, W.-J. (2006). Study of hongsambak for medicinal foods applications –nutritional composition, antioxidants contents and antioxidative activity. *J. Physiol. Pathol. Korean Med.* 20, 449–454.

Sabater-Molina, M., Larqué, E., Torrella, F., and Zamora, S. (2009). Dietary fructooligosaccharides and potential benefits on health. *J. Physiol. Biochem.* 65, 315–328. doi: 10.1007/BF03180584

Shi, D., Yan, R., Lv, L., Jiang, H., Lu, Y., Sheng, J., et al. (2021). The serum metabolome of COVID-19 patients is distinctive and predictive. *Metabolism* 118:154739. doi: 10.1016/j.metabol.2021.154739

So, S.-H., Lee, J. W., Kim, Y.-S., Hyun, S. H., and Han, C.-K. (2018). Red ginseng monograph. *J. Ginseng Res.* 42, 549–561. doi: 10.1016/j.jgr.2018.05.002

Su, F., Xu, L., Xue, Y., Xu, W., Li, J., Yu, B., et al. (2022). Immune enhancement of nanoparticle-encapsulated ginseng stem-leaf saponins on porcine epidemic diarrhea virus vaccine in mice. *Vaccines* 10:1810. doi: 10.3390/vaccines10111810

Sugimura, N., Li, Q., Chu, E. S. H., Lau, H. C. H., Fong, W., Liu, W., et al. (2022). *Lactobacillus gallinarum* modulates the gut microbiota and produces anti-cancer metabolites to protect against colorectal tumourigenesis. *Gut* 71, 2011–2021. doi: 10.1136/gutjnl-2020-323951

Tam, D., Truong, D., Nguyen, T., Quynh, L., Tran, L., Nguyen, H., et al. (2018). Ginsenoside Rh1: A systematic review of its pharmacological properties. *Planta Med.* 84, 139–152. doi: 10.1055/s-0043-124087

Thompson, H. O., Önning, G., Holmgren, K., Strandler, H. S., and Hultberg, M. (2020). Fermentation of cauliflower and white beans with *Lactobacillus plantarum* – impact on levels of riboflavin, folate, vitamin B12, and amino acid composition. *Plant Foods Hum. Nutr.* 75, 236–242. doi: 10.1007/s11130-020-00806-2

Truong, V.-L., and Jeong, W.-S. (2022). Red ginseng (*Panax ginseng* Meyer) oil: A comprehensive review of extraction technologies, chemical composition, health benefits, molecular mechanisms, and safety. *J. Ginseng Res.* 46, 214–224. doi: 10.1016/j.jgr.2021.12.006

Veronese, N., Solmi, M., Caruso, M. G., Giannelli, G., Osella, A. R., Evangelou, E., et al. (2018). Dietary fiber and health outcomes: An umbrella review of systematic reviews and meta-analyses. *Am. J. Clin. Nutr.* 107, 436–444. doi: 10.1093/ajcn/nqx082

Wang, J., Ji, H., Wang, S., Liu, H., Zhang, W., Zhang, D., et al. (2018). Probiotic *Lactobacillus plantarum* promotes intestinal barrier function by strengthening the epithelium and modulating gut microbiota. *Front. Microbiol.* 9:1953. doi: 10.3389/fmicb.2018.01953

Yu, H.-Y., Rhim, D.-B., Kim, S.-K., Ban, O.-H., Oh, S.-K., Seo, J., et al. (2022). Growth promotion effect of red ginseng dietary fiber to probiotics and transcriptome analysis of Lactiplantibacillus plantarum. *J. Ginseng Res.* 47:S122684532200118X. doi: 10.1016/j.jgr.2022.09.003

Yu, S., Xia, H., Guo, Y., Qian, X., Zou, X., Yang, H., et al. (2020). Ginsenoside Rb1 retards aging process by regulating cell cycle, apoptotic pathway and metabolism of aging mice. *J. Ethnopharmacol.* 255:112746. doi: 10.1016/j.jep.2020.112746

Yuan, H.-D., Kim, J.-T., Kim, S.-H., and Chung, S.-H. (2012). Ginseng and diabetes: The evidences from in vitro, animal and human studies. *J. Ginseng Res.* 36, 27–39. doi: 10.5142/jgr.2012.36.1.27

Zheng, N., Gu, Y., Hong, Y., Sheng, L., Chen, L., Zhang, F., et al. (2020). Vancomycin pretreatment attenuates acetaminophen-induced liver injury through 2-hydroxybutyric acid. *J. Pharm. Anal.* 10, 560–570. doi: 10.1016/j.jpha.2019.11.003

frontiers | Frontiers in Microbiology

TYPE Original Research
PUBLISHED 01 June 2023
DOI 10.3389/fmicb.2023.1202440

OPEN ACCESS

EDITED BY
Carlo Giuseppe Rizzello,
Sapienza University of Rome, Italy

REVIEWED BY
Severino Zara,
University of Sassari, Italy
Gianluca Bleve,
National Research Council (CNR), Italy

*CORRESPONDENCE
Mingzheng Huang
✉ huangmingzheng@git.edu.cn
Xiaozhu Liu
✉ liuxiaozhu_840914@163.com

RECEIVED 08 April 2023
ACCEPTED 17 May 2023
PUBLISHED 01 June 2023

CITATION
Li Y, Ding P, Tang X, Zhu W, Huang M, Kang M and Liu X (2023) Screening and oenological property analysis of ethanol-tolerant non-*Saccharomyces* yeasts isolated from *Rosa roxburghii* Tratt.
Front. Microbiol. 14:1202440.
doi: 10.3389/fmicb.2023.1202440

Screening and oenological property analysis of ethanol-tolerant non-*Saccharomyces* yeasts isolated from *Rosa roxburghii* Tratt

Yinfeng Li[1], Peipei Ding[1], Xiaoyu Tang[1], Wenli Zhu[1], Mingzheng Huang[1]*, Mei Kang[1] and Xiaozhu Liu[1,2]*

[1]Guizhou Institute of Technology, Guiyang, China, [2]Key Laboratory of Microbial Resources Collection and Preservation, Ministry of Agriculture and Rural Affairs, Beijing, China

Ethanol tolerance is crucial for the oenological yeasts. *Rosa roxburghii* Tratt, a Rosaceae plant native to China, is rich in nutritional and medicinal ingredients. In this study, ethanol-tolerant non-*Saccharomyces* yeasts were screened, and their oenological properties were further evaluated. Three ethanol-tolerant yeast strains (designated as C6, F112, and F15), which could tolerate 12% (v/v) ethanol treatment, were isolated from *R. roxburghii*, and identified as *Candida tropicalis*, *Pichia guilliermondii*, and *Wickerhamomyces anomalus*, respectively. The winemaking condition tolerances of these ethanol-tolerant yeast strains were similar to those of *Saccharomyces cerevisiae* X16. However, their growth, sugar metabolic performance and sulphureted hydrogen activities, were different. The β-glucosidase production ability of strain *W. anomalus* F15 was lower than that of *S. cerevisiae* X16, and strains of *C. tropicalis* C6 and *P. guilliermondii* F112 were similar to *S. cerevisiae* X16. Electronic sensory properties of the *R. roxburghii* wines fermented using ethanol-tolerant yeasts together with *S. cerevisiae* showed no significant differences. However, the mixed inoculation of the ethanol-tolerant yeast strains with *S. cerevisiae* could regulate the volatile aroma characteristics of the fermented *R. roxburghii* wine, enriching and enhancing the aroma flavor. Therefore, the selected ethanol-tolerant yeasts have the potential for application in the production of unique *R. roxburghii* wine.

KEYWORDS

ethanol tolerance, non-*Saccharomyces* yeast, *Rosa roxburghii* Tratt, fruit wine, volatile aroma

Introduction

The flavor characteristics and quality of fruit wine are determined by various factors, including the type of fruit, the brewing process, and the metabolic activity of the selected yeast (Wei et al., 2019). Yeast can be classified into two categories based on their fermentation characteristics and physiological properties: *Saccharomyces cerevisiae* and non-*Saccharomyces* yeasts (Jolly et al., 2014). *S. cerevisiae* is preferred for its high fermentation

activity and strong ethanol tolerance, making it a popular choice for fruit wine production, and it is readily available for purchase by producers (Parapouli et al., 2020). However, the commercial varieties of wine yeast are limited, leading to high similarity in the flavor characteristics of fermented fruit wines and a lack of complexity in taste and flavor. As a result, product homogenization is common, which does not meet the diverse needs of consumers for product diversity. Non-*Saccharomyces yeast* refers to a diverse group of yeast species that also play a crucial role in winemaking. This group includes *Hanseniaspora uvarum* (Pietrafesa et al., 2020), *Wickerhamomyces anomalus* (Padilla et al., 2018), *Candida tropicalis* (Egue et al., 2018), etc.

Research has shown that non-*Saccharomyces* yeast can metabolize a greater variety of compounds during fruit wine fermentation, resulting in more complex and aromatic wine characteristics that enhance the overall flavor quality (Morata et al., 2019). However, non-*Saccharomyces* yeast is typically more sensitive to ethanol, which accumulates during the fermentation process and can inhibit its growth and induce cell death, ultimately reducing fermentation efficiency (Contreras et al., 2014). Therefore, the screening of non-*Saccharomyces* yeast strains with higher ethanol tolerance is of great practical significance for the production of distinctive fruit wines.

Rosa roxburghii Tratt, a perennial plant belonging to the Rosaceae family and the *Rosa* genus, is widely distributed in southwestern China, such as Guizhou, Sichuan, and Yunnan (Liu X. et al., 2020). The fruit of *R. roxburghii* is rich in nutrients, such as vitamin C, polysaccharides, and carotenoids (Liu et al., 2021a). Moreover, it contains abundant bioactive substances, such as flavonoids, superoxide dismutase (SOD), and organic acids, which give it good medicinal value (Wang et al., 2021). However, due to its high content of phenolic and acidic compounds, the fresh fruit tastes sour and astringent in taste, making it unsuitable for consumption. Therefore, fermenting the fruit into *R. roxburghii* fruit wine is more appropriate (Liu et al., 2021b). Currently, the yeast strains used in *R. roxburghii* fruit wine production mostly come from the active dry yeast used in grape wine production rather than from the indigenous yeast strains of *R. roxburghii*. This leads to poor adaptability of the strains and serious homogenization of the resulting *R. roxburghii* wine. Therefore, screening and isolating excellent indigenous yeast strains of *R. roxburghii* with perfect brewing characteristics, especially non-*Saccharomyces* yeasts, will promote the healthy development of *R. roxburghii* fruit wine.

In our preliminary research, we used high-throughput sequencing technology to identify the diversity and population changes of non-*Saccharomyces* yeasts during the spontaneous fermentation process of *R. roxburghii* fruit (Liu X. Z. et al., 2020). Additionally, we isolated 80 cultivable non-*Saccharomyces* yeasts from the spontaneous fermentation broth of *R. roxburghii* fruit using culture-dependent approach (Liu X. Z. et al., 2020). In this study, ethanol-tolerant strains were screened from our previously isolated culturable non-*Saccharomyces* yeasts, and then species of these ethanol-tolerant yeasts were identified based on morphology and molecular approaches. In addition, we also analyzed brewing characteristics of these ethanol-tolerant yeasts. Moreover, aroma and quality characteristics of *R. roxburghii* fruit wines were further evaluated by co-inoculation of these non-*Saccharomyces* yeasts together with *S. cerevisiae* as fermentation starter. The results obtained from the present study were helpful to explore potential high-quality brewing strains for the production of characteristic *R. roxburghii* fruit wine.

Materials and methods

Yeast strains

The reference strain used in this study was the commercial *S. cerevisiae* X16 obtained from Laffort Company (France). A total of 80 strains of non-*Saccharomyces* yeasts, isolated from spontaneous fermentation of *R. roxburghii* were screened for ethanol-tolerant strains. All yeasts cells were cultured on yeast extract peptone dextrose (YEPD) solid medium (1% yeast extract, 2% peptone, 2% glucose, and 2% agar) containing 100 mg/L of Chloramphenicol at 28°C for 72 h and then stored at 4°C for later use.

Screening and of identification of ethanol-tolerant non-*Saccharomyces* yeast strains

Ethanol-tolerant strains were screened by culturing them in YEPD broth (1% yeast extract, 2% peptone, and 2% glucose) containing 12% (v/v) ethanol with the initial concentration of 10^8 cfu/ml, and the yeast cells were cultured at 28°C with shaking at 180 rpm for 36 h. The optical density (OD) values were measured at a wavelength of 600 nm using a spectrophotometer (Hitachi, Tokyo, Japan).

Yeast strains were identified using both morphological and molecular methods. Firstly, cells were scraped onto Wallerstein Laboratory nutrient agar and cultured for 72 h. The characteristics of the colony and cellular morphology were examined and photographed with a microscope (Olympus, Tokyo, Japan). Next, genomic DNA was extracted from three ethanol-tolerant strains (C6, F112, and F15) using a DNA extraction kit (B518257; Sangon Biotech, China) following the manufacturer's instructions. The D1/D2 domain within the 26S rDNA was amplified using the polymerase chain reaction (PCR). The yeast species were then determined by comparing the 26S rDNA D1/D2 domain sequences in the GenBank database.

Growth curve detection and sugar metabolism analysis of ethanol-tolerant non-*Saccharomyces* yeast strains

The C6, F112, and F15 strains were inoculated into YEPD broth at a concentration of 10^8 cfu/ml and cultured under agitation at 180 rpm and 28°C for 48 h. The OD of the cultures was measured at the wavelength of 600 nm every 4 h, and a growth curve was plotted based on the time and $OD_{600\ nm}$ values.

Strains C6, F112, and F15 were inoculated with a concentration of 10^8 cfu/ml into a 0.6% yeast powder solution containing 2% final concentration of glucose, sucrose, maltose, lactose, and galactose,

respectively. The yeast powder solution was placed in test tubes containing Durham tubes and incubated at 28°C for 48 h. The formation of gas bubbles in the Durham tubes was observed. A positive reaction was recorded as "+ " if bubbles formed. Otherwise, a negative reaction was recorded as "−."

Analysis of winemaking tolerances of ethanol-tolerant non-*Saccharomyces* yeast strains

Strains of C6, F112, and F15 were inoculated in YEPD broth at a concentration of 10^8 cfu/ml with (1) glucose concentrations of 100, 150, 200, 250, or 300 g/L; (2) citric acid mass fractions of 1, 1.5, 2, 2.5, or 3% (w%); and (3) a sulfur dioxide contents of 50, 100, 150, 200, or 300 mg/L. All groups were cultured at 28°C and 180 rpm for 36 h with three replicates, and then $OD_{600\ nm}$ values were measured.

Production capacity of hydrogen sulfide and β-glucosidase activity in ethanol-tolerant non-*Saccharomyces* yeast strains

The hydrogen sulfide (H_2S) production activities of C6, F112, and F15 were investigated using BiGGY agar by comparing the depth of colony color (Caridi et al., 2022).

The ability of the strains to produce β-glucosidase was analyzed using the p-nitrophenyl-β-D-glucopyranoside (p-NPG) method. Strains C6, F112, and F15 were inoculated into YEPD medium and shaken at 180 rpm at 28°C for 72 h. The supernatant was obtained after centrifugation at 3,000 *g* for 10 min and used for the determination of enzyme activity. Enzyme activity units (U) were defined as the amount of enzyme required to produce 1 μmol of p-nitrophenol (p-NP) by hydrolyzing 1 μmol of p-NPG under conditions of pH 5.0 and 50°C for 1 min.

Laboratory-scale fermentation of *R. roxburghii* fruit wine

Fresh, mature, and non-rotten *R. roxburghii* (**Supplementary Figure 1**) was juiced with juice extractor (Midea, WJE2802D, China) and then treated with 100 mg/L of potassium metabisulfite and 20 mg/L of pectinase at room temperature for 12 h. The juice was then adjusted to 24°Brix with crystalline sucrose and divided into four groups, with each group replicated in triplicate in 2 L sterile triangular flasks. For the C6 + *S.* cerevisiae X16 group, F112 + *S. cerevisiae* X16 group, and F15 + *S. cerevisiae* X16 group, each group was inoculated with 10^8 cfu/ml of the C6, F112, or F15 strain and 10^7 cfu/ml of *S. cerevisiae* X16, with a control group that was only inoculated with 10^7 cfu/ml of *S. cerevisiae* X16. The flasks were left to ferment statically at 26°C until fermentation was completed. After fermentation, the *R. roxburghii* fruit wine from each group was centrifuged at 4,000 rpm for 10 min, and the supernatant was used for the determination of the quality indicators of *R. roxburghii* fruit wine.

Analysis of flavor and quality characteristics of *R. roxburghii* fruit wine

The alcohol content, total sugar, total acidity, and volatile acid content of the *R. roxburghii* wine were determined following the methods described by Liu et al. (2021b). The sensory characteristics of the *R. roxburghii* fruit wine were analyzed using an electronic tongue system. For this, 80 ml of each group of *R. roxburghii* fruit wine was taken and added to a dedicated beaker for the electronic tongue system. The electronic tongue system was used according to the instructions in the user manual to test each group of *R. roxburghii* fruit wine. The sampling time was 120 s, the sampling speed was 1/s, each sample was measured in triplicate, and each replicate was collected four times.

The headspace solid-phase microextraction-gas chromatography-mass spectrometry system (TQ8040, Agilent, USA) was used to analyze the aroma characteristics of the *R. roxburghii* fruit wine. The aroma components of *R. roxburghii* fruit wine were extracted at 40°C for 30 min, with cyclohexanone used as the internal standard for determining the aroma components of *R. roxburghii* fruit wine. The odor activity value (OAV) of each aroma component was calculated by referring to the threshold values of each volatile aroma component.

Statistical analysis

Data results were presented as mean ± SD. Principal component analysis (PCA) and one-way ANOVA were performed using SPSS 21.0 to test for significant differences among the groups. A *p*-value of less than 0.05 was considered statistically significant. Each experiment was repeated in triplicate.

Results

Screening of ethanol-tolerant non-*Saccharomyces* yeast strains

When the native non-*Saccharomyces* yeasts isolated from *R. roxburghii* were treated with 12% (v/v) ethanol, most of them died. However, three yeast strains (designated as C6, F112, and F15) exhibited satisfactory growth with $OD_{600\,nm}$ values of 0.56 ± 0.02, 0.47 ± 0.01, and 0.48 ± 0.01, respectively. Therefore, C6, F112, and F15 were selected as ethanol-tolerant strains for further analysis.

Identification of ethanol-tolerant non-*Saccharomyces* yeast strains

The identification of the three ethanol-tolerant yeast strains was initially based on morphological characteristics on WL agar. As shown in **Figure 1**, the colony color of C6, F112, and F15 was white, and their colony topography was convex and opaque.

To confirm the identity of the ethanol-tolerant yeast strains, their 26S rDNA D1/D2 domain sequences were compared. The analysis revealed that the 26S rDNA sequences of C6, F112, and

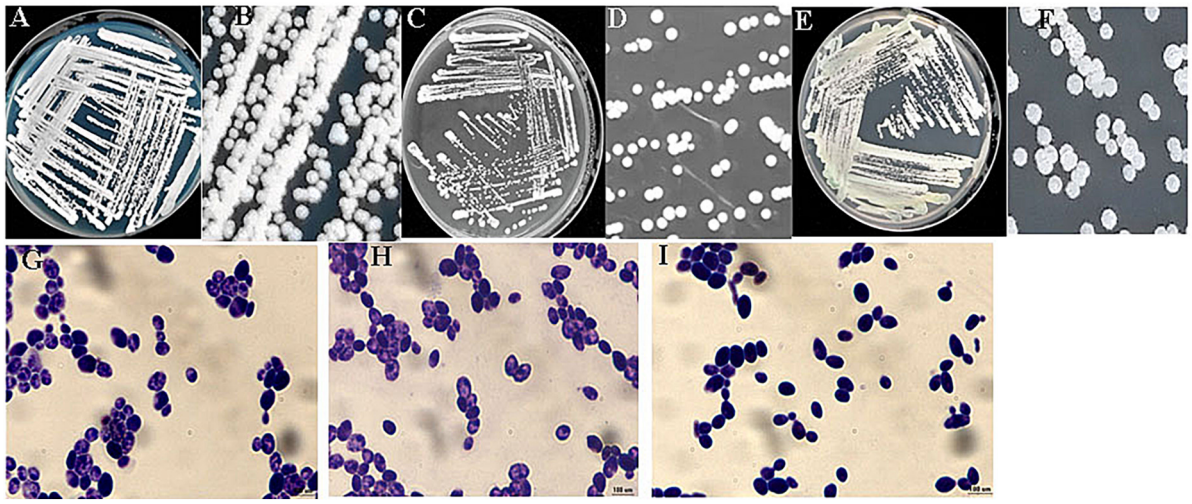

FIGURE 1
Colony and cell morphologies of ethanol-tolerant non-*Saccharomyces* yeasts isolated from *R. Roxburghii*. **(A,B)** Colony morphology of C6 on WL medium; **(C,D)** colony morphology of F112 on WL medium; **(E,F)** colony morphology of F15 on WL medium; **(G)** cell morphology of C6 following crystal violet staining (100×); **(H)** cell morphology of F112 following crystal violet staining (100×); and **(I)** cell morphology of F15 following crystal violet staining (100×).

F15 had the highest similarity to *C. tropicalis*, *Pichia guilliermondii*, and *W. anomalus*, respectively. Therefore, these three strains of ethanol-tolerant yeasts (C6, F112, and F15) were identified and named *C. tropicalis* C6, *P. guilliermondii* F112, and *W. anomalus* F15 based on the results of morphological characteristics and sequence alignment.

Growth characteristics of ethanol-tolerant non-*Saccharomyces* yeast strains

The growth curves of the strains are shown in Figure 2, with a lag phase from 0 to 4 h, a logarithmic growth phase from 4 to 20 h, and a stationary phase after 20 h. During the logarithmic growth phase, the $OD_{600\ nm}$ values of *C. tropicalis* C6, *P. guilliermondii* F112, and *W. anomalus* F15 were all lower than those of the commercial *S. cerevisiae* X16. During the stationary phase, the $OD_{600\ nm}$ of *P. guilliermondii* F112 was lower than that of *S. cerevisiae* X16. Throughout the entire growth period, the growth of *P. guilliermondii* F112 was lower than that of *S. cerevisiae* X16, while the growth of *C. tropicalis* C6 and *W. anomalus* F15 was basically consistent with that of *S. cerevisiae* X16 in the later stages of the stationary phase.

Winemaking condition tolerances of ethanol-tolerant non-*Saccharomyces* yeast strains

To assess the tolerance of the selected yeasts to winemaking conditions, their $OD_{600\ nm}$ values were measured after exposure to different concentrations of glucose, SO_2, and citric acid. Results demonstrated that all three ethanol-tolerant yeast strains exhibited

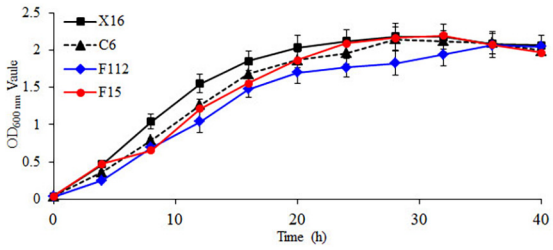

FIGURE 2
Growth curve of ethanol-tolerant non-*Saccharomyces* yeasts isolated from *R. roxburghii*.

excellent sugar tolerance, as they were able to grow in all glucose concentrations tested (100–300 mg/L) (Figure 3A). Furthermore, *C. tropicalis* C6, *P. guilliermondii* F112, and *W. anomalus* F15 displayed similar sulfur dioxide and acid tolerance to *S. cerevisiae* X16 within the tested ranges of sulfur dioxide (50–300 mg/L) and citric acid (2.5–4.0%) concentrations, respectively (Figures 3B, C). Therefore, *C. tropicalis* C6, *P. guilliermondii* F112, and *W. anomalus* F15 showed perfect tolerance to the winemaking environment.

Sugar metabolic performance of ethanol-tolerant non-*Saccharomyces* yeast strains

As shown in Table 1, different strains have different utilization characteristics for different sugars. *W. anomalus* F15 can only metabolize glucose with the least number of sugars that it can utilize. On the other hand, *C. tropicalis* C6 can metabolize all types of sugars except for galactose, with the broadest range of

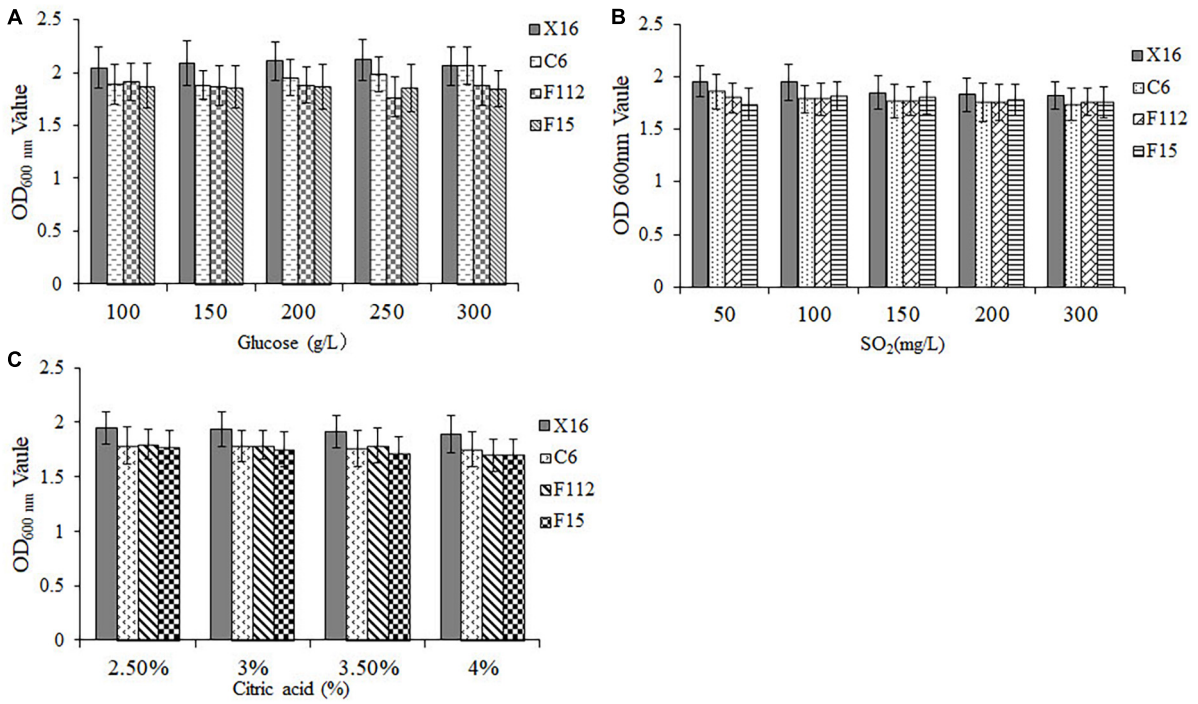

FIGURE 3
Winemaking condition tolerances of ethanol-tolerant non-*Saccharomyces* yeasts isolated from *R. roxburghii*. **(A)** Glucose tolerance; **(B)** SO_2 tolerance; and **(C)** citric acid tolerance.

TABLE 1 Sugar utilization characteristics of ethanol-tolerant non-*Saccharomyces* yeasts isolated from *R. Roxburghii*.

Strains	Glucose	Sucrose	Maltose	Lactose	Galactose
S. cerevisiae X16	+	+	+	+	+
C. tropicalis C6	+	+	+	+	–
P. guilliermondii F112	+	+	+	–	–
W. anomalus F15	+	–	–	–	–

sugar utilization. *P. guilliermondii* F112 can utilize three types of sugars (glucose, sucrose, and maltose). Therefore, *C. tropicalis* C6 has the widest range of sugar metabolism, and its sugar utilization characteristics are similar to those of *S. cerevisiae* X16, except for galactose.

Sulphureted hydrogen and β-glucosidase production abilities of ethanol-tolerant non-*Saccharomyces* yeasts strains

The ability of ethanol-tolerant yeasts to produce H_2S production ability was evaluated by observing the color depth on BiGGY agar (Caridi et al., 2022). As shown in **Figure 4**, *C. tropicalis* C6 had a similar H_2S production ability to the control (*S. cerevisiae* X16), while *P. guilliermondii* F112 and *W. anomalus* F15 exhibited stronger H_2S production abilities than the control, as evidenced by the colony depth color on the filter paper.

Flavor compounds in fruit are often present in the form of glycoconjugate, making them flavorless (Gueguen et al., 1996). β-Glucosidase are enzymes that could hydrolyze these glycosyl bonds, thereby releasing the flavor compounds to wines (Haslbeck et al., 2017). To investigate the β-glucosidases of the selected strains, namely, *C. tropicalis* C6, *P. guilliermondii* F112, and *W. anomalus* F15, p-NPG colorimetry was used. The result showed that the β-glucosidase production abilities of *C. tropicalis* C6 and *P. guilliermondii* F112 were similar to those of *S. cerevisiae* X16. However, the strain of *W. anomalus* F15 exhibited significantly lower β-glucosidase production ability than *S. cerevisiae* X16 (**Table 2**).

Winemaking properties of the ethanol-tolerant non-*Saccharomyces* yeasts in laboratory-scale

The combination of *non-saccharomyces* yeasts with *S. cerevisiae* as fermentation starters has been widely studied and accepted in wine production (Comitini et al., 2011). To further analyze the fermentative properties of the ethanol-tolerant yeast strains, *R. roxburghii* wine was fermented by co-inoculating the *C. tropicalis* C6, *P. guilliermondii* F112, or *W. anomalus* F15 together with *S. cerevisiae* X16. Dynamic changes of the non-*Saccharomyces* yeasts population during *R. roxburghii* wine fermentation were monitored by colony counting method, and the results showed that the proportion of *C. tropicalis* C6, *P. guilliermondii* F112, and *W. anomalus* F15 gradually decreased, in contrast, the proportion of *S. cerevisiae* X16 gradually increased and dominate

10.3389/fmicb.2023.1202440

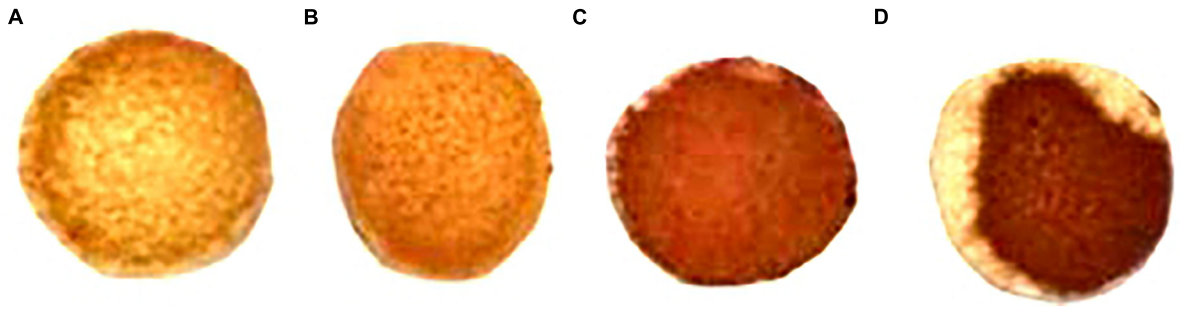

FIGURE 4
Hydrogen sulfide production ability of C6, F112, and F15 strains on BiGGY agar. **(A)** *S. cerevisiae* X16; **(B)** strain of *C. tropicalis* C6; **(C)** strain of *P. guilliermondii* F112; and **(D)** strain of *W. anomalus* F15.

TABLE 2 β-Glucosidase production capacity of ethanol-tolerant non-*Saccharomyces* yeasts isolated from *R. Roxburghii*.

Strains	β-Glucosidase activities (U/L)
S. cerevisiae X16	25.6 ± 2.13a
C. tropicalis C6	23.5 ± 1.56a
P. guilliermondii F112	21.5 ± 1.87a
W. anomalus F15	6.3 ± 0.46b

Different lowercase letters indicate a significant difference ($P < 0.05$).

at the middle and later periods of fermentation (Supplementary Figure 2).

The physicochemical parameters of the fermented *R. roxburghii* wines are listed in Table 3. Ethanol degrees of wines fermented by *P. guilliermondii* F112 or *W. anomalus* F15 were lower than the wine produced by *S. cerevisiae* X16 alone, while the *C. tropicalis* C6 fermented wine was similar to that produced by *S. cerevisiae* X16. The pH and volatile acidity parameters of the four groups of *R. roxburghii* wines were similar, with no differences found among them. The total acidity were lower in the *C. tropicalis* C6 and *P. guilliermondii* F112 groups compared to the *S. cerevisiae* X16 group.

In addition, an electronic tongue system was used to perform sensory analysis and differentiate the sensory characteristics of the *R. roxburghii* wines fermented with different yeast strains. However, no significant differences in the sensory characteristics including in sourness, bitterness, astringency, aftertaste-A, aftertaste-B, umami, richness, and saltiness were found among the three types of *R. roxburghii* wines (Figure 5).

The volatile aroma profiles of the *R. roxburghii* wines fermented with the selected yeast strains were further examined by using GC-MS analysis. A total of 66 volatile compounds, including 32 volatile esters, 10 volatile alcohols, 6 volatile acids, 3 volatile aldoketones, and 15 other volatile chemicals, were identified in the four groups of fermented *R. roxburghii* wines (Table 4). The *R. roxburghii* wines co-fermented with the three ethanol-tolerant yeast strains contained 50, 46, and 55 volatile compounds, respectively, whereas only 44 volatile compounds were detected in the *R. roxburghii* wine inoculated with *S. cerevisiae* X16 alone. Additionally, 22 chemicals, including 10 esters, 1 alcohol, 1 acid, and 10 other compounds, were specifically detected in the *R. roxburghii* wines inoculated with the ethanol-tolerant yeasts. On the other hand, octyl acetate, decanoic acid, 1-nonanal, and 2,4-di-tert-butylphenol were specifically discovered in the *S. cerevisiae* X16 group. Overall, the co-inoculation of these ethanol-tolerant yeast strains isolated from *R. roxburghii* along with *S. cerevisiae* increased the types of volatile compounds in the wine (Supplementary Figure 3).

When checking the volatile compound contents of *R. roxburghii* wines with the different ethanol-tolerant yeast strains, variations in the levels of volatile esters, alcohols, acids, aldoketones, and other chemicals were observed (Table 4). Co-inoculation with the three ethanol-tolerant yeasts resulted in an increase in volatile esters and alcohols, as well as a decrease in volatile aldoketones and other compounds (Table 4). In addition, *R. roxburghii* wines co-fermented with *W. anomalus* F15 and *S. cerevisiae* X16 exhibited higher levels of volatile acids compared to those produced with *S. cerevisiae* X16 alone.

The OAV was used to further evaluate the contribution of the main aromatic compounds to the aromatic characteristics of *R. roxburghii* wine. Compounds with OAV greater than 1 were considered to have a significant impact on the aroma, while those with OAV less than 1 were considered less important. Table 5 shows the calculated OAVs of twenty aromatic compounds in *R. roxburghii* wine. Thirteen compounds had OAVs greater than 1, while only 1 had an OAV less than 1 across all 4 groups of *R. roxburghii* wine. Specifically, ethyl 9-decenoate had an OAV greater than 1 only in the *S. cerevisiae* X16 group, whereas isobutanol had the only OAV less than 1 in the same group. The OAVs of ethyl caprate, isoamyl acetate, ethyl hexanoate, and ethyl octanoate were high in all four groups, suggesting that these compounds strongly contribute to the aroma of *R. roxburghii* wine.

Principal component analysis was used to further assess the impact of the main aromatic compounds on the characteristics of *R. roxburghii* wine. As depicted in Figure 6, the three principal components, PC1, PC2, and PC3, accounted for 62.84, 25.02, and 12.14% of the total variance, respectively, explaining 100.00% of the total variance. Most of the compounds were clustered in the positive axis of PC1 and PC2, and significant differences in distribution were observed among the four groups of fermented *R. roxburghii* wine. Ethyl palmitate might be closely related to the mixed fermentation of *C. tropicalis* C6 and *S. cerevisiae* X16, while *W. anomalus* F15 and *S. cerevisiae* X16 produced wines were characterized by compounds located in the positive PC1 and PC2,

TABLE 3 Oenological parameters of *R. roxburghii* wine fermented with ethanol-tolerant non-*Saccharomyces* yeasts in combination with *S. cerevisiae*.

Strains	Ethanol (% v/v)	pH	Total acidity (g/L)	Volatile acidity (g/L)
S. cerevisiae X16	13.79 ± 0.17a	3.71 ± 0.05a	14.06 ± 0.27a	0.26 ± 0.01a
C. tropicalis C6 + *S. cerevisiae* X16	13.34 ± 0.11a	3.77 ± 0.03a	13.34 ± 0.32b	0.22 ± 0.00a
P. guilliermondii F112 + *S. cerevisiae* X16	11.51 ± 0.26b	3.76 ± 0.03a	10.92 ± 0.32c	0.22 ± 0.00a
W. anomalus F15 + *S. cerevisiae* X16	9.28 ± 0.68c	3.76 ± 0.05a	14.37 ± 0.11a	0.28 ± 0.01a

Different lowercase letters indicate a significant difference ($P < 0.05$).

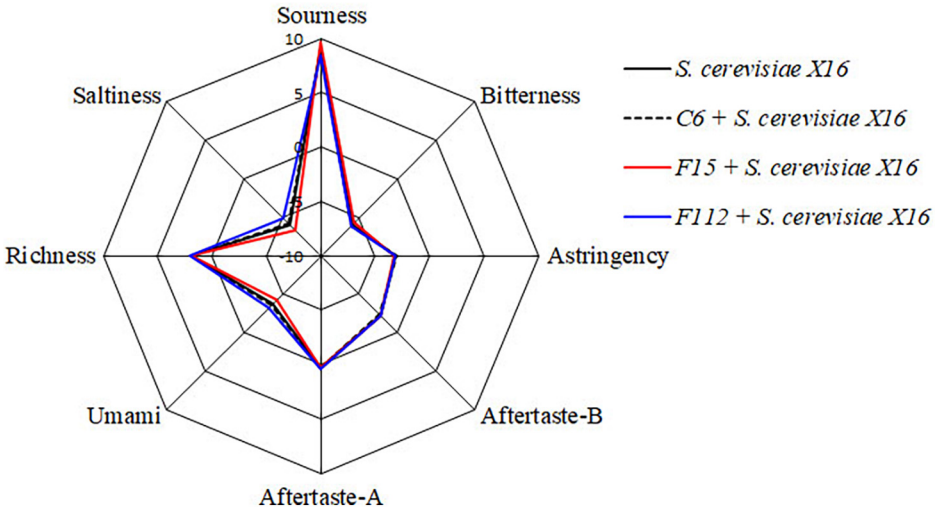

FIGURE 5
Radar chart of taste attribute of *R. Roxburghii* wine fermented with ethanol-tolerant non-*Saccharomyces* yeasts in combination with *S. cerevisiae*.

such as fruity and rosy chemicals (e.g., isobutyl acetate and ethyl 9-decenoate), which may contribute to the aroma of *S. cerevisiae* X16 fermented wine. However, it was challenging to identify the main volatile characteristics of *P. guilliermondii* F112 and *S. cerevisiae* X16 fermented *R. roxburghii* wines. Moreover, the mixed fermented wine using *W. anomalus* F15 and *S. cerevisiae* X16 was closely clustered to many esters, alcohols and acids, such as ethyl laurate, phenethyl alcohol, and octanoic acid, which may endow the wine more complex aroma characteristics.

Discussion

In order to evaluate yeast strains for winemaking, ethanol tolerance is an essential property (Novo et al., 2014). Researchers have made numerous efforts to isolate ethanol-tolerant yeasts from various sources, including fruits and fermentation conditions, for industrial purposes (Osho, 2005; Tikka et al., 2013). In a recent study, ethanol-tolerant yeast flora was isolated, identified, and screened from the Indian cashew apple, and seven strains of ethanol-tolerant yeasts were identified as *Candida* spp. (Desai et al., 2012). Besides, mutational breeding techniques were also applied to produce ethanol-tolerant yeasts. For example, the *Pichia terricola* H5 strain, which initially displayed 8% ethanol tolerance, was subjected to ultraviolet irradiation and diethyl sulfate mutagenesis to increase its ethanol tolerance (Gao et al., 2022). As a result, two mutant strains (UV5 and UV8) that demonstrated high tolerance to ethanol were obtained, and modified aroma profiles were evident in the fermentation samples exposed to these strains. In the present study, ethanol-tolerant non-*Saccharomyces* yeasts were screened for the first time from *R. roxburghii*. Three strains of yeasts displaying high ethanol tolerance were successfully obtained and subsequently identified as *C. tropicalis*, *P. guilliermondii*, and *W. anomalus* (**Figure 1**).

While *S. cerevisiae* is the most commonly isolated ethanol-tolerant yeast and widely used for wine making (Alexandre et al., 2004), non-*Saccharomyces* yeasts have been considered sensitive to ethanol and are typically dominant in the early stage of spontaneous wine fermentation (Liu et al., 2021c). However, some non-*Saccharomyces* species were proved to be tolerant to ethanol. For example, three strains of *Candida* spp. yeast isolated from Indian cashew apple were able to tolerate up to 10% (v/v) ethanol (Desai et al., 2012). Besides, a strain of *Candida stellata* was found to produce ethanol levels up to 13.48% (v/v) during the fermentation of Macabeo grape must, indicating a high tolerance to ethanol (Clemente-Jimenez et al., 2004). In this study, we obtained a strain of *C. tropicalis* that exhibited robust growth in YEPD broth containing 12% (v/v) of ethanol (**Figure 1**). These results indicated that *Candida* species may be a better source for screening ethanol-tolerant yeast.

Among non-*Saccharomyces* yeasts, *W. anomalus* has gained increasing attention in recent years due to its unique physiological characteristics and metabolic features (Liu et al., 2021d). These yeast species have been reported to tolerate various extreme

TABLE 4 Volatile compounds (mg/L) in *R. roxburghii* wines fermented with ethanol-tolerant non-*Saccharomyces* yeasts combined with *S. cerevisiae*.

Number	Volatile compound	*S. cerevisiae* X16	*C. tropicalis* C6 + *S. cerevisiae* X16	*P. guilliermondii* F112 + *S. cerevisiae* X16	*W. anomalus* F15 + *S. cerevisiae* X16
1	Ethyl acetate	60.80 ± 2.14a	61.87 ± 2.05a	57.57 ± 2.35a	61.70 ± 1.89a
2	Ethyl butyrate	5.77 ± 0.32a	4.46 ± 0.31b	4.07 ± 0.25b	4.43 ± 0.34b
3	Ethyl hexanoate	92.34 ± 4.65b	113.22 ± 5.87a	92.66 ± 5.19b	106.08 ± 6.11a
4	Ethyl 3-hexenoate	13.38 ± 0.57a	13.66 ± 0.48a	11.98 ± 0.52b	13.19 ± 0.44a
5	Ethyl octanoate	351.52 ± 26.51c	772.47 ± 48.79a	590.43 ± 37.49b	702.99 ± 49.68a
6	Ethyl pelargonate	8.71 ± 0.64a	3.63 ± 0.28b	3.37 ± 0.32b	3.44 ± 0.29b
7	Ethyl caprate	341.86 ± 30.51c	676.25 ± 46.18a	521.90 ± 40.62b	604.28 ± 49.53a
8	Ethyl 9-decenoate	51.71 ± 3.68a	6.53 ± 0.55b	4.97 ± 0.30c	5.78 ± 0.39b
9	Ethyl laurate	68.89 ± 3.54b	99.12 ± 6.98a	92.09 ± 7.04a	103.17 ± 8.79a
10	Ethyl isobutyrate	11.12 ± 0.43a	1.44 ± 0.09c	/	1.78 ± 0.07b
11	Ethyl 2-methyl butyrate	7.35 ± 0.38a	0.59 ± 0.02b	0.57 ± 0.01b	0.57 ± 0.02b
12	Ethyl tetradecanoate	/	10.45 ± 0.97b	15.64 ± 0.64a	14.16 ± 1.12a
13	Ethyl cinnamate	/	4.63 ± 0.31a	4.56 ± 0.29a	/
14	Ethyl palmitate	/	8.05 ± 0.35	/	/
15	Ethyl isovalerate	/	/	/	0.52 ± 0.06
16	Ethyl phenylacetate	/	/	1.97 ± 0.16a	2.14 ± 0.20a
17	Ethyl pentadecanoate	/	1.73 ± 0.21b	2.81 ± 0.27a	/
18	Ethyl benzoate	/	/	1.91 ± 0.13	/
19	Hexyl acetate	23.24 ± 0.87b	32.55 ± 1.15a	24.04 ± 1.09b	30.78 ± 1.64a
20	(E)-3-hexene-1-ol acetate	4.81 ± 0.18c	11.73 ± 0.87b	17.84 ± 1.64a	1.50 ± 0.09d
21	Isobutyl acetate	35.32 ± 2.64a	4.53 ± 0.25b	4.53 ± 0.31b	4.81 ± 0.19b
22	Isoamyl acetate	210.13 ± 13.15b	352.63 ± 17.22a	305.03 ± 16.18a	356.55 ± 20.87a
23	Isoamyl caprylate	12.74 ± 0.95b	16.69 ± 1.26a	14.04 ± 1.07a	16.29 ± 1.32a
24	Isoamyl decanoate	3.58 ± 0.16b	12.79 ± 0.59a	11.50 ± 0.62a	13.35 ± 0.79a
25	Isobutyl caprylate	15.68 ± 1.26a	4.48 ± 0.31b	/	4.57 ± 0.38b
26	Isobornyl acetate	/	/	1.88 ± 0.21	/
27	Methyl octanoate	5.33 ± 0.29a	2.28 ± 0.17b	1.78 ± 0.13c	
28	Methyl caprate	34.87 ± 2.89a	4.96 ± 0.27b	3.68 ± 0.29c	
29	Octyl acetate	5.76 ± 0.35	/	/	/
30	Phenethyl acetate	36.76 ± 2.18b	68.46 ± 4.61a	69.55 ± 3.98a	74.13 ± 5.14a
31	3-Acetoxy butane-2-yl acetate	/	2.58 ± 0.26a	1.50 ± 0.18b	2.50 ± 0.13a
32	Vinyl formate	/	/	0.56 ± 0.06	/
	Σ Esters	1,401.67 ± 98.29b	2,291.78 ± 139.85a	1,862.43 ± 121.34a	2,134.44 ± 149.76a
33	2,3-Butanediol	4.89 ± 0.35b	7.40 ± 0.62a	4.90 ± 0.29b	6.18 ± 0.61a
34	3-Hexene-1-ol	17.17 ± 1.63c	56.07 ± 4.36a	60.00 ± 4.62a	48.05 ± 3.75b
35	Hexanol	8.65 ± 0.62b	14.64 ± 0.98a	16.51 ± 0.89a	15.61 ± 1.26a
36	Isobutanol	26.01 ± 1.89c	47.03 ± 3.25b	62.79 ± 4.62a	53.56 ± 3.69a
37	Isoamylol	459.51 ± 29.45b	759.99 ± 52.92a	847.94 ± 65.68a	800.96 ± 59.78a
38	3-Methylthiopropanol	/	2.44 ± 0.20a	2.48 ± 0.29a	2.53 ± 0.18a
39	Methanol	3.29 ± 0.26a	3.57 ± 0.32a	1.91 ± 0.15b	2.07 ± 0.19b
40	Octanol	3.18 ± 0.26a	3.63 ± 0.38a	2.96 ± 0.26a	3.52 ± 0.32a
41	Phenethyl alcohol	146.31 ± 7.96b	245.58 ± 16.65a	259.68 ± 14.89a	276.89 ± 16.92a

(Continued)

10.3389/fmicb.2023.1202440

TABLE 4 (Continued)

Number	Volatile compound	*S. cerevisiae* X16	*C. tropicalis* C6 + *S. cerevisiae* X16	*P. guilliermondii* F112 + *S. cerevisiae* X16	*W. anomalus* F15 + *S. cerevisiae* X16
42	Propanol	2.31 ± 0.20b	2.76 ± 0.23a	3.03 ± 0.28a	2.74 ± 0.18a
	Σ Alcohols	671.32 ± 42.62b	1,143.11 ± 79.91a	1,262.2 ± 91.97a	1,212.11 ± 86.88a
43	Acetic acid	11.47 ± 0.89c	17.76 ± 0.97b	17.05 ± 1.11b	21.12 ± 1.96a
44	n-Decanoic acid	5.98 ± 0.45	/	/	/
45	Isobutyric acid	5.82 ± 0.57a	2.74 ± 0.31c	/	3.63 ± 0.29b
46	Isovaleric acid	/	/	/	8.99 ± 0.62
47	3-Methylvaleric acid	3.08 ± 0.21b	5.74 ± 0.42a	6.00 ± 0.32a	6.56 ± 0.46a
48	Octanoic acid	14.34 ± 1.14b	19.74 ± 1.56a	19.08 ± 1.62a	20.22 ± 1.45a
	Σ Acids	40.69 ± 3.26 b	45.98 ± 3.26b	42.13 ± 3.05 b	60.52 ± 4.78 a
49	Acetaldehyde	10.84 ± 1.87a	0.44 ± 0.05b	/	0.55 ± 0.07b
50	4-Methoxy-2,5-dimethyl-3(2H)-furanone	35.39 ± 2.65a	4.77 ± 0.32b	5.31 ± 0.38b	5.32 ± 0.29b
51	1-Nonanal	4.14 ± 0.23	/	/	/
52	Σ Aldoketones	50.37 ± 4.75a	5.21 ± 0.37b	5.31 ± 0.38b	5.87 ± 0.36b
53	Benzothiazole	/	2.43 ± 0.16	/	/
54	Borane-methyl sulfide complex	/	0.60 ± 0.58a	0.68 ± 0.39a	0.74 ± 0.42a
55	1,3,5,7-Cyclooctatetraene	0.89 ± 0.19b	5.49 ± 0.36a	/	/
56	Dodecane	3.84 ± 0.36a	3.21 ± 0.29a	/	2.94 ± 0.25b
57	2,4-Di-tert-butylphenol	42.10 ± 3.27	/	/	/
58	Dipentene	36.75 ± 2.35a	5.75 ± 0.34b	4.77 ± 0.16c	5.62 ± 0.64b
59	Dimethyl sulfide	/	/	/	0.52 ± 0.02
60	n-Heptadecane	/	/	/	1.50 ± 0.10
61	2-Methyl-1,5-dioxaspiro[5.5]undecane	/	3.58 ± 0.21a	1.74 ± 0.12b	1.40 ± 0.11c
62	Naphthaline	9.89 ± 0.95b	24.95 ± 1.56a	23.35 ± 1.98a	23.99 ± 1.85a
63	α-p-Dimethylstyrene	/	/	/	4.03 ± 0.23
64	n-Pentadecane	/	/	/	2.12 ± 0.12
65	p-Cymene	/	/	/	0.55 ± 0.03
66	Styrene	/	4.64 ± 0.35a	/	4.16 ± 0.29a
63	Tetradecane	/	/	2.14 ± 0.17b	3.02 ± 0.23a
	Σ Other compounds	93.07 ± 7.12a	50.65 ± 3.85b	32.68 ± 2.82c	50.59 ± 4.29b

The symbol "/" represents a compound that is not detected. Different lowercase letters indicate a significant difference ($P < 0.05$).

environmental conditions such as high/low pH, high osmotic pressure, and anaerobic conditions (Schneider et al., 2012). In our previous study, a fruity aroma-producing strain of *W. anomalus* C11 was isolated from *R. roxburghii*, which was capable of withstanding 9% (v/v) ethanol treatment (Liu et al., 2021b). In the present study, we isolated another strain of *W. anomalus* F15 from *R. roxburghii*, which displayed a higher ethanol tolerance of up to 12% (v/v) than *W. anomalus* C11. Moreover, *W. anomalus* F15 was also found to be tolerant to glucose, sulfur dioxide, and citric acid, suggesting that this strain of *W. anomalus* may have a better potential for application in winemaking (**Figure 3**).

Aroma characteristic is an important parameter in assessing wine quality (Styger et al., 2011). Combining non-*Saccharomyces* starters with *S. cerevisiae* during winemaking to enhance the richness and complexity of wine has been widely accepted by researchers and wine producers (Contreras et al., 2015). In this study, *R. roxburghii* wines were fermented by co-inoculating ethanol-tolerant non-*Saccharomyces* yeasts with *S. cerevisiae*. The results showed that the levels of volatile esters and alcohol compounds significantly increased in the three mixed-fermentation wines compared to those fermented with *S. cerevisiae* alone. On the other hand, the levels of aldoketones and other compounds significantly decreased in mixed-fermentation wines (**Table 4** and **Supplementary Figure 2**). Therefore, co-inoculating ethanol-tolerant non-*Saccharomyces* yeasts with *S. cerevisiae* can regulate the aromatic characteristics of *R. roxburghii* wine, contributing to the enrichment of different types of *R. roxburghii* wine.

10.3389/fmicb.2023.1202440

TABLE 5 The OAVs for the main compounds in *R. roxburghii* wine fermented with different yeasts.

Number	Volatile compound	Odor descriptor	Odor threshold (mg/L)	OAV			
				S. cerevisiae X16	*C. tropicalis* C6 + *S. cerevisiae* X16	*P. guilliermondii* F112 + *S. cerevisiae* X16	*W. anomalus* F15 + *S. cerevisiae* X16
A1	Ethyl acetate	Pineapple, fruity, solvent, balsamic	0.75	81.07	82.49	76.77	82.27
A2	Ethyl butyrate	Fruity	0.02	288.5	223	203.5	221.5
A3	Ethyl hexanoate		0.05	1,846.8	2,264.4	1,853.2	2,121.6
A4	Ethyl octanoate	Sweet, fruity	0.58	606.07	1,331.84	1,017.98	1,212.05
A5	Ethyl caprate	Sweet, fruity	0.20	1,709.3	3,381.25	2,609.5	3,021.25
A6	Ethyl 9-decenoate	Roses	14.10	3.67	0.46	0.35	0.41
A7	Ethyl laurate	Fruity, fatty	0.64	107.64	154.88	143.89	161.20
A8	Ethyl cinnamate	Fruity	0.01	/	463	456	/
A9	Ethyl palmitate		1.5	/	5.37	/	/
A10	Isobutyl acetate	Sweet, fruity, apple, banana	1.6	22.08	2.83	2.83	3.01
A11	Isoamyl acetate	Banana, fruity, sweet	0.16	1,313.31	2,203.93	1,906.44	2,228.44
A12	Phenethyl acetate	Floral	1.8	20.42	38.03	38.63	41.18
B1	2,3-Butanediol	Fruity	150	0.03	0.05	0.03	0.04
B2	Hexanol	Flower, green, cut grass	8	1.08	1.83	2.06	1.95
B3	Isobutanol		40	0.65	1.18	1.57	1.34
B4	Isoamylol	Burnt, alcohol	30	15.32	25.33	28.26	26.70
B5	Phenethyl alcohol	Floral, roses	10	14.63	24.56	25.97	27.69
C1	n-Decanoic acid	Fatty and rancid	6	1.00	/	/	/
C2	Isobutyric acid	Acid, fatty	0.23	25.30	11.91	/	15.78
C3	Octanoic acid	Fatty and rancid	10	1.43	1.97	1.91	2.02

The symbol "/" represents a compound that is not detected.

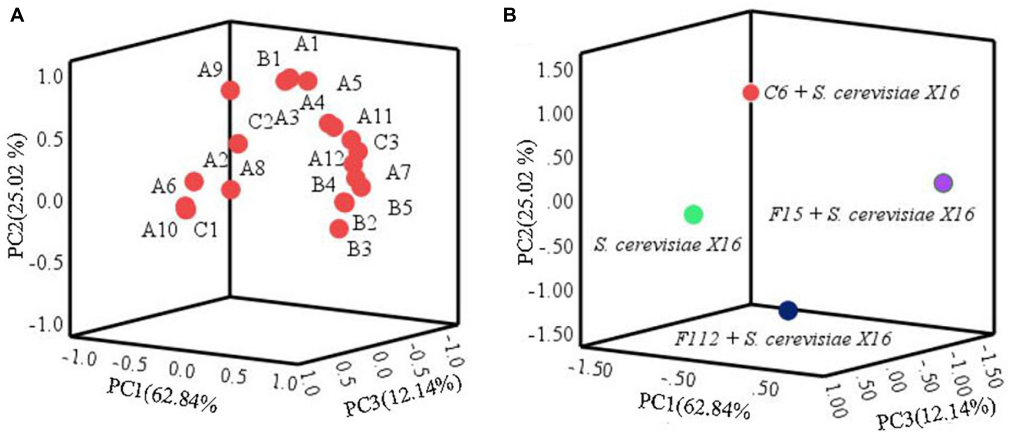

FIGURE 6
Principal component analysis of *R. roxburghii* wine fermentation with ethanol-tolerant non-*Saccharomyces* yeasts in combination with *S. cerevisiae*. **(A)** Principal component load plot of volatile aroma compounds; and **(B)** principal component score of volatile aroma compounds. A1, ethyl acetate; A2, ethyl butyrate; A3, ethyl hexanoate; A4, ethyl octanoate; A5, ethyl caprate; A6, ethyl 9-decenoate; A7, ethyl laurate; A8, ethyl cinnamate; A9, ethyl palmitate; A10, isobutyl acetate; A11, isoamyl acetate; A12, phenethyl acetate; B1, 2,3-butanediol; B2, hexanol; B3, isobutanol; B4, isoamylol; B5, phenethyl alcohol; C1, n-decanoic acid; C2, isobutyric acid; C3, octanoic acid.

Ester compounds are a type of metabolite generated during alcohol metabolism (Sumby et al., 2021). Most ester compounds exhibit floral and fruity aromatic characteristics and are important contributors to the aroma profiles of various fermented wines (Rojas et al., 2001). Our study found that using native non-*Saccharomyces* yeasts of *R. roxburghii* in combination with commercial *S. cerevisiae* can increase the diversity and concentration of volatile esters compounds (**Table 4** and **Supplementary Figure 2**). For example, the levels of ethyl octanoate, ethyl caprate, and ethyl laurate in non-*Saccharomyces* yeasts-fermented wines were higher than those in *R. roxburghii* wine fermented with *S. cerevisiae* alone (**Table 4**). Additionally, seven types of ethyl eater chemicals, including ethyl tetradecanoate, ethyl cinnamate, and ethyl palmitate, were specifically detected in the three types of *R. roxburghii* wines produced with the native non-*Saccharomyces* yeasts of *R. roxburghii* (**Table 4**).

Conclusion

This study represents the first report on the screening and oenological property analysis of ethanol-tolerant non-*Saccharomyces* yeasts isolated from *R. roxburghii*. We obtained three strains of ethanol-tolerant yeasts designated as C6, F112, and F15, which were identified as *C. tropicalis*, *P. guilliermondii*, and *W. anomalus*, respectively, after treating them with 12% (v/v) of ethanol. These strains showed similar winemaking condition tolerances to *S. cerevisiae* X16, but their growth, sugar metabolic performance, and activities of sulphureted hydrogen production were different. The β-glucosidase production ability of strain *W. anomalus* F15 was lower than that of *S. cerevisiae* X16, and strains of *C. tropicalis* C6 and *P. guilliermondii* F112 were similar to *S. cerevisiae* X16. Mixed inoculation of these ethanol-tolerant yeast strains with *S. cerevisiae* regulated the volatile aroma characteristics of the fermented *R. roxburghii* wine, enriching and enhancing its aroma flavor. Therefore, the selected ethanol-tolerant yeasts exhibit potential applications in the production of unique *R. roxburghii* wine.

Data availability statement

The original contributions presented in this study are included in the article/**Supplementary material**, further inquiries can be directed to the corresponding authors.

Author contributions

YL and XL wrote the original draft manuscript. PD, XT, WZ, and MK conducted the experiments. XL and MH conceived and designed the experiments. All authors contributed to the article and approved the submitted version.

Funding

This study was supported by the Guizhou Provincial Science and Technology Foundation [ZK (2023)137], Key Laboratory of Microbial Resources Collection and Preservation, Ministry of Agriculture and Rural Affairs (KLMRCP2021-02), National Natural Science Foundation of China (32260641), and Guizhou Fruit Wine Brewing Engineering Research Center [Qianjiaoji (2022)050].

Conflict of interest

The authors declare that the research was conducted in the absence of any commercial or financial relationships that could be construed as a potential conflict of interest.

Publisher's note

All claims expressed in this article are solely those of the authors and do not necessarily represent those of their affiliated organizations, or those of the publisher, the editors and the reviewers. Any product that may be evaluated in this article, or claim that may be made by its manufacturer, is not guaranteed or endorsed by the publisher.

Supplementary material

The Supplementary Material for this article can be found online at: https://www.frontiersin.org/articles/10.3389/fmicb.2023.1202440/full#supplementary-material

References

Alexandre, H., Costello, P. J., Remize, F., Guzzo, J., and Guilloux-Benatier, M. (2004). *Saccharomyces cerevisiae–Oenococcus oeni* interactions in wine: Current knowledge and perspectives. *Int. J. Food Microbiol.* 93, 141–154. doi: 10.1016/j.ijfoodmicro.2003.10.013

Caridi, A., Sidari, R., Pulvirenti, A., Blaiotta, G., and Ritieni, A. (2022). Clonal selection of wine yeasts with differential adsorption activities towards phenolics and ochratoxin A. *Food Biotechnol.* 36, 22–37. doi: 10.1080/08905436.2021.2006064

Clemente-Jimenez, J. M., Mingorance-Cazorla, L., Martı̀nez-Rodrı̀guez, S., Francisco Heras-Vázquez, J. L., and Rodrı̀guez-Vico, F. (2004). Molecular characterization and oenological properties of wine yeasts isolated during spontaneous fermentation of six varieties of grape must. *Food Microbiol.* 21, 149–155. doi: 10.1016/S0740-0020(03)00063-7

Comitini, F., Gobbi, M., Domizio, P., Romani, C., Lencioni, L., Mannazzu, I., et al. (2011). Selected non-*Saccharomyces* wine yeasts in controlled multistarter fermentations with *Saccharomyces cerevisiae*. *Food Microbiol.* 28, 873–882. doi: 10.1016/j.fm.2010.12.001

Contreras, A., Hidalgo, C., Henschke, P. A., Chambers, P. J., Curtin, C., and Varela, C. (2014). Evaluation of non-*Saccharomyces* yeasts for the reduction of alcohol content in wine. *Appl. Environ. Microbiol.* 80, 1670–1678. doi: 10.1128/AEM.03780-13

Contreras, A., Hidalgo, C., Schmidt, S., Henschke, P. A., Curtin, C., and Varela, C. (2015). The application of non-*Saccharomyces* yeast in fermentations with limited aeration as a strategy for the production of wine with reduced alcohol content. *Int. J. Food Microbiol.* 205, 7–15. doi: 10.1016/j.ijfoodmicro.2015.03.027

Desai, M. V., Dubey, K. V., Vakil, B. V., and Ranade, V. V. (2012). Isolation, identification and screening of the yeast flora from Indian cashew apple for sugar and ethanol tolerance. *Int. J. Biotechnol. Wellness Ind.* 1, 259–265.

Egue, L. A. N., Bouatenin, J. P. K. M., N'guessan, F. K., and Koussemon-Camara, M. (2018). Virulence factors and determination of antifungal susceptibilities of *Candida* species isolated from palm wine and sorghum beer. *Microb. Pathog.* 124, 5–10. doi: 10.1016/j.micpath.2018.08.007

Gao, J., He, X., Huang, W., You, Y., and Zhan, J. (2022). Enhancing ethanol tolerance via the mutational breeding of *Pichia terricola* H5 to improve the flavor profiles of wine. *Fermentation* 8:149. doi: 10.3390/fermentation8040149

Gueguen, Y., Chemardin, P., Janbon, G., Arnaud, A., and Galzy, P. (1996). A very efficient β-glucosidase catalyst for the hydrolysis of flavor precursors of wines and fruit juices. *J. Agric. Food Chem.* 44, 2336–2340. doi: 10.1021/jf950360j

Haslbeck, K., Jerebic, S., and Zarnkow, M. (2017). Characterization of the unfertilized and fertilized hop varieties progress and hallertauer tradition-Analysis of free and glycosidic-bound flavor compounds and β-glucosidase activity. *Brew. Sci.* 70, 148–158. doi: 10.23763/BRSC17-15HASLBECK

Jolly, N. P., Varela, C., and Pretorius, I. S. (2014). Not your ordinary yeast: Non-*Saccharomyces* yeasts in wine production uncovered. *FEMS Yeast Res.* 14, 215–237. doi: 10.1111/1567-1364.12111

Liu, X. Z., Li, Y. F., Yu, Z. H., Hardie, W. J., and Huang, M. Z. (2020). Biodiversity of non-*Saccharomyces* yeasts during natural fermentation of *Rosa roxburghii*. *Acta Microbiol. Sin.* 60, 1696–1708. doi: 10.13343/j.cnki.wsxb.20190523

Liu, X., Li, Y., Yu, Z., Liu, X., Hardie, W. J., and Huang, M. (2020). Screening and characterisation of β-glucosidase production strains from *Rosa roxburghii* Tratt. *Int. J. Food Eng.* 17, 1–9. doi: 10.1515/ijfe-2020-0152

Liu, X., Li, Y., Zhao, H., Yu, Z., and Huang, M. (2021a). Oenological property analysis of selected *Hanseniaspora uvarum* isolated from *Rosa roxburghii* Tratt. *Int. J. Food Eng.* 17, 445–454. doi: 10.1515/ijfe-2020-0331

Liu, X., Li, Y., Zhao, H., Yu, Z., Hardie, W. J., and Huang, M. (2021b). Identification and fermentative properties of an indigenous strain of *Wickerhamomyces anomalus* isolated from *Rosa roxburghii* Tratt. *Brit. Food J.* 123, 4069–4081. doi: 10.1108/BFJ-11-2020-0993

Liu, X., Li, Y., Zhang, Y., Zeng, S., and Huang, M. (2021c). Yeast diversity investigation of 'Beihong' (*V. vinifera*× *V. amurensis*) during spontaneous fermentation from Guiyang region, Guizhou, China. *Food Sci Technol. Res.* 27, 887–896. doi: 10.3136/fstr.27.887

Liu, X., Li, Y., Zhou, J., and Huang, M. (2021d). Effects of co-inoculation and sequential inoculation of *Wickerhamomyces anomalus* and *Saccharomyces cerevisiae* on the physicochemical properties and aromatic characteristics of longan (Dimocarpus longan Lour.) wine. *Qual. Assur. Saf. Crop.* 13, 56–66. doi: 10.15586/qas.v13i2.893

Morata, A., Escott, C., Bañuelos, M. A., Loira, I., Fresno, J. M., González, C., et al. (2019). Contribution of non-*Saccharomyces* yeasts to wine freshness. A review. *Biomolecules* 10:34. doi: 10.3390/biom10010034

Novo, M., Gonzalez, R., Bertran, E., Martínez, M., Yuste, M., and Morales, P. (2014). Improved fermentation kinetics by wine yeast strains evolved under ethanol stress. *LWT-Food Sci. Technol.* 58, 166–172. doi: 10.1016/j.lwt.2014.03.004

Osho, A. (2005). Ethanol and sugar tolerance of wine yeasts isolated from fermenting cashew apple juice. *Afr. J. Biotechnol.* 4, 660–662. doi: 10.5897/AJB2005.000-3119

Padilla, B., Gil, J. V., and Manzanares, P. (2018). Challenges of the non-conventional yeast *Wickerhamomyces anomalus* in winemaking. *Fermentation* 4:68. doi: 10.3390/fermentation4030068

Parapouli, M., Vasileiadis, A., Afendra, A. S., and Hatziloukas, E. (2020). *Saccharomyces cerevisiae* and its industrial applications. *AIMS Microbiol.* 6, 1–31. doi: 10.3934/microbiol.2020001

Pietrafesa, A., Capece, A., Pietrafesa, R., Bely, M., and Romano, P. (2020). *Saccharomyces cerevisiae* and *Hanseniaspora uvarum* mixed starter cultures: Influence of microbial/physical interactions on wine characteristics. *Yeast* 37, 609–621. doi: 10.1002/yea.3506

Rojas, V., Gil, J. V., Piñaga, F., and Manzanares, P. (2001). Studies on acetate ester production by non-*Saccharomyces* wine yeasts. *Int. J. Food Microbiol.* 70, 283–289. doi: 10.1016/S0168-1605(01)00552-9

Schneider, J., Rupp, O., Trost, E., Jaenicke, S., Passoth, V., Goesmann, A., et al. (2012). Genome sequence of *Wickerhamomyces anomalus* DSM 6766 reveals genetic basis of biotechnologically important antimicrobial activities. *FEMS Yeast Res.* 12, 382–386. doi: 10.1111/j.1567-1364.2012.00791.x

Styger, G., Prior, B., and Bauer, F. F. (2011). Wine flavor and aroma. *J. Ind. Microbiolo. Biotechnol.* 38, 1145–59. doi: 10.1007/s10295-011-1018-4

Sumby, K. M., Grbin, P. R., and Jiranek, V. (2021). Microbial modulation of aromatic esters in wine: Current knowledge and future prospects. *Food Chem.* 121, 1–16. doi: 10.1016/j.foodchem.2009.12.004

Tikka, C., Osuru, H. P., Atluri, N., Raghavulu, P. C. V., Yellapu, N. K., Mannur, I. S., et al. (2013). Isolation and characterization of ethanol tolerant yeast strains. *Bioinformation* 9, 421–425. doi: 10.6026/97320630009421

Wang, L., Lv, M., An, J., Fan, X., Dong, M., Zhang, S., et al. (2021). Botanical characteristics, phytochemistry and related biological activities of *Rosa roxburghii* Tratt fruit, and its potential use in functional foods: A review. *Food Funct.* 12, 1432–1451. doi: 10.1039/D0FO02603D

Wei, J., Zhang, Y., Yuan, Y., Dai, L., and Yue, T. (2019). Characteristic fruit wine production via reciprocal selection of juice and non-*Saccharomyces* species. *Food Microbiol.* 79, 66–74. doi: 10.1016/j.fm.2018.11.008

frontiers | Frontiers in Microbiology

TYPE Original Research
PUBLISHED 12 July 2023
DOI 10.3389/fmicb.2023.1229251

OPEN ACCESS

EDITED BY
Carlo Giuseppe Rizzello,
Sapienza University of Rome, Italy

REVIEWED BY
Liaoyuan Zhang,
Fujian Agriculture and Forestry University, China
Yuefang Gao,
Northwest A&F University, China
Xinghui Li,
Nanjing Agricultural University, China

*CORRESPONDENCE
Yao Zou
✉ zouyao82@163.com
Wei Xu
✉ xuweianti@sicau.edu.cn

†These authors have contributed equally to this work and share first authorship

RECEIVED 26 May 2023
ACCEPTED 26 June 2023
PUBLISHED 12 July 2023

CITATION
Zou Y, Liu M, Lai Y, Liu X, Li X, Li Y, Tang Q and Xu W (2023) The glycoside hydrolase gene family profile and microbial function of *Debaryomyces hansenii* Y4 during South-road dark tea fermentation.
Front. Microbiol. 14:1229251.
doi: 10.3389/fmicb.2023.1229251

The glycoside hydrolase gene family profile and microbial function of *Debaryomyces hansenii* Y4 during South-road dark tea fermentation

Yao Zou[1,2*†], Minqiang Liu[1,2†], Yuqing Lai[1,2], Xuyi Liu[1,2], Xian Li[1,2], Yimiao Li[1,2], Qian Tang[1,2] and Wei Xu[1,2*]

[1]Department of Tea Science, College of Horticulture, Sichuan Agricultural University, Chengdu, China, [2]Tea Refining and Innovation Key Laboratory of Sichuan Province, Chengdu, China

Microbes are crucial to the quality formation of Sichuan South-road Dark Tea (SSDT) during pile-fermentation, but their mechanism of action has not yet been elucidated. Here, the glycoside hydrolase (GH) gene family and microbial function of *Debaryomyces hansenii* Y4 during solid-state fermentation were analyzed, and the results showed that many *GH* genes being distributed in comparatively abundant GH17, GH18, GH76, GH31, GH47, and GH2 were discovered in *D. hansenii*. They encoded beta-galactosidase, alpha-D-galactoside galactohydrolase, alpha-xylosidase, mannosidase, etc., and most of the GHs were located in the exocellular space and participated in the degradation of polysaccharides and oligosaccharides. *D. hansenii* Y4 could develop the mellow mouthfeel and "reddish brown" factors of SSDT via increasing the levels of water extracts, soluble sugars and amino acids but decreasing the tea polyphenols and caffeine levels, combined with altering the levels of thearubiins and brown index. It may facilitate the isomerization between epicatechin gallate and catechin gallate. Moreover, the expression levels of *DEHA2G24860g* (Beta-galactosidase gene) and *DEHA2G08602g* (Mannan endo-1,6-alpha-mannosidase DFG5 gene) were sharply up-regulated in fermentative anaphase, and they were significantly and negatively correlated with epicatechin content, especially, the expression of *DEHA2G08602g* was significantly and negatively correlated with catechin gallate level. It was hypothesized that *D. hansenii* Y4 is likely to be an important functional microbe targeting carbohydrate destruction and catechin transformation during SSDT pile-fermentation, with *DEHA2G08602g* as a key thermotolerant functional gene.

KEYWORDS

***Debaryomyces hansenii* Y4, Sichuan South-road dark tea, glycoside hydrolase gene family, fermentation, quality**

Introduction

South-road Dark Tea (SSDT) is a well-known health beverage in China, it is produced in Ya' an City, Sichuan Province (Figure 1), and characterized by the sensory qualities of brick shape, reddish-brown appearance, mellow mouthfeel, and aged and pure aroma (Zou et al., 2022). Pile-fermentation, a spontaneous fermentation stimulated by environmental

FIGURE 1
Sichuan South-road Dark Tea. The yellow area reflects Sichuan province and the pentagram means Ya'an city, the origin of SSDT.

microorganisms in workshop, is the key procedure responsible for SSDT quality formation, during which microbial metabolism, extracellular enzyme activities and natural oxidation, etc. accelerate the transformation of complex compounds, produce various secondary metabolites, ultimately contribute to the unique flavor of dark tea (Zhang et al., 2016). Recently, some of the functional microorganisms involved in the distinctive flavor formation of dark tea have been identified, for example, *Aspergillus*, *Debaryomyces*, and *Lichtheimia* were confirmed to be the primary beneficial agents of Pu-erh tea during fermentation (Li et al., 2018; Ma et al., 2021), while *Aspergillus* and *Debaryomyces* also play an important role in the volatile metabolism of Fuzhuan tea during production (Li M. Y. et al., 2020). Furthermore, *Aspergillus niger* M10 could significantly influence the transformation of key quality components in SSDT during fermentation via the expression of *GH* genes (Zou et al., 2022, 2023). It seems that the functional microbes are very important in the production of dark tea.

The raw materials for processing SSDT are the mature leaves and branches of tea plant, which are rich in cellulose, hemicellulose and other polysaccharides. Usually, cellulose and hemicellulose are cross-linked by lignin and pectin, etc. to form plant cell walls (Burton et al., 2010). During pile-fermentation, tea leaf cell wall would be destroyed by the superposed effects of hygrothermal fermentation environment and microbial action, which promotes the conversion of chemical components and finally benefits dark tea quality (Wang et al., 2011). Published literature suggests that various carbohydrate-active enzymes (CAZymes) are involved in the degradation of leaf cell walls (Zou et al., 2023), of which GHs are the major modules responsible for hydrolyzing glycosidic linkages between carbohydrates or a carbohydrate-aglycone moiety (Tingley et al., 2021), thus playing a pivotal role in the degradation of complex carbohydrates. Generally, GHs contain different families, and members of the same family share more than 30% sequence similarity in primary structures (Henrissat, 1991), therefore present the similar functions, for instance, members of GH48 and GH6 mainly participate in destruction of cellulose, while members belonging to GH10, GH11, GH39, and GH43, etc. are primarily responsible for decomposing hemicellulose (Singh et al., 2019), some members of GH3 and GH1 could improve tea flavor by cleaving glycoside aroma precursors (Zhou et al., 2017; Xiang et al., 2020). Additionally, the researchers discovered that the expression of some *GH* genes, such as *NI_1_1714074* and *ANI_1_2704024*, may be significantly related to the degradation of polysaccharides (Zou et al., 2023). Overall, it is speculated that GHs probably play a critical role in dark tea quality formation during pile-fermentation.

Debaryomyces is a functional genus for dark tea production (Li et al., 2018), but the details of its species information and action mechanism during pile-fermentation are still obscure. We have ever isolated *Debaryomyces hansenii* Y4 (*D. hansenii* Y4) from stacked

SSDT during pile-fermentation. Given the role of *D. hansenii* in the chemical transformation during black tea fermentation (Pasha and Reddy, 2005), the object of this work is to explore the function of *D. hansenii* Y4 during SSDT fermentation via analyzing microbial *GH* gene and detecting chemical components and color parameters of SSDT. The results may provide a theoretical basis for further research on the potential functions of *GH* genes, and elucidate the mechanism of organoleptic quality development of SSDT during pile-fermentation to some extent.

Materials and methods

GH gene family analysis

The genome sequence data of *D. hansenii CBS 767* and the sequence data of GH family modules were separately downloaded from the NCBI[1] and Pfam[2] databases. Utilizing BLASTP program to identify the amino acid sequences of GHs in *D. hansenii* based on the HMMER3.0 profile of the GHs domain (Supplementary Table S1). Amino acid length, molecular weights and theoretical isoelectric point (pI) of each protein were predicted with ExPASy[3] Subcellular localization was predicated using WOLF PSORT (https://wolfpsort.hgc.jp/; Gasteiger et al., 2003). Using MEGA v.7.0 combined with neighbor joining (N-J) method to construct the phylogenetic tree, and whose reliability was tested with a bootstrap value of 1,000 (Kumar et al., 2008). Moreover, MapChart (Version 2.1) was employed to present the chromosomal distribution of *GH* genes (Li Q. et al., 2020), and their structure was generated by MapInspect.[4] Simultaneously, protein sequence motif analysis was performed with MEME (Bailey et al., 2009), the conserved motif size was set as 6–50 amino acids and the maximum number of structural domains outputted was 15, motif structure was displayed using TBtools software (Chen et al., 2020).

Solid-state fermentation

Debaryomyces hansenii Y4 (NCBI ID: OQ975970; Supplementary Figure S1) isolated from SSDT was activated and suspended in distilled water to a final concentration of 10^6cfu/ml. Subsequently, Maozhuang teas (the raw materials of SSDT) were lightly crushed and their water content was adjusted to 30%, then placed in triangular flasks with air-vent capping (35 g per flask) and sterilized by autoclave. Part of the sterilized samples were inoculated with *D. hansenii* Y4 suspension (1 ml/flask), while the rest were inoculated with equivalent volumes of sterile distilled water as control (CK). After thorough mixing, all samples were fermented for 20 days at 55°C in a constant temperature and humidity incubator (GZ-120-HSH, Guangzhi, China).

Experiments were performed in triplicate and samples were collected every 2 days. Part of the samples were used to analyze the chemical components and color parameters, while the rest were stored in a −80°C refrigerator for quantitative real-time PCR (qRT-PCR) analysis.

1 https://ftp.ncbi.nlm.nih.gov/genomes/
2 http://pfam.xfam.org/
3 https://web.expasy.org/protparam
4 https://software.informer.com/search/MapInspect

Chemical analysis and color parameters detection

According to the method described by China National Standard GB/T8305-2013, GB/T8313-2008 and GB/T8314-2013, water extract content (WE), tea polyphenols (TPs) and amino acid (AA) in tea samples were quantified, respectively. Furthermore, the levels of catechin monomers and caffeine (Caf) were determined following GB/T 8313–2018 with some modifications by Tan et al. (2021), while water-soluble sugar (SS) were detected by the method of Zou (2014). The contents of theaflavin (TF), thearubigin (TR) and theabrownin (TB) were, respectively, measured using spectrophotometric methods (Huang, 1997). Additionally, the CIELab parameters of dried tea and tea liquor were separately investigated as described by Zou et al. (2020), and the derivative parameters of tea pigments and CIELab parameters were calculated according to the formulas listed in Supplementary Table S2.

RNA extraction, cDNA synthesis, and qRT-PCR analysis

Debaryomyces hansenii Y4 in different fermentation samples were, respectively, collected by centrifugation and differential centrifugation, and then ground using liquid nitrogen. The M5 plant RNeasy Complex Mini Kit (Mei5bio, Beijing, China) was used to extract their RNA, and after checking the concentration and integrity of RNA, the M5 super plus qPCR RT Kit (Mei5bio, Beijing, China) was utilized to synthesize the cDNA, followed by qRT-PCR using the CFX96™ Real-time PCR System (Bio-Rad, California, USA). All experiments were conducted in triplicate, and the 26S rRNA was used as a reference gene to normalize gene expression. The relative expression level of *GH* gene was calculated with the $2^{-\Delta\Delta CT}$ method (Pfaffl, 2001). The primers used in this work were designed using Primer Premier 5.0 software and their details are presented in Supplementary Table S3.

Statistical analysis

Pearson correlation analysis between *GH* gene expression level and chemical component content was performed using SPSS 22.0 (SPSS, Inc., Chicago, IL), and one-way ANOVA with LSD multiple comparison test was also conducted. Orthogonal partial least squares discriminant analysis (OPLS-DA) was carried out utilizing SIMCA 14.1 (Umetrics Corporation, Umeå, Sweden).

Results

Analysis of *GH* gene family in *Debaryomyces hansenii*

A total of 30 proteins with typical GH domains were identified in *D. hansenii*, they were distributed in 13 GH families, with members of GH17, GH18, GH76, GH31, GH47 and GH2 being more abundant (Figure 2A). The phylogenetic analysis indicated that these protein sequences were classified into 3 distinct groups, among that group I was the smallest group with 6 members and contained all the genes encoding the members of GH 47; group II

contained all the genes encoding the members of GH16; while group III formed the largest group with 16 members, and contained all the genes encoding the members of GH17, GH4, GH15 and GH31(Figure 2B). Obviously, the proteins belonging to the same GH family were clustered together, whereas, the conserved motifs of DEHA2G24860g (beta-galactosidase, GH2) and DEHA2F26840g (alpha-D-galactoside galactohydrolase, GH27) seem to be highly homologous since they were branched together. Moreover, all the genes detected contained exons, but only *DEHA2G18766g* (Glucan 1,3-beta-glucosidase gene) had an intron. In order to elucidate the composition and diversity of motifs in these protein sequences, MEME Suite was utilized to search for protein motifs, finally identifying 15 distinct motifs ranging from 20 to 50 amino acids in length. Noticeably, motifs 9 and 13 were mainly detected in group I, while motifs 1, 2, 4, 6, 7, 10 and 11 were primarily identified in group II, and motifs 3, 5, 8, 9, 12, 13, 14 and 15 were principally obtained in group III, nevertheless, motifs were absent in DEHA2E00528g, DEHA2D06930g, DEHA2F09020g, DEHA2F26840g, DEHA2G24860g, DEHA2D01430g, DEHA2E09504g, DEHA2A12254g, and DEHA2E21890g (Figure 2C; Supplementary Table S4). Furthermore, all genes were found unevenly distributed on 6 chromosomes, with more genes located on NC_006046.2 and NC_006049.2, while NC_006043.2 and NC_006045.2 had only two genes. Simultaneously, the clustering phenomenon was confirmed in NC_006049.2 as *DEHA2G18700g* and *DEHA2G18766g* were accumulated on the same region of this chromosome (Figure 2D).

Additionally, 18 genes encoding glycoside hydrolase were subjected to further analysis, and the GHs comprising of beta-galactosidase, alpha-D-galactoside galactohydrolase, alpha-xylosidase, mannosidase and so on were confirmed. These GHs presented amino acid lengths ranging from 306 to 1,022, molecular mass ranging from 33.75 to 119.03 kDa, and PI between 3.87 and 8.6, besides, most of the GHs were located in the extracellular space, except for DEHA2G24860g and DEHA2F16632g located in the cytoplasm, DEHA2E09504g, DEHA2G08866g and DEHA2E00528g located in the nucleus, and DEHA2G20746g located in the endoplasmic reticulum (Table 1).

Effect of *Debaryomyces hansenii* Y4 on taste-active ingredients of SSDT during fermentation

The taste-active components levels of SSDT were apparently altered by solid-state fermentation. During fermentation, all the samples were clearly clustered into 4 groups: raw materials (0d), the 2d samples, the fermentative prophase and metaphase samples, and the fermentative anaphase samples. After fermentation, the levels of ECG, WE, GC and C in *D. hansenii* Y4 sample were significantly enhanced by 35.92,11.44, 11.8 and 14.11% ($p<0.05$),

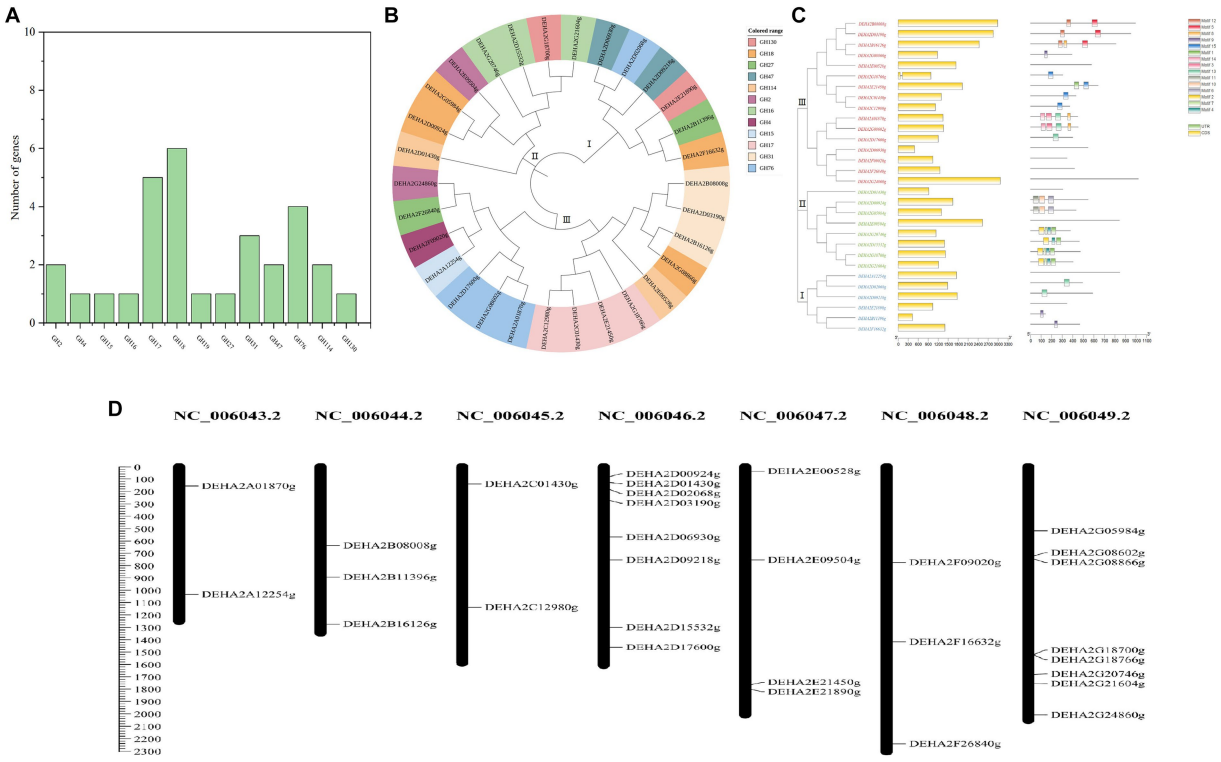

FIGURE 2
Analysis of *GH* gene family in *D. hansenii*. **(A)** GH family members in *D. hansenii*. **(B)** Phylogenetic analysis of GHs; the different colors indicate different GH families. **(C)** Exon-intron structure and conserved motifs analysis of *GH* genes in *D. hansenii*; boxes and lines, respectively, represent exons and introns in "exon-intron structure," different colored boxes represent different motifs. **(D)** Chromosomal distribution of *GH* genes; chromosome numbers are showed at the top of each bar, and the size of chromosomes are reflected by the scale bar on the left.

TABLE 1 Basic information of GH family members in *Debaryomyces hansenii*.

Gene names	Gene description	Accession number	GH family	Amino acids	Molecular weight/Da	Theoretical point	Unstable coefficient	Lipid solubility index	WoLF PSORT
DEHA2G24860g	Beta- galactosidase	XP_462623.1	GH2	1,022	119034.8	5.47	36.21	79.69	cyto
DEHA2E09504g	Mannosidase	XP_459719.1	GH2	843	97184.79	5.41	32.4	80.43	nucl
DEHA2A12254g	Glucoamylase	XP_002770029.1	GH15	545	62525.25	4.97	38.48	38.48	extr
DEHA2G21604g	Putative glycosidase of the cell wall	XP_462482.1	GH16	404	42289.55	4.32	46.69	59.21	extr
DEHA2G18700g	Putative glycosidase of the cell wall	XP_462353.1	GH16	472	49563.01	4.27	61.74	53.98	extr
DEHA2G20746g	Putative glycosidase of the cell wall	XP_462444.1	GH16	378	42673.56	4.94	32.97	76.08	E.R
DEHA2G18766g	Endo-beta-1 3-glucanase	XP_462355.1	GH17	306	33752.24	4.27	19.93	73.33	extr
DEHA2C12980g	Cell wall protein with similarity to glucanases	XP_458240.1	GH17	372	38980.85	5.06	25.55	71.29	extr
DEHA2G08866g	Chitinase	XP_461932.1	GH18	393	44573.55	6.56	37.68	73.92	nucl
DEHA2F16632g	Sporulation-specific chitinase	XP_461083.1	GH18	467	51454.29	8.67	26.3	66.64	cyto
DEHA2D00924g	Endochitinase	XP_458510.1	GH18	546	57380.75	3.87	31.7	78.77	extr
DEHA2F26840g	Alpha-D-galactoside galactohydrolase	XP_461506.1	GH27	417	46835.34	4.58	27.4	78.85	extr
DEHA2B16126g	Alpha-xylosidase	XP_457652.1	GH31	951	105819.6	4.64	40.86	77.5	extr
DEHA2D03190g	Glucoamylase	XP_458606.1	GH31	590	67544.58	5.36	30.35	73.52	extr
DEHA2D09218g	Mannosyl- oligosaccharide 1 2-alpha-mannosidase	XP_458865.1	GH47	590	67544.58	5.36	30.35	75.19	extr
DEHA2A01870g	Mannan endo-1,6-alpha-mannosidase DCW1	XP_456419.1	GH76	448	49977.85	4.48	25.48	76.65	extr
DEHA2G08602g	Mannan endo-1,6-alpha-mannosidase DFG5	XP_461921.1	GH76	452	50207.86	4.4	34.67	71.24	extr
DEHA2E00528g	Maltase	XP_459350.1	GH114	578	66747.65	4.85	37.4	74	nucl

nucl, nucleus; cyto, cytoplasm; extr, extracellular space; golg, golgi apparatus; E.R, endoplasmic reticulum.

10.3389/fmicb.2023.1229251

while SS and AA were increased by 8.73 and 2.93% (p>0.05), respectively, compared to CK. However, *D. hansenii* Y4 significantly decreased the contents of CG, EC, Caf and TPs in SSDT by 62.13, 25.29, 23.03 and 15.42%, respectively, as compared with that of CK ($p < 0.05$; Figure 3A). At the end of fermentation, although CK and *D. hansenii* Y4 samples were grouped together, but they were distinguishable from each other as shown in Figure 3B (OPLS-DA model: $R^2Y = 0.915$, $Q^2 = 0.929$; cross-validation with 500 permutation tests: intercepts of $R^2 = 0.579$, $Q^2 = -0.148$). Moreover, the differential chemical components between CK and *D. hansenii* Y4 samples after fermentation were observed with the criterion of VIP > 1 and $p < 0.05$, confirming that WE, Caf, TPs and SS were the differential taste-active chemical components between them (Figure 3B). The above results suggested that *D. hansenii* Y4 could significantly improve the mellow mouthfeel of SSDT by increasing the levels of thickness and sweetness-components but decreasing the contents of bitterness and astringency-compounds, and also altering the levels of catechins monomers.

Effect of *Debaryomyces hansenii* Y4 on color parameters of SSDT during fermentation

Tea pigments are the major parameters affecting SSDT color, in this work *D. hansenii* Y4 was discovered to significantly decrease the levels of TF, A1 (TF/(TF + TR + TB)), E5 (TF/TR) and

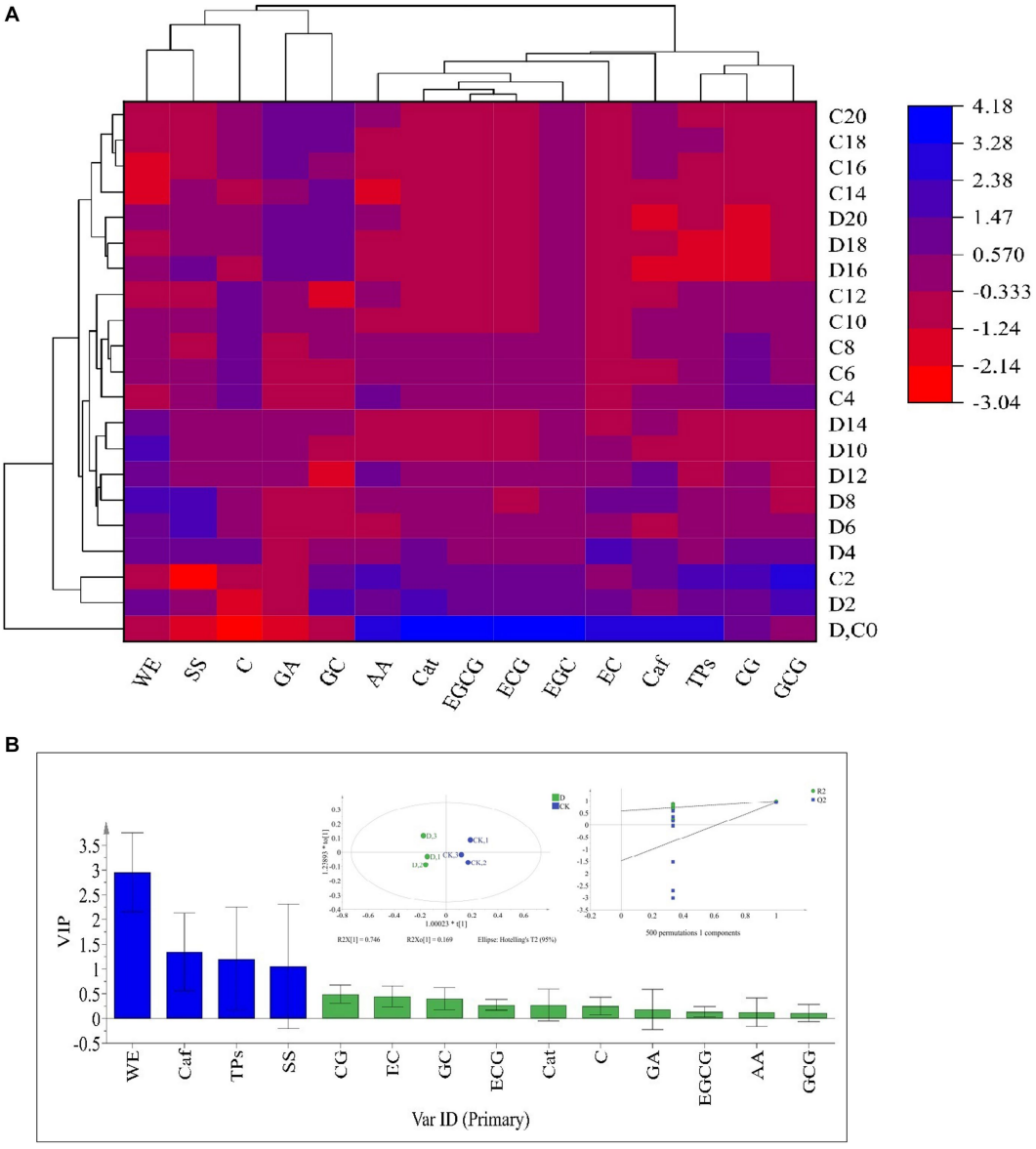

FIGURE 3
Analysis of the primary taste-active components of tea during solid-state fermentation. **(A)** heatmap of chemical ingredients; the row represents the samples at different fermentation times, C before the number represents the samples of CK, while D reflects the samples fermented by *D. hansenii* Y4, the column represents the taste-active components, the red and blue colors indicate their levels. **(B)** Orthogonal partial least square discriminant analysis (OPLS-DA) and determination of the differential chemical components.

10.3389/fmicb.2023.1229251

F6 (TF/TB) in SSDT by 35.62, 36.6, 37.44 and 36.27%, respectively ($p<0.05$), but obviously increase the levels of TR, B2 (TR/(TF + TR + TB)) and D4 (TR/TB) by 4.86, 3.08 and 4.17%, respectively ($p>0.05$), compared with CK after fermentation (Figure 4A). Moreover, *D. hansenii* Y4 apparently influenced the CIELab parameters of dried tea and tea liquor when it mediated SSDT fermentation, it dramatically increased the levels of BI, Sab, b, Cab, h, a and Hab of dried tea color by 156.37, 54.4, 50, 34.75, 27.78, 16.67 and 14.4%, respectively, while, decreased L level by 12.9%, compared to CK after fermentation (Figure 4B). At the same time, it also significantly enhanced the levels of h and Hab of tea liquor by 12.36 and 6.98% respectively, as compared with

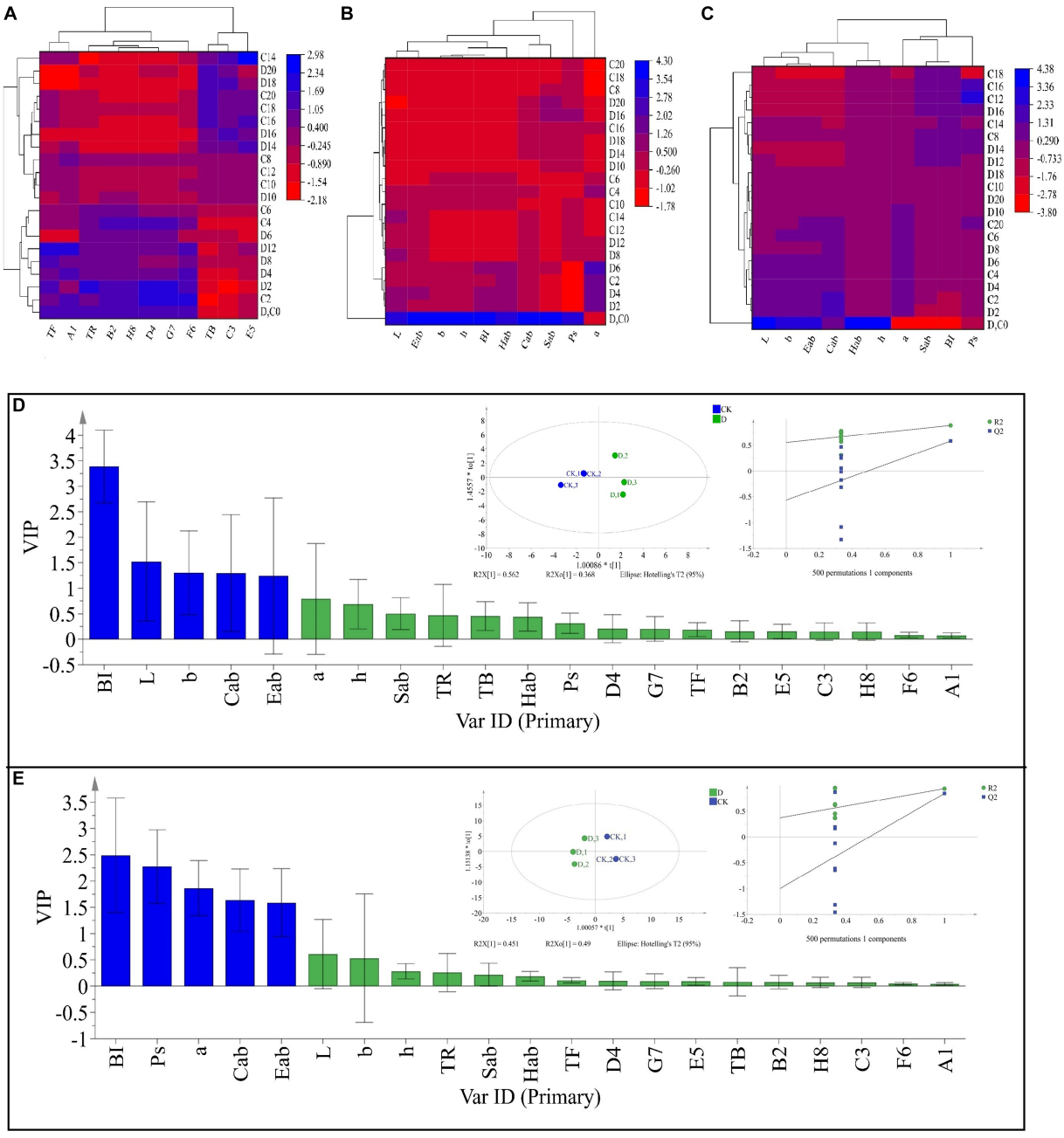

FIGURE 4
Analysis of the tea color parameters during solid-state fermentation. **(A)** heatmap of tea pigments and their derived parameters; the row represents the samples at different fermentation times, C before the number represents the samples of CK, while D reflects the samples fermented by *D. hansenii* Y4, the column represents the tea pigments and their derived parameters, A1 = TF/(TF + TR + TB), B2 = TR/(TF + TR + TB), C3 = TB/(TF + TR + TB), D4 = TR/TB, E5 = TF/TR, F6 = TF/TB, G7 = (TF + TR)/TB, H8 = (TF + TR)/(TF + TR + TB), the red and blue colors denote their levels. **(B)** Changes in CIELab parameters and their derived parameters of dried tea; the row and column represent the samples at different fermentation times and CIELab parameters, respectively. **(C)** Changes in CIELab parameters and their derived parameters of tea liquor; the row and column represent the samples at different fermentation times and CIELab parameters, respectively. **(D)** Orthogonal partial least square discriminant analysis (OPLS-DA) of color parameters of dried tea and determination of its differential color parameters. **(E)** Orthogonal partial least square discriminant analysis (OPLS-DA) of color parameters of tea liquor and determination of its differential color parameters.

CK at the end of fermentation, but obviously decreased the levels of Ps, a, Cab, Eab, and Sab of tea liquor by 58.58, 12.31, 6.27, 5.26, and 4.40%, separately (Figure 4C). It was worth noting that the CK and *D. hansenii* Y4 samples can be clearly distinguished from each other after fermentation based on their dried tea color parameters (OPLS-DA model: $R^2Y = 0.881$, $Q^2 = 0.577$; cross-validation with 500 permutation tests: intercepts of $R^2 = 0.555$, $Q^2 = -0.567$), and BI, L, b, Cab and Eab were the differential color parameters between them (Figure. 4D). Moreover, at the end of fermentation, the CK and *D. hansenii* Y4 samples could also be clearly separated from each other based on tea liquor color parameters (OPLS-DA model: $R^2Y = 0.942$, $Q^2 = 0.843$; cross-validation with 500 permutation tests: intercepts of $R^2 = 0.373$, $Q^2 = -1$), and BI, Ps, a, Cab and Eab were their differential color parameters (Figure 4E). Therefore, *D. hansenii* Y4 seriously influenced the color parameters of SSDT and exhibited a strong capacity to enhance tea "reddish brown" factors through increasing the levels of BI and TR but decreasing the levels of TF and its derived parameters.

Expression characteristics of *GH* gene in *Debaryomyces hansenii* Y4 during SSDT fermentation

Nine *GH* genes were selected for expression analysis. These genes encode GHs in the relatively abundant families and are presumably involved in cell wall degradation. It was found that the expression levels of *GH* genes showed a significant fluctuation with fermentation, of which most genes exhibited a significant up-regulation of expression. Notedly, *DEHA2G24860g* (beta-galactosidase gene) and *DEHA2G08602g* (mannan endo-1,6-alpha-mannosidase DFG5 gene) were dramatically up-regulated in the fermentative anaphase ($p < 0.05$), whose expression levels at 14d were 47.84 and 20.17-fold higher than that at 2d, respectively. Furthermore, at 18d, the expression level of *DEHA2G08602g* was 169.85-fold higher than that at 2d, while at the end of fermentation, the expression levels of *DEHA2G24860g* and *DEHA2G08602g* were 46.14 and 467.96-fold higher than that at 2d. In contrast, the expression level of *DEHA2G18766g* (glucan 1,3-beta-glucosidase gene) was significantly down-regulated during fermentation ($p < 0.05$), while the expression levels of *DEHA2A12254g* (glucoamylase gene) and *DEHA2D09218g* (mannosyl-oligosaccharide 1,2-alpha-mannosidase gene) presented a down-regulation trend during fermentative metaphase and anaphase (Figure 5A). Additionally, the correlation between the expression level of *GH* gene and the content of chemical component was analyzed. It was evident that the expression of most *GH* genes was significantly correlated with the content of catechin monomers. Among them, the expression level of *DEHA2G08602g* was significantly and positively related to GA and GC contents, but negatively correlated to EC, CG, Caf and TPs levels ($p < 0.05$), while *DEHA2D03190g* was significantly and positively related to GA level, but negatively correlated to CG level ($p < 0.05$). Moreover, *DEHA2G24860g* was significantly and negatively related to EC content, while *DEHA2D09218g* and *DEHA2A12254g* were significantly and negatively correlated to ECG and EGCG contents, and *DEHA2A12254g* was also significantly and negatively related to Caf and TPs ($p < 0.05$). It seems that *DEHA2G08602g* is a pivotal functional gene in *D. hansenii* Y4 affecting SSDT quality formation during fermentation.

Discussion

Debaryomyces is beneficial for the development of dark tea flavor during production (Li M. Y. et al., 2020). Usually, *D. hansenii* discovered in protein-rich fermented products exhibits the characteristics of being metabolically versatile, non-pathogenic and tolerant to low temperatures (Viana et al., 2011). However, *D. hansenii* Y4 used in this work was isolated from the high-temperature location of piled SSDT and subjected to high-temperature solid-state fermentation, implying that *D. hansenii* Y4 may be a thermophilic yeast.

Glycoside hydrolases are famous for their excellent capacity to catalyze the hydrolysis of glycosidic linkages (Davies and Henrissat, 1995; Drula et al., 2022). Some GHs identified in *D. hansenii* may strongly participate in the hydrolysis of polysaccharides and oligosaccharides, for example, α-D-galactoside galactohydrolase is mainly responsible for cleaving terminal α-1,6-linked D-galactosyl residues from oligosaccharides substrates, while β-galactosidase could efficiently hydrolyze disaccharide lactose to generate galactose and glucose, and also has the ability to facilitate the transgalactosylation reaction of lactose to allolactose, which is finally cleaved to monosaccharides. Furthermore, both beta-mannosidase and beta-galactosidase are oligosaccharide-degrading enzymes (Mhuantong et al., 2015). It was demonstrated that *D. hansenii* Y4 may mediate the metabolism of polysaccharides or oligosaccharide in tea leaves during fermentation via GHs, then part of the resultant monosaccharides would be used to sustain microbial growth, and the remainder may increase the SS level and finally benefit SSDT sweetness. Additionally, most of the GHs detected were located in the extracellular space, that means they can act directly on the tea leaves to stimulate chemical reactions. Regrettably, the *GH* genes detected in *D. hansenii* Y4 were not as abundant as those found in *Aspergillus* fungi (Ma et al., 2021; Zou et al., 2022, 2023).

In general, the transformation of the chemical component in SSDT during pile-fermentation always results from a synergistic effect of moist heat and microbial activity (Zou et al., 2022), whereas, after excluding the effect of hygrothermal action used the control treatment, apparently, *D. hansenii* Y4 seriously reduced the contents of TPs and Caf, and altered the levels of catechin monomers in tea. Previous literature suggested that GHs, tannase, glycosyltransferases and so on could catalyze the hydrolysis of phenolic glycosides and phenolic esters, oxidation or polymerization of phenolic compounds, and destruction of the aromatic rings in phenolic compounds, thus significantly reducing the TPs levels in tea during fermentation (Ma et al., 2021). Moreover, *D. hansenii* was reported to be a tannin-tolerant yeast with an excellent capacity of secreting tannase (Kanpiengjai et al., 2016), combined with the GHs detected in this work, it was speculated that *D. hansenii* Y4 may be an important functional microbe influencing the conversion of bitterness and astringency-active compounds during SSDT pile-fermentation.

Catechins are the major constituents of TPs, *D. hansenii* Y4 seems to strongly affect the conversion of catechin monomers in this work. It dramatically enhanced ECG level, but decreased CG level in tea after fermentation, implying that this yeast may efficiently facilitate the isomerization reaction between ECG and

10.3389/fmicb.2023.1229251

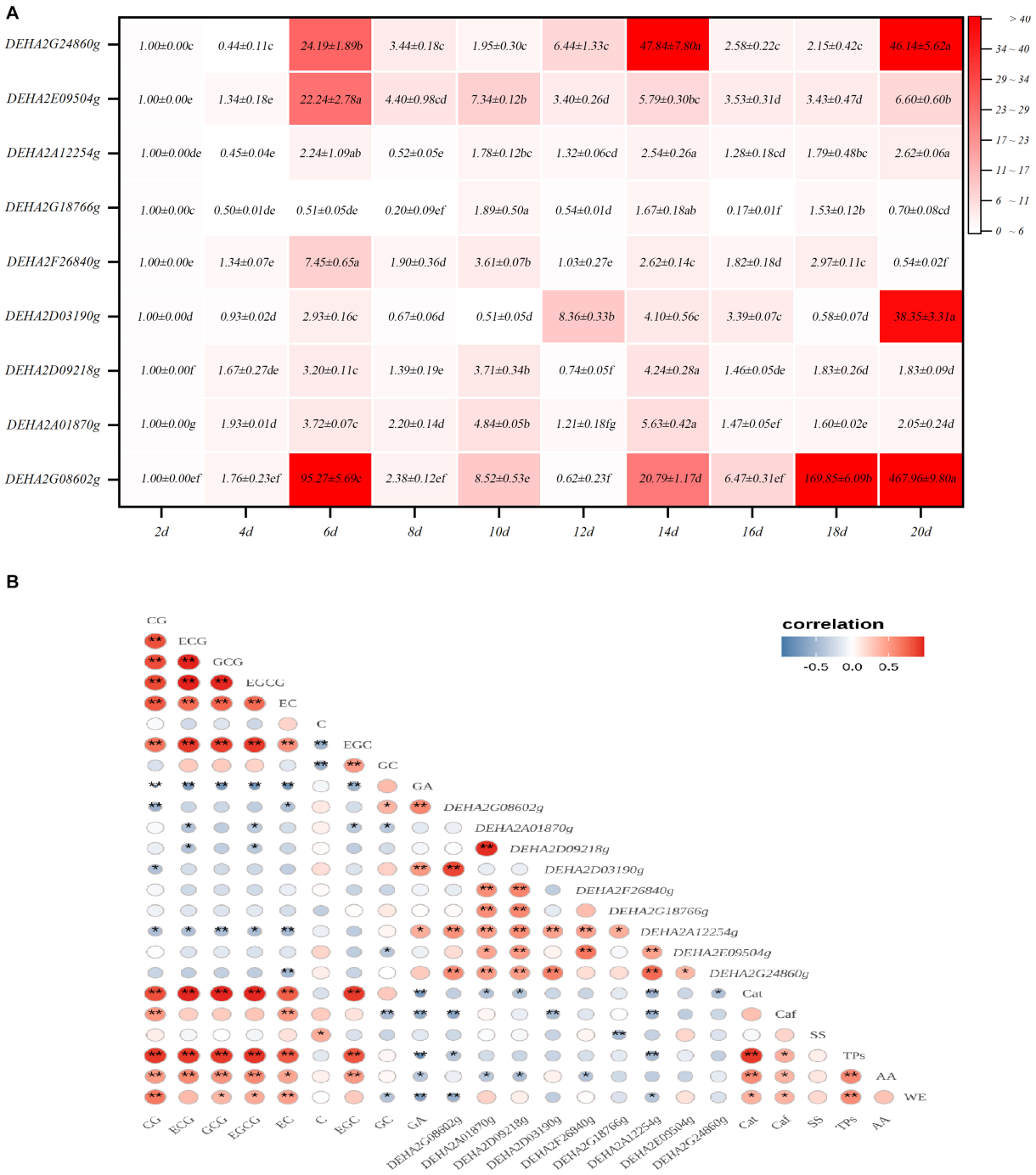

FIGURE 5
Analysis of *GH* gene expression characteristics in *D. hansenii* Y4 during solid-state fermentation. **(A)** Expression characteristics of *GH* genes; different letters on the gradient color block denote a significant difference at $p = 0.05$. **(B)** Correlation analysis on the *GH* gene expression level and Chemical component level, * and ** reflect a significant difference at $p = 0.05$ and $p = 0.01$, respectively.

CG. Unexpectedly, some interesting relationships between the contents of catechin monomers and the expression levels of *GH* genes were detected, for instance, the content of EC was significantly and negatively related to the expression levels of *DEHA2G24860g* and *DEHA2G08602g*, respectively, while the content of CG was significantly and negatively correlated with the expression levels of *DEHA2G08602g* and *DEHA2D03190g*, respectively. In view of the apparent decrease in the levels of EC, EGCG and so forth after fermentation and the relationship between catechin monomers and *GH* genes, it cannot be excluded that the expression of some *GH* genes probably leads to an obvious decrease in the levels of specific catechin monomers by mediating the glycosylation of catechins, as researchers have discovered that certain GHs can catalyze transglycosylation reactions, e.g.,

transferring a sugar unit to a nucleophilic acceptor other than water under certain conditions (Prieto et al., 2021; Wang et al., 2022). Cho et al. (2011) have employed amylosucrase from *Deinococcus geothermalis* DSM 11300 to biosynthesize (+)-catechin glycosides via linking glucose or maltose molecule to (+)-catechin, and Méndez-Líter et al. (2022) also successfully synthesized 3 novel EGCG-glycosides utilizing engineered transformed β-glucosidase and β-xylosidase from *Talaromyces amestolkiae*. The production of glycosylated catechin will result in an evident reduction in the levels of some unique catechin monomers. Besides, *DEHA2G24860g* and *DEHA2G08602g* were sharply up-regulated in the anaphase of high-temperature fermentation, suggesting that they are likely to be thermotolerant genes.

In this work some functions of *D. hansenii* Y4 during SSDT fermentation were verified, but compared to the functional research of filamentous fungi during dark tea fermentation, which is obviously insufficient (Ma et al., 2021; Zou et al., 2022, 2023; Liao et al., 2023). We expect to explore more functional microbes during SSDT production, and we will continue to investigate the activities of unique GHs in *D. hansenii* Y4 for elucidating its action mechanism during SSDT pile-fermentation and facilitating its application in our subsequent work.

Conclusion

In this work, many genes encoding GHs, distributed in a comparatively abundant GH17, GH18, GH76, GH31, GH47 and GH2, were detected in *D. hansenii*, and most of the GHs were located in the exocellular space. *D. hansenii* Y4 exhibited an excellent ability to improve the mellow mouthfeel of SSDT via increasing the WE, SS and AA contents, but reducing the TPs and Caf levels. It seriously influenced the "reddish-brown" factors of SSDT and possibly accelerated the isomerization reaction between ECG and CG. *DEHA2G08602g* (mannan endo-1,6-alpha-mannosidase DFG5 gene) in *D. hansenii* Y4 was dramatically up-regulated in fermentative anaphase, and its expression was significantly and negatively correlated to EC and CG levels. Overall, *D. hansenii* Y4 may be an important functional microbe targeting carbohydrates degradation and catechin transformation during SSDT pile-fermentation, with *DEHA2G08602g* as a pivotal thermotolerant *GH* gene. These results may provide a novel complement to the traditional theory of dark tea pile-fermentation.

Data availability statement

The original contributions presented in the study are included in the article/Supplementary material, further inquiries can be directed to the corresponding author.

Author contributions

YZ and WX designed the experiments. ML, YuL, XuL, XiL, and YiL performed experiments. YZ and ML wrote the manuscript. QT reviewed and edited the manuscript. All authors contributed to the article and approved the submitted version.

Funding

This work was supported by the National Natural Science Foundation of China (32102434), Tea Refining and Innovation Key Laboratory of Sichuan Province, and the "Disciplinary Construction Double Support Program" of Sichuan Agricultural University.

Conflict of interest

The authors declare that the research was conducted in the absence of any commercial or financial relationships that could be construed as a potential conflict of interest.

Publisher's note

All claims expressed in this article are solely those of the authors and do not necessarily represent those of their affiliated organizations, or those of the publisher, the editors and the reviewers. Any product that may be evaluated in this article, or claim that may be made by its manufacturer, is not guaranteed or endorsed by the publisher.

Supplementary material

The Supplementary material for this article can be found online at: https://www.frontiersin.org/articles/10.3389/fmicb.2023.1229251/full#supplementary-material

References

Bailey, T. L., Boden, M., Buske, F. A., Frith, M., Grant, C. E., Clementi, L., et al. (2009). MEME SUITE: tools for motif discovery and searching. *Nucleic Acids Res.* 37, W202–W208. doi: 10.1093/nar/gkp335

Burton, R. A., Gidley, M. J., and Fincher, G. B. (2010). Heterogeneity in the chemistry, structure and function of plant cell walls. *Nat. Chem. Biol.* 6, 724–732. doi: 10.1038/nchembio.439

Chen, C., Chen, H., Zhang, Y., Thomas, H. R., Frank, M. H., He, Y., et al. (2020). TBtools - an integrative toolkit developed for interactive analyses of big biological data. *Mol. Plant* 13, 1194–1202. doi: 10.1016/j.molp.2020.06.009

Cho, H. K., Kim, H. H., Seo, D. H., Jung, J. H., Park, J. H., Baek, N. I., et al. (2011). Biosynthesis of (+)-catechin glycosides using recombinant amylosucrase from *Deinococcus geothermalis* DSM 11300. *Enzym. Microb. Technol.* 49, 246–253. doi: 10.1016/j.enzmictec.2011.05.007

Davies, G., and Henrissat, B. (1995). Structures and mechanisms of Glycosyl hydrolases. *Structure* 3, 853–859. doi: 10.1016/S0969-2126(01)00220-9

Drula, E., Garron, M. L., Dogan, S., Lombard, V., Henrissat, B., and Terrapon, N. (2022). The carbohydrate-active enzyme database: functions and literature. *Nucleic Acids Res.* 50, D571–D577. doi: 10.1093/nar/gkab1045

Gasteiger, E., Gattiker, A., Hoogland, C., Ivanyi, I., Appel, R. D., and Bairoch, A. (2003). ExPASy: the proteomics server for in-depth protein knowledge and analysis. *Nucleic Acids Res.* 31, 3784–3788. doi: 10.1093/nar/gkg563

Henrissat, B. (1991). A classification of glycosyl hydrolases based on amino acid sequence similarities. *Biochem. J.* 280, 309–316. doi: 10.1042/bj2800309

Huang, Y. H. *Tea science experimental techniques*. Beijing: China Agriculture Press. (1997). 120–128.

Kanpiengjai, A., Chui-Chai, N., Chaikaew, S., and Khanongnuch, C. (2016). Distribution of tannin-'tolerant yeasts isolated from Miang, a traditional fermented tea leaf (*Camellia sinensis var. assamica*) in northern Thailand. *Int. J. Food Microbiol.* 238, 121–131. doi: 10.1016/j.ijfoodmicro.2016.08.044

Kumar, S., Nei, M., Dudley, J., and Tamura, K. (2008). MEGA: a biologist-centric software for evolutionary analysis of DNA and protein sequences. *Brief. Bioinform.* 9, 299–306. doi: 10.1093/bib/bbn017

Li, Z. Y., Feng, C. X., Luo, X. G., Yao, H. L., Zhang, D. C., and Zhang, T. C. (2018). Revealing the influence of microbiota on the quality of Pu-erh tea during fermentation process by shotgun metagenomic and metabolomic analysis. *Food Microbiol.* 76, 405–415. doi: 10.1016/j.fm.2018.07.001

Li, M. Y., He, Q., Zhang, Y., Sun, B., Luo, Y., Zhang, Y., et al. (2020). New insights into the evolution of the SBP-box family and expression analysis of genes in the growth and development of *Brassica juncea*. *Biotechnol. Biotec. EQ.* 34, 810–824. doi: 10.1080/13102818.2020.1803131

Li, Q., Li, Y. D., Luo, Y., Xiao, L. Z., Wang, K. B., Huang, J. A., et al. (2020). Characterization of the key aroma compounds and microorganisms during the manufacturing process of Fu brick tea. *LWT Food Sci. Technol.* 127:109355. doi: 10.1016/j.lwt.2020.109355

Liao, S. Y., Zhao, Y. Q., Jia, W. B., Niu, L., Bouphun, T., Li, P. W., et al. (2023). Untargeted metabolomics and quantification analysis reveal the shift of chemical constituents between instant dark teas individually liquid-state fermented by *Aspergillus cristatus, Aspergillus niger*, and *Aspergillus tubingensis*. *Front. Microbiol.* 14:1124546. doi: 10.3389/fmicb.2023.112454

Ma, Y., Ling, T. J., Su, X. Q., Jiang, B., Nian, B., Chen, L. J., et al. (2021). Integrated proteomics and metabolomics analysis of tea leaves fermented by *Aspergillus Niger*, *Aspergillus tamarii* and *Aspergillus fumigatus*. *Food Chem.* 334:127560. doi: 10.1016/j.foodchem.2020.127560

Méndez-Líter, J. A., Pozo-Rodríguez, A., Madruga, E., Rubert, M., Santana, A. G., de Eugenio, L. I., et al. (2022). Glycosylation of epigallocatechin Gallate by engineered glycoside hydrolases from Talaromyces amestolkiae: potential Antiproliferative and neuroprotective effect of these molecules. *Antioxidants* 11:1325. doi: 10.3390/antiox11071325

Mhuantong, W., Charoensawan, V., Kanokratana, P., Tangphatsornruang, S., and Champreda, V. (2015). Comparative analysis of sugarcane bagasse metagenome reveals unique and conserved biomass-degrading enzymes among lignocellulolytic microbial communities. *Biotechnol. Biofuels* 8, 1–17. doi: 10.1186/s13068-015-0200-8

Pasha, C., and Reddy, G. (2005). Nutritional and medicinal improvement of black tea by yeast fermentation. *Food Chem.* 89, 449–453. doi: 10.1016/j.foodchem.2004.02.054

Pfaffl, M. W. (2001). A new mathematical model for relative quantification in real-time RT–PCR. *Nucleic Acids Res.* 29:e45. doi: 10.1093/nar/29.9.e45

Prieto, A., de Eugenio, L., Méndez-Líter, J. A., Nieto-Domínguez, M., Murgiondo, C., Barriuso, J., et al. (2021). Fungal glycosyl hydrolases for sustainable plant biomass valorization: Talaromyces amestolkiae as a model fungus. *Int. Microbiol.* 24, 545–558. doi: 10.1007/s10123-021-00202-z

Singh, R., Bennett, J., Gupta, M., Sharma, M., Eqbal, D., Alessi, A. M., et al. (2019). Mining the biomass deconstructing capabilities of rice yellow stem borer symbionts. *Biotechnol. Biofuels* 12:265. doi: 10.1186/s13068-019-1603-8

Tan, L. Q., Yang, C. J., Zhou, B., Wang, L. B., Zou, Y., Chen, W., et al. (2021). Inheritance and quantitative trait loci analyses of the anthocyanins and catechins of *Camellia sinensis* cultivar 'Ziyan' with dark-purple leaves. *Physiol. Plant.* 1, 109–119. doi: 10.1111/ppl.13114

Tingley, J. P., Low, K. E., Xing, X. H., and Abbott, D. W. (2021). Combined whole cell wall analysis and streamlined in silico carbohydrate-active enzyme discovery to improve biocatalytic conversion of agricultural crop residues. *Biotechnol. Biofuels* 14:16. doi: 10.1186/s13068-020-01869-8

Viana, P. A., de Rezende, S. T., Passos, F. M. L., Machado, S. G., Maitan, G. P., da Silva Coelho, V. T., et al. (2011). α-Galactosidases production by *Debaryomyces hansenii* UFV-1. *Food Sci. Biotechnol.* 20, 601–606. doi: 10.1007/s10068-011-0085-7

Wang, Q. P., Peng, C. X., and Gong, J. X. (2011). Effects of enzymatic action on the formation of theabrownin during solid state fermentation of Pu-erh tea. *J. Sci. Food Agric.* 91, 2412–2418. doi: 10.1002/jsfa.4480

Wang, Q., Wu, Y., Peng, A., Cui, J., Zhao, M., Pan, Y., et al. (2022). Single-cell transcriptome atlas reveals developmental trajectories and a novel metabolic pathway of catechin esters in tea leaves. *Plant Biotechnol. J.* 20, 2089–2106. doi: 10.1111/pbi.13891

Xiang, H. L., Chen, L., Yu, W. Q., and Zhang, Y. G. (2020). Identification of the GH1 gene family in Camellia sinensis and expression analysis during the withering process of fresh tea leaves. *Chin. J. App. Environ. Biol.* 26, 878–885.

Zhang, W., Yang, R. J., Fang, W. J., Yan, L., Lu, J., Sheng, J., et al. (2016). Characterization of thermophilic fungal community associated with pile fermentation of Pu-erh tea. *J. Food Microbiol.* 227, 29–33. doi: 10.1016/j.ijfoodmicro.2016.03.025

Zhou, Y., Zeng, L. T., Gui, J. D., Liao, Y. Y., Li, J. L., Tang, J. C., et al. (2017). Functional characterizations of β-glucosidases involved in aroma compound formation in tea (*Camellia sinensis*). *Food Res. Int.* 96, 206–214. doi: 10.1016/j.foodres.2017.03.049

Zou, Y. (2014). Effects of microorganisms on quality formation of Sichuan dark tea during post-fermentation. Ph.D. thesis. Ya'an: Sichuan Agricultural University.

Zou, Y., Ma, W. J., Tang, Q., Xu, W., Tan, L. Q., Han, D. Y., et al. (2020). A high-precision method evaluating color quality of Sichuan dark tea based on colorimeter combined with multi-layer perceptron. *J. Food Process Eng.* 43:e13444. doi: 10.1111/jfpe.13444

Zou, Y., Yuan, Y., Liu, M. Q., Li, X., Lai, Y. Q., Liu, X. Y., et al. (2023). Metagenomics reveal the role of microorganism and GH genes contribute to Sichuan south-road dark tea quality formation during pile fermentation. *LWT Food Sci. Technol.* 178:114618. doi: 10.1016/j.lwt.2023.114618

Zou, Y., Zhang, Y., Tian, Y., Liu, M. Q., Yuan, Y., Lai, Y. Q., et al. (2022). Microbial community analysis in Sichuan south-road dark tea piled center at pile-fermentation metaphase and insight into organoleptic quality development mediated by *Aspergillus niger* M10. *Front. Microbiol.* 13:930477. doi: 10.3389/fmicb.2022.930477

10.3389/fmicb.2023.1229251

Glossary

WE	Water extracts
AA	Amino acids
SS	Water-soluble sugar
Cat	Total catechins
TPs	Tea polyphenols
Caf	Caffeine
TR	Thearubiin
TF	Theaflavins
TB	Theabrownin
GA	Galic acid
C	Catechin
EC	Epicatechin
ECG	Epicatechin gallate
EGC	Epigallocatechin
GC	Gallocatechin
ECCG	Epigallocatechin gallate
CG	Catechin gallate
GCG	Gallocatechin gallate
BI	Brown index
Eab	Total color value
Cab	Chroma
Sab	Color saturation
Hab	Hue angle
h	Hue
Ps	Yellow brightness degree

frontiers | Frontiers in Microbiology

TYPE Original Research
PUBLISHED 27 July 2023
DOI 10.3389/fmicb.2023.1234884

OPEN ACCESS

EDITED BY
Michela Verni,
Sapienza University of Rome, Italy

REVIEWED BY
Gustavo Cordero-Bueso,
University of Cádiz, Spain
Roberto Pérez-Torrado,
Spanish National Research Council (CSIC), Spain

*CORRESPONDENCE
Maria Tufariello
✉ maria.tufariello@ispa.cnr.it
Lorenzo Palombi
✉ l.palombi@ifac.cnr.it

†These authors have contributed equally to this work
‡These authors have contributed equally to this work and share first authorship

RECEIVED 05 June 2023
ACCEPTED 11 July 2023
PUBLISHED 27 July 2023

CITATION
Pietrafesa R, Siesto G, Tufariello M, Palombi L, Baiano A, Gerardi C, Braghieri A, Genovese F, Grieco F and Capece A (2023) A multivariate approach to explore the volatolomic and sensory profiles of craft Italian Grape Ale beers produced with novel *Saccharomyces cerevisiae* strains.
Front. Microbiol. 14:1234884.
doi: 10.3389/fmicb.2023.1234884

A multivariate approach to explore the volatolomic and sensory profiles of craft Italian Grape Ale beers produced with novel *Saccharomyces cerevisiae* strains

Rocchina Pietrafesa[1‡], Gabriella Siesto[1,2‡], Maria Tufariello[3*†], Lorenzo Palombi[4*†], Antonietta Baiano[5], Carmela Gerardi[3], Ada Braghieri[1], Francesco Genovese[1], Francesco Grieco[3] and Angela Capece[1,2]

[1]Scuola di Scienze Agrarie, Forestali, Alimentari ed Ambientali, Università degli Studi della Basilicata, Potenza, Italy, [2]Spinoff StarFInn S.r.l.s., Scuola di Scienze Agrarie, Forestali, Alimentari ed Ambientali, Università degli Studi della Basilicata, Potenza, Italy, [3]Consiglio Nazionale delle Ricerche, Istituto di Scienze delle Produzioni Alimentari (ISPA), Lecce, Italy, [4]Consiglio Nazionale delle Ricerche, Istituto di Fisica Applicata "Nello Carrara", Firenze, Italy, [5]Dipartimento di Scienze Agrarie, degli Alimenti e dell'Ambiente, Università di Foggia, Foggia, Italy

This study investigated the influence of three *Saccharomyces cerevisiae* strains, selected from different matrices - CHE-3 (cherry), P4 (sourdough) and TA4-10 (grape must) - on characteristics of Italian Grape Ale (IGA) beers obtained at microbrewery scale. A multidisciplinary approach, combining results from analysis of chemical, volatile and organoleptic profiles of the beers, was adopted to underline the relationships between yeast starter and the quality of final products. Detection volatile organic compounds (VOCs) by Gas-Chromatography coupled with Mass Spectrometry (GC-MS) after extraction carried out by head-space micro-extraction (HS-SPME) revealed that the beer obtained by P4 strain differed from the others for its higher concentrations of esters, alcohols, and terpenes as confirmed by PCA (principal component analysis) and Cluster heatmap. Furthermore, sensorial analysis and consumer test showed that this sample differed from others by more pronounced notes of "fruity smell and floral" and "olfactory finesse," and it was the most appreciated beer for smell, taste, and overall quality. Conversely, CHE-3 was the sample with the lowest concentrations of the identified volatiles and, together TA4-10, showed the highest scores for smoked, yeast, malt, and hop notes. As far as we know, these are the first results on the application of indigenous *S. cerevisiae* strains in the production of craft IGA beers analyzed through a complex multivariate approach.

KEYWORDS

fruit beer, indigenous strains, volatile organic compounds, sensory analysis, multivariate statistical analysis

1. Introduction

The Beer Judges Certification Program (BJCP) recently recognized a new subcategory of special fruit beers, denoted as Italian Grape Ale (IGA; BJCP, 2015). Produced primarily by craft breweries, this new style of beer joins two key products of the Italian beverage industry, i.e., beer and wine. IGA beers are produced with the addition of grapes or must or winemaking waste in a range from 5 to 40% of the total weight of the wort. The must addition significantly influences the sensory profile, thus offering to the brewers the opportunity to diversify their production, through the obtainment of beers characterized by a complex sensorial profile (Castro Marin et al., 2021). Indeed, an increase of phenolic acids and volatile molecules was detected in IGAs produced by adding must from grapes of the cv Lambrusco (Castro Marin et al., 2021). IGAs belong to the group of ale beers and are obtained from the fermentation process driven by strains belonging to the *Saccharomyces cerevisiae* species. Esters, alcohols, acids, aldehydes, ketones, hydrocarbons, sulfur compounds and volatile phenols are the main volatiles detected in beer, they being able to influence their aroma and flavor both individually and in a synergistic or antagonistic way (Pinho et al., 2006). Different strains of *S. cerevisiae* can produce significantly different flavor profiles when fermenting the same substrate and this is a consequence of two factors: the differential ability of yeast strains to release varietal volatile compounds from their non-volatile precursors, and the differential ability to *de novo* synthesize yeast-derived volatile compounds (Vilanova and Sieiro, 2006).

The use of pure yeast cultures, pioneered by Christian Hansen in the 1880s, greatly improved the consistency and quality of beer. Moreover, the increasing popularity of both the craft beer market (Garavaglia and Swinnen, 2018) and the consumer interest in new beer styles (Aquilani et al., 2015; Romano et al., 2023) have stimulated the research for new brewing yeasts (Gibson et al., 2017; Hittinger et al., 2018). Nowadays, different strategies are available for providing new starter cultures, such as evolution, mutagenesis, breeding, and yeast isolation from various environmental niches (Steensels et al., 2014a,b; Berbegal et al., 2019). The latter option represents one of the most attractive tools for the obtainment of alternative yeasts with brewing potential as it takes advantage of the natural biodiversity of the microorganisms found within specific geographical regions, which can incorporate novel flavor and aroma compounds into the fermented products. In fact, the use of locally selected yeast strains with strain-specific metabolic characteristics could positively affect the final quality of fermented beverage (Capece et al., 2010; Berbegal et al., 2018) and ensure the maintenance of the typical sensory properties of products deriving from any given region (Valles et al., 2008; De Simone et al., 2021). In the last years, yeast research has turned toward the use of food substrates that represent a potentially valuable source of strains with beneficial characteristics such as an increased resistance or new flavor and aroma profiles, which could be applied in a controlled manner to industrial brewing systems (Cubillos et al., 2019). Yeasts potentially useful for brewing have been isolated from cacao, kombucha, and sourdough cultures (Mascia et al., 2015; Bellut et al., 2018; Holt et al., 2018). With this in mind, in order to improve the quality of new craft beer styles, the producers have sought not only to diversify the choice of raw materials, but also by applying the microbial cross-over, which is the use of new yeast starter cultures, usually employed in other fermentation process (Dank et al., 2021).

In line with this strategy, three indigenous *S. cerevisiae* selected from different matrices, CHE-3 (cherry), P4 (sourdough) and TA4-10 (grape must), were recently applied in brewing trials for IGA production at a laboratory scale; these selected yeast strains resulted potentially able for differentiation and quality improvement of IGA beer production (Siesto et al., 2023). In the present study, these indigenous strains were tested during inoculated fermentations at microbrewery scale. The strain influence on chemical, aromatic and sensory profiles of final products was evaluated through a chemometric approach (principal component analysis, Cluster Heatmap, Partial least square-correlation) in order to validate these strains as novel starters for IGA production. To the best of our knowledge, this investigation is the first one concerning the application of the microbial crossover for the production of craft IGA beer in Southern Italy.

2. Materials and methods

2.1. Yeast starters

In this study, four *Saccharomyces cerevisiae* strains, already tested during brewing trials at laboratory scale (Siesto et al., 2023) were used. Three strains (CHE-3, P4 and TA4-10) were indigenous yeasts, previously isolated from different foods and belonging to the UNIBAS Yeast Collection (UBYC), University of Basilicata (Potenza, Italy), whereas the commercial starter SafAle US-05 (US-05)—American top-fermenting yeast (Fermentis, Marq en Baroeul, France) was used as reference strain. The yeasts were cultured aerobically in Erlenmeyer flasks containing 2 liters of YPD medium (yeast extract 10 g/L, peptone 20 g/L, dextrose 20 g/L) and incubated for 24 h at 20°C under stirring at 180 rpm, using a digital orbital shaker. These cultures were used as pre-inoculum for biomass production for micro brewing trials, following the procedure previously described (Capece et al., 2011). Briefly, the pre-cultures were inoculated in a vessel containing 4.5 L of YPD liquid by using the BioFlo/CelliGen 110 bioreactor (Eppendorf, Germany), with the following growth parameters: temperature at 20°C; stirring at 400 rpm; oxygen at 4 vvm. After 24 h, the biomass was recovered by centrifugation carried out at 5000 rpm for 10 min at 4°C; the recovered cell pellets were washed with saline solution (0.9% NaCl) and maintained at 4°C until their use. The cell density of biomass was assessed by viable cell count on YPD medium.

2.2. Beer production

The four strains were tested in a micro brewing plant (Birrificio Sorrento, Sorrento, Italy). Ten hectoliters of wort, prepared by using the commercial extract malt for Pale Ale beer (MrMalt®, Udine, Italy) already tested during laboratory scale trials (Siesto et al., 2023); the wort was boiled for 20 min with hop of Cascade variety. At the end of boiling, the beer wort was blended with 15% of frozen grape must (Falanghina variety). This percentage was chosen as it gave the best results during laboratory-scale trials and it was the most frequently used by this producer. The obtained wort, characterized by a content of total soluble solids of 11.4° Plato

(corresponding to an original gravity of 1.044), was inoculated with each starter at inoculum level of 1×10^7 CFU/mL.

The analysis of viable cells in fermentation wort was assayed by plate counting on Wallerstein Laboratory Nutrient Agar medium (WL, Oxoid, Hampshire, UK), a yeast differential culture medium (Pallmann et al., 2001).

The primary fermentation lasted 10 days, and then the samples were transferred into other steel tanks for the maturation step, performed at low temperatures (10°C) for 1 month. The secondary fermentation was carried out by disposing the samples in 500 mL bottles in the presence of 5 g/L of sucrose for 2 weeks at 10°C. At the end of secondary fermentation, the samples were maintained at 4°C for 2 months in order to allow flavor maturation and stability. Afterward, the beers were evaluated for analytical and aromatic composition.

During fermentation, the starter evolution was monitored by yeast viable cell counts on WL nutrient agar medium (Wallerstein Laboratory; Oxoid, Hampshire, UK) and by plate incubation at 26°C for 5 days. In details, the following sampling points were considered: after 24 h of inoculation, at the end of primary and secondary fermentations. For each isolation time, the plates containing a statistically representative number of colonies were counted and around 20 colonies were purified on YPD plates for identification by 5.8S ITS-RFLP analysis.

2.3. Standard quality attributes

The content of total soluble solids (°Plato) was determined by using a refractometer (Hanna Instruments, Padua, Italy). For bitterness determination, craft beers were decarbonated and 10 mL of samples were submitted to extraction of bitter substances by using 1 mL of hydrochloric acid 3M and 20 mL of pure iso-octane (Popescu et al., 2013). After that, the samples were shaken vigorously for 5 min at room temperature and centrifuged for 15 min at 4000 rpm. The iso-octane phase was decanted and drained, whereas the sample tube was maintained in dark for at least 30 min before measuring the absorption at 275 nm by a spectrophotometer (SPECTRO Star Nano, BGM Labtech). For calculation of bitterness, expressed as International Bittering Units (IBU), the average values of three determinations were used and the following equation was applied:

$$IBU = 50 \times A275$$

where A275 correspond to the absorbance at 275 nm.

The beer color, was expressed as European Brewing Convention (EBC) units, determined by a colorimeter (SA-130, S.A.M.A. Italia S.r.l., Viareggio, Italy) and calculated as follows:

$$EBC\ color: 25.5 \times (A430 - A700)$$

where A430 and A700 correspond to the absorbance at 430 and 700 nm, respectively.

The turbidity was measured in a turbidimeter (TL23, Hach®, Loveland, Colorado, US) and expressed in nephelometric turbidity units (NTU).

2.4. HPLC analysis

Organic acids were identified using an Agilent Hi-Plex H column (300 × 7.7 mm; 8.0 μm internal particles; Agilent Technologies, Santa Clara, CA, USA). The temperature of the column compartment was maintained at 70°C. The flow rate applied was 0.4 mL/min with a run time of 30 min. The phase was represented by 4.0 mM/L H_2SO_4 in ultrapure water. Standard solutions were injected to obtain the retention time for each compound. A Diode Array Detector settled at 210 nm was used.

The concentrations of maltodextrin, sucrose, maltose, maltotriose, glucose, fructose, glycerol, and ethanol were quantified using the same type of column used for organic acids. The mobile phase was represented by deionized water and a constant flow rate of 0.6 mL/min. A run time of 30 min was applied. Sugar detection was carried out through a Refractive Index Detector (RID). Quantification of individual organic acids and sugars was performed directly by the Chem-Station software (Agilent) using a five-point regression curve ($R^2 \geq 0.99$) based on authentic standards.

2.5. Volatolomic profile of IGA beers

Acetaldehyde, ethyl acetate, acetoin, n-propanol, isobutanol, n-butanol, 2-methyl-1-butanol and 3-methyl-1-butanol, were quantified by direct injection of 1 mL of beer samples into a packed glass column (80/120 Carbopak B/5% Carbowax 20 M, Supelco, Sigma-Aldrich, Milano, Italy) by using an Agilent 7890A Gas-Chromatograph, following the protocol previously reported (Capece et al., 2021).

Volatile organic compounds (VOCs) were identified and quantified by Gas-Chromatography coupled with Mass Spectrometry (GC-MS) after extraction carried out by head-space micro-extraction (HS-SPME) according to Palombi et al. (2023). Briefly, 100 μL of internal standard solution (ISTD, 4-methyl-2-pentanol, 300 mg/L) was added to a volume of 5 mL of beer in a 20 mL headspace vial (Alltech Corp., Deerfield, IL, USA). A 50/30 DVB-CAR-PDMS fiber (Supelco, Bellofonte, PA) was inserted into the vial and let to adsorb volatiles for 30 min at 40°C and then transferred to the injector port (250°C) where desorption occurred in 2 min. *Splitless* mode was selected as injection mode. GC-MS analyses were performed on a GC 6890 (Agilent Technologies, Palo Alto, CA) coupled to an Agilent MSD 5973 Network detector using a HP-INNOWAX capillary column (60 m × 0.25 mm, 0.25 μm, J&W Scientific Inc., Folsom, CA, USA) as reported by Tufariello et al. (2019). Concentrations of volatiles were assessed by the internal standard method. The GC/MS data subjected to subsequent statistical processing consist of the average values of three replicates obtained by carrying out three different extraction procedures for each sample.

2.6. Sensory analysis

A trained panel of ten judges between 40 and 65 years of age, experienced in alcoholic beverage sensory evaluation, carried out a Quantitative Descriptive Analysis (QDA) in a room free of noise, odors and with white light. Fifty milliliters of each beer were served to the panelists in crystal goblets at a temperature of 5 ± 1°C. The parameters evaluated by the judges were selected among those found in the literature (Baiano et al., 2023) and

those generated by the panel to both give a complete product description and avoid overlapping. Data were collected using a combined profile sheet including 3 appearance (color, amount, and persistence of foam), 12 olfactory (malty, hoppy, floral, fruity, spicy, honey, caramel, yeast, smoked, aromatic herbs; olfactory finesse and the overall olfactory intensity), 11 gustatory (sweetness, bitterness, saltiness, acidity/sourness, malty, hoppy, floral, fruity, spicy, toasted, alcoholic), and 2 tactile (effervescence and body) parameters. Panelists were also asked to evaluate the overall quality of each beer. All descriptors and the overall quality were evaluated on a 5-point scale with the exception of those referred to foam color, which were evaluated on a 4-point scale (**Supplementary Table 1**). Drinking water was used for mouth-rinsing between tastings.

2.7. Consumer test

The consumer test was conducted with 42 consumers (female 29 and men 13), with age ranging between 21 and 75 years. The prerequisites for participating in the study were that the individual habitually consumed beer and they were selected on the basis of other criteria, such as not reporting any conditions affecting the senses of sight, taste or smell, The test was conducted in the sensory laboratory from the School of Agricultural, Forestry, Food and Environmental Sciences of Basilicata University using individual sensory booth equipped with sensory data collection software (Smart Sensory box version 2.3.5., Smart Sensory Solution, Italy). The test was conducted to assess liking for appearance, odor, taste, and overall liking, using a using a 9-point hedonic scale in which 1 = dislike extremely, 5 = neither like nor dislike and 9 = like extremely (Peryam and Pilgrim, 1957). The samples were randomly coded with 3-digit numbers, and the order of the sample presentation was randomized to minimize first-serving order bias. Each participant received about 15 mL of sample, served at refrigerator temperature (4°C); water and crackers were used as palate cleansers.

2.8. Statistical analysis

One-way ANalysis Of VAriance (ANOVA) applied to chemical, sensory, and volatolomic data determined significant quantitative differences among samples. Differences were considered statistically significant for p-values of the null hypothesis less than or equal to 0.05. Partial Least Squares Correlation (PLSC) was applied to volatile compound data and sensory analysis data to study their multivariate covariance. PLSC (Tucker, 1958; Streissguth et al., 1993) is a multivariate statistical method used to analyze, through correlation, the relationship between two sets of variables. Volatolomic data were also used to create a clustergram consisting of a heatmap and dendrograms. The heatmap indicated, in a scale of false colors, the standardized concentration of each volatile compound for each of the samples considered. Samples and volatiles were organized according to the corresponding hierarchical clustering dendrograms. Euclidean distance as metric and unweighted average distance as linkage criterion, were considered. The calculations and visualization of the ANOVA, PCA, PLSC, and clustergrams results were performed using MATLAB Version: 9.14.0 (R2023a).

TABLE 1 Growth of inoculated starters, expressed as Log UFC/mL, during the different steps of IGA production.

	TA4-10	P4	CHE-3	US-05
After 24 h	7.71 ± 0.71	7.72 ± 0.57	7.94 ± 0.14	7.15 ± 0.35
End primary fermentation	7.02 ± 0.35	8.51 ± 0.58	8.15 ± 0.25	6.96 ± 0.43
After refermentation	6.18 ± 0.30	6.57 ± 0.26	7.05 ± 0.64	5.59 ± 0.35

3. Results and discussion

3.1. Starter evolution during fermentation

The strains growth was monitored during the fermentation process by a microbiological assay (**Table 1**). The viable count on WL medium, followed by ITS-RFLP analysis, revealed that all the isolated colonies during the process belong to *S. cerevisiae* species in order to confirm that no contamination occurred during the fermentation trials. The theoretical inoculum ratio resulted as planned; in fact, 24 h after inoculation, for all the trials the yeast population ranging between 7.1 and 7.9 Log CFU/mL. At this time, the three indigenous strains reached levels higher than those of the control strain US-05 (7.15 Log CFU/mL); the highest count (7.94 Log CFU/mL) were displayed by the strain CHE-3. At the end of primary fermentation, an increase of yeast population was observed for P4 and CHE-3 strains (0.8 and 0.2 Log cycles, respectively), a slight decrease to 6.96 Log CFU/mL was observed for the control strain US-05, whereas a 0.7 Log cycles decrease was registered for the strain TA4-10. After the secondary fermentation, the end of monitoring, all the fermentations showed a decrease of yeast levels; the highest value (7.05 Log CFU/mL) was detected for CHE-3 strain, whereas the lowest level was found for the control strain US-05, which was the strain showing the lowest count along all the process. However, the high yeast vitality found during the process for all the starters is crucial for improving fermentation and product quality as it is related to the efficiency and predictability of fermentation. This aspect, together the presence of only *S. cerevisiae* cells, are pivotal for beer quality, in particular for craft beers, which are more prone to spoilage than beer produced in large-scale breweries, in consequence of absence of pasteurization or sterile-filtration processes.

3.2. Physicochemical analyses

The IGA beers were analyzed for the main quality attributes, such as ethanol content, attributes related to turbidity, color and bitterness (**Table 2**). The ethanol ranged between 4.4 and 5.1 (% v/v), with the highest content in beer fermented with the commercial starter, this result being likely correlated with the very low maltotriose residual found in this beer.

All the beers presented a bitterness (International Bitterness Units, IBU) ranging between 8 and 13.3. The lowest values, found in TA4-10 and US-05 samples (9 and 8, respectively), were slightly lower than indications given by the Beer Judges Certification Program (BJCP), whereas IBU values significantly higher were found in beers fermented with CHE-3 and P4. Hops are the raw

TABLE 2 Principal quality parameters of the IGA beers obtained in the micro brewing plant.

Sample	Final gravity	Ethanol (%v/v)	Bitterness (IBU)	Color (EBC-unit)	Turbidity (NTU)
CHE-3	1011.13 ± 0.18^{a}	4.88 ± 0.61^{a}	12.60 ± 0.32^{a}	18.37 ± 0.31^{a}	15.63 ± 0.25^{c}
P4	1010.12 ± 0.18^{b}	4.44 ± 0.16^{ab}	13.4 ± 1.1^{a}	16.49 ± 0.16^{b}	34.23 ± 0.12^{a}
TA4-10	1009.25 ± 0.35^{b}	4.76 ± 0.03^{a}	9.19 ± 0.37^{b}	16.46 ± 0.06^{b}	33.7 ± 1.2^{a}
US-05	1009.93 ± 0.11^{b}	5.11 ± 0.20^{ac}	8.14 ± 0.16^{b}	20.73 ± 0.11^{c}	54.53 ± 0.12^{b}

Data are reported as mean ± standard deviation of two independent replicates. Different superscript letters indicate significant differences ($p < 0.05$) among the four samples.

TABLE 3A Carbohydrate content of experimental beers (g/L).

Samples	Maltodextrins	Maltotriose	Maltose	Glucose	Fructose
Wort	15.14 ± 0.12	15.17 ± 0.14	34.56 ± 0.25	17.13 ± 0.14	13.16 ± 0.11
TA4-10	14.54 ± 0.06	14.58 ± 0.19	ND	ND	0.49 ± 0.14
CHE3	14.53 ± 0.03	13.1 ± 1.2	ND	ND	0.35 ± 0.04
P4	14.6 ± 1.0	13.53 ± 0.83	ND	ND	0.33 ± 0.04
US-O5	15.32 ± 0.26	5.33 ± 0.16*	ND*	ND	0.35 ± 0.04

Data are reported as mean ± standard deviation of two independent replicates; ND, not detected; *$p < 0.05$.

material in beer mainly responsible for beer bitterness. Indeed, it provides α-acids, which during the technological process are transformed into the more bitter iso-α-acids. By considering that the variety and quantity of hop were kept constant among all beer samples, the difference in beer IBU might be correlated to the different capacity of yeast strain used for fermentation to preserve the α-acids from hop. These results enhance the role of starter on beer bitterness, conversely to data reported in other studies in which no differences in IBU were found among beers fermented with different starters (Matukas et al., 2022). Beer color, a commercial parameter crucial for quality product, is affected by amount and quality of the used malt; it usually can range from pale (0–15 EBC), amber (15–35 EBC), and dark (35–80 EBC). The analyzed samples had a color in the range 15-35 EBC; the highest value was found in beer produced with the commercial starter, whereas the lowest levels were found in P4 and TA4-10 beers, which were very similar among them. A similar trend was observed also for turbidity levels, with similar values for IGA produced by inoculating P4 and TA4-10 strains, and the highest turbidity (54.53 NTU) in US-05 beer. The turbidity is another parameter important for beer quality and for consumer acceptability. Following the EBC (European Brewery Convention) indications, beer is considered very hazy when it shows a turbidity level higher than 32 NTU (De Francesco et al., 2021); the IGAs produced with P4 and TA4-10 strains showed values slightly higher than this level, whereas very low turbidity was observed in CHE-3 beer.

The profile of carbohydrate present in the produced beers are shown in **Table 3A**. The monosaccharides maltose and glucose were almost very fermented. In fact, no residual maltose and glucose were found in all the produced beers indicating that the four strains efficiently utilized maltose during fermentation. Otherwise, some fructose residual was found in all the produced IGA beers. Furthermore, the three crossover strains did not proficiently catabolize the maltotriose, whereas a low residue of this compound was found in beer produced with reference strain US-05. The catabolism of maltotriose in yeasts is species-specific (Li et al., 2020). However, most yeast species catabolize maltotriose slowly and often incompletely (Cubillos et al., 2019). The beers contained a maltodextrin level very similar to wort, as expected, by considering that *S. cerevisiae* yeast is not able to utilize the dextrins (Armijo et al., 2016), with exception of *S. cerevisiae* var. *diastaticus*. As reported in **Table 3B**, the highest glycerol content was found in P4 sample, while acetic acid was higher in sample fermented with TA4-10 (isolated from grape must) and US-05 strains. The glycerol concentration in beer is affected, among other factors, by the yeast strain used and condition of the fermentation process. A higher glycerol concentration affects the sensory characteristics of the product as it enhances the perception of a sweet taste and increases product viscosity (Zhao et al., 2015). Citric, malic and tartaric acids derive from wort and/or from added grape must and all the fermentation samples showed not statistically different amounts of these organic acids, except for tartaric acid.

3.3. Volatile profile of IGA beers

Thirty-one volatile compounds grouped in the esters, alcohols, terpenes and volatile acids families, were identified in the analyzed IGA beers (**Table 4**). The alcohols group was quantitatively the most important one, with a total concentration ranging from 332.03 mg/L in CHE-3 to 411.54 mg/L in P4. Among alcohols, significant differences ($p < 0.05$, $p < 0.01$) were found for 2-methyl-1-butanol, 3-methyl-1-butanol and isobutanol. The higher alcohols may influence the sensory profile of beer by giving an alcoholic or solvent-like aroma and a warm mouthfeel (Meilgaard and Peppard, 1986). These compounds play a direct role in taste perception or through interactions with other beer components due to the synergistic and antagonistic effects that these compounds induce on taste perception. Among the identified compounds belonging to this class, only the 3-methylbutanol (solvent and fruity flavor) was above the perception threshold, as previously reported in a study aimed to a characterization of a wide number of commercial IGA samples (De Francesco et al., 2021). This compound influences the drinkability of beer since sensory analysis describes beer flavor as heavier when the content of amyl alcohol increases (Olaniran et al., 2017).

TABLE 3B Organic acids, glycerol and ethanol of experimental beers (g/L).

Samples	Citric acid	Malic acid	Tartaric acid	Succinic acid	Lactic acid	Acetic acid	Glycerol
Wort	1.81 ± 0.11	2.27 ± 0.09	0.82 ± 0.10	ND	0.05 ± 0.01	0.38 ± 0.01	0.44 ± 0.03
TA4-10	2.09 ± 0.04	1.86 ± 0.02	0.48 ± 0.00	0.76 ± 0.19	0.36 ± 0.03	0.24 ± 0.08	4.78 ± 0.06
CHE3	2.01 ± 0.17	2.56 ± 0.14	0.50 ± 0.16	0.75 ± 0.05	0.44 ± 0.03	0.14 ± 0.03	4.26 ± 0.39
P4	1.27 ± 0.18	2.26 ± 0.04	0.64 ± 0.06	1.16 ± 0.00	0.32 ± 0.01	0.19 ± 0.02	5.50 ± 0.05
US-O5	2.08 ± 0.59	2.04 ± 0.81	0.68 ± 0.23	0.78 ± 0.04	0.34 ± 0.02	0.25 ± 0.03	4.40 ± 0.23

Data are reported as mean ± standard deviation of two independent replicates; ND, not detected.

Furthermore, 2-methylbutanol and 3-methylbutanol were found at level significantly higher in beers obtained with indigenous strains than beer fermented with the reference strain US-05. These alcohols are produced in fermented beverages as a result of the metabolism of amino acids, such as isoleucine and valine. Differences found in their concentrations despite the use of wort with identical composition as fermentation medium, which should have the same concentration of the above-mentioned amino acids, may indicate that indigenous strains are characterized by a different metabolism compared to typical brewer yeast US-05.

The higher alcohols are also involved in the biochemical pathways leading to the synthesis of esters, which is another important group for beer aroma. The most described flavor-active esters in beer are ethyl acetate (solvent-buttery like aroma), ethyl caproate, ethyl caprylate (sour apple-like flavor and aroma), isoamyl acetate (fruity, banana aroma), isobutyl acetate, phenylethyl acetate, and ethyl octanoate (honey, fruity, roses, flowery aroma). In our samples, ethyl esters and acetates represented the second most abundant group of volatile compounds (**Table 4**), ranging from 0.72 mg/L in CHE-3 to 3.28 mg/L in P4. Significant differences in concentrations of different flavor-active esters, such as isoamyl acetate, ethyl hexanoate, hexyl acetate, ethyl octanoate, ethyl decanoate and phenylethyl acetate were found among beers obtained by different starters. Indeed, ester concentration is the result of the enzymatic balance of synthesis by alcohol acetyltransferases (AATases) and acyl-CoA/ethanol O-acyltransferases (AEATases) and breakdown by esterases. The activity of these enzymes is strain-specific (Marconi et al., 2016). The ethyl octanoate concentration was the highest in the US-05 sample, whereas the P4 beer showed the highest amount of the other above esters, probably due to the fermentative performance of this yeast strain and/or the higher ester synthase activity than esterase activity of P4 strain.

Phenyl acetate and ethyl hexanoate were above their perception thresholds for TA4-10 and P4 beers, contributing with rose, honey, and green notes to the aroma of these samples. Among esters, ethyl hexanoate, isoamyl acetate and phenyl acetate were in concentrations above their respective perception thresholds in P4 contributing significantly to the overall aroma (Rossi et al., 2014). However, both sensory and gas-chromatographic analyses revealed that esters might affect beer flavor also if these aromatic compounds are present at concentration below their individual threshold values (Rodrigues et al., 2008). It was reported that the presence of the different esters could play synergistic effects on individual flavors, interfering with the overall aromatic profile of the beer. Furthermore, since most esters are present in concentrations ranging in the threshold value, little variations in their concentration may significantly affect the organoleptic properties of the beer (Humia et al., 2019).

Acids are the third most abundant group in beers studied, but not statistically significant differences have been detected in the amount found in the different samples. The acids are produced during fermentation process but their amount depend both on yeast activity and on the composition of raw materials (Schreier and Jennings, 1979).

Three terpenes have been found in IGA beers, i.e., linalool, citronellol and nerolidol. In all samples, linalool and citronellol were found in concentrations above their odor thresholds, thus enhancing the aromatic profiles of IGA beers with fruity and floral notes. Moreover, IGA are beer made with a variable percentage of grape must, which is mainly characterized by primary aromatic compounds derived from grapes, such as terpenes, sulfur compounds, pyrazines, and norisoprenoids (Crupi et al., 2010; Slegers et al., 2015).

To highlight the effects of yeast strains on volatile molecules concentration, a *Pearson* principal component analysis (PCA) was carried out. **Figure 1** shows the projection of the beer samples on a factor plane in which the first two principal components explained 54.96 and 28.49% of the total variance, respectively. US-05 is described by negative PC1 and PC2, and it was associated with higher values of methyl octanoate and decanoate, 2 octanone, 1-heptanol, linalool and citronellol. P4 is characterized by positive PC1 and negative PC2 due to higher concentrations of most volatiles identified. Indeed, it was the sample with the most complex and rich volatile profile. Finally, TA4-10 and CHE-3 group together and were characterized by a positive value of PC2 that is due to a greater content in acetic acid, 2-ethyl-1-hexanol and nerolidol. Overall, our results, based on the quantification of volatile compounds, showed that the yeast strain has a statistically significant impact on the majority of target volatile compounds. This result is in line with previous research showing that the yeast strain is a significant factor in the formation of main volatile compounds in beer and starter selection is a key factor to modulate beer characteristics (De Simone et al., 2021; Matukas et al., 2022). A clustergram, which consists of a heatmap of standardized compound concentrations and dendrograms, was utilized as a tool for exploratory multivariate analysis of the volatile profiles of beers. This clustergram provided valuable insights into the relationships between the different yeast strains tested and the quantified compounds (as shown in **Figure 2**). The dendrograms, both by samples and by compounds, were generated through a

TABLE 4 Organic volatile compounds determined in IGA beers by means GC-MS and GC-FID.

Volatile molecules (mg/L)	US05	sd	TA4_10	sd	P4	sd	CHE-3	sd	OTH (mg/L)	Sensory notes	One-way Anova
Esters											
Ethyl acetate	0.07	0.01	0.05	0.02	0.08	0.02	0.06	0.02	25–30	Fruity-solvent-apple	ns
Isoamyl acetate	0.08	0.02	0.27	0.04	**0.65**	0.14	0.21	0.08	0.6–2	Banana	*
Ethyl hexanoate	**0.20**	0.04	**0.46**	0.02	**1.29**	0.34	nd		0.2–0.23	Apple-fruit	*
Hexyl acetate	nd		0.06	0.02	0.06	0.02	nd			Fruit	*
Methyl octanoate	0.05	0.01	0.02	0.01	0.02	0.00	0.02	0.01			ns
Ethyl octanoate	0.50	0.17	nd		0.38	0.07	nd		0.9–1.0	Apple-aniseed-cheesy	*
Methyl decanoate	0.06	0.02	0.06	0.02	0.07	0.03	0.05	0.02			ns
Ethyl decanoate	0.06	0.02	0.08	0.03	0.32	0.01	0.08	0.01	1.5	Apple	**
Ethyl-9-decenoate	0.04	0.02	0.07	0.02	0.09	0.03	0.05	0.02			ns
Methyl dodecanoate	0.11	0.03	0.12	0.03	0.09	0.03	0.10	0.02			ns
Phenylethyl acetate	0.03	0.01	**0.29**	0.06	**0.30**	0.01	0.18	0.04	0.25	Roses-honey	*
Ethyl dodecanoate	0.06	0.01	0.06	0.01	0.06	0.02	0.05	0.02			ns
Sum	1.26		1.54		3.41		0.80				
Alcohols											
n-propanol^	15.5	3.4	11.49	0.86	14.39	0.98	11.43	0.62			ns
Isobutanol^	90.1	4.1	91.3	5.6	94.5	4.8	61.8	4.1	100	Solvent	*
n-butanolo^	122	13	123.2	8.7	142.8	5.4	115	11			ns
2 methyl butanol^	29.9	2.5	40.3	2.9	53.4	5.2	37.9	3.8	65		*
3 methyl butanol^	**90.4**	7.2	**133.1**	8.9	**119.9**	11.5	**117.1**	9.8	70	Alcoholic-banana	*
1-hexanol	nd		nd		0.05	0.01	0.03	0.01	8	Green	ns
Phenylethanol	0.28	0.08	0.40	0.02	0.94	0.25	0.38	0.11	40-100	Roses	ns
2-ethyl-1-hexanol	0.05	0.01	0.06	0.02	0.04	0.01	0.06	0.02	8	Mild green	ns
Sum	332.72		388.32		411.58		332.05				
Volatile acids											
Hexanoic acid	0.03	0.01	0.03	0.01	0.08	0.02	0.03	0.01	5		ns
Octanoic acid	0.20	0.07	0.27	0.01	0.45	0.17	0.20	0.06	10		ns
n-decanoic acid	0.01	0.00	0.08	0.03	0.11	0.01	0.04	0.01	10		ns

(Continued)

10.3389/fmicb.2023.1234884

TABLE 4 (Continued)

Volatile molecules (mg/L)	US05	sd	TA4_10	sd	P4	sd	CHE-3	sd	OTH (mg/L)	Sensory notes	One-way Anova
Linoleic acid	0.07	0.01	0.03	0.01	0.03	0.01	0.05	0.02			
Sum	0.31		0.41		0.67		0.32				
Terpenes											
Linalool	**0.03**	0.01	**0.02**	0.01	**0.02**	0.01	**0.04**	0.01	0.001-0.1	Green-lemon	ns
Citronellol	**0.07**	0.01	**0.04**	0.02	**0.05**	0.02	**0.04**	0.01	0.009-0.04	Rose-sweet	ns
Nerolidol	0.06	0.01	0.04	0.01	nd		nd		1	Rose-apple-citrus	ns
Sum	0.16		0.10		0.07		0.08				
Other compound											
Acetoin^	3.35	0.46	12.94	2.47	nd		10.83	0.68	150		*
Acetaldehyde^	30.7	2.2	31.4	3.8	36.9	4.1	34.1	2.8			
Styrene	0.05	0.02	nd		0.04	0.02	0.05	0.01			ns
2-octanone	0.04	0.01	0.03	0.01	0.03	0.01	0.04	0.02			ns
Sum	34.17		44.36		36.89		45.00				

sd, standard deviation; nd, not detected; OTH, odor threshold; ^molecules determined by GC-FID; *significant differences $p \leq 0.05$, **significant differences $p \leq 0.01$. In bold the concentrations above odor threshold.

hierarchical clustering analysis using the Euclidean metric to assess similarity/dissimilarity and the unweighted average distance as the linkage criterion. As shown in **Figure 2**, the red color in the heatmap indicated the highest standardized concentrations of each substance while blue represents the lowest one. The beers produced with the four yeast strains constitute four independent clusters, they being dissimilar to each other's. Consistent with the PCA results, however, samples CHE-3 and TA4-10 are more similar to each other.

Overall, the samples were characterized by different standardized concentrations of the analyzed volatiles. Indeed, US-05, the commercial strain used as control, was characterized by higher production of molecules ranging from styrene to isobutanol; sample obtained with P4 strain showed high values of compounds ranging from phenylethyl acetate and ethyl acetate; however, this beer was characterized by the highest amounts of most detected volatiles, confirming the interesting findings of this strains previously obtained during brewing trials at laboratory scale (Capece et al., 2018, 2021). The TA4-10 sample is distinguished from the others by higher concentrations of volatiles ranged from nerolidol and hexyl acetate.

Finally, CHE-3 beer appeared to be the sample with fewer dominant volatile molecules, including 2-octanone, styrene, isoamyl alcohols, 2-ethyl-1-hexanol, acetoin and 1-hexanol. Our results underscore the ability of the yeast strain to influence the volatolomic profile, from a quantitative point of view, by affecting the sensory perception of notes associated with the detected molecules.

3.4. Descriptive sensory analysis

In order to investigate the impact of the three cross-over strains on the sensory quality of beers obtained by using malt fortified with grape must, a sensory analysis was carried out. This study offers valuable insight into the sensory response of Italian consumers on this new version of beer, which has a particular aromatic complexity strongly influenced by the combination of malt and grape must.

The **Supplementary Table 2** reported the mean values of sensory descriptors used by trained panelists to describe visive, tactile, olfactory and gustative aspects of beers. Sensory analysis revealed that the yeast strain can significantly ($p < 0.05$) affect some of the attributes considered, including foam color, amount and persistence of foam, effervescence, olfactory finesse, floral, yeast and fruity smell, acidity, and finally overall quality. Spider plots for the aroma (visive, tactile, olfactory attributes) and taste profiles, reporting the mean values of samples, are shown in **Figures 3A, B**.

The comparison of the ANOVA results (**Supplementary Table 2**) and the sensory radar plots (A-B) (**Figure 3**), indicated that all IGA beers showed high scores (≥3) for "olfactory finesse" and "olfactory intensity," probably due to the complexity of volatile profiles characterized by molecules belonging to different classes. Some of them, having an OAV > 1, directly affected odor perception, while the molecules having an OAV < 1 might have contributed to the beer flavor through the additive effects of compounds with similar structure or odor (Francis and Newton, 2005). All beers were characterized by medium-high scores for fruity and floral descriptors, which are influenced by wine must

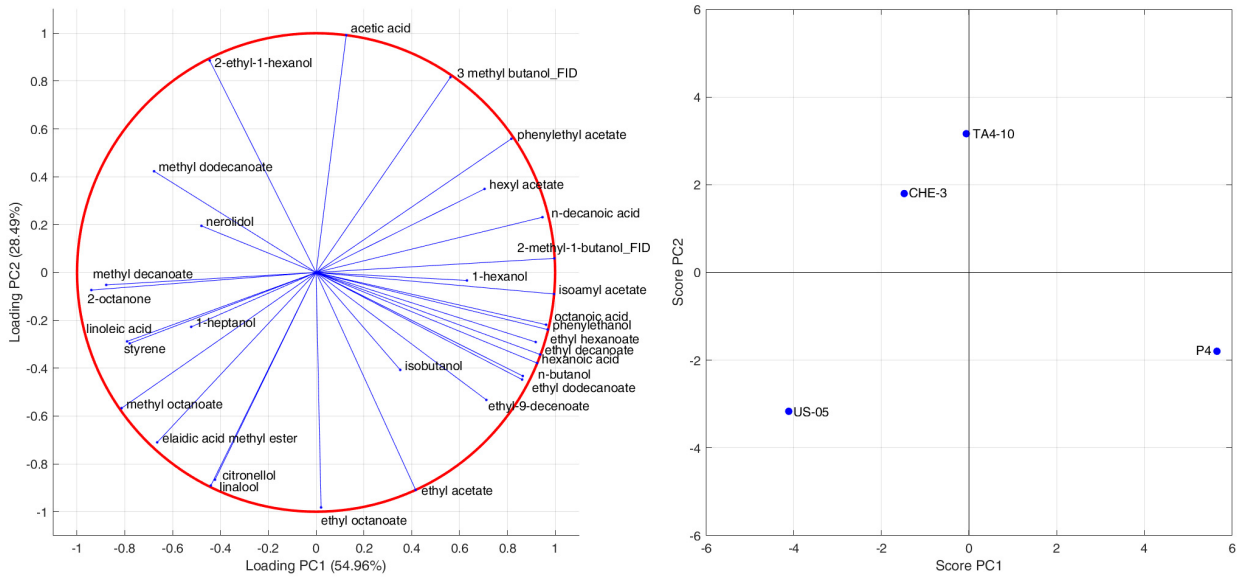

FIGURE 1
Pearson principal component analysis performed on GC-MS data for the detection of volatile compounds.

addition and then by yeast action (De Francesco et al., 2021). The floral notes are associated with terpenes, varietal molecules found in grapes, while the fruity character is mainly related to alcohols (i.e., phenyl ethanol) and esters, fermentation by-products. P4 beer was judged to have the higher score for fruity (4.25) than others, probably linked to the high ester content. Yeast smell was a descriptor with the higher score (3.25) in CHE-3 and TA4-10. **Figure 3B** illustrated the radar plot of taste profile. Among gustative descriptors, acidity was perceived in scores significantly different, with high values (3.75) in TA4-10. Medium scores for sweetness are detected in all IGAs, ranged from 2 (US-05) to 2.5 (TA4-10; CHE-3), probably due to low sugar residual content.

A PCA was applied to analyze the covariance of sensory descriptors judged by panelists (**Figures 4A, B**). The first two principal components explained the 94.08% of the variance (78.74 and 15.34% for PC1 and PC2, respectively). PC1 components separated P4 from the other samples. Indeed, P4 beer was positioned at negative values of PC1, which can be related to its olfactory finesse and overall olfactory intensity, as well as caramel, floral and fruity descriptors intensity. By contrast, CHE-3 and T4-10, clustering in the same quadrant delimited by positive PC1 and PC2, contributed to variance thanks to smoked, yeast, malt and hop olfactory descriptors. The body, effervescence, spices smell and then particular characteristics of foam, described by positive PC1 and negative PC2, influenced US05. Undoubtedly, foam is one of the key attributes of beer that differentiates it from other beverages. Different factors, endogenous or exogenous, significantly affect foam consistency and persistence, including protein components, hop acids, non-starch polysaccharides, metal ions, lipids, proteolytic enzymes, ethanol concentration, basic amino acids, as well as malting and brewing processes (Blasco et al., 2011; Donadini et al., 2011). Moreover, yeast proteins also play a secondary role in enhancing the foam (Lao et al., 1999). In particular, the beer produced with the TA4-10 strain was characterized by the visive attributes "amount and persistence of foam," the gustative descriptor "acidity," and then "overall quality," whereas the P4 one was distinguished by olfactory notes "fruity smell and floral" and "olfactory finesse."

In our research, Partial Least Square-Correlation (PLSC) analysis was applied to study the relationship between two different groups of data obtained with different techniques, as reported in literature (Aznar et al., 2003; Vilanova et al., 2010; Delgado et al., 2022; Palombi et al., 2023). In particular, PLSC was used to study the correlation between volatile compounds and olfactive and visive descriptors scores and **Figure 5** showed the score and loading plot of the first two PLSC components for the volatiles/olfactive-visive descriptors. The first two components explained, respectively the 48.9% and 32.5% of the multivariate covariance between the two datasets. In detail, the correlation coefficient between the scores of the first component of volatiles data and the scores of the first component of sensory data was 0.9873 (p-value = 0.013), whereas for the second components the correlation coefficient was 0.9825 (p-value = 0.0175).

The P4 strain contributed to the overall correlation between the datasets with higher concentration of ethyl esters (ethyl hexanoate, ethyl decanoate, ethyl dodecanoate), acetate esters (isoamyl acetate, ethyl-9-decenoate), hexanoic acid. These molecules were correlated to the fruity smell and olfactory finesse, indicating the contribution of esters on fruity notes in IGA beers. US-05 was positively correlated with terpenes (citronellol, linalool), ethyl octanoate, ethyl acetate, isobutanol and was characterized by "floral, spicy and caramel" notes and more pronounced "overall olfactory intensity."

Finally, CHE-3 and TA4-10, differed from the others for a positive correlation with few volatiles, including 2-ethyl-1-hexanol, acetic acid, methyl dodecanoate and nerolidol, while, on the sensorial-olfactory level, they displayed high correlation with "smoked, yeast and malt smell" and then a good quality of foam.

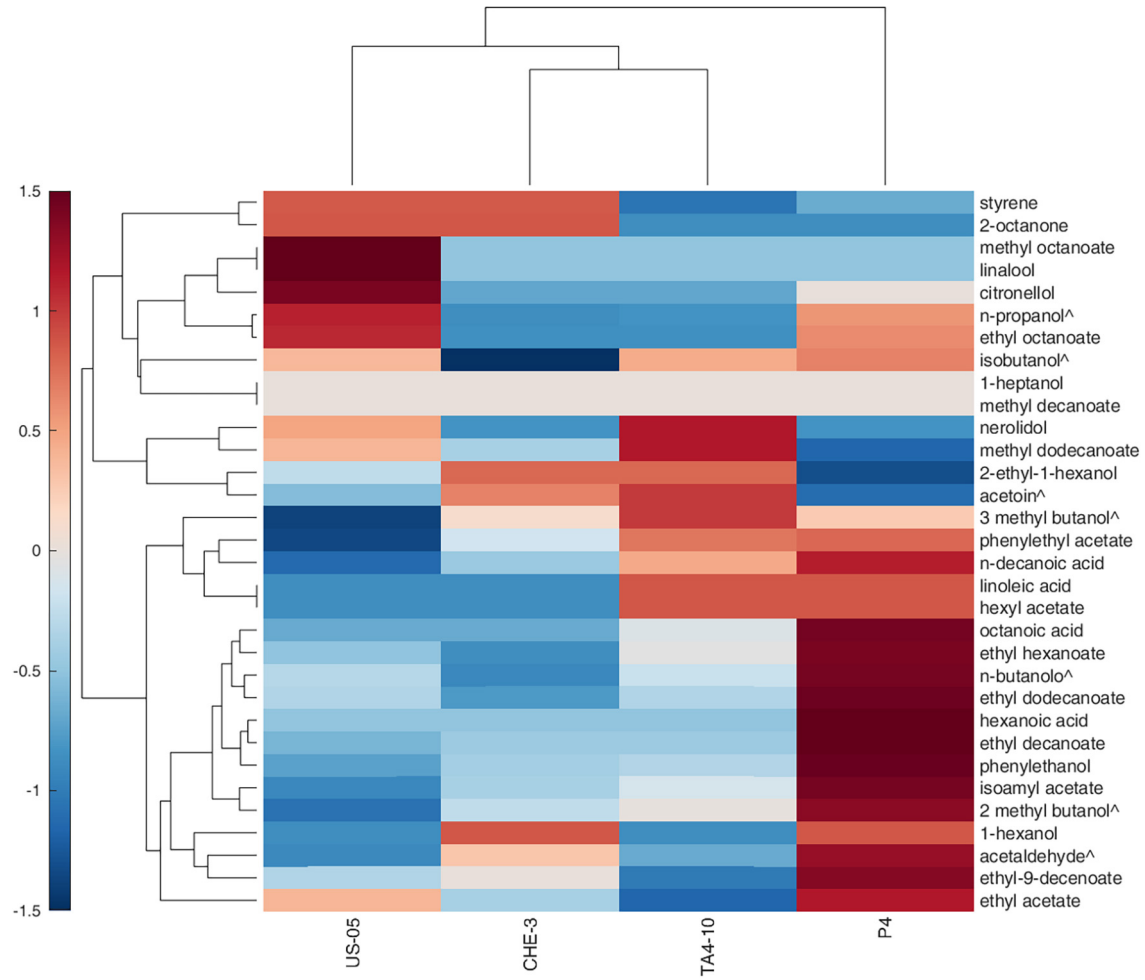

FIGURE 2
Hierarchical clustering heat map performed on the GC-MS normalized data (distance measure using Euclidean and clustering algorithm using average). Each colored cell on the map corresponds to a concentration value in the data table, with samples in columns and metabolites in rows. Molecules indicated with ^ are detected by GC-FID.

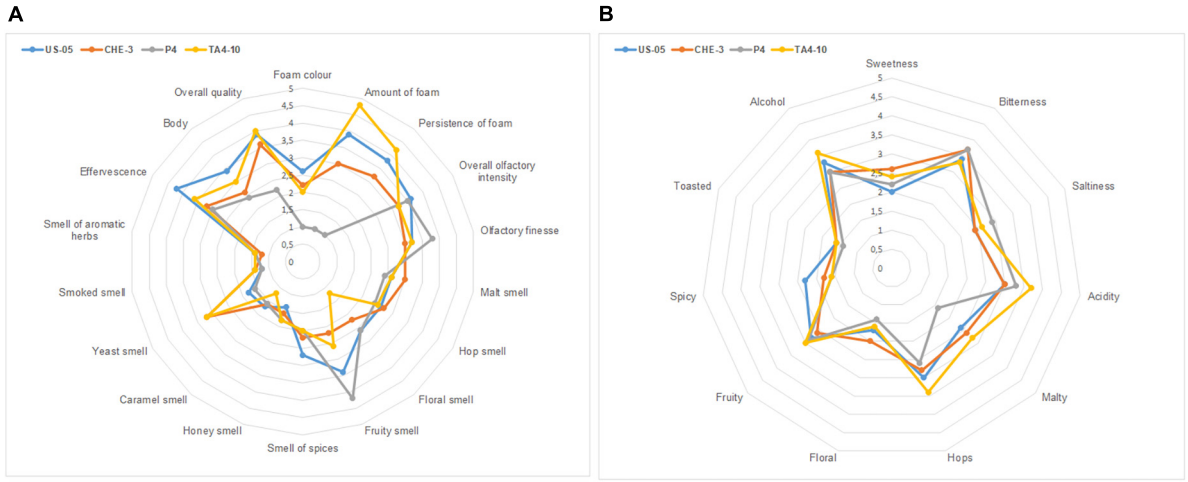

FIGURE 3
Radar plots of visive, tactile, olfactory **(A)** and gustative **(B)** descriptors indicated by panelists.

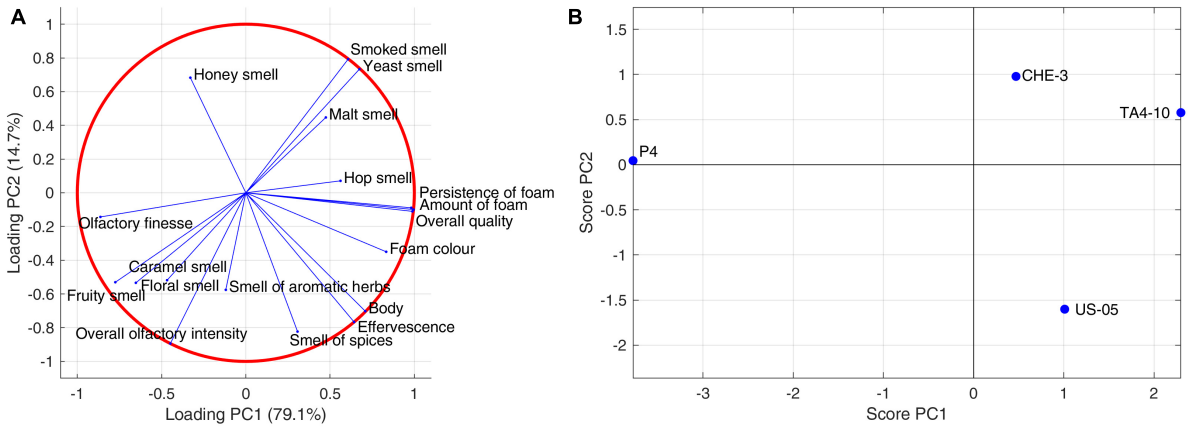

FIGURE 4
Principal component analysis performed on sensory (olfactive-tactile and visive) descriptors: **(A)** sensory data correlation circle; **(B)** sensory data score plot.

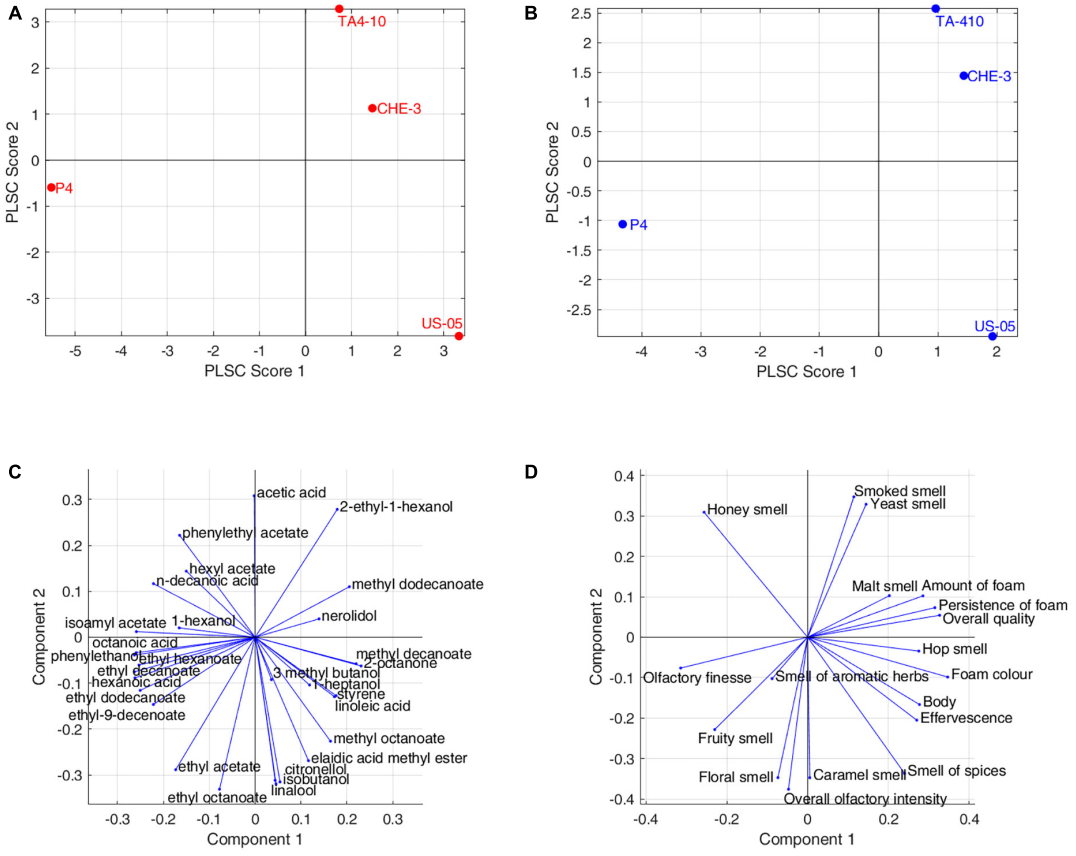

FIGURE 5
Partial least squares correlation between volatolomic and olfactory profiles: **(A)** volatolomic score plot; **(B)** olfactory score plot; **(C)** volatolomic loadings plot; **(D)** olfactory loadings plot.

3.5. Consumer test

In the last step of the research, the beer samples were submitted to evaluation of consumer liking. This is fundamental to identify the reason for the success (or failure) of a product and its market opportunities, giving useful indication about the suitability of a testing beer for full scale production in the breweries. The panel was composed of 69% females and 31% males, with an average consumer age of 44 ± 14 years old and ranged from 21 to 75 years old. The recruited consumers rated the following parameters: appearance liking, taste liking, odor liking and then overall liking. The mean values and standard deviations for each descriptor are reported in **Supplementary Table 3**. One-way ANOVA and multi-way ANOVA (with and without factors interaction) were

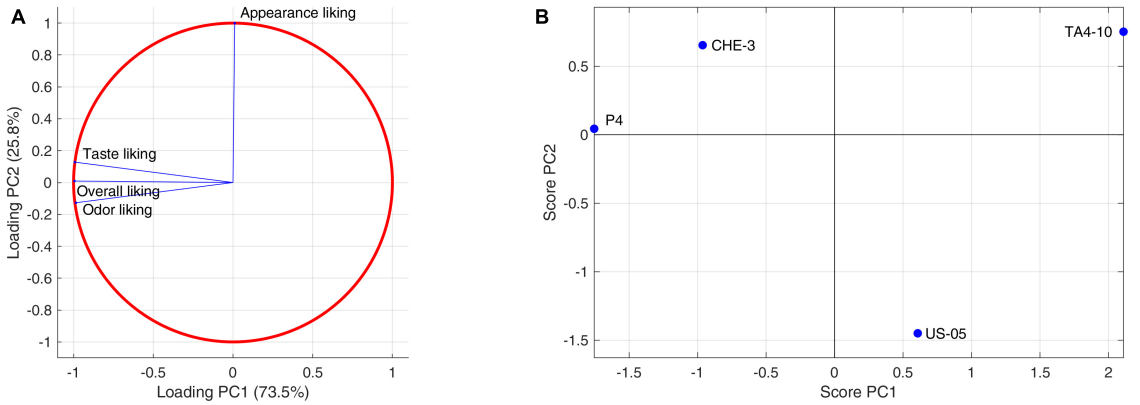

FIGURE 6
Principal component analysis performed on consumers descriptors: **(A)** consumers liking data correlation circle; **(B)** consumers liking data score plot.

conducted to explore the hedonic responses of the consumers. The factors taken into account were the different beer samples, the gender and the consumer age (this divided in three classes: 18 to 31 years, 31 to 45 years and 46 to 60 years). Results showed no significant differences ($p < 0.05$), for beer sample, gender and age class. No statistically significant interactions were found.

A PCA was applied also to liking attributes judged by the consumers (Figures 6A, B). Although the samples differences are not statistically significant, the plane identified by the first two components, describing 99% of the total variance, shows a clear differentiation of the samples. PC1 (73.5%) is closely related to smell, taste, and overall liking, attributes that are highly correlated with each other. Sample scores allow us to establish a higher liking for P4 and CHE-3 beers as regards these attributes, with above-average liking values. Lower approval ratings were associated with US05 and TA4-10 beers. PC2 (25.8%), on the other hand, is almost exclusively linked to appearance, an attribute perceived to a greater extent in the CHE-3 and TA4-10 samples, to an average extent in P4, and to a lesser extent in the control US-05.

Both sensory analysis and consumers' test indicated that beer obtained by using P4 (Figures 4B, 6B, respectively), characterized by higher fruity and floral notes, which significantly influenced the finesse and olfactory intensity, was the most appreciated beer for smell, taste, and overall quality. On the other hand, the CHE-3 and TA4-10 samples, with better visual properties related to the consistency and color of the foam influencing the overall quality, were appreciated above all for their appearance. Given all that, the cross-over strains tested contributed positively to the improvement of the various sensory aspects of the beers produced, validating the results previously obtained during laboratory-scale fermentations (Siesto et al., 2023).

4. Conclusion

In the present study, the applicability of *S. cerevisiae* strains selected from different food matrices for the production of craft IGA beers was investigated for the first time through a multidisciplinary chemistry-multivariate approach. Overall, the strains tested showed the ability to degrade maltose during fermentation and contribute to the qualitative complexity of the final products. In particular, beer obtained by inoculating P4 strain showed high content of some classes of volatile molecules, including alcohols, esters, and volatile acids, as shown by the cluster heatmap and PCA. In agreement with the chemical data, the sensory analysis performed by a trained panel on P4 sample revealed more pronounced fruity and floral notes. On the other hand, TA4-10 differed from the control (US-05) and from the other samples (CHE-3, P4) especially for the visual attributes "quantity and persistence of foam," for the taste descriptor "acidity" and for its "overall quality."

In terms of consumer acceptability, the overall liking, odor-taste-appearance liking were not significantly different among four beers, but consumer group showed a preference for P4, concerning odor-taste-overall liking, whereas CHE-3 and TA4-10 were preferred for appearance. An interesting result is the highest consumer preference toward beers obtained by using indigenous *S. cerevisiae* strains.

Moreover, the PLSC clearly indicated how crucial the interaction between analytical and sensory data is in obtaining a snapshot of the overall quality of the fermented beverage, which is useful in standardizing a fermentation process. In conclusion, this work represents the first phase of a wider project for the qualitative improvement of IGA beers, which will industrially employ indigenous cross over starter cultures as potential approach to improve the organoleptic profile of this innovative beverage and to tie it to the culture and history of the production area.

Data availability statement

The original contributions presented in this study are included in the article/Supplementary material, further inquiries can be directed to the corresponding authors.

Author contributions

MT: conceptualization, investigation, data curation, writing–original draft, and writing–review and editing. LP: data

curation, formal analysis, data acquisition, software, validation, writing–original draft, and writing–review and editing. FG: conceptualization, writing–original draft, and writing–review and editing. CG, ABr, and FGe: data acquisition and writing–review and editing. AC: conceptualization, funding acquisition, investigation, data acquisition, writing–original draft, and writing–review and editing. GS and RP: investigation, methodology, data acquisition, data curation, and writing–review and editing. ABa: data acquisition, writing–original draft, and writing–review and editing. All authors contributed to the article and approved the submitted version.

Funding

This work was granted by the European Commission – NextGenerationEU, Project "Strengthening the MIRRI Italian Research Infrastructure for Sustainable Bioscience and Bioeconomy," code no. IR0000005.

Acknowledgments

We wish to thank the Birrificio Sorrento Microbrewery (Sorrento, Italy) for making the microbrewery available and Dr. Giuseppe Schisano for supporting the technical experimental design during brewing.

Conflict of interest

GS and AC were employed by Spinoff StarFInn S.r.l.s.

The remaining authors declare that the research was conducted in the absence of any commercial or financial relationships that could be construed as a potential conflict of interest.

Publisher's note

All claims expressed in this article are solely those of the authors and do not necessarily represent those of their affiliated organizations, or those of the publisher, the editors and the reviewers. Any product that may be evaluated in this article, or claim that may be made by its manufacturer, is not guaranteed or endorsed by the publisher.

Supplementary material

The Supplementary Material for this article can be found online at: https://www.frontiersin.org/articles/10.3389/fmicb.2023.1234884/full#supplementary-material

References

Aquilani, B., Laureti, T., Poponi, S., and Secondi, L. (2015). Beer choice and consumption determinants when craft beers are tasted: an exploratory study of consumer preferences. *Food Qual. Prefer.* 41, 214–224. doi: 10.1016/j.foodqual.2014.12.005

Armijo, G., Schlechter, R., Agurto, M., Mũnoz, D., Nuñez, C., and Arce-Johnson, P. (2016). Grapevine pathogenic microorganisms: understanding infection strategies and host response scenarios. *Front. Plant Sci.* 7:382. doi: 10.3389/fpls.2016.00382

Aznar, M., López, R., Cacho, J., and Ferreira, V. (2003). Prediction of aged red wine aroma properties from aroma chemical composition. Partial least squares regression models. *J. Agric. Food Chem.* 51, 2700–2707. doi: 10.1021/jf026115z

Baiano, A., Fiore, A., la Gatta, B., Tufariello, M., Gerardi, C., Savino, M., et al. (2023). Single and interactive effects of unmalted cereals, hops, and yeasts on quality of white-inspired craft beers. *Beverages* 9:9. doi: 10.3390/beverages9010009

Bellut, K., Michel, M., Zarnkow, M., Hutzler, M., Jacob, F., De Schutter, D., et al. (2018). Application of non-*Saccharomyces* yeasts isolated from Kombucha in the production of alcohol-free beer. *Fermentation* 4:66. doi: 10.3390/fermentation4030066

Berbegal, C., Fragasso, M., Russo, P., Bimbo, F., Grieco, F., Spano, G., et al. (2019). Climate changes and food quality: the potential of microbial activities as mitigating strategies in the wine sector. *Fermentation* 5:85. doi: 10.3390/fermentation5040085

Berbegal, C., Spano, G., Fragasso, M., Grieco, F., Russo, P., and Capozzi, V. (2018). Starter cultures as biocontrol strategy to prevent *Brettanomyces bruxellensis* proliferation in wine. *Appl. Microbiol. Biotechnol.* 102, 569–576. doi: 10.1007/s00253-017-8666-x

BJCP, (2015). *Beer style guidlines, Beer Judge Certification Program*. Available online at: https://www.bjcp.org/download/2021_Guidelines_Beer.pdf (accessed May 17, 2023).

Blasco, L., Viñas, M., and Villa, T. (2011). Proteins influencing foam formation in wine and beer: the role of yeast. *Int. Microbiol.* 14, 61–71. doi: 10.2436/20.1501.01.136

Capece, A., De Fusco, D., Pietrafesa, R., Siesto, G., and Romano, P. (2021). Performance of wild non- conventional yeasts in fermentation of wort based on different malt extracts to select novel starters for low-alcohol beers. *Appl. Sci.* 11:801. doi: 10.3390/app11020801

Capece, A., Pietrafesa, R., and Romano, P. (2011). Experimental approach for target selection of wild wine yeasts from spontaneous fermentation of "Inzolia" grapes. *World J. Microbiol. Biotechnol.* 27, 2775–2783. doi: 10.1007/s11274-011-0753-z

Capece, A., Romaniello, R., Pietrafesa, A., Siesto, G., Pietrafesa, R., Zambuto, M., et al. (2018). Use of *Saccharomyces cerevisiae* var. *boulardii* in co-fermentations with *S. cerevisiae* for the production of craft beers with potential healthy value-added. *Int. J. Food Microbiol.* 284, 22–30. doi: 10.1016/j.ijfoodmicro.2018.06.028

Capece, A., Romaniello, R., Siesto, G., Pietrafesa, R., Massari, C., Poeta, C., et al. (2010). Selection of indigenous *Saccharomyces cerevisiae* strains for Nero d'Avola wine and evaluation of selected starter implantation in pilot fermentation. *Int. J. Food Microbiol.* 144, 187–192. doi: 10.1016/j.ijfoodmicro.2010.09.009

Castro Marin, A., Baris, F., Romanini, E., Lambri, M., Montevecchi, G., and Chinnici, F. (2021). Physico-chemical and sensory characterization of a fruit beer obtained with the addition of cv. Lambrusco grapes must. *Beverages* 7:34. doi: 10.3390/beverages7020034

Crupi, P., Coletta, A., and Antonacci, D. (2010). Analysis of carotenoids in grapes to predict norisoprenoid varietal aroma of wines from Apulia. *J. Agric. Food Chem.* 58, 9647–9656. doi: 10.1021/jf100564v

Cubillos, F. A., Gibson, B., Grijalva-Vallejos, N., Krogerus, K., and Nikulin, J. (2019). Bioprospecting for brewers: exploiting natural diversity for naturally diverse beers. *Yeast* 36, 383–398. doi: 10.1002/yea.3380

Dank, A., van Mastrigt, O., Yang, Z., Dinesh, V., Lillevang, S., Weij, C., et al. (2021). The cross-over fermentation concept and its application in a novel food product: the dairy miso case study. *LWT* 142:111041. doi: 10.1016/j.lwt.2021.111041

De Francesco, G., Marconi, O., Sileoni, V., and Perretti, G. (2021). Barley malt wort and grape must blending to produce a new kind of fermented beverage: a physicochemical composition and sensory survey of commercial products. *J. Food Composit. Anal.* 103:104112. doi: 10.1016/j.jfca.2021.104112

De Simone, N., Russo, P., Tufariello, M., Fragasso, M., Solimando, M., Capozzi, V., et al. (2021). Autochthonous biological resources for the production of regional craft beers: exploring possible contributions of cereals, hops, microbes, and other ingredients. *Foods* 10:1831. doi: 10.3390/foods10081831

Delgado, J., Sánchez-Palomo, E., Alises, M. O., and Viñas, M. (2022). Chemical and sensory aroma typicity of La Mancha Petit Verdot wines. *LWT* 162:113418. doi: 10.1016/j.lwt.2022.113418

Donadini, G. N., Fumi, M., and De Faveri, M. (2011). How foam appearance influences the Italian consumer's beer perception and preference. *J. Inst. Brew* 117, 523–533. doi: 10.1002/j.2050-0416.2011.tb00500.x

Francis, I. L., and Newton, J. L. (2005). Determining wine aroma from compositional data. *Aust. J. Grape Wine Res.* 11, 114–126. doi: 10.1111/j.1755-0238.2005.tb00283.x

Garavaglia, C., and Swinnen, J. (2018). *Economic perspectives on craft beer: a revolution in the global beer industry*. Berlin: Springer.

Gibson, B., Geertman, J., Hittinger, C., Krogerus, K., Libkind, D., Louis, E., et al. (2017). New yeasts—new brews: modern approaches to brewing yeast design and development. *FEMS Yeast Res.* 17:fox038. doi: 10.1093/femsyr/fox038

Hittinger, C., Steele, J., and Ryder, D. (2018). Diverse yeasts for diverse fermented beverages and foods. *Curr. Opin. Biotechnol.* 49, 199–206. doi: 10.1016/j.copbio.2017.10.004

Holt, S., Mukherjee, V., Lievens, B., Verstrepen, K., and Thevelein, J. (2018). Bioflavoring by non-conventional yeasts in sequential beer fermentations. *Food Microbiol.* 72, 55–66. doi: 10.1016/j.fm.2017.11.008

Humia, B. V., Santos, K., Barbosa, A., Sawata, M., Mendonça, M., and Padilha, F. (2019). Beer molecules and its sensory and biological properties: a review. *Molecules* 24:1568. doi: 10.3390/molecules24081568

Lao, C., Santamaria, A., López-Tamames, E., Bujan, J., Buxaderas, S., and De la Torre-Boronat, M. C. (1999). Effect of grape pectic enzyme treatment on foaming properties of white musts and wines. *Food Chem.* 65, 169–173. doi: 10.1016/S0308-8146(98)00181-2

Li, M., Du, J., and Zhang, K. (2020). Profiling of carbohydrates in commercial beers and their influence on beer quality. *J. Sci. Food Agric.* 100, 3062–3070. doi: 10.1002/jsfa.10337

Marconi, O., Rossi, S., Galgano, F., Sileoni, V., and Perretti, G. (2016). Influence of yeast strain, priming solution and temperature on beer bottle conditioning. *J. Sci. Food Agric.* 96, 4106–4115. doi: 10.1002/jsfa.7611

Mascia, I., Fadda, C., Dostálek, P., Karabín, M., Zara, G., Budroni, M., et al. (2015). Is it possible to create an innovative craft durum wheat beer with sourdough yeasts? A case study. *J. Inst. Brew* 121, 283–286. doi: 10.1002/jib.215

Matukas, M., Starkute, V., Zokaityte, E., Zokaityte, G., Klupsaite, D., Mockus, E., et al. (2022). Effect of different yeast strains on biogenic amines, volatile compounds and sensory profile of beer. *Foods* 11:2317. doi: 10.3390/foods11152317

Meilgaard, M., and Peppard, T. (1986). "Food flavours: part b, the flavour of beverages," in *The Flavour of Beer*, eds I. D. Morton and A. J. Macleod (Amsterdam: Elsevier), 99–170.

Olaniran, A., Hiralal, L., Mokoena, M., and Pillay, B. (2017). Flavour-active volatile compounds in beer: production, regulation and control. *J. Inst. Brew* 123, 13–23. doi: 10.1002/jib.389

Pallmann, C., Brown, J., Olineka, T., Cocolin, L., Mills, D., and Bisson, L. (2001). Use of WL medium to profile native flora fermentations. *Am. J. Enol. Viticult.* 52, 198–203. doi: 10.5344/ajev.2001.52.3.198

Palombi, L., Tufariello, M., Durante, M., Fiore, A., Baiano, A., and Grieco, F. (2023). Assessment of the impact of unmalted cereals, hops, and yeast strains on volatolomic and olfactory profiles of Blanche craft beers: a chemometric approach. *Food Chem.* 416:135783. doi: 10.1016/j.foodchem.2023.135783

Peryam, D. R., and Pilgrim, F. J. (1957). Hedonic scale method of measuring food preferences. *Food Technol.* 11(Suppl.), 9–14.

Pinho, O., Ferreira, I., and Santos, L. (2006). Method optimization by solid-phase microextraction in combination with gas chromatography with mass spectrometry for analysis of beer volatile fraction. *J. Chromatogr. A.* 1121, 145–153. doi: 10.1016/j.chroma.2006.04.013

Popescu, V., Soceanu, A., Dobrinas, S., and Stanciu, G. (2013). A study of beer bitterness loss during the various stages of the Romanian beer production process. *J. Inst. Brew* 119, 111–115. doi: 10.1002/jib.82

Rodrigues, F., Caldeira, M., and Câmara, J. (2008). Development of a dynamic headspace solid-phase microextraction procedure coupled to GC–qMSD for evaluation the chemical profile in alcoholic beverages. *Anal. Chem. Acta* 609, 82–104. doi: 10.1016/j.aca.2007.12.041

Romano, G., Tufariello, M., Calabriso, N., Del Coco, L., Fanizzi, F., Blanco, A., et al. (2023). Laddomada B. Pigmented cereals and legume grains as healthier alternatives for brewing beers. *Food Biosci.* 52:102463. doi: 10.1016/j.fbio.2023.102463

Rossi, S., Sileoni, V., Perretti, G., and Marconi, O. (2014). Characterization of the volatile profiles of beer using headspace solid-phase microextraction and gas chromatography–mass spectrometry. *J. Sci. Food Agric.* 94, 919–928. doi: 10.1002/jsfa.6336

Schreier, P., and Jennings, W. (1979). Flavor composition of wines: a review. *Crit. Rev. Food Sci. Nutr.* 12, 59–111. doi: 10.1080/10408397909527273

Siesto, G., Pietrafesa, R., Tufariello, M., Gerardi, C., Grieco, F., and Capece, A. (2023). Application of microbial cross-over for the production of Italian grape ale (IGA), a fruit beer obtained by grape must addition. *Food Biosci.* 52:102487. doi: 10.1016/j.fbio.2023.102487

Slegers, A., Angers, P., Ouellet, E., Truchon, T., and Pedneault, K. (2015). Volatile compounds from grape skin, juice and wine from five interspecific hybrid grape cultivars grown in Quebec (Canada) for wine production. *Molecules* 20, 10980–11016. doi: 10.3390/molecules200610980

Steensels, J., Meersman, E., Snoek, T., Saels, V., and Verstrepen, K. (2014a). Large-scale selection and breeding to generate industrial yeasts with superior aroma production. *Appl. Environ. Microbiol.* 80, 6965–6975. doi: 10.1128/AEM.02235-14

Steensels, J., Snoek, T., Meersman, E., Nicolino, M., Voordeckers, K., and Verstrepen, K. (2014b). Improving industrial yeast strains: exploiting natural and artificial diversity. *FEMS Microbiol. Rev.* 38, 947–995. doi: 10.1111/1574-6976.12073

Streissguth, A., Bookstein, F., Sampson, P., and Barr, H. (1993). *Methods of latent variable modeling by partial least squares. The enduring effects of prenatal alcohol exposure on child development*. Ann Arbor, MI: University of Michigan Press.

Tucker, L. R. (1958). An inter-battery method of factor analysis. *Psychometrika* 23, 111–136. doi: 10.1007/BF02289009

Tufariello, M., Maiorano, G., Rampino, P., Spano, G., Grieco, F., Perrotta, C., et al. (2019). Selection of an autochthonous yeast starter culture for industrial production of Primitivo "Gioia del Colle" PDO/DOC in Apulia (Southern Italy). *LWT* 99, 188–196. doi: 10.1016/j.lwt.2018.09.067

Valles, B., Bedriñana, R., Queipo, A., and Alonso, J. (2008). Screening of cider yeasts for sparkling cider production (*Champenoise* method). *Food Microbiol.* 25, 690–697. doi: 10.1016/j.fm.2008.03.004

Vilanova, M., and Sieiro, C. (2006). Contribution by *Saccharomyces cerevisiae* yeast to fermentative flavour compounds in wines from cv. Albariño. *J. Ind. Microbiol. Biotechnol.* 33, 929–933. doi: 10.1007/s10295-006-0162-8

Vilanova, M., Genisheva, Z., Masa, A., and Oliveira, J. M. (2010). Correlation between volatile composition and sensory properties in Spanish Albariño wines. *Microchem. J.* 95, 240–246. doi: 10.1016/j.microc.2009.12.007

Zhao, X., Procopio, S., and Becker, T. (2015). Flavor impacts of glycerol in the processing of yeast fermented beverages: a review. *J. Food Sci. Technol.* 52, 7588–7598. doi: 10.1007/s13197-015-1977-y

frontiers | Frontiers in Microbiology

TYPE Original Research
PUBLISHED 07 August 2023
DOI 10.3389/fmicb.2023.1205767

OPEN ACCESS

EDITED BY
Michela Verni,
Sapienza University of Rome, Italy

REVIEWED BY
Luis Henrique Souza Guimarães,
University of São Paulo, Brazil
Eliane Ferreira Noronha,
University of Brasilia, Brazil
Guadalupe Gutiérrez,
Universidad Autonoma de Nuevo, Mexico

*CORRESPONDENCE
Yongping Xu
✉ xyping@dlut.edu.cn

RECEIVED 14 April 2023
ACCEPTED 25 July 2023
PUBLISHED 07 August 2023

CITATION
Li G, Yuan Y, Jin B, Zhang Z, Murtaza B, Zhao H, Li X, Wang L and Xu Y (2023) Feasibility insights into the application of *Paenibacillus pabuli* E1 in animal feed to eliminate non-starch polysaccharides.
Front. Microbiol. 14:1205767.
doi: 10.3389/fmicb.2023.1205767

Feasibility insights into the application of *Paenibacillus pabuli* E1 in animal feed to eliminate non-starch polysaccharides

Gen Li[1], Yue Yuan[2], Bowen Jin[1], Zhiqiang Zhang[1], Bilal Murtaza[1], Hong Zhao[1], Xiaoyu Li[1], Lili Wang[1] and Yongping Xu[1]*

[1]School of Bioengineering, Dalian University of Technology, Dalian, China, [2]School of Biological Engineering, Dalian Polytechnic University, Dalian, China

The goal of the research was to find alternative protein sources for animal farming that are efficient and cost-effective. The researchers focused on distillers dried grains with solubles (DDGS), a co-product of bioethanol production that is rich in protein but limited in its use as a feed ingredient due to its high non-starch polysaccharides (NSPs) content, particularly for monogastric animals. The analysis of the *Paenibacillus pabuli* E1 genome revealed the presence of 372 genes related to Carbohydrate-Active enzymes (CAZymes), with 98 of them associated with NSPs degrading enzymes that target cellulose, hemicellulose, and pectin. Additionally, although lignin is not an NSP, two lignin-degrading enzymes were also examined because the presence of lignin alongside NSPs can hinder the catalytic effect of enzymes on NSPs. To confirm the catalytic ability of the degrading enzymes, an *in vitro* enzyme activity assay was conducted. The results demonstrated that the endoglucanase activity reached 5.37 U/mL, while beta-glucosidase activity was 4.60 U/mL. The filter paper experiments did not detect any reducing sugars. The xylanase and beta-xylosidase activities were measured at 11.05 and 4.16 U/mL, respectively. Furthermore, the pectate lyase and pectin lyase activities were found to be 8.19 and 2.43 U/mL, respectively. The activities of laccase and MnP were determined as 1.87 and 4.30 U/mL, respectively. The researchers also investigated the effect of *P. pabuli* E1 on the degradation of NSPs through the solid-state fermentation of DDGS. After 240 h of fermentation, the results showed degradation rates of 11.86% for hemicellulose, 11.53% for cellulose, and 8.78% for lignin. Moreover, the crude protein (CP) content of DDGS increased from 26.59% to 30.59%. In conclusion, this study demonstrated that *P. pabuli* E1 possesses various potential NSPs degrading enzymes that can effectively eliminate NSPs in feed. This process improves the quality and availability of the feed, which is important for animal farming as it seeks alternative protein sources to replace traditional nutrients.

KEYWORDS

NSPs, DDGS, degradation, *Paenibacillus*, fermentation

1. Introduction

Pigs play a pivotal role as a primary source of meat and protein for human consumption (Casellas et al., 2013). The demand for pig feed is exceptionally high, accounting for over 20% of the total animal feed production (Mottet et al., 2017). With the current global maize production reaching 114.8 million tons (Wang et al., 2021), maize serves as the predominant

raw material in swine feed formulation. However, the escalating demand for maize in the swine industry poses a significant challenge, as it competes directly with human food sources, thereby compromising long-term sustainability. Consequently, the development of nutritious and efficient swine feeds assumes strategic significance in addressing the pressing issue of global food shortages.

The United States and Brazil hold significant prominence as the foremost global producers of fuel ethanol. In the year 2021, the collective global production of bioethanol amounted to a substantial 27.22 billion gallons. Among the major contributors, the United States spearheaded the production with a noteworthy output of 15.01 billion gallons, closely followed by Brazil at 7.43 billion gallons. Remarkably, the combined efforts of the United States and Brazil accounted for an impressive 82.3% of the world's total ethanol production (Filipe et al., 2023). Currently, corn ethanol production is predominant in the United States, while sugarcane ethanol production is predominant in Brazil. A significant by-product of sugarcane processing is bagasse (Sugarcane Bagasse SB), which contains approximately 2.1% to 2.9% crude protein, 79.4% to 88.3% neutral detergent fiber, 62.2% to 69.8% acid detergent fiber, 22.1% total lignin, 10.3% to 10.5% acid detergent lignin, 1.4% ash, and some extracts (Arntzen et al., 2021; de Lucas et al., 2021). Bagasse has low crude protein content and high cellulose and lignin content, making it suitable for ruminant feed. Ruminants have various microorganisms in their rumen that can digest and decompose cellulose and hemicellulose (de Almeida et al., 2018). On the other hand, distillers dried grains with solubles (DDGS), a co-product of corn fermentation, is high in protein and can serve as a substitute protein feed ingredient (Streams, 2006; Pahm et al., 2009). Corn is the primary grain used for ethanol production in the United States and China. Approximately 1.4 L of ethanol and 1 kilogram of DDGS are produced from every 3 kilograms of fermented corn (Mohammadi Shad et al., 2021). DDGS has been recognized as a valuable source of protein, energy, water-soluble vitamins, lutein, and linoleic acid (Lumpkins et al., 2005) and is utilized as an alternative ingredient in swine feed. The global annual output of DDGS exceeds 40 million tons, with China alone producing over 15 million tons. As a new high-quality protein resource, DDGS can help reduce the overall amount of feed required and partially alleviate the significant feed shortage (Abd El-Hack et al., 2018).

Non-starch polysaccharides (NSPs) are widely distributed anti-nutritional factors found in plant-derived feeds. Cereals, including corn, have high levels of NSPs, mainly composed of pentosan, glucan, and cellulose. Compared to corn, DDGS has varying crude protein content ranging from 26.7% to 32.9%, with concentrated levels of NSPs (Min et al., 2009). DDGS contains xylan ranging from 9.1% to 18.4% and cellulose ranging from 6.3% to 14.7%. Monogastric animals lack the enzymes necessary to digest cellulose and xylan. NSPs increase chyme viscosity and hinder the interaction between digestive enzymes and nutrients, thereby greatly affecting nutrient absorption and utilization (Xu et al., 2009). As anti-nutritional factors, NSPs disrupt the physiological activities of intestinal microorganisms, reduce animal production performance, and have a more significant impact on young animals (Pedersen et al., 2014; Swiatkiewicz et al., 2016). Cellulose, a linear polymer of D-glucose units linked by beta-1,4-glycosidic bonds, forms microfibril units through hydrogen bonding between cellulose chains. These microfibril units assemble to create cellulose fibers, enhancing the stability and resistance of the cell wall against degradation (Thapa et al., 2020). Endo-1,4-beta-D-glucanases hydrolyze beta-1,4 linkages randomly in both soluble and insoluble cellulose chains. Cellobiohydrolases (CBHs) release cellobiose from the reducing (CBH II) and non-reducing (CBH I) ends of cellulose chains. Beta-glucosidases liberate D-glucose. Hemicellulose consists of pentose sugars (beta-D-xylose, alpha-L-arabinose), hexose sugars (beta-D-mannose, beta-D-glucose, and alpha-D-galactose), and aldonic acid (alpha-D-glucuronic acid; Girio et al., 2010; Escamilla-Alvarado et al., 2017). Hemicellulases can be categorized into three types: endoenzymes that act within the interior of polysaccharides, exoenzymes that hydrolyze from either the reducing or non-reducing ends, and coenzymes that act on branched chains. Hemicellulases encompass various enzymes such as xylanases, mannanases, beta-glucanases, galactanases, ferulic acid esterases, acetyl esterases, and arabinofuranosidases. Lignin, a three-dimensional biopolymer, forms complex structures composed of random propanol groups. It acts as a barrier, preventing cellulolytic enzymes from accessing their substrates by physically obstructing enzyme-cellulose interaction and hindering contact with hemicelluloses, leading to non-productive enzyme adsorption (Meng et al., 2020). Lignin-degrading enzymes primarily include laccases, manganese peroxidases, and lignin peroxidases (Bugg and Rahmanpour, 2015).

Consequently, the elimination of NSPs in feed ingredients is necessary. *Paenibacillus* species are widely distributed in various environments, particularly in soil, where they play roles in detoxification through biological nitrogen fixation (Xie et al., 2014), phosphate dissolution (Xie et al., 2016), production of the plant hormone indole-3-acetic acid (IAA; Patten et al., 2013), and release of siderophores (Raza and Shen, 2010), which promote crop growth. Some bacteria, including *Paenibacillus* species, produce antimicrobial agents such as bacteriocins and antimicrobial peptides that can be used to control phytopathogenic microorganisms, reducing the need for chemical fungicides that may negatively impact the environment (Xie et al., 2016). Various *Paenibacillus* species found in the soil produce glucans, chitinases, cellulases, and proteases involved in the degradation of eukaryotic cell walls (Grady et al., 2016; Seo et al., 2016). However, there are limited reports on the systematic study of non-starch polysaccharide degradation by *Paenibacillus*. The target bacteria in this study belong to the *Paenibacillus* genus. The purpose of this study is to explore the degradation effect of the target bacteria on non-starch polysaccharides in DDGS and improve the feeding value of DDGS.

Paenibacillus pabuli E1 was isolated from surface soil and stored in our laboratory. It has been thoroughly characterized and its genome has been completely sequenced. Carbohydrate-active enzymes (CAZymes) are a group of enzymes that degrade, modify, or generate glycosidic bonds, enabling efficient carbohydrate utilization. The CAZy database categorizes CAZymes into four types: glycoside hydrolases (GHs), glycosyl transferases (GTs), polysaccharide lyases (PLs), and carbohydrate esterases (CEs). The database also includes carbohydrate-binding modules (CBMs; Cantarel et al., 2009). In this study, we report the annotation of carbohydrate-active enzymes (CAZymes) of *P. pabuli* E1. The NSPs-degrading genes in the *P. pabuli* E1 genome were identified, and the structural information of different NSPs-degrading enzymes was comprehensively analyzed. The identification results based on CAZymes provide insights into the degradation mechanism of NSPs in feed and contribute to the design and development of useful microorganisms and enzyme preparations

for agriculture or feed. This study investigated the degradation ability of *P. pabuli* E1 on NSPs in DDGS and provides guidance for the fermentation application of *P. pabuli* E1 in eliminating NSPs in feed. The results offer a theoretical basis for the subsequent development of NSPs enzyme preparations.

2. Materials and methods

2.1. CAZyme annotation

The GenBank accession number for *P. pabuli* E1 is MT322455, and the strain preservation number is CGMCC NO.20517 (Li et al., 2021). All protein-encoding ORFs from *P. pabuli* E1 genomes were subjected to CAZy annotation using a two-step procedure of annotation and identification. BLASTp or Markov models were employed to confirm that the sequences belonged to the CAZyme family, and the information for each protein was collected (Bayer et al., 2008). The identification of CAZymes in *P. pabuli* E1 was performed using the HMMER (e-value < $1e^{-15}$, coverage > 0.35), and DIAMOND (e-value < $1e^{-102}$) tools in dbCAN (Tamaru et al., 2011). The results were analyzed to determine the presence of a secretory signal peptide or a transmembrane domain for each identified enzyme (Fabrice et al., 2002).

2.2. Growth condition

Luria-Bertani (LB) medium was composed of tryptone (20 g/L), yeast (10 g/L), and NaCl (20 g/L). Minimal mineral (MM) medium consisted of $(NH_4)_2SO_4$ (1 g/L), NaH_2PO_4 (0.5 g/L), K_2HPO_4 (0.5 g/L), $MgSO_4$ (0.2 g/L) and $CaCl_2$ (0.1 g/L). The polysaccharide medium was MM solid medium supplemented with agar (15 g/L) and different polysaccharides (1 g/L) such as carboxyl methyl cellulose (CMC), filter paper, cellulose powder, xylan, and pectin. LB medium supplemented with the above-mentioned polysaccharides (0.5 g/L) in addition to cellulose powder was used to produce degradative enzymes. The ability to degrade lignin was also tested because it is closely related to the above polysaccharides. All media were autoclaved at 121°C for 20 min. Before each experiment, *P. pabuli* E1 was reactivated in a fresh LB liquid medium. Cultures were incubated at 37°C on a shaker at 160 rpm for 48 h. The presence of spores can hinder the production of degradative enzymes in *P. pabuli* E1 cultures for more than 48 h. Hence, a 48-h incubation time was adopted for our experiments.

2.3. Enzyme assay

Paenibacillus pabuli E1 was cultivated in the LB medium for 48 h. After 10 min centrifugation of liquid culture (6,000 ×*g* at 4°C), both supernatant and cell pellets were collected. The supernatant was used as crude enzyme source, while cell pellets were disrupted by ultrasonication (300 W, 2 s interval 4 s, 7 min) in an ice bath and then centrifuged at 4°C, 6,000 ×*g* for 10 min. The filter paper disintegration experiment assessed the supernatant and cell insoluble fraction separately. To initiate the experiment, 50 mL of the medium was added with 0.05 g of circular filter paper and incubated at 37°C and 160 rpm, with phosphate buffered saline (PBS) solution serving as a control. The endo-cellulase activity was determined using the 3,5-dinitrosalicylic acid (DNS) method, as described by Miller (1959). The assay was conducted by combining approximately 0.05 mL of crude enzyme with 0.3 mL of 1% carboxymethyl cellulose (CMC) that was solubilized in a 0.05 M PBS (pH 7.0). The mixture was then incubated at 40°C in a water bath for a duration of 30 min. Subsequently, 0.285 mL of DNS solution was added, and the reaction was stopped by boiling the mixture in a water bath for 10 min. The liberated sugars were quantified by measuring the absorbance at 540 nm. The xylanase and pectate lyase activities were quantified using the DNS method, with xylan and pectin employed as the respective substrates. Beta-glucosidase activity was estimated by spectroscopic measurement of *p*-nitrophenol (pNP) released from *p*-nitrophenyl-beta-glucopyranoside (pNPG). The reaction mixture contained 0.4 mL of 1 mM pNPG, 0.5 mL of 0.1 M PBS buffer (pH 7.0), and 0.1 mL of crude enzyme solution. The reaction mixture was incubated at 37°C for 30 min. The reaction was stopped by the addition of 1.0 mL of 0.5 M Na_2CO_3, centrifuged at 6,000 ×*g* for 5 min at 4°C, and measured the absorbance at 400 nm. Beta-xylosidase activity was similarly estimated under the same conditions by measurement of pNP released from *p*-nitrophenyl-beta-D-xylopyranoside (pNPX). Pectin lyase acted on the alpha-1,4 glycosidic bonds in pectin, generating unsaturated oligogalacturonic acid with unsaturated bonds between C4 and C5 at the reducing end, which exhibited a characteristic absorption peak at 235 nm. Laccase decomposed 2,2-azino-bis(3-ethylbenz-thiazoline-6-sulfonate; ABTS) to produce ABTS radicals, with a significantly higher absorption coefficient at 420 nm than the substrate ABTS. The molar extinction coefficient of ABTS was 36,000 $L \cdot mol^{-1} \cdot cm^{-1}$. In the presence of Mn^{2+}, manganese peroxidase oxidized guaiacol to 4-o-methoxy phenol, which had an absorption peak at 465 nm. The activity of manganese peroxidase was determined by monitoring the change in absorbance at 465 nm. The molar extinction coefficient of guaiacol was 12,100 $L \cdot mol^{-1} \cdot cm^{-1}$. The MnP Enzyme Activity Detection Kit was obtained from Beijing Solarbio Science & Technology Co., Ltd., and other reagents were purchased from Sangon Biotech (Shanghai) Co., Ltd. The enzyme unit (U/mL) was calculated as the amount of enzyme required to release one μmol of reducing sugar or product per mL per minute.

2.4. Solid-state fermentation

DDGS was obtained from Weifang Yingxuan Industrial Co., LTD (Shandong, China). The inoculum concentration for DDGS fermentation was 10^7–10^8 CFU/mL. Sterile water was added to 50 g of feed, and the humidity was adjusted to 50% using a hygrometer. The mixture was then placed in a sterile fermentation bag with a one-way filter valve. Solid-state fermentation was conducted at 37°C for 240 h. The humidity of the solid-state ferment was monitored daily, and if reduced, it was supplemented with sterile water as needed. Samples were collected every 48 h for nutritional composition analysis. DDGS samples were dried at 105°C until a constant weight was achieved. Crude protein (CP) was determined by the Kjeldahl method (Belyea et al., 2004). The content of crude fiber (*CF*) was determined following the AOCS Ba 6a-5 standard method (Dey et al., 2021). The content of cellulose, hemicellulose, and Klason lignin was determined using a two-step acid treatment (Leite et al., 2016). Ash content was

determined by incinerating samples in a muffle furnace at 450°C for 4 h.

2.5. Statistical analysis

Enzyme assays and solid-state fermentation experiments were performed in triplicate. Origin 2023 (Origin 2023 program, OriginLab) and SPSS v 25.0 were used for variance (ANOVA) and statistical comparisons, as well as for data visualization. Results were presented as means of more than three replicates.

3. Results

3.1. CAZy database annotation

The *P. pabuli* E1 genome harbors a considerable number of carbohydrate-degrading enzymes. However, limited information on *Paenibacillus* species for feed is available in the existing database. Therefore, this study aimed to analyze the carbohydrate distribution in the *P. pabuli* E1 genome to provide fundamental data for the development and utilization of degrading enzymes. A total of 372 genes were assigned to CAZymes families. Among these, the GH family was the most predominant, followed by CBM, GT, CE, PL, and AA families, with gene counts of 228, 69, 33, 26, 14, and 2, respectively (Figure 1A). The GH family comprises a versatile group of enzymes involved in the hydrolysis of glycosidic bonds in carbohydrates. The abundance of GH family enzymes in *P. pabuli* E1 is advantageous for its growth and reproduction by facilitating the degradation of complex polysaccharides. Specifically, there are 24 GH families associated with cellulose degradation and 46 GH families related to hemicellulose degradation. Additionally, the PLs families encompass 16 pectin-degrading enzymes, while the CEs families comprise three and nine enzymes involved in hemicellulose and pectin degradation, respectively (Figure 1B).

3.1.1. Cellulose degradation

Complete cellulose degradation necessitates the presence of endo-1,4-beta-D-glucanase, cellobiohydrolase, and beta-glucosidase enzymes (Figure 2A). Endo-1,4-beta-D-glucanase enzymes randomly cleave O-glycoside bonds. Among the annotated genes, seven were identified as endo-1,4-beta-D-glucanases, with six of them containing signal peptides and one being an intracellular protein. These seven proteins belong to five distinct GH families: GH5, GH8, GH9, GH12, and GH74. Notably, E1GL002997 and E1GL006765 of the GH5 family possess a CBM46 domain at their C-terminal ends. Cellobiosidase (exo-cellulase) catalyzes the processive hydrolysis of cellulose chains toward the crystalline region, generating cellobiose. Two genes, E1GL01119 and E1GL01285, were annotated as cellobiosidases. E1GL01119 belongs to GH6 and is linked to a CBM3 domain at its C-terminal, while E1GL001284, E1GL002456, E1GL001119, and E1GL001285 are all associated with a CBM3 domain at their C-terminal ends. Beta-glucosidase (BG) acts on cellobiose, producing glucose as the final product. Among the annotated genes, 12 were identified as beta-glucosidases, with only E1006056 belonging to the GH1 family and the rest belonging to the GH3 family. Notably, E1GL00945 possesses a signal peptide for extracellular secretion, whereas E1GL002415 and E1GL006476 possess a CBM6 domain at their C-terminal ends. Additionally, E1001978 and E1006424 were annotated as cellobiose phosphorylases (CBP), which differ from beta-glucosidases as they act on cellobiose through the phosphorolysis pathway, resulting in glucose and glucose-1-phosphate as the final products. CBP belongs to the GH94 family and exhibits strict substrate specificity.

3.1.2. Hemicellulose degradation

Paenibacillus pabuli E1 is equipped with the necessary enzymes for complete xylan hydrolysis (Figure 3). Five genes were annotated as beta-1,4-endo-D-xylanases, with four of them possessing signal peptides. E1GL000825, E1GL003990, and E1GL006811 belong to the GH10 family, while E1GL003315 belongs to the GH11 family. E1GL000825 is linked to CBM9 and CBM22 domains at its C-terminal

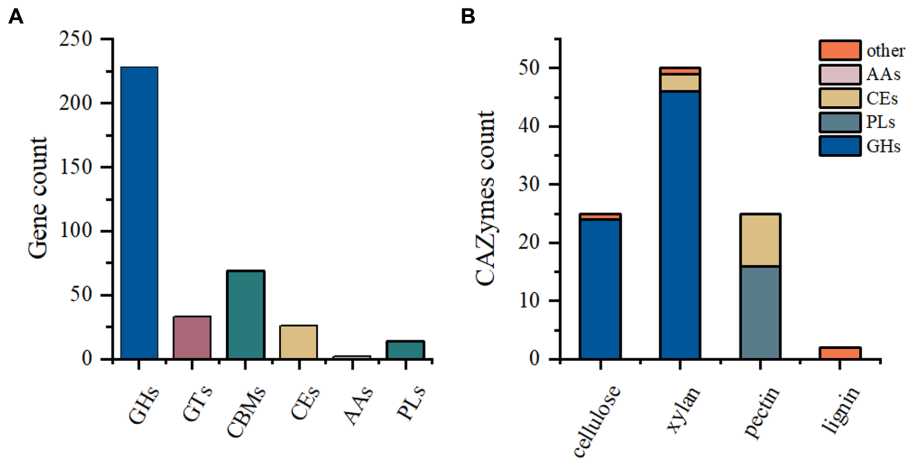

FIGURE 1
CAZyme annotation. **(A)** A total of 372 genes were assigned to CAZyme families. The GH family exhibited the highest abundance, followed by CBM, GT, CE, PL, and AA families, with 228, 69, 33, 26, 14, and 2 genes, respectively. **(B)** Among the GH families, 24 and 46 were associated with the degradation of cellulose and hemicellulose, respectively. The PL families contained 16 pectin-degrading enzymes. In the CE families, three and nine enzymes were related to the degradation of hemicellulose and pectin, respectively.

10.3389/fmicb.2023.1205767

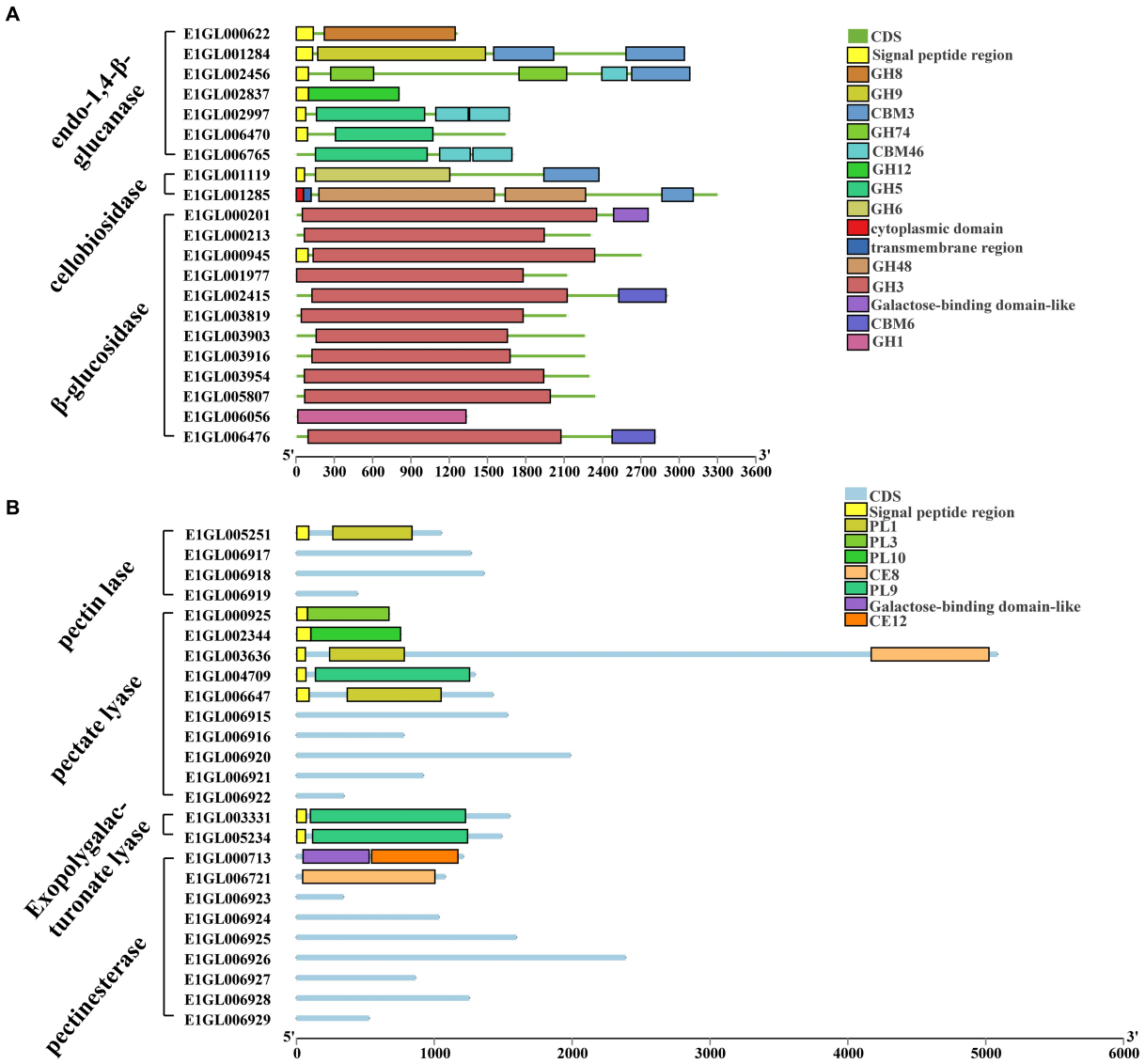

FIGURE 2
Cellulose and pectin degrading enzyme gene ID and CAZyme family/domain. **(A)** Cellulose degrading enzyme. Seven genes were annotated as endo-1,4-beta-D-glucanase. Two genes were annotated as cellobiosidase. There are 12 genes annotated as beta-glucosidase. **(B)** Pectin degrading enzymes. Four genes were annotated to pectin lyases. Ten genes were annotated to pectate lyases. Two genes were annotated as exo-polygalacturonate lyases. Nine genes were annotated as pectate esterases.

end, and E1GL002701 is connected to the CBM36 domain. Moreover, eight genes were annotated as exo-1,4-beta-xylosidases. E1GL003470 and E1GL003905 belong to the GH52 and GH39 families, respectively, while the remaining six genes belong to the GH43 family. Natural xylan comprises various substituent groups on the main chain and side chain sugar groups, including arabinoyl and glucuronyl. Seven genes were annotated as alpha-L-arabinosidases, all of which belong to the exo-glycosidases. Specifically, E1GL000109, E1GL001288, E1GL003221, and E1GL004074 are classified under the GH51 family, while E1GL001321, E1GL003870, and E1GL003989 belong to the GH43 family. Alpha-galactosidase catalyzes the hydrolysis of galactose residues from the side chains of xylans or galactomannans at non-reducing ends. This study identified 10 annotated genes for alpha-galactosidase, with E1GL002357 and E1GL003820 possessing signal peptides. These enzymes belong to the GH4, GH27, and GH36 families. E1GL003471 was the sole annotated alpha-glucuronidase in *P. pabuli* E1, belonging to the GH67 family. Additionally, hemicellulose is typically acetylated, and the presence of acetyl groups limits the action of xylan-degrading enzymes. E1GL002453 and E1GL006825 were annotated as acetyl xylan esterases, with E1GL006825 belonging to the CE2 domain. Furthermore, E1GL003852 was annotated as a ferulic acid esterase responsible for cleaving the ester bond between ferulic acid and arabinose residues.

The backbone of mannan consists of beta-1,4-linked mannose or a combination of mannose and glucose residues, often substituted by alpha-1,6-linked galactose. The main enzymes involved in mannan degradation are beta-mannanase and beta-mannosidase, along with additional enzymes such as alpha-galactosidase and acetyl mannan esterase to remove side groups from the mannan main chain. Three genes, E1GL001833, E1GL002988, and E1GL004125, were annotated as

10.3389/fmicb.2023.1205767

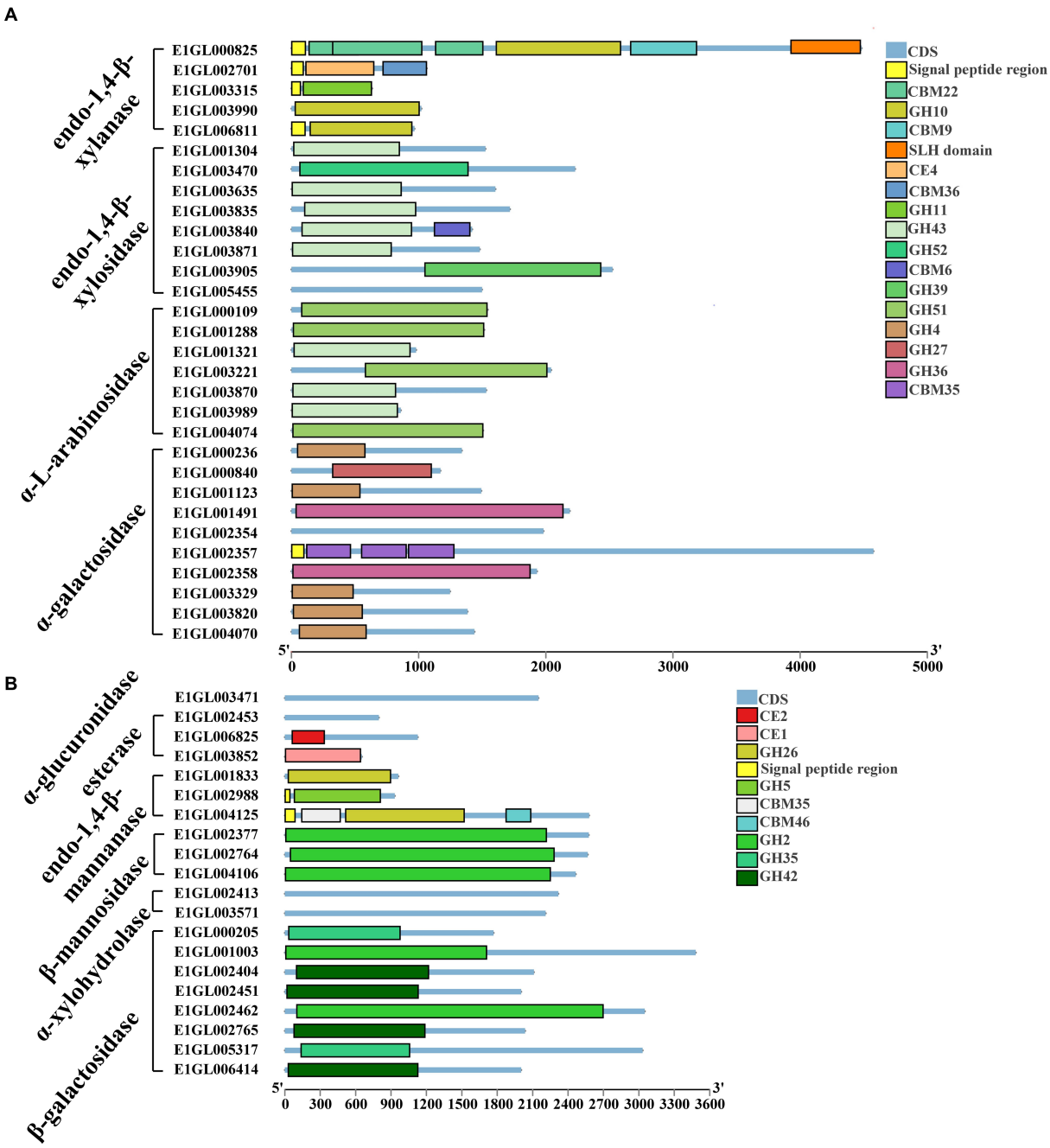

FIGURE 3
Hemicellulose degrading enzyme gene ID and CAZyme family/domain. **(A)** Five genes were annotated as beta-1,4-endo-D-xylanase. Eight genes were annotated as exo-1,4-beta-xylosidase. Seven genes were annotated as alpha-L-arabinosidase. Ten genes were annotated as alpha-galactosidase. **(B)** One gene was annotated as alpha-glucuronidase. Three genes were annotated as acetyl xylan esterases. Three genes were annotated as endo-1,4-beta-mannanase. Three genes were annotated as beta-mannosidase. Two genes were annotated as alpha-xylosidases. Two genes were annotated as alpha-xylohydrolase. Eight genes were annotated as beta-galactosidases.

endo-1,4-beta-mannanases. E1GL001833 and E1GL004123 belong to the GH26 family, while E1GL002988 belongs to the GH5 family. These three genes are linked to different CBM domains at their C-terminal ends. Additionally, E1GL002377, E1GL002764, and E1GL004106 were annotated as beta-mannosidases, all belonging to the GH2 family.

Xyloglucan serves as the primary hemicellulose in the primary cell walls of dicots and non-graminous monocots. Two genes, E1GL002413 and E1GL003571, were annotated as alpha-xylosidases, and classified under the GH31 family. GH31 enzymes catalyze the hydrolysis of terminal unsubstituted xylosides at the reducing ends of xylogluco-oligosaccharides. Eight genes were annotated as beta-galactosidases, distributed across the GH2, GH35, and GH42 families. Specifically, E1GL001003, E1GL002404, and E1GL002462 belong to the GH2 family. Moreover, E1GL001003 and E1GL002404 are linked to the

10.3389/fmicb.2023.1205767

TABLE 1 Growth in polysaccharide medium.

Polysaccharide type	Growth
No sugar	–
Cellulose powder	+
CMC	+
Filter paper	–
Xylan	+
Pectin	+

TABLE 2 Enzymatic activities detected.

Enzyme type	Enzyme activity (U/mL)
Endoglucanase	5.37
Beta-glucosidase	4.60
FPAase	-
Beta-xylanase	11.05
Beta-xylosidase	4.16
Pectate lyase	8.19
Pectin lyase	2.43
Laccase	1.87
MnP	4.30

CBM6 domain at their C-terminal ends, while E1GL002462 is linked to the CBM51 domain.

3.1.3. Pectin degradation

The *P. pabuli* E1 genome contains 10 pectate lyases (PGL) and four pectin lyases (PMGL) belonging to the polysaccharide lyases (PL) family, distributed across PL1, PL3, PL9, and PL10 (Figure 2B). Among these, only the pectin lyase E1GL005251 belongs to the PL1 family, while the others lack PL1 domain characteristics. The pectate lyases E1GL000925, E1GL002344, E1GL003636, E1GL004709, and E1GL006647 all possess signal peptides. E1GL000925, E1GL002344, and E1GL004709 belong to PL3, PL10, and PL9, respectively, while E1GL003636 and E1GL006647 belong to PL1. Additionally, E1GL003331 and E1GL005234 were annotated as exo-polygalacturonate lyases, both with signal peptides and classified under PL9. Nine genes were annotated as pectate esterases, with E1GL000713 and E1GL006647 belonging to CE12 and CE8, respectively, while the remaining genes lacked a clear domain match.

3.1.4. Lignin degradation

The potential lignin-degrading enzymes identified in *P. pabuli* E1 are MnP (from E1GL004832) and laccase (from E1GL004895). The E1GL004832 showed 100% similarity to the reported manganese catalase (WP_076288188.1) from *Lactobacillus plantarum* when analyzed using the blastp tool. Manganese catalase exhibits a hexameric structure that is stabilized through extensive contacts between subunits. Each subunit contains a dimanganese active site. Similarly, the sequence E1GL004895 exhibited 100% similarity to the reported polyphenol oxidase (CAH1208948.1) from *Paenibacillus* sp. JJ-223 when analyzed using blastp. The COG database annotation identifies it as a Copper oxidase (laccase).

3.2. Growth in different polysaccharide mediums

Paenibacillus pabuli E1 exhibited growth in polysaccharide media supplemented with carboxymethyl cellulose (CMC), xylan, and pectin. However, the growth was limited when cellulose powder was used, and no growth was observed when filter paper was used as the sole carbon source (Table 1). Lignin, a non-polysaccharide compound, was also tested, and growth was observed in a minimal medium supplemented with lignin. To investigate the potential induction of cellulase, filter paper or CMC was added to the LB activation culture medium. The results showed that no reducing sugar activity was detected regardless of whether filter paper or CMC was pre-added to the activation medium. The disintegration of filter paper was observed to varying degrees after incubating with the supernatant and cell insoluble fraction for 4 h, with the control group being PBS solution (Supplementary Figure S1). The cell insoluble fraction showed a stronger disintegration effect on filter paper, but no reducing sugar was detected in either case.

3.3. Enzyme assay

The endoglucanase (CMCase) activity of *P. pabuli* E1 was measured to be 5.37 U/mL, while the beta-glucosidase activity was 4.60 U/mL. No reducing sugars were detected in the filter paper experiments. In the degradation of xylan, the concerted action of complex enzymes is required, with beta-xylanase and beta-xylosidase being the most crucial enzymes involved. These enzymes are capable of degrading the main chain structure of xylan. Therefore, in the present experiment, the activities of beta-xylanase and beta-xylosidase were tested. The beta-xylanase and beta-xylosidase activities were determined to be 11.05 U/mL and 4.16 U/mL, respectively. Pectate lyase and pectin lyase activities reached 8.19 U/mL and 2.43 U/mL, respectively. Lignin, a highly complex aromatic polymer, poses challenges for degradation due to its intricate structure. The activities of laccase and MnP in *P. pabuli* E1 were measured to be 1.87 U/mL and 4.30 U/mL, respectively. Laccase and MnP are responsible for lignin degradation in bacteria. All enzyme activity values are shown in Table 2.

3.4. Solid-state fermentation

Solid-state fermentation was employed to reduce NSPs such as lignocellulose. After 7 days of fermentation, the neutral detergent fiber (NDF) content in DDGS decreased from 46.9% to 41.33%, while the acid detergent fiber (ADF) decreased from 22.15% to 20.65%. Similarly, the acid detergent lignin (ADL) content decreased from 4.63% to 4.23%. These results demonstrate that *P. pabuli* E1 effectively reduced the lignocellulosic content of DDGS through fermentation. The ash content in DDGS increased from 4.46% to 4.90%, potentially due to the addition of inorganic salt ions during the preparation of *P. pabuli* E1. *CF*, which serves as an important parameter in feed formulation, decreased from 15.62% to 11.76%. Furthermore, CP content in DDGS increased from 26.59% to 30.59% (Figure 4). NDF comprises cellulose, hemicellulose, lignin, and ash, while ADF contains the latter three components. By calculating the differences

between NDF, ADF, ADL, and ash, the content of cellulose, hemicellulose, and lignin can be obtained. After 240 h of DDGS fermentation ($p < 0.001$), the degradation rates of hemicellulose, cellulose, and lignin were determined to be 11.86%, 11.53%, and 8.78%, respectively (Figure 5).

4. Discussion

4.1. Cellulose degradation

The disintegration of filter paper without the presence of reducing sugars suggests that *P. pabuli* E1 may produce cellulose accessory proteins that disrupt the crystalline structure of cellulose without exhibiting hydrolase activity. Previous studies have reported the production of auxiliary proteins such as expansin and swollenin by some microorganisms. These proteins loosen the cellulose structure by breaking hydrogen bonds between microfibrils, thus increasing the accessibility of cellulase to the substrate (Hendriks and Zeeman, 2009). Kim et al. (2009) demonstrated that expansin from *Bacillus subtilis* synergistically increased cellulase activity by 5.7-fold. Therefore, it is speculated that the disintegration of filter paper observed in *P. pabuli* E1 may be caused by an auxiliary protein that disrupts the network structure of the cellulose surface without detectable reducing sugars but significantly enhances cellulase hydrolytic activity. Expansins are present in various plants and microorganisms, and they share homology with the GH45 family of glycoside hydrolases. However, expansins lack a complete catalytic mechanism, and no hydrolytic activity has been detected (Georgelis et al., 2015). Expansins from *B. subtilis* do not possess hydrolytic activity but contribute to the loosening of cellulose structure, thereby facilitating cellulose biotransformation (Kim et al., 2009). Swollenin, a non-enzymatic protein with high sequence similarity to expansins, has also been found in *Trichoderma reesei*. Swollenin swells cotton fibers without producing detectable reducing sugars (Chen et al., 2010). The application of swollenin effectively alleviates the hindering effect of the crystallization region of the substrate on the hydrolysis reaction and increases the affinity between the enzyme and the

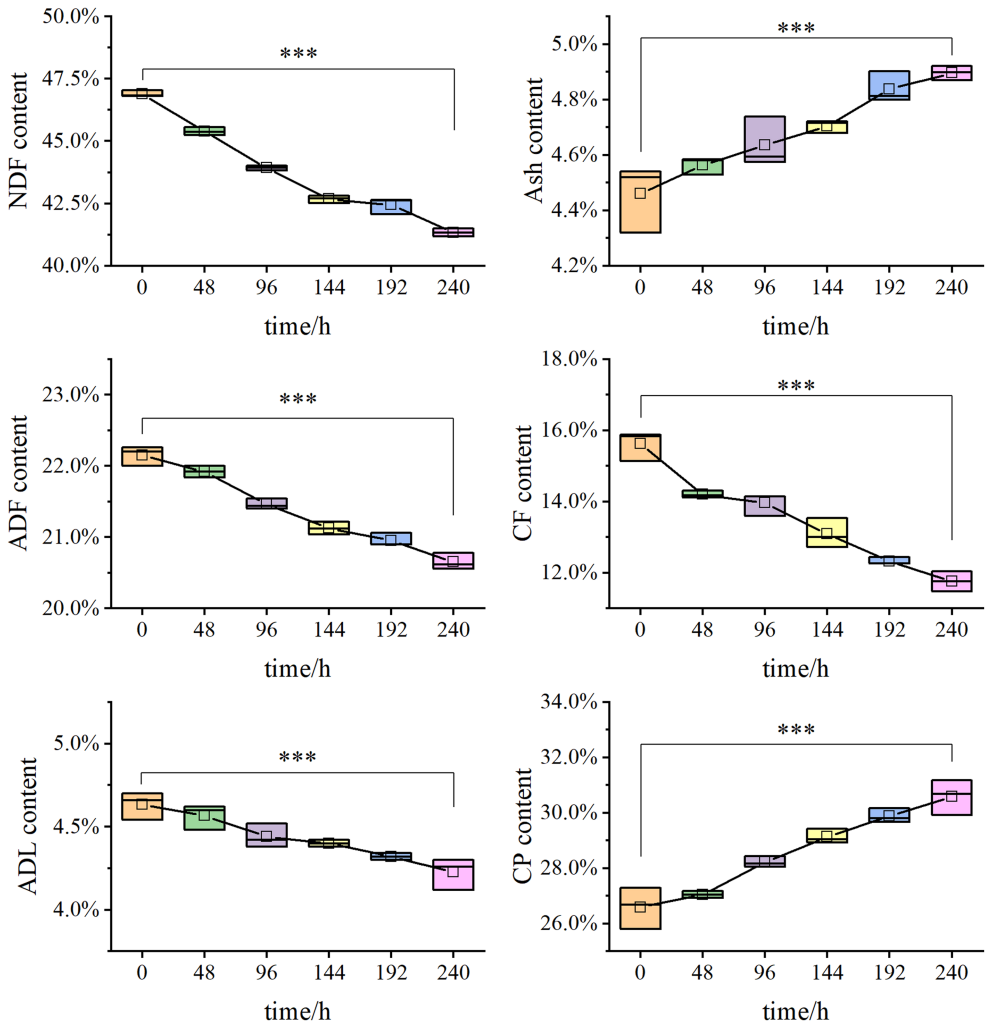

FIGURE 4
Degradation rates of cellulose, hemicellulose, and lignin in solid-state fermentation. The NDF content decreased from 46.9% to 41.33%, the ADF decreased from 22.15% to 20.65%, and ADL decreased from 4.63% to 4.23%. Ash increased from 4.46% to 4.90%. CF reduced from 15.62% to 11.76%. CP increased from 26.59% to 30.59%. *** Indicates p-value < 0.001, which is considered extremely significant.

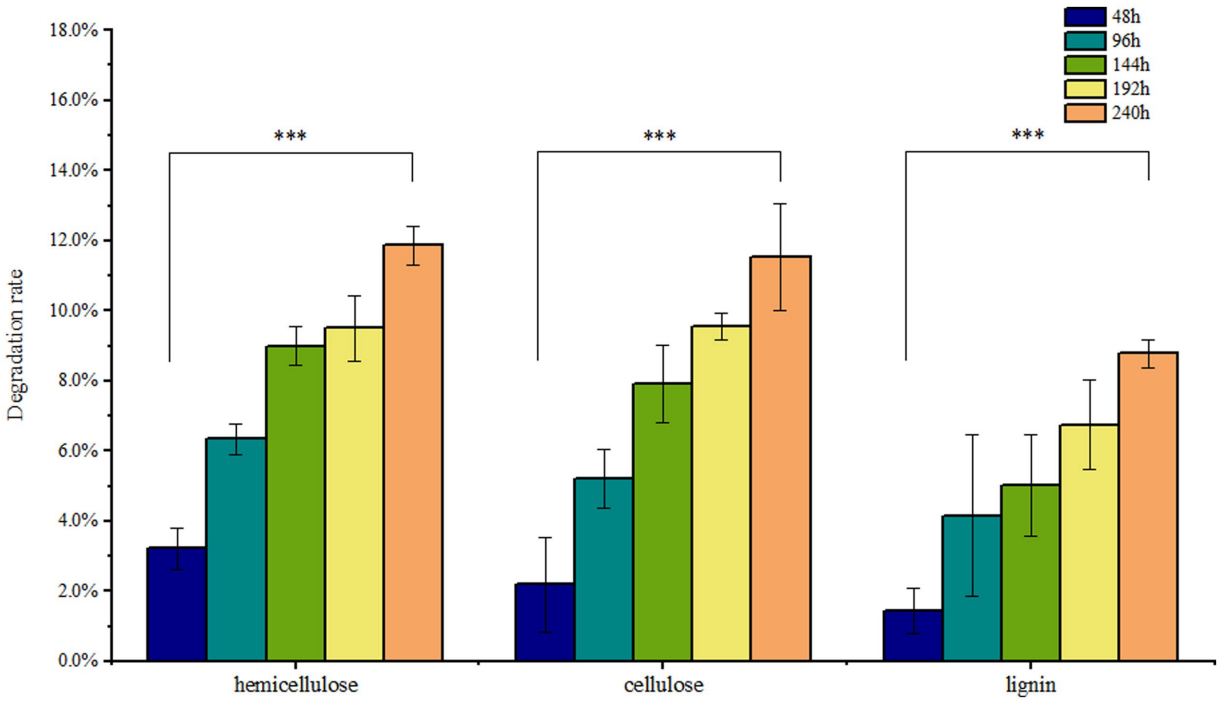

FIGURE 5
Nutrients in DDGS at different fermentation times. After 240 h of DDGS fermentation, the degradation rates of hemicellulose, cellulose, and lignin were 11.86%, 11.53%, and 8.78%, respectively ($p < 0.001$). *** Indicates p-value < 0.001, which is considered extremely significant.

substrate, thus enhancing cellulase hydrolysis activity (Saloheimo et al., 2002). Unfortunately, the genome of *P. pabuli* E1 did not match any proteins similar to the reported auxiliary proteins. There are few studies on auxiliary proteins in bacteria, and it is not ruled out that there are novel auxiliary proteins.

Cellulolytic enzymes are essential to break down cellulose thoroughly, although the role of accessory proteins is indispensable. Fungi, known for their potent ability to degrade lignocellulose, have been extensively studied as the primary group of microorganisms involved in plant biomass degradation. This is attributed to their remarkable enzyme secretion capacity and the robustness of their degradation enzymes. Among the cellulose-degrading microorganisms, *A. Niger* and *T. reesei* are the most extensively investigated. The study revealed the complete secretomes of *A. Niger* and *T. reesei* are involved in lignocellulose degradation. These secretomes include the well-known GH7 and GH6 cellobiohydrolases, GH5 endoglucanases, beta-glucosidases, as well as additional enzymes that target other components of the plant cell wall (Borin et al., 2015). A total of 430 CAZymes were annotated in *T. harzianum*. These included 259 GHs, 101 GTs, 6 PLs, 22 CEs, 42 AAs and 46 CBMs (Ferreira Filho et al., 2017).

When compared to fungi, bacteria generally exhibit lower cellulase activity. However, the characterization of novel enzymes has increasingly focused on bacterial sources due to the high specific activity (Obeng et al., 2017). Among the bacterial strains isolated for their ability to degrade crystalline cellulose, the majority belong to specific lineages within the four major phyla: Actinobacteria, Firmicutes, Proteobacteria, and Bacteroidetes (Koeck et al., 2014). The primary cellulase-producing bacteria are often from the genus *Bacillus*, such as *B. licheniformis* and *B. subtilis*, as well as from the genus *Clostridium*. Anaerobic bacteria play a significant role among cellulose-degrading bacteria. In anaerobic bacteria, cellulases are typically associated with the bacterial surface in the form of cellulosomes. Certain anaerobic members of the *Clostridia* group are known to produce cellulosomes, which are highly efficient multienzyme complexes attached to the outer surface of bacterial cell (Wilson, 2008). This arrangement allows for enzyme recycling and rapid assimilation of hydrolytic products. Whole genome sequencing has led to the characterization of key components of cellulosomes. The structure of cellulosomes can vary in complexity among different bacterial species. The most prominent enzymes integrated into cellulosomes typically belong to GH48, GH9, and GH5 families, which are involved in cellulose degradation (Artzi et al., 2017). However, it should be noted that the genome of *P. pabuli* E1 does not contain the structural skeleton proteins typically associated with cellulosomes.

In contrast, aerobic bacteria are capable of secreting extracellular enzymes involved in cellulose degradation. Members of the *Bacillus* and *Paenibacillus* exhibit significant cellulolytic capability, which is attributed to the presence of a wide range of glycoside hydrolase (GH) enzymes in their genomes (Ma et al., 2020). For instance, *B. velezensis* LC1 demonstrated promising cellulase activity. Carbohydrate-active enzyme annotation revealed 136 genes associated with CAZy families. The cellulase activities of strain LC1 were then determined. The endoglucanase activity was measured as 0.689 ± 0.011 U/mL on day 1 and increased to 0.752 ± 0.013 U/mL on day 6. The exoglucanase activity ranged from 0.359 ± 0.016 U/mL to 0.385 ± 0.022 U/mL (Li et al., 2020).

The agricultural waste hydrolyzing capabilities of *Paenibacillus dendritiformis* CRN18 were investigated. The strain exhibited enzyme

activities for exo-glucanase, beta-glucosidase, beta-glucuronidase, endo-1,4-beta-xylanases, arabinosidase, and alpha-galactosidase at levels of 0.1, 0.3, 0.09, 0.1, 0.05, and 0.41 U/mL, respectively (Srivastava et al., 2020). Genomic analysis of *Paenibacillus lautus* BHU3 strain predicted 6,234 protein-coding genes, with 316 genes associated with sugar metabolism. This analysis suggests an important role in enhancing cellulolytic properties (Kim et al., 2018). Similarly, *Paenibacillus* sp. strains IHB B 3415, a cellulase-producing psychrotrophic bacterium, contained 1,011 genes assigned for carbohydrate metabolism, including 16 genes predicted for cellulases, supporting its cellulose degradation capabilities (Dhar et al., 2015). Among the examined isolates, *Paenibacillus* sp. O199 demonstrated the highest efficiency for cellulose deconstruction. Its genome contained 476 genes associated with CAZyme families, including 100 genes coding for GHs potentially involved in cellulose and hemicellulose degradation (Lopez-Mondejar et al., 2016). *Paenibacillus pabuli* E1 possesses multiple types of endo-1,4-beta-D-glucanases with different substrate affinities. The GH8 family exhibits broad substrate specificity and catalyzes various polysaccharides such as carboxymethylcellulose (CMC), chitosan, barley-beta-glucan, lichenin, and xylan sugars (Ontanon et al., 2019). GH74 is considered an important family of endoglucanases, but recent studies have shown high specificity for xyloglucan (Wang et al., 2022). CBM46 enhances the enzyme's affinity for cellulose, and some studies have indicated that the catalytic activity of enzymes depends entirely on the CBM46 domain (Liberato et al., 2016).

Cellobiosidases are classified into CBH I and CBH II based on the reducing properties of the bound chain ends. GH6 is a typical representative of CBH II enzymes that act on the non-reducing end of cellulose molecules. Most GH6 enzymes exhibit processive catalysis, and their catalytic domains have a short connecting peptide to the CBM domain, which is essential for enzyme activity (Irwin et al., 1998). E1GL01285, belonging to the GH48 domain, is a CBH I enzyme that acts on the reducing end of cellulose and is present in many bacterial cellulase systems. GH48 enzymes have inherently low cellulolytic activity but exhibit strong synergy with GH9 endoglucanases, even at low ratios. CBM3 can enhance cellulose adsorption capacity, which is beneficial for the catalysis of endo-cellulases and cellobiosidases.

The presence of endo-1,4-beta-D-glucanases and cellobiosidases is crucial for the initial degradation of cellulose. Endo-glucanases randomly bind to non-crystalline regions of microfibrils, generating new reducing ends, while exo-cellulases bind to the reducing or non-reducing end of a single cellulose chain and processively degrade the crystalline region. Studies have indicated that the loss of exo-cellulase activity is a major factor in the reduced rate of enzymatic cellulose hydrolysis (Wang et al., 2006). Although cellulose is the primary resource in feed for ruminant livestock, monogastric animals such as pigs and chickens have limited ability to degrade cellulose. *Paenibacillus pabuli* E1 possesses the necessary enzymes to break down cell walls, thereby releasing nutrients and significantly improving feed nutrient absorption rates.

4.2. Hemicellulose degradation

Xylan, as an anti-nutritional factor present in feed, poses obstacles to the absorption and utilization of nutrients in livestock (Dikeman and Fahey, 2006). Among the constituents of feed ingredients, hemicellulose primarily comprises xylan, mannan, and xyloglucan (de Vries and Visser, 2001). When the culture temperature was raised to 37°C and the initial pH was set at 8.5, the xylanase activity of *Paenibacillus glycanilyticus* X1 peaked at 189.6 mU after 72 h (Wang and Liang, 2021). Another study focused on *Paenibacillus* sp. BL11 strain, which exhibited the highest enzyme activity at an initial pH of 8 and a culture temperature of 37°C. This strain displayed greater xylanase activity under neutral to slightly alkaline conditions and at moderate to high temperatures (Ko et al., 2010). The endo-beta-1,4-xylanase derived from *Paenibacillus curdlanolyticus* B-6, belonging to the GH10 family, was found to possess CBM22 and CBM3 domains at its C-terminus (Sermsathanaswadi et al., 2017). Additionally, a novel GH6 cellobiohydrolase from the same strain, *Paenibacillus curdlanolyticus* B-6, demonstrated high substrate specificity toward amorphous cellulose and lower specificity toward crystalline cellulose. However, this enzyme did not exhibit activity on substitution substrates such as carboxymethyl cellulose and xylan (Baramee et al., 2017). *Paenibacillus* sp. LS1 exhibited the ability to utilize different types of xylans. Genome analysis revealed a comprehensive set of xylan-active CAZymes, indicating its capacity for efficient degradation of xylan (Mukherjee et al., 2023). Moreover, *Paenibacillus* sp. strains DA-C8 completely degraded 1% beechwood xylan within 4 days under anaerobic conditions, while it was capable of growth on xylan medium under aerobic conditions (Chhe et al., 2021a,b). In the case of *Paenibacillus physcomitrellae* XB, different xylan degradation abilities were observed for various substrates such as corncob xylan, oat spelled xylan, and wheat flour arabinoxylan. The bifunctional enzymes Ppxyl43A and Ppxyl43B identified in this strain hold promise for xylan biomass conversion (Zhang et al., 2021).

Paenibacillus pabuli E1 exhibits higher levels of beta-xylanase and beta-xylosidase compared to similar strains (Ghio et al., 2020). Xylanases are commonly classified into two families. GH10 xylanases have a high molecular weight and possess four or five substrate binding sites, while GH11 xylanases catalyze xylans with a minimum of three adjacent xyloses without substituents (Mendis et al., 2016; Chang et al., 2017). GH11 xylanases demonstrate higher specificity, with superior hydrolytic activity toward long-chain xylan compared to GH10 xylanases. The presence of CBM9 and CBM22 domains enhances the adsorption capacity of xylan. CBM22 aids in delivering xylan to the adjacent catalytic domain of GH10 by promoting binding to xylan, whereas CBM9 enhances xylan degradation by binding to cellulose (Tanimoto et al., 2016). CBM36 is a novel carbohydrate-binding module that exhibits Ca^{2+}-dependent affinity for xylan. Additionally, the CBM2 domain exhibits broad substrate recognition and can bind xylan, cellulose, and chitin (Tanimoto et al., 2016). Xylanases are responsible for cleaving the glycosidic linkages in the xylan backbone, leading to the generation of xylooligosaccharides. Beta-1,4-xylosidase further hydrolyzes xylooligosaccharides into xylose, which is crucial for complete xylan degradation. The activity of beta-1,4-xylosidase derived from Bacillus sp. in the GH52 family gradually decreases as the length of the main chain increases (Teramoto et al., 2021). Alpha-L-arabinosidase acts on alpha-nitrophenol-furan arabinoside or branched arabinan. Some xylanases cannot degrade glycosidic bonds between xylose units with substituted side chains, while others can only hydrolyze side chain substituents on xylooligosaccharides. Alpha-L-arabinosidase is classified into the GH43 and GH51 families. The presence of metal ions enhances the enzyme activity of the GH43 family, whereas the GH51 enzyme hydrolyzes alpha-1,2 or alpha-1,3-linked arabinofuranose residues.

The synergy between GH51 and GH43 enzymes improves the debranching efficiency of arabinoxylans (Koutaniemi and Tenkanen, 2016). Alpha-glucuronidase, as the rate-limiting enzyme in xylan degradation, plays a crucial role in the biodegradation of xylan hemicellulose. It acts specifically on small molecules of 4-O-methylglucurono-oligosaccharides with residues, hydrolyzing the side chain of the non-reducing end of 4-O-methylglucuronic acid (de Wet et al., 2006). *Paenibacillus* sp. TH501b isolates from soil samples contain alpha-glucuronidase. This enzyme is most active at pH 6.0–7.0 and 30°C (Iihashi et al., 2009). Acetyl xylan esterase primarily acts on the 2- or 3-position O-acetyl groups of xylose residues in acetylated xylan. The CE2 domain exhibits strong specificity for the 4-position acetyl group of xylopyranose residues. The degree of 2-O- and 3-O-acetyl substituents in xylan is challenging to determine, and the release of O-acetyl groups reduces pH, which inhibits fermenting microorganisms (Basen et al., 2014). Ferulic acid, found as monomers and dimers linked to arabinoxylan residues, is enzymatically hydrolyzed from the hemicellulose substrate, loosening the cell wall structure and increasing the rate of cellulose degradation (Krueger et al., 2008).

Mannan, another type of anti-nutritional factor present in plant-based feedstuffs such as soybean meal, rapeseed meal, sesame meal, and corn, can be degraded by beta-mannanase. Among them, the highest content of beta-mannan in soybean meal is 1.1%–1.3% (Seo et al., 2015). Beta-mannanase facilitates the release of nutrients encapsulated in the cell wall and reduces chyme viscosity, thereby improving nutrient absorption in animals. Enzyme supplementation enhances feed digestion, utilization, and animal production performance (Chauhan et al., 2012). CBM6-associated beta-galactosidases not only adsorb amorphous cellulose but also bind to beta-1,3-glucan, beta-1,3/1,4-glucan, and beta-1,4-glucan. Although research on CBM51 is limited, its members demonstrate specificity for eukaryotic glycans (Gregg et al., 2008).

Xyloglucan is initially hydrolyzed by endo-1,4-beta-glucanase, producing xyloglucan oligosaccharides (XGOs) that are further hydrolyzed by beta-galactosidase, releasing galactose monomers. Alpha-xylosidase removes xylosyl residues in oligosaccharides, while beta-glucosidase hydrolyzes glucose residues in the xyloglucan backbone (Attia and Brumer, 2016). The structural complexity of hemicelluloses, with their varied main chains and modified side chain groups, poses challenges for complete degradation. *Paenibacillus pabuli* E1 possesses a repertoire of enzymes targeting both the main chains and side chains, which are essential for efficient hemicellulose degradation. The *P. pabuli* E1 genome contains enzymes that degrade different types of xylan, which is also helpful for eliminating xylan in other cereals not limited to those in DDGS.

4.3. Pectin degradation

Pectin is composed of D-galacturonic acid units connected via alpha-1,4-glycosidic linkages, with side chains comprising rhamnose, arabinose, galactose, and xylose. Pectin is classified into four types: pectic acid, pectinic acid, pectin, and protopectin. In *Paenibacillus amylolyticus* 27C64, a comprehensive analysis identified a total of 314 putative carbohydrate-active enzymes (CAZymes) distributed among 108 distinct families. Further investigation of the culture supernatants revealed the presence of pectinase activities (Keggi and Doran-Peterson, 2019). An alkaline pectate lyase gene derived from *Paenibacillus polymyxa* KF-1 was also studied. This gene encodes a protein consisting of 449 amino acid residues and belongs to the polysaccharide lyase family 9 (PL9). The optimal conditions for its enzymatic activity were determined to be at pH 10.0 and a temperature of 40°C (Zhao et al., 2018; Yuan et al., 2019).

Structurally, lyases from PL1, PL3, and PL9 families exhibit a parallel beta-helix conformation, while the PL10 family adopts an (alpha/alpha)3-barrel structure. Galacturonic acid plays a vital role in maintaining the pectin structure, making the degradation of polygalactose essential. Additionally, nine pectin esterases promote the hydrolysis of pectin esters by removing methyl groups, thus facilitating the production of pectinic acid. PMGL, on the other hand, directly degrades high-methoxyl pectin without the need for esterases to remove methyl ester groups. Most pectin methylesterases (PGLs) degrade polygalacturonic acid and low-methoxyl pectin but exhibit less activity toward high-methoxyl pectin. In animals, the absence of endogenous pectinases hampers the digestion of pectin, making pectinase supplementation crucial for improving crude fiber utilization (Sharma et al., 2012; Lima et al., 2017; Yang et al., 2020). Pectate lyase and pectin lyase act on the alpha-1,4-glycosidic bonds of pectin or pectinic acid, generating unsaturated pectin oligosaccharides without producing highly toxic methanol. Pectinase finds applications in various industries such as food fermentation, paper biopulping, animal feed, and environmental protection (Kohli and Gupta, 2015).

4.4. Lignin degradation

Microbial degradation of lignin represents a promising approach for mitigating its deleterious effects. Among microorganisms, fungi possess a diverse array of lignin depolymerase systems, with significant research attention directed toward white-rot and brown-rot fungi (Wang et al., 2019). However, our understanding of bacterial ligninases remains limited, despite their potential importance in lignin degradation. *Paenibacillus* sp. DLE-14, isolated from plant roots, demonstrates the potential to degrade lignin. Lignin degradation is commonly associated with the action of two prominent enzymes, namely laccase and manganese peroxidase (MnP). However, the presence and activity of these enzymes in the *Paenibacillus* species have received limited research attention. To date, only one study has reported the purification of MnP from *Paenibacillus* sp., revealing an enzyme activity of 4.3 U/L under optimal conditions (De et al., 2009).

MnP activity is primarily dependent on Mn^{2+} ions, which are oxidized to Mn^{3+} and form complexes with glycolic acid and oxalic acid present in the system. MnP exhibits a low oxidation/reduction potential and selectively degrades phenolic lignin (Xu et al., 2018). Laccase, belonging to the blue multi-copper oxidase family, is a polyphenol oxidase with a broad range of substrates, including phenols, aromatic amines, carboxylic acids, and steroids. It catalyzes the oxidation of phenols by generating phenoxy radicals, thereby promoting lignin degradation (McMahon et al., 2007).

Laccases are found in fungi, plants, and other bacteria. However, most laccases cannot directly oxidize non-phenolic compounds due to their high redox potential compared to the "normal hydrogen electrode" (NHE), whereas the redox potential of laccases is lower than 0.8 V (Canas and Camarero, 2010). Nevertheless, there are two basidiomycetes known to produce laccases with high redox potential (Hernández-Martínez et al., 2017, 2018). White-rot fungi are generally more efficient in lignin degradation, but their enzymes are susceptible

to loss of activity under extreme temperature and pH conditions. However, heat-resistant laccases produced by *Pycnoporus sanguineus* CS43 (LacI and LacII) have demonstrated high resistance to organic solvents such as acetonitrile, ethanol, and acetone (Ramírez-Cavazos et al., 2014). Enzymes with superior tolerance are more suitable for industrial and agricultural applications. In comparison to fungal laccases, bacterial laccases exhibit high activity at elevated temperatures, alkaline pH, and high chloride and copper ion concentrations, making them compatible with various industrial processes (Ausec et al., 2011; Chandra and Chowdhary, 2015). Bacteria may also possess the ability to modify lignin and release smaller aromatic compounds that can be imported into cells and metabolized through aromatic catabolism (Brown and Chang, 2014). Bacterial enzymes show significant potential in lignin degradation and have become candidates for commercial production. While *P. pabuli* E1 enzymes have lower oxidation/reduction potentials and inferior lignin degradation ability compared to fungi, bacteria's strong environmental adaptability and biodiversity have sparked interest in bacterial lignin degradation research (Wang X. et al., 2018).

4.5. Solid-state fermentation

CF refers to the content of fiber in a sample, and it is important to note that the use of acid–base reagents during sample preparation may lead to the destruction of some cellulose and hemicellulose, resulting in a measured value smaller than the actual value. ADF comprises cellulose, lignin, and a small amount of acid-insoluble silicate ash, and there is a strong correlation between ADF and CF in DDGS (Pekel et al., 2013; Liu et al., 2018). DDGS typically contain varying amounts of NDF, ADF, CF, and ADL (Kannadhason et al., 2009). The NDF content is generally higher than the ADF content, indicating a higher hemicellulose content in DDGS (Sharma et al., 2016). Solid-state fermentation has been shown to effectively reduce the content of NSPs in DDGS and improve its nutritional value. Studies have demonstrated that solid-state fermentation using *B. subtilis* and *L. plantarum* can reduce lignin, ADF, and NDF contents by 1.1%, 5%, and 20.4% respectively (Wang C. et al., 2018). Supplementation of cornmeal with *Lactobacillus plantarum* can reduce *CF* content by approximately 77% (Terefe et al., 2021).

Fungi are commonly employed in the fermentation of DDGS. Research has indicated that the addition of Trichoderma can reduce the CF content of corn stalks by approximately 23.5% (Li et al., 2022), while fermentation with *A. niger* can increase the protein content by about 22% (Fan et al., 2022). The increase in protein content is particularly important in providing cost-effective feed, as access to affordable and high-quality feed is a crucial constraint in animal nutrition. Solid-state fermentation of DDGS not only reduces anti-nutritional factors but also increases protein content through bacterial proliferation. Despite the relatively long fermentation period, the increased CP content significantly enhances the competitiveness of DDGS as a high-protein feed.

Studies have demonstrated that feeding fermented DDGS significantly enhances the average daily gain of swine, reduces average daily feed intake and feed-to-weight ratio, and induces beneficial changes in the microbial flora of swine manure (Wang et al., 2017). In summary, solid-state fermentation of DDGS substantially reduces lignocellulosic content and eliminates the negative effects of anti-nutritional factors in the feed on monogastric animals. Concurrently, the increase in CP content improves the competitiveness of DDGS as a protein feed.

5. Conclusion

NSPs include cellulose, xylan, pectin, and smaller amounts of mannan and galactomannan. These complex carbohydrates can have detrimental effects on animal performance as animals lack the necessary digestive enzymes to break them down. Additionally, certain NSPs possess high viscosity due to their network structure, leading to the inhibition of nutrient digestion by adsorbing digestive enzymes. Therefore, it is crucial to identify microorganisms that possess the ability to extensively degrade NSPs. In this study, we conducted a systematic analysis of the potential NSPs-degrading enzymes present in the genome of *P. pabuli* E1. The genome of *P. pabuli* E1 encodes a diverse range of carbohydrate-degrading enzymes. By examining the distribution of carbohydrates, this study provides essential data that can be utilized for the development and application of degrading enzymes. *In vitro* enzyme activity assays were conducted, which demonstrated that *P. pabuli* E1 produces enzymes capable of effectively degrading NSPs. Furthermore, fermentation experiments using DDGS confirmed the practical applicability of *P. pabuli* E1 in eliminating non-starch polysaccharides. Given the presence of numerous potential NSPs-degrading enzymes in *P. pabuli* E1, this microorganism holds significant promise as a candidate for the development of highly efficient enzyme preparations.

Data availability statement

The datasets presented in this study can be found in online repositories. The names of the repository/repositories and accession number(s) can be found at: https://www.ncbi.nlm.nih.gov/genbank/, MT322455.

Author contributions

GL contributed to performing the experiments, analyzing data, and writing the initial draft. YY performed bioinformatics analysis of NSPs enzyme. BJ and ZZ were responsible for testing samples and collecting data. HZ and BM performed the instrument and revised the language of the article. The project fund management and final manuscript preparation were performed by YX, XL, and LW. All authors contributed to the article and approved the submitted version.

Funding

This project was supported by the International (Regional) Cooperation and Exchange Program of the National Natural Science Foundation of China (grant no. 41861124004).

Acknowledgments

The authors are especially grateful to Chi for providing DDGS samples and Wei for his advice on DDGS fermentation.

Conflict of interest

The authors declare that the research was conducted in the absence of any commercial or financial relationships that could be construed as a potential conflict of interest.

Publisher's note

All claims expressed in this article are solely those of the authors and do not necessarily represent those of their affiliated organizations, or those of the publisher, the editors and the reviewers. Any product that may be evaluated in this article, or claim that may be made by its manufacturer, is not guaranteed or endorsed by the publisher.

Supplementary material

The Supplementary material for this article can be found online at: https://www.frontiersin.org/articles/10.3389/fmicb.2023.1205767/full#supplementary-material

References

Abd El-Hack, M. E., Chaudhry, M. T., Mahrose, K. M., Noreldin, A., Emam, M., and Alagawany, M. (2018). The efficacy of using exogenous enzymes cocktail on production, egg quality, egg nutrients and blood metabolites of laying hens fed distiller's dried grains with solubles. *J. Anim. Physiol. Anim. Nutr.* 102, e726–e735. doi: 10.1111/jpn.12825

Arntzen, M. O., Pedersen, B., Klau, L. J., Stokke, R., Oftebro, M., Antonsen, S. G., et al. (2021). Alginate degradation: insights obtained through characterization of a thermophilic exolytic alginate Lyase. *Appl. Environ. Microbiol.* 87:e02399. doi: 10.1128/AEM.02399-20

Artzi, L., Bayer, E. A., and Morais, S. (2017). Cellulosomes: bacterial nanomachines for dismantling plant polysaccharides. *Nat. Rev. Microbiol.* 15, 83–95. doi: 10.1038/nrmicro.2016.164

Attia, M. A., and Brumer, H. (2016). Recent structural insights into the enzymology of the ubiquitous plant cell wall glycan xyloglucan. *Curr. Opin. Struct. Biol.* 40, 43–53. doi: 10.1016/j.sbi.2016.07.005

Ausec, L., Zakrzewski, M., Goesmann, A., Schluter, A., and Mandic-Mulec, I. (2011). Bioinformatic analysis reveals high diversity of bacterial genes for laccase-like enzymes. *PLoS One* 6:e25724. doi: 10.1371/journal.pone.0025724

Baramee, S., Teeravivattanakit, T., Phitsuwan, P., Waeonukul, R., Pason, P., Tachaapaikoon, C., et al. (2017). A novel GH6 cellobiohydrolase from *Paenibacillus curdlanolyticus* B-6 and its synergistic action on cellulose degradation. *Appl. Microbiol. Biotechnol.* 101, 1175–1188. doi: 10.1007/s00253-016-7895-8

Basen, M., Rhaesa, A. M., Kataeva, I., Prybol, C. J., Scott, I. M., Poole, F. L., et al. (2014). Degradation of high loads of crystalline cellulose and of unpretreated plant biomass by the thermophilic bacterium *Caldicellulosiruptor bescii*. *Bioresour. Technol.* 152, 384–392. doi: 10.1016/j.biortech.2013.11.024

Bayer, E. A., Lamed, R., White, B. A., and Flint, H. J. (2008). From cellulosomes to cellulosomics. *Chem. Rec.* 8, 364–377. doi: 10.1002/tcr.20160

Belyea, R. L., Rausch, K. D., and Tumbleson, M. E. (2004). Composition of corn and distillers dried grains with solubles from dry grind ethanol processing. *Bioresour. Technol.* 94, 293–298. doi: 10.1016/j.biortech.2004.01.001

Borin, G. P., Sanchez, C. C., de Souza, A. P., de Santana, E. S., de Souza, A. T., Paes Leme, A. F., et al. (2015). Comparative Secretome analysis of Trichoderma reesei and aspergillus Niger during growth on sugarcane biomass. *PLoS One* 10:e0129275. doi: 10.1371/journal.pone.0129275

Brown, M. E., and Chang, M. C. (2014). Exploring bacterial lignin degradation. *Curr. Opin. Chem. Biol.* 19, 1–7. doi: 10.1016/j.cbpa.2013.11.015

Bugg, T. D., and Rahmanpour, R. (2015). Enzymatic conversion of lignin into renewable chemicals. *Curr. Opin. Chem. Biol.* 29, 10–17. doi: 10.1016/j.cbpa.2015.06.009

Canas, A. I., and Camarero, S. (2010). Laccases and their natural mediators: biotechnological tools for sustainable eco-friendly processes. *Biotechnol. Adv.* 28, 694–705. doi: 10.1016/j.biotechadv.2010.05.002

Cantarel, B. L., Coutinho, P. M., Rancurel, C., Bernard, T., Lombard, V., and Henrissat, B. (2009). The carbohydrate-active EnZymes database (CAZy): an expert resource for Glycogenomics. *Nucleic Acids Res.* 37, D233–D238. doi: 10.1093/nar/gkn663

Casellas, J., Vidal, O., Pena, R. N., Gallardo, D., Manunza, A., Quintanilla, R., et al. (2013). Genetics of serum and muscle lipids in pigs. *Anim. Genet.* 44, 609–619. doi: 10.1111/age.12049

Chandra, R., and Chowdhary, P. (2015). Properties of bacterial laccases and their application in bioremediation of industrial wastes. *Environ Sci Process Impacts* 17, 326–342. doi: 10.1039/C4EM00627E

Chang, X., Xu, B., Bai, Y., Luo, H., Ma, R., Shi, P., et al. (2017). Role of N-linked glycosylation in the enzymatic properties of a thermophilic GH 10 xylanase from *Aspergillus fumigatus* expressed in Pichia pastoris. *PLoS One* 12:e0171111. doi: 10.1371/journal.pone.0171111

Chauhan, P. S., Puri, N., Sharma, P., and Gupta, N. (2012). Mannanases: microbial sources, production, properties and potential biotechnological applications. *Appl. Microbiol. Biotechnol.* 93, 1817–1830. doi: 10.1007/s00253-012-3887-5

Chen, X. A., Ishida, N., Todaka, N., Nakamura, R., Maruyama, J., Takahashi, H., et al. (2010). Promotion of efficient Saccharification of crystalline cellulose by *Aspergillus fumigatus* Swo1. *Appl. Environ. Microbiol.* 76, 2556–2561. doi: 10.1128/AEM.02499-09

Chhe, C., Uke, A., Baramee, S., Tachaapaikoon, C., Pason, P., Waeonukul, R., et al. (2021a). Characterization of a thermophilic facultatively anaerobic bacterium Paenibacillus sp. strain DA-C8 that exhibits xylan degradation under anaerobic conditions. *J. Biotechnol.* 342, 64–71. doi: 10.1016/j.jbiotec.2021.10.008

Chhe, C., Uke, A., Baramee, S., Ungkulpasvich, U., Tachaapaikoon, C., Pason, P., et al. (2021b). Draft genome sequence data of the facultative, thermophilic, xylanolytic bacterium Paenibacillus sp. strain DA-C8. *Data Brief* 35:106784. doi: 10.1016/j.dib.2021.106784

de Almeida, G. A. P., de Andrade Ferreira, M., de Lima Silva, J., Chagas, J. C. C., Veras, A. S. C., de Barros, L. J. A., et al. (2018). Sugarcane bagasse as exclusive roughage for dairy cows in smallholder livestock system. *Asian Australas. J. Anim. Sci.* 31, 379–385. doi: 10.5713/ajas.17.0205

de Lucas, R. C., de Oliveira, T. B., Lima, M. S., Pasin, T. M., Scarcella, A. S. A., Ribeiro, L. F. C., et al. (2021). The profile secretion of aspergillus clavatus: different pre-treatments of sugarcane bagasse distinctly induces holocellulases for the lignocellulosic biomass conversion into sugar. *Renew. Energy* 165, 748–757. doi: 10.1016/j.renene.2020.11.072

De, O., Teixeira, D., Nunes, P. A., and Regina, D. L. (2009). Purification and partial characterization of manganese peroxidase from bacillus pumilus and paenibacillus sp. *Braz. J. Microbiol.* 40, 818–826. doi: 10.1590/S1517-838220090004000012

de Vries, R. P., and Visser, J. (2001). Aspergillus enzymes involved in degradation of plant cell wall polysaccharides. *Microbiol. Mol. Biol. Rev.* 65, 497–522. doi: 10.1128/MMBR.65.4.497-522.2001

de Wet, B. J. M., van Zyl, W. H., and Prior, B. A. (2006). Characterization of the Aureobasidium pullulans α-glucuronidase expressed in *Saccharomyces cerevisiae*. *Enzyme Microb. Technol.* 38, 649–656. doi: 10.1016/j.enzmictec.2005.07.018

Dey, D., Gu, B.-J., Ek, P., Rangira, I., Saunders, S. R., Kiszonas, A. M., et al. (2021). Apple pomace pretreated with hydrochloric acid exhibited better adherence with the corn starch during extrusion expansion. *Carbohydr Polymer Technol Applic* 2:100089. doi: 10.1016/j.carpta.2021.100089

Dhar, H., Swarnkar, M. K., Gulati, A., Singh, A. K., and Kasana, R. C. (2015). Draft genome sequence of a Cellulase-producing Psychrotrophic Paenibacillus strain, IHB B 3415, isolated from the cold environment of the Western Himalayas, India. *Genome Announc.* 3, 1–2. doi: 10.1128/genomeA.01581-14

Dikeman, C. L., and Fahey, G. C. (2006). Viscosity as related to dietary fiber: a review. *Crit. Rev. Food Sci. Nutr.* 46, 649–663. doi: 10.1080/10408390500511862

Escamilla-Alvarado, C., Pérez-Pimienta, J. A., Ponce-Noyola, T., and Poggi-Varaldo, H. M. (2017). An overview of the enzyme potential in bioenergy-producing biorefineries. *J. Chem. Technol. Biotechnol.* 92, 906–924. doi: 10.1002/jctb.5088

Fabrice, S., Anne, B. C., and Philippe, S. (2002). Characterization of the cellulolytic complex (cellulosome). *FEMS Microbiol. Lett.* 217, 15–22. doi: 10.1111/j.1574-6968.2002.tb11450.x

Fan, W., Huang, X., Liu, K., Xu, Y., Hu, B., and Chi, Z. (2022). Nutrition component adjustment of distilled dried grain with Solubles via aspergillus Niger and its change about dynamic physiological metabolism. *Fermentation* 8:264. doi: 10.3390/fermentation8060264

Ferreira Filho, J. A., Horta, M. A. C., Beloti, L. L., Dos Santos, C. A., and de Souza, A. P. (2017). Carbohydrate-active enzymes in Trichoderma harzianum: a bioinformatic analysis bioprospecting for key enzymes for the biofuels industry. *BMC Genomics* 18:779. doi: 10.1186/s12864-017-4181-9

Filipe, D., Dias, M., Magalhães, R., Fernandes, H., Salgado, J., Belo, I., et al. (2023). Solid-state fermentation of Distiller's dried grains with Solubles improves digestibility for European seabass (*Dicentrarchus labrax*) juveniles. *Aust. Fish.* 8:90. doi: 10.3390/fishes8020090

Georgelis, N., Nikolaidis, N., and Cosgrove, D. J. (2015). Bacterial expansins and related proteins from the world of microbes. *Appl. Microbiol. Biotechnol.* 99, 3807–3823. doi: 10.1007/s00253-015-6534-0

Ghio, S., Bradanini, M. B., Garrido, M. M., Ontanon, O. M., Piccinni, F. E., Diaz, M., et al. (2020). Synergic activity of Cel8Pa beta-1,4 endoglucanase and Bg1Pa beta-glucosidase from Paenibacillus xylanivorans A59 in beta-glucan conversion. *Biotechnol. Rep.* 28:e00526. doi: 10.1016/j.btre.2020.e00526

Girio, F. M., Fonseca, C., Carvalheiro, F., Duarte, L. C., Marques, S., and Bogel-Lukasik, R. (2010). Hemicelluloses for fuel ethanol: A review. *Bioresour. Technol.* 101, 4775–4800. doi: 10.1016/j.biortech.2010.01.088

Grady, E. N., MacDonald, J., Liu, L., Richman, A., and Yuan, Z. C. (2016). Current knowledge and perspectives of Paenibacillus: a review. *Microb. Cell Fact.* 15:203. doi: 10.1186/s12934-016-0603-7

Gregg, K. J., Finn, R., Abbott, D. W., and Boraston, A. B. (2008). Divergent modes of glycan recognition by a new family of carbohydrate-binding modules. *J. Biol. Chem.* 283, 12604–12613. doi: 10.1074/jbc.M709865200

Hendriks, A. T., and Zeeman, G. (2009). Pretreatments to enhance the digestibility of lignocellulosic biomass. *Bioresour. Technol.* 100, 10–18. doi: 10.1016/j.biortech.2008.05.027

Hernández-Martínez, C. A., Maldonado Herrera, J. A., Méndez-Zamora, G., Hernández-Luna, C. E., and Gutierréz-Soto, G. (2017). ENZYMATIC EXTRACT OF Trametes maxima CU1 ON PRODUCTIVE PARAMETERS AND CARCASS YIELD OF RABBITS. *Can. J. Anim. Sci.* 97:150. doi: 10.1139/CJAS-2016-0150

Hernández-Martínez, C. A., Treviño-Cabrera, G. F., Hernández-Luna, C. E., Silva-Vázquez, R., Hume, M. E., Gutiérrez-Soto, G., et al. (2018). The effects of hydrolysed sorghum on growth performance and meat quality of rabbits. *World Rabbit Sci.* 26:155. doi: 10.4995/wrs.2018.7822

Iihashi, N., Nagayama, J., Habu, N., Konno, N., and Isogai, A. (2009). Enzymatic degradation of amylouronate (α-(1→4)-linked glucuronan) by α-glucuronidase from Paenibacillus sp. TH501b. *Carbohydr. Polym.* 77, 59–64. doi: 10.1016/j.carbpol.2008.12.004

Irwin, D., Shin, D. H., Sheng, Z., Barr, B. K., and Wilson, D. B. (1998). Roles of the catalytic domain and two cellulose binding domains of *Thermomonospora fusca* E4 in cellulose hydrolysis. *J. Bacteriol.* 180, 1709–1714. doi: 10.1128/JB.180.7.1709-1714.1998

Kannadhason, S., Muthukumarappan, K., and Rosentrater, K. A. (2009). Effects of ingredients and extrusion parameters on aquafeeds containing DDGS and potato starch. *J Aquacult Feed Sci Nutr.* 1, 22–28.

Keggi, C., and Doran-Peterson, J. (2019). *Paenibacillus amylolyticus* 27C64 has a diverse set of carbohydrate-active enzymes and complete pectin deconstruction system. *J. Ind. Microbiol. Biotechnol.* 46, 1–11. doi: 10.1007/s10295-018-2098-1

Kim, E. S., Kim, B. S., Kim, K. Y., Woo, H. M., Lee, S. M., and Um, Y. (2018). Aerobic and anaerobic cellulose utilization by Paenibacillus sp. CAA11 and enhancement of its cellulolytic ability by expressing a heterologous endoglucanase. *J. Biotechnol.* 268, 21–27. doi: 10.1016/j.jbiotec.2018.01.007

Kim, E. S., Lee, H. J., Bang, W. G., Choi, I. G., and Kim, K. H. (2009). Functional characterization of a bacterial expansin from *Bacillus subtilis* for enhanced enzymatic hydrolysis of cellulose. *Biotechnol. Bioeng.* 102, 1342–1353. doi: 10.1002/bit.22193

Ko, C., Lin, Z., Tu, J., Tsai, C., Liu, C., Chen, H., et al. (2010). Xylanase production by Paenibacillus campinasensis BL11 and its pretreatment of hardwood Kraft pulp bleaching. *Int. Biodeter. Biodegr.* 64, 13–19. doi: 10.1016/j.ibiod.2009.10.001

Koeck, D. E., Pechtl, A., Zverlov, V. V., and Schwarz, W. H. (2014). Genomics of cellulolytic bacteria. *Curr. Opin. Biotechnol.* 29, 171–183. doi: 10.1016/j.copbio.2014.07.002

Kohli, P., and Gupta, R. (2015). Alkaline pectinases: A review. *Biocatal. Agric. Biotechnol.* 4, 279–285. doi: 10.1016/j.bcab.2015.07.001

Koutaniemi, S., and Tenkanen, M. (2016). Action of three GH51 and one GH54 alpha-arabinofuranosidases on internally and terminally located arabinofuranosyl branches. *J. Biotechnol.* 229, 22–30. doi: 10.1016/j.jbiotec.2016.04.050

Krueger, N. A., Adesogan, A. T., Staples, C. R., Krueger, W. K., Dean, D. B., and Littell, R. C. (2008). The potential to increase digestibility of tropical grasses with a fungal, ferulic acid esterase enzyme preparation. *Anim. Feed Sci. Technol.* 145, 95–108. doi: 10.1016/j.anifeedsci.2007.05.042

Leite, P., Salgado, J. M., Venancio, A., Dominguez, J. M., and Belo, I. (2016). Ultrasounds pretreatment of olive pomace to improve xylanase and cellulase production by solid-state fermentation. *Bioresour. Technol.* 214, 737–746. doi: 10.1016/j.biortech.2016.05.028

Li, Y., Lei, L., Zheng, L., Xiao, X., Tang, H., and Luo, C. (2020). Genome sequencing of gut symbiotic *Bacillus velezensis* LC1 for bioethanol production from bamboo shoots. *Biotechnol. Biofuels* 13:34. doi: 10.1186/s13068-020-1671-9

Li, G., Li, X., Dong, L., Li, C., Zou, P., Saleemi, M. K., et al. (2021). Isolation, identification and characterization of *Paenibacillus pabuli* E1 to explore its aflatoxin B(1) degradation potential. *Curr. Microbiol.* 78, 3686–3695. doi: 10.1007/s00284-021-02624-4

Li, W., Zhao, L., and He, X. (2022). Degradation potential of different lignocellulosic residues by Trichoderma longibrachiatum and Trichoderma afroharzianum under solid state fermentation. *Process Biochem.* 112, 6–17. doi: 10.1016/j.procbio.2021.11.011

Liberato, M. V., Silveira, R. L., Prates, E. T., de Araujo, E. A., Pellegrini, V. O., Camilo, C. M., et al. (2016). Molecular characterization of a family 5 glycoside hydrolase suggests an induced-fit enzymatic mechanism. *Sci. Rep.* 6:23473. doi: 10.1038/srep23473

Lima, J. O., Pereira, J. F., Araujo, E. F., and Queiroz, M. V. (2017). Pectin lyase overproduction by Penicillium griseoroseum mutants resistant to catabolite repression. *Braz. J. Microbiol.* 48, 602–606. doi: 10.1016/j.bjm.2016.12.009

Liu, L., Fuchang, L. I., Yang, P., and Zhang, C. (2018). Study of components in residues of crude Fiber, neutral detergent Fiber and acid detergent Fiber in feed. *Chin J Anim Nutr* 30, 1044–1051.

Lopez-Mondejar, R., Zuhlke, D., Vetrovsky, T., Becher, D., Riedel, K., and Baldrian, P. (2016). Decoding the complete arsenal for cellulose and hemicellulose deconstruction in the highly efficient cellulose decomposer Paenibacillus 0199. *Biotechnol. Biofuels* 9:104. doi: 10.1186/s13068-016-0518-x

Lumpkins, B., Batal, A., and Dale, N. (2005). Use of distillers dried grains plus Solubles in laying hen diets. *J. Appl. Poultry Res.* 14, 25–31. doi: 10.1093/japr/14.1.25

Ma, L., Lu, Y., Yan, H., Wang, X., Yi, Y., Shan, Y., et al. (2020). Screening of cellulolytic bacteria from rotten wood of Qinling (China) for biomass degradation and cloning of cellulases from *Bacillus methylotrophicus*. *BMC Biotechnol.* 20:2. doi: 10.1186/s12896-019-0593-8

McMahon, A. M., Doyle, E. M., Brooks, S., and O'Connor, K. E. (2007). Biochemical characterisation of the coexisting tyrosinase and laccase in the soil bacterium *Pseudomonas putida* F6. *Enzyme Microb. Technol.* 40, 1435–1441. doi: 10.1016/j.enzmictec.2006.10.020

Mendis, M., Leclerc, E., and Simsek, S. (2016). Arabinoxylans, gut microbiota and immunity. *Carbohydr. Polym.* 139, 159–166. doi: 10.1016/j.carbpol.2015.11.068

Meng, X., Ma, L., Li, T., Zhu, H., Guo, K., Liu, D., et al. (2020). The functioning of a novel protein, Swollenin, in promoting the lignocellulose degradation capacity of Trichoderma guizhouense NJAU4742 from a proteomic perspective. *Bioresour. Technol.* 317:123992. doi: 10.1016/j.biortech.2020.123992

Miller, G. L. (1959). Use of Dinitrosalicylic acid reagent for determination of reducing sugar. *Anal. Chem.* 31, 420–428.

Min, Y. N., Yan, F., Liu, F. Z., Coto, C., and Waldroup, P. W. (2009). Effect of various dietary enzymes on energy digestibility of diets high in distillers dried grains with solubles for broilers. *J. Appl. Poultry Res.* 18, 734–740. doi: 10.3382/japr.2009-00046

Mohammadi Shad, Z., Venkitasamy, C., and Wen, Z. (2021). Corn distillers dried grains with solubles: production, properties, and potential uses. *Cereal Chem.* 98, 999–1019. doi: 10.1002/cche.10445

Mottet, A., de Haan, C., Falcucci, A., Tempio, G., Opio, C., and Gerber, P. (2017). Livestock: on our plates or eating at our table? A new analysis of the feed/food debate. *Glob. Food Sec.* 14, 1–8. doi: 10.1016/j.gfs.2017.01.001

Mukherjee, S., Lodha, T., and Madhuprakash, J. (2023). Comprehensive genome analysis of cellulose and Xylan-active CAZymes from the GenusPaenibacillus: special emphasis on the novel XylanolyticPaenibacillussp. LS1. *Microbiol Spectr.* 11:e0502822. doi: 10.1128/spectrum.05028-22

Obeng, E. M., Adam, S. N. N., Budiman, C., Ongkudon, C. M., Maas, R., and Jose, J. (2017). Lignocellulases: a review of emerging and developing enzymes, systems, and practices. *Bioresourc Bioprocess* 4:8. doi: 10.1186/s40643-017-0146-8

Ontanon, O. M., Ghio, S., Diaz, M., de Villegas, R., Garrido, M. M., Talia, P. M., et al. (2019). A thermostable GH8 endoglucanase of Enterobacter sp. R1 is suitable for beta-glucan deconstruction. *Food Chem.* 298:124999. doi: 10.1016/j.foodchem.2019.124999

Pahm, A. A., Scherer, C. S., Pettigrew, J. E., Baker, D. H., Parsons, C. M., and Stein, H. H. (2009). Standardized amino acid digestibility in cecectomized roosters and lysine bioavailability in chicks fed distillers dried grains with solubles. *Poult. Sci.* 88, 571–578. doi: 10.3382/ps.2008-00184

Patten, C. L., Blakney, A. J., and Coulson, T. J. (2013). Activity, distribution and function of indole-3-acetic acid biosynthetic pathways in bacteria. *Crit. Rev. Microbiol.* 39, 395–415. doi: 10.3109/1040841X.2012.716819

Pedersen, M. B., Dalsgaard, S., Knudsen, K. E. B., Yu, S., and Lærke, H. N. (2014). Compositional profile and variation of distillers dried grains with Solubles from various origins with focus on non-starch polysaccharides. *Anim. Feed Sci. Technol.* 197, 130–141. doi: 10.1016/j.anifeedsci.2014.07.011

Pekel, A. Y., Çakır, E. O., Polat, M., Çakır, K., İnan, G., and Kocabağlı, N. (2013). Correlations between chemical assays and near-infrared reflectance spectroscopy for nutrient components and correlations between nutrients and color scores of distillers dried grains with solubles. *J. Appl. Poultry Res.* 22, 814–824. doi: 10.3382/japr.2013-00728

Ramírez-Cavazos, L. I., Junghanns, C., Ornelas-Soto, N., Cárdenas-Chávez, D. L., Hernández-Luna, C., Demarche, P., et al. (2014). Purification and characterization of two thermostable laccases from Pycnoporus sanguineus and potential role in degradation of endocrine disrupting chemicals. *J. Mol. Catal. B: Enzym.* 108, 32–42. doi: 10.1016/j.molcatb.2014.06.006

Raza, W., and Shen, Q. (2010). Growth, Fe3+ reductase activity, and siderophore production by *Paenibacillus polymyxa* SQR-21 under differential iron conditions. *Curr. Microbiol.* 61, 390–395. doi: 10.1007/s00284-010-9624-3

Saloheimo, M., Paloheimo, M., Hakola, S., Pere, J., Swanson, B., Nyyssonen, E., et al. (2002). Swollenin, a Trichoderma reesei protein with sequence similarity to the plant

expansins, exhibits disruption activity on cellulosic materials. *Eur. J. Biochem.* 269, 4202–4211. doi: 10.1046/j.1432-1033.2002.03095.x

Seo, J., Kim, W., Kim, J., Kim, J. K., Kim, S. C., Jang, Y., et al. (2015). Effects of palm kernel expellers on growth performance, nutrient digestibility, and blood profiles of weaned pigs. *Asian Australas. J. Anim. Sci.* 28, 987–992. doi: 10.5713/ajas.14.0842

Seo, D. J., Lee, Y. S., Kim, K. Y., and Jung, W. J. (2016). Antifungal activity of chitinase obtained from *Paenibacillus ehimensis* MA2012 against conidial of Collectotrichum gloeosporioides in vitro. *Microb. Pathog.* 96, 10–14. doi: 10.1016/j.micpath.2016.04.016

Sermsathanaswadi, J., Baramee, S., Tachaapaikoon, C., Pason, P., Ratanakhanokchai, K., and Kosugi, A. (2017). The family 22 carbohydrate-binding module of bifunctional xylanase/beta-glucanase Xyn10E from *Paenibacillus curdlanolyticus* B-6 has an important role in lignocellulose degradation. *Enzyme Microb. Technol.* 96, 75–84. doi: 10.1016/j.enzmictec.2016.09.015

Sharma, R., Lamsal, B. P., and Colonna, W. J. (2016). Pretreatment of fibrous biomass and growth of biosurfactant-producing *Bacillus subtilis* on biomass-derived fermentable sugars. *Bioprocess Biosyst. Eng.* 39, 105–113. doi: 10.1007/s00449-015-1494-4

Sharma, N., Rathore, M., and Sharma, M. (2012). Microbial pectinase: sources, characterization and applications. *Rev. Environ. Sci. Biotechnol.* 12, 45–60. doi: 10.1007/s11157-012-9276-9

Srivastava, S., Dafale, N. A., and Purohit, H. J. (2020). Functional genomics assessment of lytic polysaccharide mono-oxygenase with glycoside hydrolases in *Paenibacillus dendritiformis* CRN18. *Int. J. Biol. Macromol.* 164, 3729–3738. doi: 10.1016/j.ijbiomac.2020.08.147

Streams (2006). Methodology to determine soluble content in dry grind ethanol coproduct streams. *Appl. Eng. Agric.* 22:244. doi: 10.13031/2013.22244

Swiatkiewicz, S., Swiatkiewicz, M., Arczewska-Wlosek, A., and Jozefiak, D. (2016). Efficacy of feed enzymes in pig and poultry diets containing distillers dried grains with solubles: a review. *J. Anim. Physiol. Anim. Nutr.* 100, 15–26. doi: 10.1111/jpn.12351

Tamaru, Y., Miyake, H., Kuroda, K., Nakanishi, A., Matsushima, C., Doi, R. H., et al. (2011). Comparison of the mesophilic cellulosome-producing *Clostridium cellulovorans* genome with other cellulosome-related clostridial genomes. *J. Microbial. Biotechnol.* 4, 64–73. doi: 10.1111/j.1751-7915.2010.00210.x

Tanimoto, S., Higashi, M., Yoshida, N., and Nakano, H. (2016). The ion dependence of carbohydrate binding of CBM36: an MD and 3D-RISM study. *J. Phys. Condens. Matter* 28:344005. doi: 10.1088/0953-8984/28/34/344005

Teramoto, K., Tsutsui, S., Sato, T., Fujimoto, Z., and Kaneko, S. (2021). Substrate specificities of GH8, GH39, and GH52 beta-xylosidases from *Bacillus halodurans* C-125 toward substituted Xylooligosaccharides. *Appl. Biochem. Biotechnol.* 193, 1042–1055. doi: 10.1007/s12010-020-03451-2

Terefe, Z. K., Omwamba, M. N., and Nduko, J. M. (2021). Effect of solid state fermentation on proximate composition, antinutritional factors and in vitro protein digestibility of maize flour. *Food Sci. Nutr.* 9, 6343–6352. doi: 10.1002/fsn3.2599

Thapa, S., Mishra, J., Arora, N., Mishra, P., Li, H., O'Hair, J., et al. (2020). Microbial cellulolytic enzymes: diversity and biotechnology with reference to lignocellulosic biomass degradation. *Rev. Environ. Sci. Biotechnol.* 19, 621–648. doi: 10.1007/s11157-020-09536-y

Wang, B., Chen, K., Zhang, P., Long, L., and Ding, S. (2022). Comparison of the biochemical properties and roles in the xyloglucan-rich biomass degradation of a GH74 Xyloglucanase and its CBM-deleted variant from Thielavia terrestris. *Int. J. Mol. Sci.* 23:5276. doi: 10.3390/ijms23095276

Wang, J., Han, Y., Zhao, J.-Z., Zhou, Z.-J., and Fan, H. (2017). Consuming fermented distillers' dried grains with solubles (DDGS) feed reveals a shift in the faecal microbiota of growing and fattening pigs using 454 pyrosequencing. *J. Integr. Agric.* 16, 900–910. doi: 10.1016/S2095-3119(16)61523-X

Wang, S., Huang, X., Zhang, Y., Yin, C., and Richel, A. (2021). The effect of corn straw return on corn production in Northeast China: an integrated regional evaluation with meta-analysis and system dynamics. *Resour. Conserv. Recycl.* 167:105402. doi: 10.1016/j.resconrec.2021.105402

Wang, W. K., and Liang, C. M. (2021). Enhancing the compost maturation of swine manure and rice straw by applying bioaugmentation. *Sci. Rep.* 11:6103. doi: 10.1038/s41598-021-85615-6

Wang, H., Pu, Y., Ragauskas, A., and Yang, B. (2019). From lignin to valuable products-strategies, challenges, and prospects. *Bioresour. Technol.* 271, 449–461. doi: 10.1016/j.biortech.2018.09.072

Wang, C., Su, W., Zhang, Y., Hao, L., Wang, F., Lu, Z., et al. (2018). Solid-state fermentation of distilled dried grain with solubles with probiotics for degrading lignocellulose and upgrading nutrient utilization. *AMB Exp* 8:188. doi: 10.1186/s13568-018-0715-z

Wang, X., Yao, B., and Su, X. (2018). Linking enzymatic oxidative degradation of lignin to organics detoxification. *Int. J. Mol. Sci.* 19:3373. doi: 10.3390/ijms19113373

Wang, L., Zhang, Y., Gao, P., Shi, D., Liu, H., and Gao, H. (2006). Changes in the structural properties and rate of hydrolysis of cotton fibers during extended enzymatic hydrolysis. *Biotechnol. Bioeng.* 93, 443–456. doi: 10.1002/bit.20730

Wilson, D. B. (2008). Three microbial strategies for plant cell wall degradation. *Ann. N. Y. Acad. Sci.* 1125, 289–297. doi: 10.1196/annals.1419.026

Xie, J. B., Du, Z., Bai, L., Tian, C., Zhang, Y., Xie, J. Y., et al. (2014). Comparative genomic analysis of N2-fixing and non-N2-fixing Paenibacillus spp.: organization, evolution and expression of the nitrogen fixation genes. *PLoS Genet.* 10:e1004231. doi: 10.1371/journal.pgen.1004231

Xie, J., Shi, H., Du, Z., Wang, T., Liu, X., and Chen, S. (2016). Comparative genomic and functional analysis reveal conservation of plant growth promoting traits in Paenibacillus polymyxa and its closely related species. *Sci. Rep.* 6:21329. doi: 10.1038/srep21329

Xu, W., Reddy, N., and Yang, Y. (2009). Extraction, characterization and potential applications of cellulose in corn kernels and distillers' dried grains with solubles (DDGS). *Carbohydr. Polym.* 76, 521–527. doi: 10.1016/j.carbpol.2008.11.017

Xu, R., Zhang, K., Liu, P., Han, H., Zhao, S., Kakade, A., et al. (2018). Lignin depolymerization and utilization by bacteria. *Bioresour. Technol.* 269, 557–566. doi: 10.1016/j.biortech.2018.08.118

Yang, G., Chen, W., Tan, H., Li, K., Li, J., and Yin, H. (2020). Biochemical characterization and evolutionary analysis of a novel pectate lyase from aspergillus parasiticus. *Int. J. Biol. Macromol.* 152, 180–188. doi: 10.1016/j.ijbiomac.2020.02.279

Yuan, Y., Zhang, X. Y., Zhao, Y., Zhang, H., Zhou, Y. F., and Gao, J. (2019). A novel PL9 pectate Lyase from *Paenibacillus polymyxa* KF-1: cloning, expression, and its application in pectin degradation. *Int. J. Mol. Sci.* 20:3060. doi: 10.3390/ijms20123060

Zhang, X. J., Wang, L., Wang, S., Chen, Z. L., and Li, Y. H. (2021). Contributions and characteristics of two bifunctional GH43 beta-xylosidase /alpha-L-arabinofuranosidases with different structures on the xylan degradation of Paenibacillus physcomitrellae strain XB. *Microbiol. Res.* 253:126886. doi: 10.1016/j.micres.2021.126886

Zhao, Y., Yuan, Y., Zhang, X., Li, Y., Li, Q., Zhou, Y., et al. (2018). Screening of a novel polysaccharide Lyase family 10 pectate Lyase from *Paenibacillus polymyxa* KF-1: cloning, Expression and Characterization. *Molecules* 23:2774. doi: 10.3390/molecules23112774

frontiers | Frontiers in Microbiology

TYPE Original Research
PUBLISHED 04 September 2023
DOI 10.3389/fmicb.2023.1237442

OPEN ACCESS

EDITED BY
Michela Verni,
Sapienza University of Rome, Italy

REVIEWED BY
María Esteban-Torres,
Spanish National Research Council (CSIC), Spain
Byung Hee Chun,
Pukyong National University, Republic of Korea
Do-Won Jeong,
Dongduk Women's University, Republic of Korea

*CORRESPONDENCE
Nam Soo Han
✉ namsoo@cbnu.ac.kr

†These authors have contributed equally to this work and share first authorship

RECEIVED 09 June 2023
ACCEPTED 18 August 2023
PUBLISHED 04 September 2023

CITATION
Kim DH, Kim S-A, Jo NG, Bae J-H, Nguyen MT, Jo YM and Han NS (2023) Phenotypic and genomic analyses of bacteriocin-producing probiotic *Enterococcus faecium* EFEL8600 isolated from Korean soy-meju. *Front. Microbiol.* 14:1237442. doi: 10.3389/fmicb.2023.1237442

Phenotypic and genomic analyses of bacteriocin-producing probiotic *Enterococcus faecium* EFEL8600 isolated from Korean soy-meju

Da Hye Kim†, Seul-Ah Kim†, Na Gyeong Jo, Jae-Han Bae, Minh Tri Nguyen, Yu Mi Jo and Nam Soo Han*

Brain Korea 21 Center for Bio-Health Industry, Division of Animal, Horticultural, and Food Sciences, Chungbuk National University, Cheongju, Republic of Korea

Enterococcus faecium is a prevalent species found in fermented soybean products, known for its contributions to flavor development and inhibition of pathogenic microorganisms during fermentation. This study aims to provide comprehensive phenotypic and genomic evidence supporting the probiotic characteristics of *E. faecium* EFEL8600, a bacteriocin-producing strain isolated from Korean soy-meju. Phenotypic analysis revealed that EFEL8600 produced a peptide with inhibitory activity against *Listeria monocytogenes*, estimated to be 4.6 kDa, corresponding to the size of enterocins P or Q. Furthermore, EFEL8600 exhibited probiotic traits, such as resilience in gastrointestinal conditions, antioxidant and anti-inflammatory activities, and protection of the intestinal barrier. Safety assessments demonstrated no hemolytic and bile salt deconjugation activities. Genomic analysis revealed the presence of several genes associated with probiotic characteristics and bacteriocin production, while few deleterious genes with a low likelihood of expression or transferring were detected. Overall, this study highlights *E. faecium* EFEL8600 as a potent anti-listeria probiotic strain suitable for use as a starter culture in soymilk fermentation, providing potential health benefits to consumers.

KEYWORDS

probiotic, lactic acid bacteria, soy-milk, bacteriocin, *Enterococcus faecium*, *Listeria* inhibition

1. Introduction

Soybean, a widely consumed legume, contains a diverse array of functional components, including isoflavones, soyasaponins, terpenes, and sterols, alongside anti-nutritional factors such as phytates and trypsin inhibitors (Licandro et al., 2020). The fermentation mediated by lactic acid bacteria (LAB) can effectively reduce phytates and trypsin inhibitors, and also facilitate the hydrolysis of tannic acid through their tannase activities leading to the generation of novel compounds that were not originally present in raw soybean (Jang et al., 2021). However, *Listeria monocytogenes*, a gram-positive foodborne pathogen, has been detected or presented a high risk of contamination in soy-based products, including soymilk (Haraguchi et al., 2019), soybean paste (Nam et al., 2012), and tempeh (Ashenafi, 1991). Consequently, the development of an effective fermentation process to ensure the safety of soy products has become an imperative task.

Bacteriocins are defined as a narrow range of antimicrobial peptides produced by major lineages of bacteria and some members of the Archaea (Bharti et al., 2015). Bacteriocin production can be beneficial to the host microbes by inhibiting or competing with other bacteria in the same environmental niche (Deegan et al., 2006). Many bacteriocins produced from lactic acid bacteria can be applied in the industry for food fermentation because they can suppress the growth of many problematic microorganisms in processed foods (Cotter et al., 2005). In the case of nisin, which is produced by *Lactococcus lactis,* has already been approved as a GRAS (generally regarded as safe) for food additive (Özel et al., 2018).

Enterococci are increasingly investigated as a potential probiotic candidate, and *Enterococcus faecium* is typically available as a probiotic on the market (Zommiti et al., 2018). The health-beneficial effects of *E. faecium* were reported as lowering cholesterol levels (Singhal et al., 2019), alleviating diarrhea (Torres-Henderson et al., 2017), and regulating the immune system (Franz et al., 2011). Notably, several studies reported that *Enterococcus* spp. can produce bacteriocins against foodborne pathogens such as *Listeria* spp. which belonging to various classes (Favaro et al., 2014). Especially, enterocin, which is representative bacteriocin produced by *Enterococcus*, is composed of small molecular weight peptides and has specific anti-microbial activity against gram-positive and putrefactive bacteria (Franz et al., 2011). Previously, several studies were reported on bacteriocin produced by *E. faecium*, including enterocin A, B, P, L50a, L50b, and Q (Valledor et al., 2022).

Meju, a solid-state soybean preculture consisting of a microbial consortium including bacteria and fungi, plays a crucial role as both an inoculum and a substrate in the fermentation process of traditional Korean soy-based foods such as doenjang (soybean paste) and ganjang (soybean sauce) (Jung et al., 2014). Throughout the fermentation process, the diverse enzymes secreted by the microbial community present in meju facilitate the hydrolysis of soybean polypeptides, carbohydrates, lipids, and isoflavone glycosides, resulting in the production of amino acids, sugars, organic acids, aglycones, and flavor compounds (Han et al., 2023). Notably, among the bacterial species inhabiting meju, *Enterococcus faecium* has been identified as the predominant microorganism due to its fast growth rate in soybean cultures and its ability to contribute to the development of desirable flavors in fermented foods (Jeong et al., 2019; Kumari et al., 2022).

Within the same context, we isolated various *E. faecium* strains from soy-meju and tested their anti-microbial and probiotic activities. Following comprehensive analysis, we identified *E. faecium* EFEL8600 as a superior strain. This study presents an in-depth investigation into the phenotypic characteristics of *E. faecium* EFEL8600, encompassing microbial and biochemical traits, probiotic properties (including safety, gastrointestinal stability, and health-promoting effects), and its capacity for bacteriocin production. Additionally, we provide insights into the genetic characteristics of EFEL8600, focusing on the presence of genes associated with safety, probiotic properties, and bacteriocin production. By elucidating these aspects, our study contributes to the understanding of *E. faecium* EFEL8600 as a promising candidate for potential applications in soybean fermentation.

2. Materials and methods

2.1. Bacterial isolation and culture conditions

E. faecium EFEL8600 was isolated from soy-meju and cultured in MRS medium (BD Difco™, Sparks, MD, United States) supplemented with 0.002% of bromophenol blue at a temperature of 37°C under aerobic condition without shaking. *Listeria monocytogenes* KCTC 3569 used as pathogenic bacteria were cultivated in BHI medium (BD Difco™) at a temperature of 37°C under anaerobic condition. The specific cultural conditions and growth media employed for other microorganisms utilized in this study are detailed in Table 1. *Lacticaseibacillus rhamnosus* GG (LGG) and *Lactiplantibacillus plantarum* WCFS1 (WCFS1) were selected as the reference probiotic strains for comparative analysis.

2.2. Antimicrobial activity analysis

The antimicrobial activity of the isolates was determined using the agar well diffusion assay, as described by Jozala et al. (2005). Briefly, the isolates were cultured in MRS medium for 15 h and adjusted the optical density as 1.0. The supernatant fractions were obtained by centrifugation (10,000 × *g* for 10 min) and filtration through a 0.22 μm filter to obtain cell-free supernatants (CFS). The CFS was neutralized with 5 N NaOH. Subsequently, 100 μL of the filtered supernatants was added to 10 mm diameter wells created in a BHI agar plate previously spread with overnight-cultured *Listeria monocytogenes*. The plates were incubated at 37°C overnight, and the inhibitory activity was determined by measuring the size of the inhibition halo around the well, compared to ampicillin (1 mg/mL) as a control.

TABLE 1 Microorganism used in this study.

Species	Collections	Culture condition
Enterococcus faecium EFEL8600	KCTC 14743BP	37°C, MRS
Enterococcus faecium	DSM 20477	37°C, MRS
Lacticaseibacillus rhamnosus GG	KCTC 5033	37°C, MRS
Lactiplantibacillus plantarum WCFS1	ATCC BAA-793	37°C, MRS
Listeria monocytogenes	KCTC 3569	37°C, BHI
Limosilactobacillus reuteri	ATCC 23272	37°C, MRS
Enterococcus faecalis	KCCM 11729	37°C, BHI
Enterococcus faecium	ATCC 19434	37°C, MRS

2.3. Molecular characterization of bacteriocin

The neutralized CFS was used for bacteriocin purification. In details, ammonium sulfate (Sigma-Aldrich) was gently added to the sample to obtain 60% saturation and stirred for 15 h at 4°C. Then, it was desalted by dialysis with a cellulose semipermeable membrane (Spectra/Por dialysis tube membrane, MW cut-off 1 kDa, no. 132638; Spectrum Labs, Irving, TX, United States) in 20 mM potassium phosphate buffer (pH 7.0). Then, bacteriocin was purified with anion exchange chromatography (DEAE cellulose; Sigma-Aldrich). To determine the molecular weight of the purified bacteriocin, tricine-sodium dodecyl sulfate-polyacrylamide gel electrophoresis (Tricine SDS-PAGE) and gel overlay assay against *L. monocytogenes* KCTC 3569 (10^6 CFU/mL) were conducted. The active bacteriocin area was determined by visual observation after incubating overnight at 37°C and the titers of an antimicrobial peptide expressed as arbitrary units (AU; mL^{-1} of medium). To determine mass spectra of bacteriocin, autoflex maX MALDI-TOF/TOF (Bruker Daltonics, Bremen, Germany) was used in the linear positive mode. The purified bacteriocin sample was desalted with C18-ziptip. FlexControl 3.4 software (Bruker Daltonics) was applied to acquire and process the spectra. Sample was mixed with matrix solution [Super-DHB (2,5-dihydroxybenzoic acid: 2-hydroxy-5-methoxy benzoic acid = 9: 1 (w/w)) in 0.1% trifluoroacetic acid/cetonitrile (1:1, v/v)] directly on the MALDI target and vacuum drying. Charged ions were distinguished in the *m/z* range of 1,000–10,000 Da, and 500 shots were accumulated per one spectrum.

2.4. Safety assessment

The hemolytic activity of EFEL8600 was analyzed by cultivating the strain on BHI medium containing 7% horse blood (MB CELL, Seoul, Republic of Korea) at 37°C for 24 h (Ryu and Chang, 2013). Then, hemolytic zones were compared with that of *L. monocytogenes* used as a positive control. The bile acid deconjugating activity of the strains were determined by culturing the strains on MRS agar with 0.5% taurodeoxycholic acid (w/v) under anaerobic conditions at 37°C for 48 h. Deconjugation of taurodeoxycholic acid created a white opaque precipitate of deoxycholate in the surrounding area of colonies. The concentration of DL-lactate was determined using high-performance liquid chromatography (HPLC) with an Agilent 1260 Infinity HPLC system (Agilent Technologies, CA, United States). For the analysis, a Shodex ORpak CRX-853 column (8.0 × 50 mm, Showa Denko, Tokyo, Japan) coupled with a CRX-G column (Showa Denko) was used. The supernatant was collected and filtered using a 0.22 μm microfilter membrane (Whatman) after cultivation in MRS medium for 15 h and the filtrate was used for HPLC analysis. $CuSO_4$ (1 mM) was used as an eluent with 1 mL/min of flow rate at room temperature. Hyaluronidase activity was measured by incubating EFEL8600 strain with hyaluronic acid (3 mg/mL) in 12.5 mM $CaCl_2$ at 37°C for 40 min (Ölgen et al., 2007). After reaction, a coloring reagent, *p*-dimethyl amino benzaldehyde (*p*DMAB) in glacial acetic acid and hydrochloric acid (1.5 mL, 9:1, v/v), was added, resulting in a reddish-purple colored product detected at 585 nm. All safety assessments in this study were conducted following the guidelines primarily established by FAO/WHO (2002).

2.5. Antibiotic resistance

Antibiotic resistance of EFEL8600 was determined by minimum inhibitory concentration (MIC) based on the Clinical and Laboratory Standards Institute (CLSI) method CLSI (2019). The ten antibiotics ampicillin, vancomycin, gentamicin, kanamycin, streptomycin, erythromycin, clindamycin, tetracycline, chloramphenicol, tylosine were tested followed by EFSA (2018) guideline. Then pre-cultured EFEL8600 (final concentration 5×10^5 CFU/mL) was inoculated into Mueller-Hinton broth (Sigma-Aldrich, St. Louis, MO, United States) (100 μL) containing each antibiotic range of 0.125 to 256 mg/L. The plate was cultured under anaerobic conditions at 37°C for 48 h. The minimum concentration at which the strain did not survive was determined as MIC by visual observation.

2.6. Gastrointestinal stability

Tolerance to artificial gastrointestinal conditions were investigated by culturing the strain in pH adjusted PBS with HCl (pH 3.0 and pH 2.5) or PBS solution containing 0.3% (w/v) bile salt (Sigma-Aldrich) (Conway et al., 1987). After 0, 90, and 180 min incubation at 37°C, survival rate was estimated by viable cell counting on MRS agar and compared with reference strains. The adhesion of EFEL8600 to intestinal epithelial cells was assessed using Caco-2 and HT-29 epithelial cell lines, obtained from the Korean Cell Line Bank (Seoul, Republic of Korea). The cells were cultured in DMEM (Dulbecco's modified Eagle's medium; Hyclone, UT, United States) supplemented with fetal bovine serum (FBS; Hyclone), 1% penicillin (10,000 U/mL), and 1% streptomycin (10 mg/mL). Caco-2 and HT-29 cells were seeded at a density of 4.7×10^5 cells/well in 24-well tissue culture plates without antibiotics. Bacterial cells (1×10^8 CFU/mL) were resuspended in DMEM without antibiotics and applied to the Caco-2 and HT-29 cell monolayers. After incubating for 2 h at 37°C in a 5% CO_2 incubator, a detachment solution containing 0.1% Triton X-100 and 0.1% trypsin-EDTA (Sigma-Aldrich) was used to detach the cells for 15 min. The detached cells were then washed with PBS and cultured on MRS agar plates to enumerate the adherent bacteria. The adherent bacteria were compared with reference probiotics. The experiments were performed in triplicate.

2.7. Protective effects on H_2O_2-induced intestinal damages

To analyze the gut barrier function of EFEL8600, the intestinal permeability was measured in the epithelial barrier model using 12 well Transwell® inserts (polyester membrane with 0.4 μm pore size, 12 mm diameter; Costar, Corning Life Science, Kennebunk, United States) at a density of 5×10^4 cells per cm^2 of Caco-2 cell (Miyauchi et al., 2012). Caco-2 cell was cultivated until the transepithelial/transendothelial electrical resistance (TEER) value reached 200 Ω·cm^2 which regarded as confluent by changing the medium every 48 h using Millicell-ERS (Millipore, Burlington, MA, United States). Then, 100 μM of H_2O_2 was treated to the Caco-2 cells (5×10^7 CFU/well) for 30 min and TEER value was analyzed every 30 min after sensitization. The results were expressed as % TEER compared with the initial TEER value at T_0 (before the addition of

H_2O_2) for each insert using the formula: TEER ($\Omega \cdot cm^2$)/initial TEER ($\Omega \cdot cm^2$) × 100 (%). In addition, 100 μg/mL of fluorescein isothiocyanate (FITC)-dextran was treated to upper chamber in the dark condition at room temperature for 4 h. Samples (100 μL) from the lower chamber of each well were moved to an opaque black 96-well plate. Then, intensity of fluorescence was measured by a fluorescence spectrometer (LS55, Perkin Elmer Instruments, Waltham, United States) at excitation (485 nm) and emission (535 nm) wavelengths. The experiments were conducted in triplicate.

2.8. Antioxidative activity

The antioxidant activity of EFEL8600 was assessed by 2,2-diphenyl-1-picrylhydrazyl (DPPH) scavenging ability (Das and Goyal, 2015) using the three fractions: intact cells, cell-free culture supernatants (CFS) and, cell-free extracts (CFE). DPPH solution was prepared as 0.4 mmol/L and concentration of cultured cells were adjusted as 5×10^8 cells/mL. Intact cells were made by resuspending in 0.85% NaCl, and CFS was collected by centrifugation after the pH was adjusted to 7.0 with 1 M of NaOH. For CFE preparation, cells were broken by sonicator (VP-050 N; Taitec Corp., Saitama, Japan) for 10 min (pulse 5 s on/5 s off at 35% amplitude), and the cell debris was eliminated by centrifugation (10,000 × *g*, 30 min). Then, 100 μL of each sample or ethanol (negative control) was reacted with 100 μL of prepared DPPH solution at 37°C in the dark condition for 30 min. Then, absorbance of samples was assessed at 517 nm by microplate reader (BioTek, Winooski, United States). The experiments were conducted in triplicate.

2.9. Nitric oxide assay

The inhibitory activities of the EFEL8600 on nitric oxide (NO) production were analyzed using LPS-induced RAW 264.7 cells (Yu et al., 2019). For heat-kill cell, bacterial cells (5×10^8 cells/mL) were exposed to a heat treatment at 95°C for 30 min, and cell lysates were prepared as described in manufacturing CFE. The murine macrophage cell line RAW 264.7 (2×10^5 cells/well) was retained in DMEM supplemented with 10% FBS (Hyclone) containing 1% penicillin–streptomycin at 37°C in 5% CO_2 incubator. The 1 μg/mL LPS was treated to RAW 264.7 to induce NO production and heat-killed cells or lysates (5×10^7 cells/well) were treated sequentially. After 24 h incubation, Griess reagent (Sigma-Aldrich) was treated to supernatant obtained from the each well and reacted in dark at 25°C for 15 min. Every absorbance at 540 nm was measured by a microplate reader (Bio-Tek). The experiments were conducted in triplicate.

2.10. Biochemical characteristics

The carbohydrate utilization ability of the *E. faecium* EFEL8600 was assessed using the API CHL kit (BioMériux Co., Marcy-l'Étoile, France) following the manufacturer's instructions. After cultivation, bacterial cells were harvested and resuspended in API 50CH medium. A 120 μL aliquot of the suspension was inoculated into a tube containing strips. Mineral oil was then added to cover the tube, and the setup was incubated at 37°C for 48 h. The fermentation pattern was observed and recorded. A positive result was recorded when the blue indicator in the medium changed to yellow, indicating carbohydrate utilization.

2.11. Whole genome sequencing

To perform whole genome analysis, the genomic DNA of *E. faecium* EFEL8600 was extracted from the 15 h cultured cells in MRS medium (Difco) at 37°C using a bacterial genomic DNA prep kit (Solgent, Daejeon, Republic of Korea) according to the manufacturer's instructions. The prepared genomic DNA was kept at −20°C for future use. DNA libraries were generated with Nanopore for long reads using MinION kit (Barcoding kit, EXP-NDB114; Ligation sequencing kit, LSK-109; Oxford Nanopore Technologies, Oxford, United Kingdom) and with Illumina Hi-seq for short read using TruSeq Nano DNA kit (Illumina, CA, United States). The quality of the reads was checked using FastQC v0.11.9 (Andrews et al., 2010), and Trimmomatic v0.36 program (Bolger et al., 2014) was used for filtering quality and removing Illumina adapter sequences. Hybrid genome assembly was conducted using short reads (Illumina) data and long reads (MinION) in SPAdes v3.15.2 (Bankevich et al., 2012). Finally, the complete genome sequence of EFEL8600 was annotated using the Prokka (prokaryotic genome annotation v1.13; Tatusova et al., 2016). Average nucleotide identity (ANI) is a measurement of genomic similarity in nucleotide-level between the coding sequence of two genomes, and OrthoANI is an improved method that compares orthologous fragment pairs (Lee et al., 2016). Orthologous (Ortho) ANI was analyzed using CJ Bioscience's OrthoANI Tool (OAT), available on the EzBioCloud server.

2.12. *In silico analysis* of safety and probiotic properties

Genes related to virulence factors and toxin genes in EFEL8600 were analyzed by virulence factor database (VFDB) at http://www.mgc.ac.cn/cgi-bin/VFs/v5/main.cgi (Liu et al., 2022). The genome file in FASTA format was uploaded, and the genus was specified as *Enterococcus* to investigate the virulence factors predominantly found within this genus. A stringent search with cut-off values at >80% identity and >60% coverage and a less stringent search with cut-off values at >60% similarity, >60% coverage, and *E*-values <1e−10 were employed to discover putative virulence genes. In addition, BlastKoala search tool in the Kyoto Encyclopedia of Genes and Genomes (KEGG) database (Version 90.1) at https://www.kegg.jp/blastkoala/ was used to determine virulence factors and antibiotics resistance genes (Oh et al., 2022). Their transferability was analyzed by PHASTER at http://phaster.ca/ (Arndt et al., 2019).

Genes associated with probiotic properties, including resistance to gastrointestinal conditions, temperature, osmotic stress, oxidation, as well as genes related to bacteriocin production, were identified in EFEL8600 by searching the NCBI database. The sequence similarity of these genes was then compared using BLASTP (Lebeer et al., 2008). The presence of genes encoding bacteriocin in the EFEL8600 genome was determined using the web-based bacteriocin genome mining tool, BAGEL4, available at http://bagel4.molgenrug.nl/index.php. BAGEL tool identifies bacteriocins and their related clusters (van Heel et al.,

2018). In details, it detects all genes related to bacteriocin processing, regulation, modification, passage, and immunity protein commonly located in near the putative bacteriocin sequence.

3. Results

3.1. Phenotype analysis of *Enterococcus faecium* EFEL8600

3.1.1. Anti-microbial activity

To analyze the antimicrobial activity of *E. faecium* EFEL8600, the agar well diffusion assay was conducted by measuring the halo size around the well. As shown in Figure 1A, the neutralized cell-free supernatant from *E. faecium* EFEL8600 demonstrated a 4 mm clear inhibition zone and the positive control displayed a 10 mm clear zone of inhibition in the agar where *L. monocytogenes* was cultured as an indicator strain. Conversely, the negative control did not exhibit any observable zone of inhibition. This result revealed that the culture supernatant of EFEL8600 contained the antimicrobial compounds against *L. monocytogenes*.

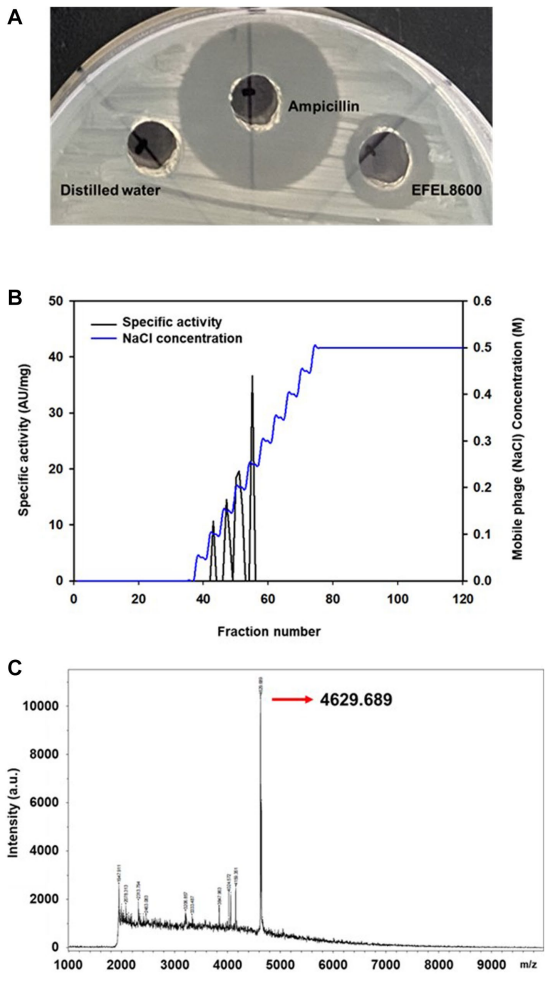

FIGURE 1
Antimicrobial activity of *Enterococcus faecium* EFEL8600 and purification of neutralized cell-free supernatant by anion exchange chromatography **(A)** Antimicrobial activity of neutralized cell-free supernatant from *E. faecium* EFEL8600 against *Listeria monocytogenes*. Positive control, ampicillin (1 mg/mL); negative control, distilled water. **(B)** The elution profiles of bacteriocin produced by *E. faecium* EFEL8600. Bacteriocin was eluted from the DEAE cellulose using a 11-step gradient with 0 to 0.5 M NaCl. The specific activity and corresponding mobile phage (NaCl) concentrations are indicated by the left and right y-axis, respectively. **(C)** MALDI-TOF/TOF spectrum of purified active bacteriocin sample (anion exchange chromatography).

3.1.2. Molecular characterization of bacteriocin

Antimicrobial compounds of EFEL8600 strain were obtained by precipitating the culture supernatant using 60% ammonium sulfate, and the specific activities of the culture supernatant and precipitate fractions were measured as 1.28 and 36.98 AU/mg protein, respectively. This indicated a significant 28.89-fold increase in specific activity, revealing protein(bacteriocin)-like properties of the antimicrobial compounds. Subsequently, anion exchange chromatography (DEAE-cellulose) was employed to separate the active fraction, as shown in Figure 1B. Among the eluted fractions, fraction 55, obtained with 0.25 M NaCl, exhibited the highest activity against *L. monocytogenes*. This step led to a 28.74-fold increase in antimicrobial activity (Table 2). To determine the molecular weight of the purified bacteriocin, a gel overlay assay was performed (Supplementary Figure S1). Tricine SDS-PAGE analysis of the active fraction obtained from anion exchange chromatography revealed multiple peptide bands, while a distinct clear zone surrounding the 5 kDa region appeared upon incubation with *L. monocytogenes*. Comparing the marker proteins on the Tricine SDS-PAGE gel, the molecular weight of the bacteriocin was estimated to be approximately 4–5 kDa. To obtain an accurate measurement of the molecular weight, MALDI-TOF/TOF analysis was conducted on the 4–5 kDa peptide. As shown in Figure 1C, the mass spectrometry spectrum exhibited a sharp peak corresponding to a molecular weight of 4629.689 Da.

3.1.3. Safety assessment

Safety evaluation of EFEL8600 for food use involved the analysis of hemolytic activity, bile salt deconjugation activity, hyaluronidase activity, antibiotic resistance, and D- and L-lactate production. Hemolytic activity was assessed on 7% horse blood agar, and no clear zones were observed around EFEL8600 colonies, while a clear zone was observed for *L. monocytogenes* (Figure 2A). Bile salt deconjugation activity was analyzed on MRS agar supplemented with 0.5% taurodeoxycholic acid. EFEL8600 and LGG showed no deconjugation activity, while *E. faecium* ATCC 1943 (positive control) resulted in a white precipitate of deoxycholate (Figure 2B). Hyaluronidase activity was determined by incubating whole cells, supernatant, and lysate fractions of EFEL8600 with hyaluronic acid. EFEL8600 and LGG showed no color changes, whereas *Staphylococcus aureus* KCTC 1692 (positive control) exhibited purple color, indicating hyaluronidase activity (Figure 2C). The D- and L-lactate production profile of EFEL8600 was analyzed by measuring lactate concentrations in the culture medium. Only L-lactate was detected at a concentration of 110 mM, indicating exclusive production of L-lactate without synthesis of the D-form stereoisomer (Figure 2D). To examine antibiotic resistance, a minimum inhibitory concentration (MIC) test was conducted following EFSA guidelines (Table 3). Among the nine tested antibiotics, EFEL8600 exhibited MIC levels within the cut-off values for nine antibiotics. However, erythromycin exceeded the cut-off value, showing a MIC of 128 μg/mL.

TABLE 2 Purification steps of bacteriocin produced by *Enterococcus faecium* EFEL8600.

Purification stage	Volume (mL)	Protein concentration (mg/mL)	Total activity (AU)	Specific activity (AU/mg)	Purification fold
Culture supernatant	1,000	7.8 ± 0.15[a]	10,000	1.28 ± 0.02	1.00 ± 0.00
Ammonium sulfate precipitation	30	4.32 ± 0.14	4,800	37.03 ± 1.25	28.89 ± 0.79
Anion exchange chromatography	5	0.55 ± 0.05	100	36.82 ± 3.06	28.74 ± 2.4

[a]Data represents means ± standard deviation (SD) from triplicate determinations.

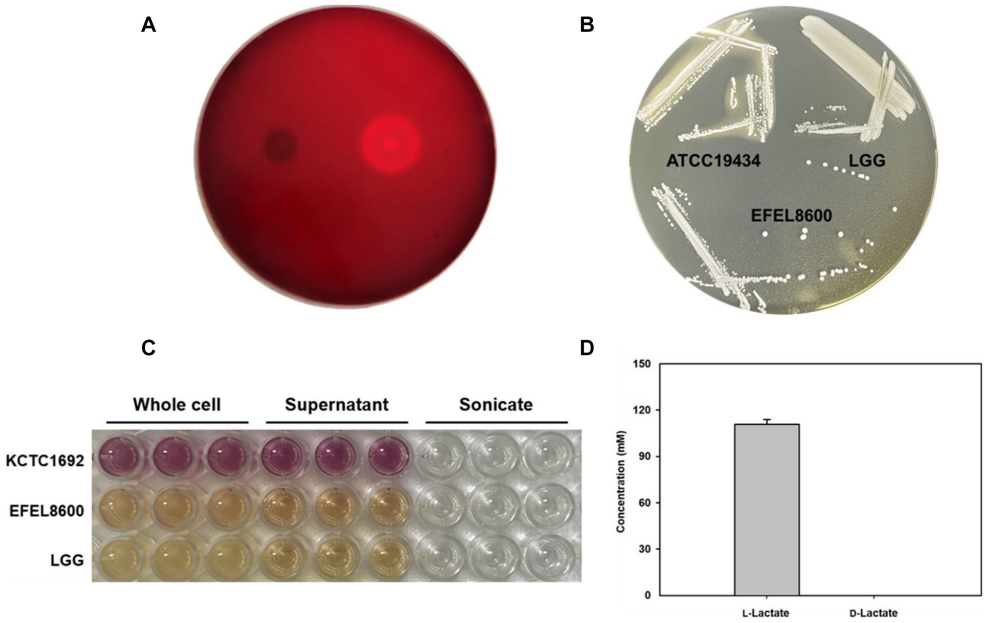

FIGURE 2
Safety analysis of *Enterococcus faecium* EFEL8600 *in vitro*. **(A)** Hemolytic activity analysis of *E. faecium* EFEL8600. Hemolytic activity was measured on BHI agar medium containing 7% horse blood. Right, positive control, *Listeria monocytogenes*, showing clear zone around the cell drop; left, the EFEL8600 strain. **(B)** Bile salt hydrolase activity of *E. faecium* EFEL8600. Plates were incubated anaerobically for 48 h at 37°C. ATCC 19434, *Enterococcus faecium* ATCC 19434 used as positive control; LGG, *Lacticaseibacillus* GG used as a negative control. **(C)** Hyaluronidase activity by optical density at 585 nm. Hyaluronidase enzyme is responsible for the degradation of hyaluronic acid, resulting in the production of N-acetylglucosamine which reacts with the DMAB reagent, causing a color change from yellow to purple. KCTC 1692, *Staphylococcus aureus* KCTC 1692. **(D)** DL-lactate level in the supernatant of the *E. faecium* EFEL8600 strain. Results are expressed as means ± SD ($n = 3$).

Based on the results, EFEL8600 demonstrated no significant hemolytic activity, bile salt deconjugation activity, hyaluronidase activity, or D-lactate production, indicating its safety for food use. However, the observed resistance to erythromycin raises concerns regarding the potential transferability of resistance genes to other members of the intestinal microbiome. Given that mobile elements such as plasmids or phages are the main vehicles for gene transfer in lactic acid bacteria, genetic analysis is required to determine whether the antibiotic resistance genes in EFEL8600 are intrinsic or acquired. The details of this analysis will be discussed in the subsequent section of this study.

3.1.4. Stability under low pH and bile salt and cell adhesion ability

The stability of EFEL8600 under gastrointestinal conditions was examined by measuring its tolerance to acid and bile salts (Figures 3A–C). The EFEL8600 strain demonstrated significantly higher resistance at pH 3.0 (7.9 log CFU/mL) and pH 2.5 (6.4 log CFU/mL) after a 180 min compared to the reference probiotic LGG. Moreover, when incubated in a 0.3% bile salt solution for 180 min, the EFEL8600 strain exhibited greater cell survival (7.6 log CFU/mL) compared to LGG (7.0 log CFU/mL) (Figure 3C). This result showed that EFEL8600 possesses high viability under simulated gastrointestinal conditions, suggesting its potential to reach the large intestine in a viable state. Subsequently, the ability of EFEL8600 to adhere to intestinal epithelial cells was analyzed by incubating the strain on a Caco-2 and HT-29 cell monolayer (Figures 3D,E). The result revealed that a total of 1,808 ± 142 cells adhered to 100 Caco-2 cells, and 345 ± 16 cells adhered to 100 HT-29 cells. Notably, the adhesion ability of EFEL8600 was comparable to that of WCFS1 in HT29 cells. This result indicated that EFEL8600 exhibits proficient adhesion capacity similar to that of a commercially available probiotic strain.

3.1.5. Protective activity on intestinal barrier

The protective effect of EFEL8600 on gut barrier function was assessed by measuring permeability with TEER values and the fluorescence level of FITC dextran using H_2O_2-induced confluent Caco-2 cell monolayers (Figure 4). The addition of H_2O_2 to Caco-2 cell monolayers led to a decrease in TEER by 63.6% after 120 min,

indicating increased monolayer permeability. However, treatment with EFEL8600 resulted in a higher TEER value of 84.4%, compared to the positive control LGG (78.4%) (Figures 4A,B). This result showed the protective effect of EFEL8600 against H_2O_2-induced epithelial cell damage. Similarly, when the permeability of Caco-2 cells was assessed using FITC-dextran, EFEL8600 exhibited lower permeability (58.6%) than LGG (75.3%) and the control group (100%, $p < 0.01$) (Figure 4C). Collectively, these results indicated that treatment with EFEL8600 has a defensive effect on gut barrier function by protecting the epithelial membrane against H_2O_2-induced oxidative damage.

TABLE 3 Antibiotic resistance of *Enterococcus faecium* EFEL8600.

Antimicrobial agent	MIC[a] (μg/mL)	EFSA cut off[b] (μg/mL)
Ampicillin	0.5	2
Vancomycin	0.25	4
Gentamicin	32	32
Kanamycin	512	1,024
Streptomycin	64	128
Erythromycin	128	4
Clindamycin	2	4
Tetracycline	0.5	4
Chloramphenicol	4	16
Tylosine	4	4

[a]MIC, minimum inhibitory concentration.
[b]Microbiological cut-off values of *Enterococcus faecium* according to EFSA (2018).

3.1.6. Antioxidative and anti-inflammatory activities

The antioxidative activity of EFEL8600 was evaluated by measuring its DPPH scavenging ability using intact cells, cell-free extract (CFE), and cell-free supernatant (CFS) (Figure 5A). The three fractions of EFEL8600 exhibited higher DPPH scavenging ability, with the highest value observed in CFS (17.5%), followed by CFE (11.7%) and intact cells (8.7%), compared to the positive controls, LGG (0.6%) and WCFS1 (8.0%). This result indicated that EFEL8600 possesses a protective effect against oxidative stress in the human intestine. Furthermore, the anti-inflammatory effect of EFEL8600 was assessed by analyzing the inhibitory activities of heat-killed cells or cell lysate on NO production in LPS-induced RAW 264.7 cells (Figure 5B). The result demonstrated that both heat-killed cells and cell lysate significantly suppressed NO production, with values of 5.2 μM and 2.7 μM, respectively, at corresponding levels of 5 μM and 20 μM of methyl arginine, a NO synthase inhibitor. These findings indicated that EFEL8600 possesses superior antioxidative and anti-inflammatory activities.

3.1.7. Biochemical characterization

The biochemical characteristics of *E. faecium* EFEL8600 were compared to the type strain, *E. faecium* ATCC 19434. As shown in Supplementary Table S1, both strains shared the ability to

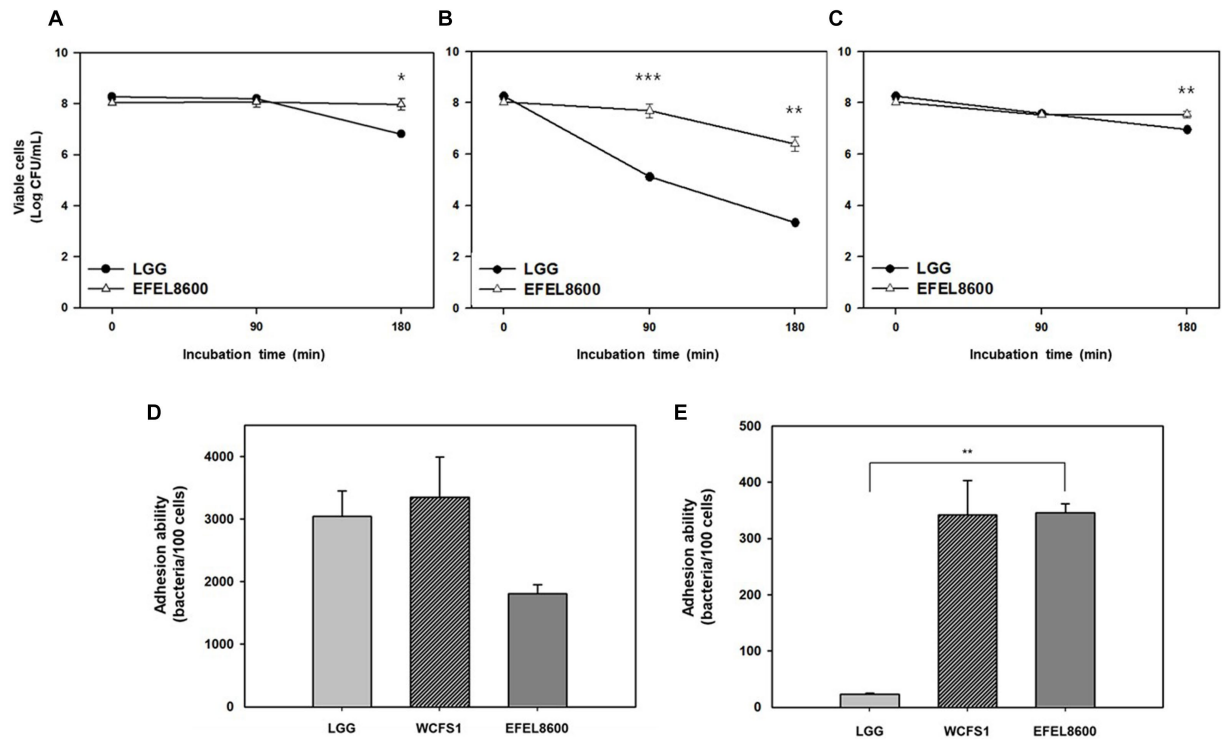

FIGURE 3
Intestinal stability and adhesion ability of *Enterococcus faecium* EFEL8600. Viability of *E. faecium* EFEL8600 under various simulated gastrointestinal condition **(A)** pH 3.0, **(B)** pH 2.5, and **(C)** 0.3% bile salt. Significant differences compared with *Lacticaseibacillus rhamnosus* GG (LGG) are represented with asterisks (*$p < 0.05$, **$p < 0.01$, ***$p < 0.001$). Intestinal adhesion ability of *E. faecium* EFEL8600 against **(D)** Caco-2 cells, and **(E)** HT-29 cells as colonic epithelial cells. Results are expressed as means ± SD ($n = 3$).

10.3389/fmicb.2023.1237442

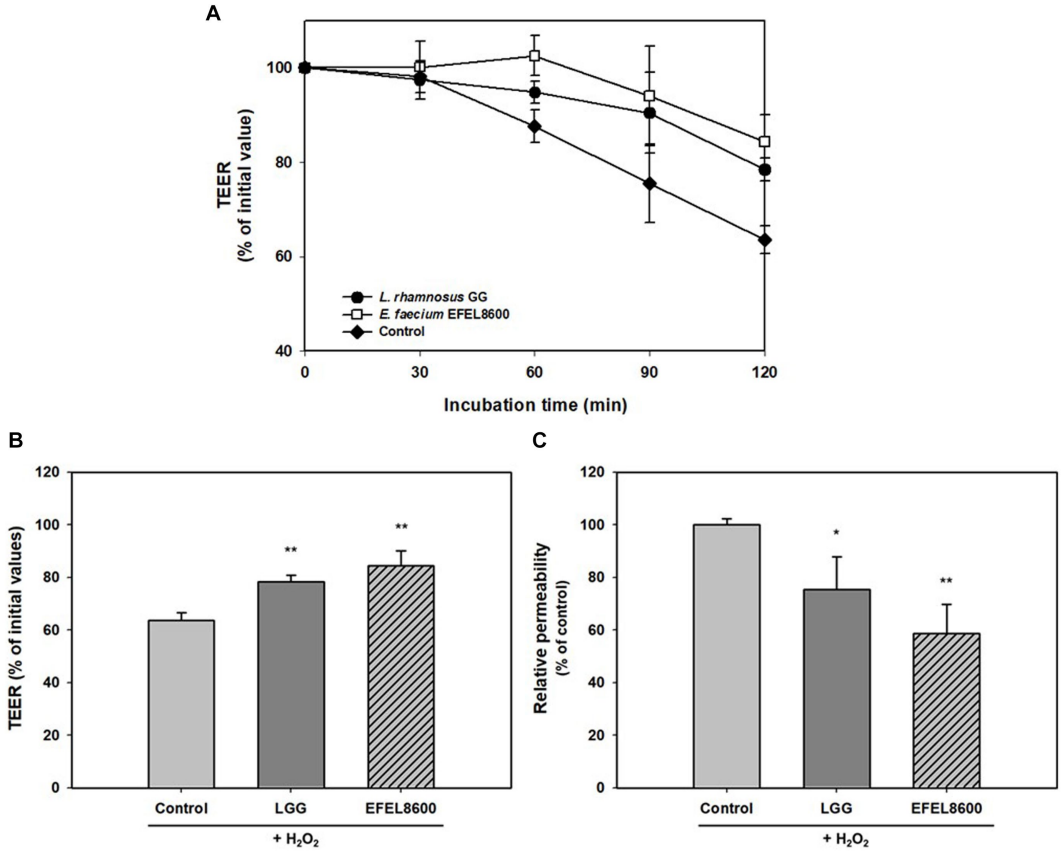

FIGURE 4
Protective effect of *Enterococcus faecium* EFEL8600 on intestinal barrier function. Caco-2 cell monolayers were pretreated with bacterial strain for 30 min, and the monolayers were exposed to H_2O_2 (1 mM). TEER was measured every 30 min **(A)** until 2 h **(B)** after H_2O_2 treatment. FITC-dextran fluorescence intensity **(C)** was measured at 4 h later after TEER measurement and expressed in % compared to control value. *Lacticaseibacillus rhamnosus* GG (LGG) was used as a positive control (*$p < 0.05$, **$p < 0.01$). All data are expressed as mean ± SD ($n = 3$).

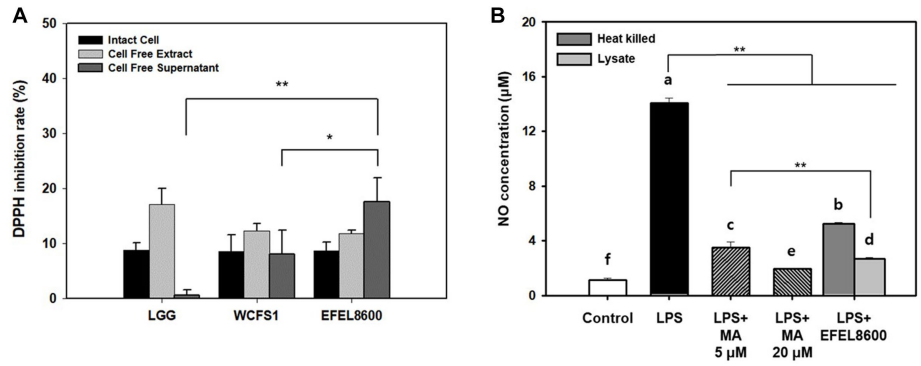

FIGURE 5
Antioxidant and anti-inflammatory activity of *Enterococcus faecium* EFEL8600. **(A)** Antioxidant activity of *E. faecium* EFEL8600 measured by the DPPH inhibition assay. Fractions of intact cells, cell-free extract, and cell-free culture supernatant were used. **(B)** Anti-inflammatory activity of *E. faecium* EFEL8600 in LPS-induced RAW 264.7 cells. Asterisks on the error bars indicate significant differences, and one-way analysis of variance (ANOVA) with Tukey's method was used to analyze differences between multiple groups (*$p < 0.05$, **$p < 0.01$). All data are expressed as mean ± SD ($n = 3$).

metabolize L-arabinose, ribose, D-galactose, glucose, fructose, mannose, mannitol, mannopyranoside, N-acetyl-glucosamine, arbutin, esculin, salicin, cellobiose, maltose, lactose, melibiose, sucrose, trehalose, and gentiobiose. However, EFEL8600 exhibited additional metabolic capabilities, including the utilization of glycerol, raffinose, and starch, which were not observed in the type strain. This finding highlights the unique carbohydrate metabolic pathways present in EFEL8600. EFEL8600 has been deposited in the Korean Collection for Type Cultures (KCTC) under accession no. KCTC 14743BP.

3.2. Genome-based analysis *Enterococcus faecium* EFEL 8600

3.2.1. Whole genome sequence analysis

The genetic characteristics of EFEL8600 were analyzed through the sequencing of its genomic DNA using the Nanopore and Illumina platforms. Nanopore sequencing generated 118,536 high-quality reads, resulting in a total of 1,518,801,768 base pairs (bp) with an average read length of 12,813 bp. Illumina sequencing produced a total of 14,865,056 high-quality reads, yielding 2,244,623,456 bp with an average read length of 151 bp. The hybrid genome assembly process (Figure 6A) led to the generation of a circular chromosome measuring 2,604,539 bp with a G+C content of 38.47%. Additionally, three plasmids were identified with sizes of 190,207 bp (G+C content: 35.10%), 34,464 bp (G+C content: 34.99%), and 6,964 bp (G+C content: 33.66%). The genomic features of EFEL8600, including the presence of 2,750 protein-coding genes, 69 tRNA genes, 18 rRNA genes, and 1 ncRNA, are summarized in Supplementary Table S2. No CRISPR sequence was detected. To determine the taxonomy of EFEL8600, a comparative analysis was conducted by calculating its OrthoANI value with other Enterococci and lactic acid bacteria (Figure 6B). The result indicated that EFEL8600 exhibited OrthoANI values of 94.93 and 97.79% with *E. faecium* ATCC 19433 (DSM 20477) and *E. faecium* T110, respectively. It is worth noting that ANI values above 95%–96% are typically considered indicative of the same species (Yoon et al., 2017). Therefore, based on this genomic comparison, it is evident that EFEL8600 belongs to the species *E. faecium*.

3.2.2. Safety-related genes

To investigate the presence of virulence factors in the genome of EFEL8600, two databases, the virulence factor database (VFDB) and BlastKOALA, were utilized. A total of 12 genes associated with virulence factors or undesirable metabolites were identified (Table 4). In VFDB, with *Enterococcus* specified as the genus, genes associated with adherence factors (*acm*, *cna*, and *sagA*), capsulation (*cpsA* and *cpsB*), biofilm formation (*bopD*), and hyaluronidase (*hyals*) were identified. These genes are commonly found in *Enterococcus* regardless of whether they are pathogenic or non-pathogenic (Natarajan and Parani, 2014). The genes related to adherence factors are often found as pseudo genes in *Enterococcus* due to insertion of phage sequence or deletion of nucleotide (Freitas et al., 2018). However, considering that there were no insertions or deletions in the amino acid sequence of these genes, and no phage sequences were identified, it is estimated that these genes are likely to exist in an intact form. It is worth noting that certain factors contributing to enterococcal virulence, such as adherence-related genes and biofilm formation, are advantageous in probiotic strains as they facilitate effective gut colonization, enhance adherence to intestinal walls, modulate the immune system indirectly, and provide protection against harmful bacteria (Krawczyk et al., 2021). Concerning capsule production-related genes, only seven genes (*cpsC*, *cpsD*, *cpsE*, *cpsG*, *cpsI*, *cpsJ*, and *cpsK*) are essential, and *cpsA* or *cpsB* do not produce capsules (Penas et al., 2013). While the *bopD* gene associated with biofilm formation is present, its expression could potentially be hindered due to the absence of the fsrABC operon, a regulator of its transcriptional activity (Shridhar et al., 2022). Regarding the hyaluronidase gene, despite its presence in the chromosomal DNA, no enzymatic activity was detected in the enzyme activity assay (Figure 2C). The Virulence Factor Database (VFDB) offers comprehensive information and analytical platform on bacterial virulence factors, initially compiled from experimentally validated sources, and augmented with genetic data from GenBank using Perl scripts (Chen et al., 2005). For this reason, while the prevalence of

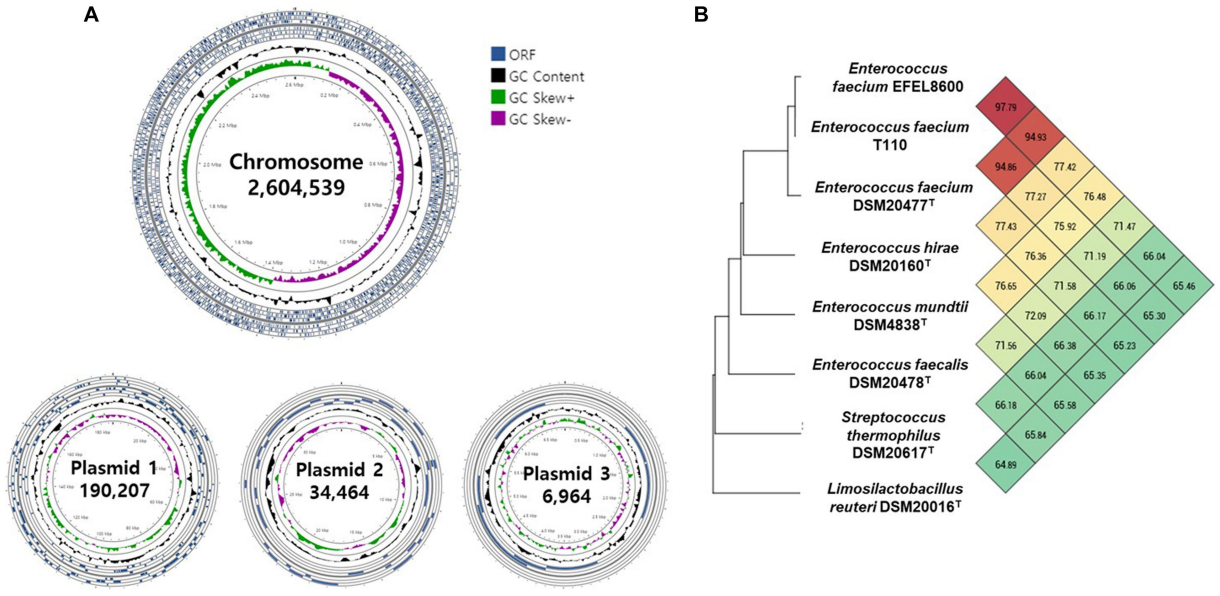

FIGURE 6
Graphical genome maps and OrthoANI analysis of *Enterococcus faecium* EFEL8600 compared with other lactic acid bacteria. **(A)** Graphical maps of the *E. faecium* EFEL8600 chromosome and plasmids created by the CG View Server. **(B)** Heat map of OrthoANI of *E. faecium* EFEL8600 compared with other lactic acid bacteria. Each cell represents the OrthoANI values between the row and the corresponding genomes of the column. The phylogenetic tree on the left represents a phylogenetic distance constructed by CJ Bioscience's OAT, available on the EzBioCloud server.

TABLE 4 List of virulence and undesirable genes detected in the genome of *Enterococcus faecium* EFEL8600 analyzed by database.

Database	Virulence factor class	Virulence factors[a]	Related genes[b]	Location
Virulence factor database (VFDB)	Adherence	Collagen adhesin precursor	*acm*	Chromosome
		Collagen binding protein	*cna*	Chromosome
		Fibronectin-binding protein	*sagA*	Chromosome
	Antiphagocytosis	Capsule	*cpsA/uppS*	Chromosome
		Capsule	*cpsB/uppS*	Chromosome
	Biofilm formation	BopD	*bopD*	Chromosome
	Enzyme	Hyaluronidase	undetermined	Chromosome
		Hyaluronidase	undetermined	Chromosome
BlastKOALA	Signaling and cellular processes	Exfoliative toxin A/B	*eta*	Chromosome
		Magnesium and cobalt exporter	*tlyC*	Chromosome
		Hemolysin III	*hlyIII*	Chromosome
	Amino acid metabolism	Tyrosine decarboxylase	*tdc-1*	Chromosome

[a]Virulence factors include toxins, adhesion proteins, and pathogenic hydrolases that allow microorganisms to settle in a particular host and cause disease.
[b]Name of virulence factor related genes.

TABLE 5 List of antimicrobial resistance gene analyzed by BlastKOALA and their locations in the genome of *Enterococcus faecium* EFEL8600.

Resistance	KEGG ID	Gene name	Protein ID	Region position	Location
Tetracycline resistance genes	K08151	MFS transporter, tetracycline resistance protein	HELCIOKC_00202	197,502–198,689	Chromosome
Macrolide resistance genes	K18231	Macrolide transport system ATP-binding/permease protein	HELCIOKC_01289	1,279,171–1,280,649	
	K19350	Lincosamide and streptogramin A transport system	HELCIOKC_01980	2,015,439–2,016,941	
	K08217	MFS transporter, DHA3 family, macrolide efflux protein	HELCIOKC_01888	1,917,404–1,918,681	
Vancomycin resistance	K07260	Zinc D-Ala-D-Ala carboxypeptidase	HELCIOKC_00336	334,559–335,383	
Cationic antimicrobial peptide (CAMP) resistance, dltABCD operon	K03367	D-alanine-poly(phosphoribitol) ligase subunit 1	HELCIOKC_00775	747,295–748,809	
	K03739	Membrane protein involved in D-alanine export	HELCIOKC_00774	746,093–747,298	
	K14188	D-alanine--poly(phosphoribitol) ligase subunit 2	HELCIOKC_00773	745,815–746,048	
	K03740	D-alanine transfer protein	HELCIOKC_00772	744,547–745,812	
Cationic antimicrobial peptide (CAMP) resistance, lysyl-phosphatidylglycerol (L-PG) synthase MprF	K14205	Phosphatidylglycerol lysyltransferase	HELCIOKC_00441	441,266–443,866	
			HELCIOKC_01260	1,248,947–1,251,520	

annotation errors may not be significant, their potential occurrence is influenced by various factors such as inaccuracies in data, evolutionary divergence, homology with non-virulence elements, and insufficient experimental validation. Therefore, depending on necessity, further validation through experimentation may be demanded for a more accurate verification. In BlastKOALA, genes associated with bacterial toxins, pore-forming toxins, and tyramine production were identified. However, despite the presence of pore-forming genes in the chromosomal DNA of EFEL8600, no hemolytic activity was observed *in vitro* (Figure 2A). These results indicated none-expression of virulence-related genes or defects in the catalytic action of the corresponding proteins. Regarding antibiotic resistance genes, a search was conducted in the genome of EFEL8600 using BlastKOALA (Table 5). A total of ten genes associated with antibiotic resistance were detected in the chromosome. To assess their transferability to other microorganisms in the human intestine, their presence in plasmid or phage-derived regions within the chromosome was analyzed (Supplementary Table S3). Analysis using PHASTER revealed the presence of a total of 9 phage regions (five in the chromosome and four in plasmid 1). Fortunately, the antibiotic resistance genes were not located within these phage sequences, suggesting a low likelihood of transfer to other bacteria. In summary, even though EFEL8600 contains some genes that may pose potential risks, it does not appear to have any highly severe genes that would negatively impact human health.

3.2.3. Probiotic-related genes

To investigate the probiotic properties of EFEL8600 at the genomic level, genome annotation was performed using Prokka v 1.14. As shown in Table 6, genes associated with probiotic traits were identified, which are associated with acid or bile salt tolerance, adhesion to epithelial cells, stress scavenging, and bacteriocin production. Specifically, the EFEL8600 genome retained F0F1 ATP synthase subunits and cation antiporters, which are involved in low pH tolerance. These genes contribute to the regulation of cytoplasmic pH by hydrolyzing ATP to pump H^+ ions out of cells, maintaining pH homeostasis (Soni et al., 2022). These genes are commonly found in other *Enterococcus* spp. that contribute to their stress resistance, especially acid tolerance (Kopit et al., 2014). Moreover, choloylglycine hydrolase and 3-dehydro-bile acid delta(4,6)-reductase were identified

10.3389/fmicb.2023.1237442

TABLE 6 Genes related with probiotic characteristics in genome of *Enterococcus faecium* EFEL8600 searched in NCBI database.

Categories	Related protein	Protein ID	Location
pH	Alkaline phosphatase synthesis sensor protein PhoR	HELCIOKC_02258	2297771.2298475
	Alkaline phosphatase synthesis transcriptional regulatory protein PhoP	HELCIOKC_02259	2297771.2298475
	ATP synthase subunit a	HELCIOKC_02115	2152928.2153647
	ATP synthase subunit c	HELCIOKC_02116	2153700.2153915
	ATP synthase subunit b	HELCIOKC_02117	2154006.2154530
	ATP synthase subunit delta	HELCIOKC_02118	2154517.2155059
	ATP synthase subunit alpha	HELCIOKC_02119	2155082.2156638
	ATP synthase gamma chain	HELCIOKC_02120	2156652.2157554
	ATP synthase subunit beta	HELCIOKC_02121	2157577.2158983
	ATP synthase epsilon chain	HELCIOKC_02122	2158997.2159419
	Na(+)/H(+) antiporter	HELCIOKC_00070	60873.62024
	Sodium, potassium, lithium and rubidium/H(+) antiporter	HELCIOKC_00405	403381.405459
	Cadmium, cobalt and zinc/H(+)-K(+) antiporter	HELCIOKC_00602	599184.600083
	Cadmium, zinc and cobalt-transporting ATPase	HELCIOKC_02240	2273209.2275293
Bile	Choloylglycine hydrolase	HELCIOKC_02395	2396881.2397855
	3-dehydro-bile acid delta(4,6)-reductase	HELCIOKC_02378	2385385.2386638
Temperature	Cold shock-like protein CspLA	HELCIOKC_00004	2163.2360
		HELCIOKC_00836	805838.806038
		HELCIOKC_02232	2263849.2264049
	Cold shock protein 1	HELCIOKC_00025	20750.20950
	Cold shock-like protein	HELCIOKC_00178	170417.170647
	Cold shock protein CspD	HELCIOKC_00599	597639.597839
	Copper chaperone CopZ	HELCIOKC_01658	1666024.1666251
	Chaperone protein DnaJ	HELCIOKC_01817	1839293.1840060
	Copper chaperone CopZ	HELCIOKC_02244	2278245.2278454
	Chaperone protein DnaK	HELCIOKC_02482	2481359.2483188
	Chaperone protein DnaJ	HELCIOKC_02483	2483339.2484505
	Chaperone protein ClpB	HELCIOKC_02581	2596575.2599184
	60 kDa chaperonin	HELCIOKC_01006	987838.989463
Osmotic stress	Potassium/sodium uptake protein NtpJ	HELCIOKC_02084	2121415.2122770
Oxidation	Glutathione amide reductase	HELCIOKC_00360	357813.359135
	Glutathione reductase	HELCIOKC_01351	1355702.1357048
	Glutathione transport system permease protein	HELCIOKC_01484	1481033.1481995
	Glutathione biosynthesis bifunctional protein	HELCIOKC_01491	1491394.1493661
	Glutathione peroxidase	HELCIOKC_01812	1834603.1834713
	Glutathione-regulated potassium-efflux system ancillary protein KefG	HELCIOKC_01836	1860969.1861646
	NADH oxidase	HELCIOKC_01719	1727534.1728829
	NADH peroxidase	HELCIOKC_01828	1851520.1852899
	NADH oxidase	HELCIOKC_02058	2090585.2091949
	NADH dehydrogenase	HELCIOKC_00073	63382.64911
	Thioredoxin-like protein YtpP	HELCIOKC_01623	1631077.1631397
	Thioredoxin	HELCIOKC_02069	2104621.2104935
	Thioredoxin reductase	HELCIOKC_02179	2214907.2215833
	Thioredoxin-like protein YtpP	HELCIOKC_01623	1631077.1631397
	Quinone oxidoreductase 2	HELCIOKC_01296	1290560.1291411
	Quinone reductase	HELCIOKC_02266	2303892.2304446
	Hydroperoxide reductase C	HELCIOKC_00074	64921.65484
Bacteriocin	Bacteriocin enterocin-P	OEFIBKHD_00190	181054.181269

as genes related to bile salt tolerance in EFEL8600 (Kim et al., 2020). In response to temperature stress, several cold shock proteins and chaperone proteins were detected. Additionally, the potassium/sodium uptake protein NtpJ was found to be involved in osmotic stress response (Checchetto et al., 2016). Furthermore, several antioxidant-related genes, including glutathione amide reductase,

NADH oxidase, NADH dehydrogenase-like protein, and thioredoxin reductase, were identified. These genes play a role in interrupting chain reactions by eliminating intermediate free radicals and preventing oxidation by neutralizing reactive oxygen species (Mishra et al., 2015). In addition, these genes represent mechanisms frequently found in *Enterococcus* to resist oxidative stress conditions (Zhao et al., 2010). Finally, a bacteriocin-related gene, enterocin P, was found on plasmid 1 of EFEL8600.

3.2.4. Bacteriocin-producing genes

To identify genes associated with bacteriocin production, BAGEL 4 and SignalP-6.0 were used to investigate detailed gene clusters and signal peptide presence (Table 7). As a result, three bacteriocins were found on plasmid 1, namely Enterocin L50a, Enterocin P, and Enterolysin A, while one bacteriocin, Enterocin Q, was detected on plasmid 3. The genes and their clusters were summarized in Table 7. Enterocin L50a, Enterocin P, and Enterocin Q exhibited a 100% match with the bacteriocins derived from *E. faecium* listed in the BAGEL 4 database. In contrast, Enterolysin A displayed a relatively low match percentage of 35.93% with the bacteriocins listed in the database, and its specific origin remains unclear. In addition, the predicted sizes of Enterocin L50a, Enterocin P, Enterolysin A, and Enterocin Q were 4.84, 7.81, 44.11, and 3.74 kDa, respectively. Among them, only Enterocin P possessed a signal peptide for protein secretion, and its size, excluding the signal peptide, was 4.84 kDa. Interestingly, in this study, a molecular weight determination revealed the presence of an antimicrobial peptide with an observed size of 4.63 kDa (Supplementary Figure S1). This peptide is believed to correspond to either Enterocin L50a or Enterocin P, as they are among the four bacteriocin genes encoded in the EFEL8600 genome. The other bacteriocin genes were determined to have low expression levels or were not expressed.

4. Discussion

Soymilk, a protein and mineral-rich liquid extract of soybean grains (Jinapong et al., 2008), is an affordable alternative to cow's milk for individuals with lactose intolerance, milk protein allergy, or those who exclude milk from their diet (Yu et al., 2021). Fermentation of soymilk with lactic acid bacteria can enhance its sensory qualities by reducing undesirable beany flavors, producing organic acids and aromatic compounds (Kumari et al., 2022), and altering its rheological properties (Yang et al., 2021). Previous studies have shown that use of *Lactobacillus harbinensis* M1 increased the levels of aromatic compounds, 2,3-butanedione and acetoin and use of *L. fermentum* decreased the levels of off-flavors in soymilk (Zheng et al., 2020; Zhu et al., 2020). The use of lactic acid bacteria in fermentation can also improve the nutritional value of soymilk by increasing the bioavailability of minerals and indigestible oligosaccharides, such as raffinose and stachyose, through the action of β-glucosidase and α-galactosidase (Baú et al., 2015). Additionally, previous studies have reported the isoflavone bioconversion to aglycones and inhibition of angiotensin-converting enzyme (ACE) in fermented soymilk using *L. fermentum* and *L. casei* (Trupti et al., 2021). Nevertheless, soymilk is highly susceptible to *L. monocytogenes* contamination due to its nutrient-rich composition (Hsieh et al., 2011; Zhang et al., 2012). In this context, *E. faecium* EFEL8600 can be utilized as an effective starter

TABLE 7 Bacteriocin related gene of *Enterococcus faecium* EFEL8600 predicted by BAGEL 4 (Bacteriocin Genomics Elimination 4).

Name	Orgin	Start	End	Match (%)	Sequence	Molecular weight (kDa)	Location
Enterocin L50a	*E. faecium*	167,506	167,640	100	MGAIAKLVAKFGWPIVKKYYKQIMQFIGEGWAINKIIEWIKKHI	4.84	Plasmid 1
Enterocin P	*E. faecium*	181,054	181,269	100	[a]MRKKLFSLALIGIFGIVVTNFGTKVDAATRSYGNGVYCNNSKCWVNWGEAKENIAGIVISGWASGLAGMGH	7.81 [b]4.84	Plasmid 1
Enterolysin A	Undear	19,876	21,081	35.93	MENQNESLIKQYVKRRAKRRLFIWLFGTSAGLITILITVFVTLFLILAAGSIDNSDSDSSSGGEAFTGEYSEGLPIYKEIKGRGPFSDEIAQYAVGAAVKYKLLPSVILSQYGY ESAFGTSASARNDLNYFGITWFDGCLFPKGTARGIGGIEGGWYMKFPNSKAAFSYYGFMVAITQSNFNACVGNKSPGASLLILGRGGYAAAAGITEDSPYYTGCMSIITSN KLITEYDEFAIKHWGEGGNDNGTITTGEWTNPFPGSSLDKSSFSGGQLFGTNPGGEFRPNGFHDGLDFGSVDHPGSEIHAVHGGKVVYYGNPGISGLGACVIVINYDGL NMVYQEFANSTGNSRVKVGDQVKVGQQVIGIRDTAHLHLGFAARTDWRQAQGHAFTDDGTWIDPLPFLNSSKK	44.11	Plasmid 1
Enterocin Q	*E. faecium*	239	341	100	MNFLKNGIAKWMTGAELQAYKKKYGCLPWEKISC	3.74	Plasmid 3

[a]Underlined are the signal peptide sequences predicted by SignalP-6.0.
[b]Molecular weight (kDa) excluding signal peptide.

in the fermentation of soymilk, aiming to prevent contamination by *L. monocytogenes*.

E. faecium is a prevalent species found in traditional Korean fermented soybean paste, meju (Jeong et al., 2019). This species possesses favorable characteristics for soybean fermentation, including rapid growth, flavor enhancement, and inhibition of pathogenic microorganisms in soybean cultures (Kumari et al., 2022). Additionally, *E. faecium* is equipped with several proteolytic enzymes capable of hydrolyzing soy proteins into small peptides or free amino acids (Moumita et al., 2018). However, due to its low resistance to salt, *E. faecium* is considered more suitable as a starter culture for soymilk rather than for high-salt soy products (>12% NaCl), such as doenjang (soybean paste) and ganjang (soybean sauce) (Martinez-Villaluenga et al., 2012).

Regarding *E. faecium* EFEL8600, it has demonstrated significant potential as a starter culture for fermented soymilk. Firstly, EFEL8600 exhibited rapid growth in soymilk, utilizing raffinose as a substrate, which is abundant in soybeans (Supplementary Table S1). Secondly, EFEL8600 does not raise major safety concerns, as it lacked hemolytic and bile salt deconjugation activities (Figures 2A,B) and showed a low risk of transferring antibiotic resistance genes (Table 5; Supplementary Table S3). Thirdly, EFEL8600 displayed notable protective effects on the intestinal barrier, as well as antioxidant and anti-inflammatory activities, while maintaining high gastrointestinal stability. Finally, EFEL8600 retains genes responsible for probiotic characteristics and bacteriocin production.

In recent years, the antibacterial activity of bacteriocins produced by enterococci, particularly *E. faecium* and *E. faecalis*, has been studied due to their potential use in controlling pathogenic bacteria such as *L. monocytogenes* (Fugaban et al., 2021). This advantageous characteristic has led to the utilization of various enterococcal strains in inhibiting the growth of foodborne pathogens during soymilk fermentation (Aspri et al., 2017). In our study, we found that the culture supernatant of EFEL8600 showed significant antibacterial activity against *L. monocytogenes* (Figure 1A). Further analysis of the antibacterial compound using mass spectrometry identified it as a bacteriocin with a molecular weight of 4.63 kDa, which is the similar molecular weight as enterocin L50a or enterocin P (Figure 1C). Based on the data, we have tried to determine the amino acid sequence of the bacteriocin by using MALDI-TOF-MS. However, this analysis presented a challenge as it was difficult to identify the correct amino acid sequence, probably due to the presence of remaining peptides. Instead, we predicted the sequence of bacteriocin based on genome sequence and sequence analysis tools. In cluster analysis, Enterocin L50a and Enterocin P, which are frequently detected in other *Enterococcus* species, were found to have secretion systems that corresponded to previous studies (Supplementary Table S4). In details, Enterocin L50a, the involvement of the ABC transporter system in the secretion of the bacteriocin from the producing cell has been reported (Teso-Pérez et al., 2021). This highlights the significance of ABC transporters in facilitating the export of Enterocin L50a across the cell membrane. In contrast, Enterocin P contains a signal peptide, typically located at the N-terminus of the protein (Martín et al., 2007). After synthesis, the signal peptide of Enterocin P is recognized, cleaved, and removed by specific enzymes, allowing it to be expelled with the protein during secretion, enabling its function outside the cell. No genes encoding transport proteins or signal peptides were detected for other bacteriocins such as Enterolysin A or Enterocin Q in this study. Based on the analysis of molecular weight and secretion mechanisms of bacteriocin, we predict that the 4.63 kDa bacteriocin corresponds to either Enterocin L50a or Enterocin P.

In conclusion, we demonstrated that *E. faecium* EFEL8600 is an antimicrobial probiotic that has health-promoting effects, such as improvement of gut barrier functions, antioxidant and anti-inflammatory activities. Therefore, *E. faecium* EFEL8600 can be applicable as probiotic starter for fermented soymilk with a health-promoting and antimicrobial safety function.

Data availability statement

The original contributions presented in the study are included in the article/Supplementary material, further inquiries can be directed to the corresponding author.

Author contributions

DHK: experiments/data collection, primary author (drafted the paper). S-AK: data analysis, primary author (drafted the paper). NGJ and J-HB: experiments/data collection. MTN and YMJ: data analysis. NSH: principal investigator (advisor, head of project, manager). All authors contributed to the article and approved the submitted version.

Funding

This work was supported by Korea Institute of Planning and Evaluation for Technology in Food, Agriculture and Forestry (IPET) through High Value-added Food Technology Development Program, funded by Ministry of Agriculture, Food and Rural Affairs (MAFRA) (322009-04-1-SB010).

Conflict of interest

The authors declare that the research was conducted in the absence of any commercial or financial relationships that could be construed as a potential conflict of interest.

Publisher's note

Supplementary material

The Supplementary material for this article can be found online at: https://www.frontiersin.org/articles/10.3389/fmicb.2023.1237442/full#supplementary-material

References

Andrews, S., Krueger, F., Segonds-Pichon, A., Biggins, L., Krueger, C., and Wingett, S. (2010). FastQC. A quality control tool for high throughput sequence data, 370. Available at: https://www.bioinformatics.babraham.ac.uk/projects/fastqc/.

Arndt, D., Marcu, A., Liang, Y., and Wishart, D. S. (2019). PHAST, PHASTER and PHASTEST: tools for finding prophage in bacterial genomes. *Brief. Bioinform.* 20, 1560–1567. doi: 10.1093/bib/bbx121

Ashenafi, M. (1991). Growth of *Listeria monocytogenes* in fermenting tempeh made of various beans and its inhibition by *Lactobacillus plantarum*. *Food Microbiol.* 8, 303–310. doi: 10.1016/S0740-0020(05)80004-8

Aspri, M., O'Connor, P. M., Field, D., Cotter, P. D., Ross, P., Hill, C., et al. (2017). Application of bacteriocin-producing *Enterococcus faecium* isolated from donkey milk in the bio-control of *Listeria monocytogenes* in fresh whey cheese. *Int. Dairy J.* 73, 1–9. doi: 10.1016/j.idairyj.2017.04.008

Bankevich, A., Nurk, S., Antipov, D., Gurevich, A. A., Dvorkin, M., Kulikov, A. S., et al. (2012). SPAdes: a new genome assembly algorithm and its applications to single-cell sequencing. *J. Comput. Biol.* 19, 455–477. doi: 10.1089/cmb.2012.0021

Baú, T. R., Garcia, S., and Ida, E. I. (2015). Changes in soymilk during fermentation with kefir culture: oligosaccharides hydrolysis and isoflavone aglycone production. *Int. J. Food Sci. Nutr.* 66, 845–850. doi: 10.3109/09637486.2015.1095861

Bharti, V., Mehta, A., Singh Jain, N., Ahirwal, L., and Mehta, S. (2015). Bacteriocin: a novel approach for preservation of food. *Int J Pharm Pharm Sci* 7, 20–29.

Bolger, A. M., Lohse, M., and Usadel, B. (2014). Trimmomatic: a flexible trimmer for Illumina sequence data. *Bioinformatics* 30, 2114–2120. doi: 10.1093/bioinformatics/btu170

Checchetto, V., Segalla, A., Sato, Y., Bergantino, E., Szabo, I., and Uozumi, N. (2016). Involvement of potassium transport systems in the response of *Synechocystis* PCC 6803 Cyanobacteria to external pH change, high-intensity light stress and heavy metal stress. *Plant Cell Physiol.* 57, 862–877. doi: 10.1093/pcp/pcw032

Chen, L., Yang, J., Yu, J., Yao, Z., Sun, L., Shen, Y., et al. (2005). VFDB: a reference database for bacterial virulence factors. *Nucleic Acids Res.* 33, D325–D328. doi: 10.1093/nar/gki008

CLSI (2019). Performance standards for antimicrobial susceptibility testing. M100, 29th ed. Clinical and laboratory standards institute, Wayne, PA.

Conway, P. L., Gorbach, S. L., and Goldin, B. R. (1987). Survival of lactic acid bacteria in the human stomach and adhesion to intestinal cells. *J. Dairy Sci.* 70, 1–12. doi: 10.3168/jds.S0022-0302(87)79974-3

Cotter, P. D., Hill, C., and Ross, R. P. (2005). Bacteriocins: developing innate immunity for food. *Nat. Rev. Microbiol.* 3, 777–788. doi: 10.1038/nrmicro1273

Das, D., and Goyal, A. (2015). Antioxidant activity and γ-aminobutyric acid (GABA) producing ability of probiotic *Lactobacillus plantarum* DM5 isolated from Marcha of Sikkim. *LWT* 61, 263–268. doi: 10.1016/j.lwt.2014.11.013

Deegan, L. H., Cotter, P. D., Hill, C., and Ross, P. (2006). Bacteriocins: biological tools for bio-preservation and shelf-life extension. *Int. Dairy J.* 16, 1058–1071. doi: 10.1016/j.idairyj.2005.10.026

EFSA Panel on Additives and Products or Substances used in Animal Feed (FEEDAP) (2018). Guidance on the characterization of microorganisms used as feed additives or as production organisms. *EFSA J.* 16:e05206. doi: 10.2903/j.efsa.2018.5206

FAO/WHO (2002). *Guidelines for the Evaluation of Probiotics in Food, report of a joint FAO/WHO working group on drafting guidelines for the evaluation of probiotics in food*, London, ON, Canada, April 30 and May 1, 2002 1–11.

Favaro, L., Basaglia, M., Casella, S., Hue, I., Dousset, X., de Melo Franco, B. D. G., et al. (2014). Bacteriocinogenic potential and safety evaluation of non-starter *Enterococcus faecium* strains isolated from homemade white brine cheese. *Food Microbiol.* 38, 228–239. doi: 10.1016/j.fm.2013.09.008

Franz, C. M., Huch, M., Abriouel, H., Holzapfel, W., and Gálvez, A. (2011). Enterococci as probiotics and their implications in food safety. *Int. J. Food Microbiol.* 151, 125–140. doi: 10.1016/j.ijfoodmicro.2011.08.014

Freitas, A. R., Tedim, A. P., Novais, C., Coque, T. M., and Peixe, L. (2018). Distribution of putative virulence markers in *Enterococcus faecium*: towards a safety profile review. *J. Antimicrob. Chemother.* 73, 306–319. doi: 10.1093/jac/dkx387

Fugaban, J. I. I., Holzapfel, W. H., and Todorov, S. D. (2021). Probiotic potential and safety assessment of bacteriocinogenic *Enterococcus faecium* strains with antibacterial activity against *Listeria* and vancomycin-resistant enterococci. *Curr. Res. Microb. Sci.* 2:100070. doi: 10.1016/j.crmicr.2021.100070

Han, D. M., Baek, J. H., Chun, B. H., and Jeon, C. O. (2023). Fermentative features of *Bacillus velezensis* and *Leuconostoc mesenteroides* in doenjang-meju, a Korean traditional fermented soybean brick. *Food Microbiol.* 110:104186. doi: 10.1016/j.fm.2022.104186

Haraguchi, Y., Goto, M., Kuda, T., Fukunaga, M., Shikano, A., Takahashi, H., et al. (2019). Inhibitory effect of *Lactobacillus plantarum* Tennozu-SU2 and *Lactococcus lactis* subsp. lactis BF1 on *Salmonella typhimurium* and *Listeria monocytogenes* during and post fermentation of soymilk. *LWT* 102, 379–384. doi: 10.1016/j.lwt.2018.12.042

Hsieh, Y. H., Yan, M., Liu, J. G., and Hwang, J. C. (2011). The synergistic effect of nisin and garlic shoot juice against *Listeria* spp. in soymilk. *J. Taiwan Inst. Chem. Eng.* 42, 576–579. doi: 10.1016/j.jtice.2010.11.006

Jang, C. H., Oh, J., Lim, J. S., Kim, H. J., and Kim, J. S. (2021). Fermented soy products: beneficial potential in neurodegenerative diseases. *Foods* 10:636. doi: 10.3390/foods10030636

Jeong, D. W., Lee, H., Jeong, K., Kim, C. T., Shim, S. T., and Lee, J. H. (2019). Effects of starter candidates and NaCl on the production of volatile compounds during soybean fermentation. *J. Microbiol. Biotechnol.* 29, 191–199. doi: 10.4014/jmb.1811.11012

Jinapong, N., Suphantharika, M., and Jamnong, P. (2008). Production of instant soymilk powders by ultrafiltration, spray drying and fluidized bed agglomeration. *J. Food Eng.* 84, 194–205. doi: 10.1016/j.jfoodeng.2007.04.032

Jozala, A. F., de Lencastre Novaes, L. C., Cholewa, O., and Penna, T. C. V. (2005). Increase of nisin production by *Lactococcus lactis* in different media. *Afr. J. Biotechnol.* 4, 262–265. Available at: https://www.ajol.info/index.php/ajb/article/view/15092

Jung, J. Y., Lee, S. H., and Jeon, C. O. (2014). Microbial community dynamics during fermentation of doenjang-meju, traditional Korean fermented soybean. *Int. J. Food Microbiol.* 185, 112–120. doi: 10.1016/j.ijfoodmicro.2014.06.003

Kim, E., Chang, H. C., and Kim, H. Y. (2020). Complete genome sequence of *Lactobacillus plantarum* EM, a putative probiotic strain with the cholesterol-lowering effect and antimicrobial activity. *Curr. Microbiol.* 77, 1871–1882. doi: 10.1007/s00284-020-02000-8

Kopit, L. M., Kim, E. B., Siezen, R. J., Harris, L. J., and Marco, M. L. (2014). Safety of the surrogate microorganism *Enterococcus faecium* NRRL B-2354 for use in thermal process validation. *Appl. Environ. Microbiol.* 80, 1899–1909. doi: 10.1128/AEM.03859-13

Krawczyk, B., Wityk, P., Gałęcka, M., and Michalik, M. (2021). The many faces of *Enterococcus* spp.—commensal, probiotic and opportunistic pathogen. *Microorganisms* 9:1900. doi: 10.3390/microorganisms9091900

Kumari, M., Patel, H. K., Kokkiligadda, A., Bhushan, B., and Tomar, S. K. (2022). Characterization of probiotic lactobacilli and development of fermented soymilk with improved technological properties. *LWT* 154:112827. doi: 10.1016/j.lwt.2021.112827

Lebeer, S., Vanderleyden, J., and De Keersmaecker, S. C. (2008). Genes and molecules of lactobacilli supporting probiotic action. *Microbiol. Mol. Biol. Rev.* 72, 728–764. doi: 10.1128/MMBR.00017-08

Lee, I., Ouk Kim, Y., Park, S. C., and Chun, J. (2016). OrthoANI: an improved algorithm and software for calculating average nucleotide identity. *Int. J. Syst. Evol. Microbiol.* 66, 1100–1103. doi: 10.1099/ijsem.0.000760

Licandro, H., Ho, P. H., Nguyen, T. K. C., Petchkongkaew, A., Van Nguyen, H., Chu-Ky, S., et al. (2020). How fermentation by lactic acid bacteria can address safety issues in legumes food products? *Food Control* 110:106957. doi: 10.1016/j.foodcont.2019.106957

Liu, B., Zheng, D., Zhou, S., Chen, L., and Yang, J. (2022). VFDB 2022: a general classification scheme for bacterial virulence factors. *Nucleic Acids Res.* 50, D912–D917. doi: 10.1093/nar/gkab1107

Martinez-Villaluenga, C., Torino, M. I., Martín, V., Arroyo, R., Garcia-Mora, P., Estrella Pedrola, I., et al. (2012). Multifunctional properties of soy milk fermented by *Enterococcus faecium* strains isolated from raw soy milk. *J. Agric. Food Chem.* 60, 10235–10244. doi: 10.1021/jf302751m

Martín, M., Gutiérrez, J., Criado, R., Herranz, C., Cintas, L. M., and Hernández, P. E. (2007). Cloning, production and expression of the bacteriocin enterocin A produced by Enterococcus faecium PLBC21 in Lactococcus lactis. *Applied microbiology and biotechnology*, 76, 667–675. doi: 10.1007/s00253-007-1044-3

Mishra, V., Shah, C., Mokashe, N., Chavan, R., Yadav, H., and Prajapati, J. (2015). Probiotics as potential antioxidants: a systematic review. *J. Agric. Food Chem.* 63, 3615–3626. doi: 10.1021/jf506326t

Miyauchi, E., Morita, M., Rossi, M., Morita, H., Suzuki, T., and Tanabe, S. (2012). Effect of D-alanine in teichoic acid from the *Streptococcus thermophilus* cell wall on the barrier-protection of intestinal epithelial cells. *Biosci. Biotechnol. Biochem.* 76, 283–288. doi: 10.1271/bbb.110646

Moumita, S., Das, B., Sundaray, A., Satpathi, S., Thangaraj, P., Marimuthu, S., et al. (2018). Study of soy-fortified green tea curd formulated using potential hypocholesterolemic and hypotensive probiotics isolated from locally made curd. *Food Chem.* 268, 558–566. doi: 10.1016/j.foodchem.2018.06.114

Nam, Y. D., Lee, S. Y., and Lim, S. I. (2012). Microbial community analysis of Korean soybean pastes by next-generation sequencing. *Int. J. Food Microbiol.* 155, 36–42. doi: 10.1016/j.ijfoodmicro.2012.01.013

Natarajan, P., and Parani, M. (2014). First complete genome sequence of a probiotic *Enterococcus faecium* strain T-110 and its comparative genome analysis with pathogenic and non-pathogenic *Enterococcus faecium* genomes. *J. Genet. Genomics* 42, 43–46. doi: 10.1016/j.jgg.2014.07.002

Oh, Y. J., Kim, S. A., Yang, S. H., Kim, D. H., Cheng, Y. Y., Kang, J. I., et al. (2022). Integrated genome-based assessment of safety and probiotic characteristics of

Lactiplantibacillus plantarum PMO 08 isolated from kimchi. *PLoS One* 17:e0273986. doi: 10.1371/journal.pone.0273986

Ölgen, S., Kaeßler, A., Nebioğlu, D., and Jose, J. (2007). New potent indole derivatives as hyaluronidase inhibitors. *Chem. Biol. Drug Des.* 70, 547–551. doi: 10.1111/j.1747-0285.2007.00590.x

Özel, B., Şimşek, Ö., Akçelik, M., and Saris, P. E. (2018). Innovative approaches to nisin production. *Appl. Microbiol. Biotechnol.* 102, 6299–6307. doi: 10.1007/s00253-018-9098-y

Penas, P. P., Mayer, M. P., Gomes, B. P., Endo, M., Pignatari, A. C., Bauab, K. C., et al (2013). Analysis of genetic lineages and their correlation with virulence genes in Enterococcus faecalis clinical isolates from root canal and systemic infections. *Journal of Endodontics*, 39, 858–864. doi: 10.1016/j.joen.2013.01.009

Ryu, E. H., and Chang, H. C. (2013). *In vitro* study of potentially probiotic lactic acid bacteria strains isolated from kimchi. *Ann. Microbiol.* 63, 1387–1395. doi: 10.1007/s13213-013-0599-8

Shridhar, P. B., Amachawadi, R. G., Tokach, M., Patel, I., Gangiredla, J., Mammel, M., et al. (2022). Whole genome sequence analyses-based assessment of virulence potential and antimicrobial susceptibilities and resistance of *Enterococcus faecium* strains isolated from commercial swine and cattle probiotic products. *J. Anim. Sci.* 100:skac030. doi: 10.1093/jas/skac030

Singhal, N., Maurya, A. K., Mohanty, S., Kumar, M., and Virdi, J. S. (2019). Evaluation of bile salt hydrolases, cholesterol-lowering capabilities, and probiotic potential of *Enterococcus faecium* isolated from rhizosphere. *Front. Microbiol.* 10:1567. doi: 10.3389/fmicb.2019.01567

Soni, R., Keharia, H., Dunlap, C., Pandit, N., and Doshi, J. (2022). Functional annotation unravels probiotic properties of a poultry isolate, *Bacillus velezensis* CGS1.1. *LWT* 153:112471. doi: 10.1016/j.lwt.2021.112471

Tatusova, T., DiCuccio, M., Badretdin, A., Chetvernin, V., Nawrocki, E. P., Zaslavsky, L., et al. (2016). NCBI prokaryotic genome annotation pipeline. *Nucleic Acids Res.* 44, 6614–6624. doi: 10.1093/nar/gkw569

Teso-Pérez, C., Martínez-Bueno, M., Peralta-Sánchez, J. M., Valdivia, E., Maqueda, M., Fárez-Vidal, M. E., et al (2021). Enterocin cross-resistance mediated by ABC transport systems. *Microorganisms*, 9:1411. doi: 10.3390/microorganisms9071411

Torres-Henderson, C., Summers, S., Suchodolski, J., and Lappin, M. R. (2017). Effect of *Enterococcus faecium* strain SF68 on gastrointestinal signs and fecal microbiome in cats administered amoxicillin-clavulanate. *Top. Companion Anim. Med.* 32, 104–108. doi: 10.1053/j.tcam.2017.11.002

Trupti, J., Das, S., Solanki, D., Kinariwala, D., and Hati, S. (2021). Bioactivities and ACE-inhibitory peptides releasing potential of lactic acid bacteria in fermented soy milk. *Food Prod. Process. Nutr.* 81, 3131–3138. doi: 10.3168/jds.S0022-0302(98)75878-3

Valledor, S. J. D., Dioso, C. M., Bucheli, J. E. V., Park, Y. J., Suh, D. H., Jung, E. S., et al. (2022). Characterization and safety evaluation of two beneficial, enterocin-producing *Enterococcus faecium* strains isolated from kimchi, a Korean fermented cabbage. *Food Microbiol.* 102:103886. doi: 10.1016/j.fm.2021.103886

van Heel, A. J., de Jong, A., Song, C., Viel, J. H., Kok, J., and Kuipers, O. P. (2018). BAGEL4: a user-friendly web server to thoroughly mine RiPPs and bacteriocins. *Nucleic Acids Res.* 46, W278–W281. doi: 10.1093/nar/gky383

Yang, X., Ke, C., and Li, L. (2021). Physicochemical, rheological and digestive characteristics of soy protein isolate gel induced by lactic acid bacteria. *J. Food Eng.* 292:110243. doi: 10.1016/j.jfoodeng.2020.110243

Yoon, S. H., Ha, S. M., Lim, J., Kwon, S., and Chun, J. (2017). A large-scale evaluation of algorithms to calculate average nucleotide identity. *Antonie Van Leeuwenhoek* 110, 1281–1286. doi: 10.1007/s10482-017-0844-4

Yu, H. S., Lee, N. K., Choi, A. J., Choe, J. S., Bae, C. H., and Paik, H. D. (2019). Anti-inflammatory potential of probiotic strain *Weissella cibaria* JW15 isolated from kimchi through regulation of NF-κB and MAPKs pathways in LPS-induced RAW 264.7 cells. *J. Microbiol. Biotechnol.* 29, 1022–1032. doi: 10.4014/jmb.1903.03014

Yu, X., Meenu, M., Xu, B., and Yu, H. (2021). Impact of processing technologies on isoflavones, phenolic acids, and antioxidant capacities of soymilk prepared from 15 soybean varieties. *Food Chem.* 345:128612. doi: 10.1016/j.foodchem.2020.128612

Zhang, H., Bao, H., Billington, C., Hudson, J. A., and Wang, R. (2012). Isolation and lytic activity of the *Listeria* bacteriophage endolysin LysZ5 against *Listeria monocytogenes* in soya milk. *Food Microbiol.* 31, 133–136. doi: 10.1016/j.fm.2012.01.005

Zhao, C., Hartke, A., La Sorda, M., Posteraro, B., Laplace, J. M., Auffray, Y., et al. (2010). Role of methionine sulfoxide reductases A and B of *Enterococcus faecalis* in oxidative stress and virulence. *Infect. Immun.* 78, 3889–3897. doi: 10.1128/iai.00165-10

Zheng, Y., Fei, Y., Yang, Y., Jin, Z., Yu, B., and Li, L. (2020). A potential flavor culture: *Lactobacillus harbinensis* M1 improves the organoleptic quality of fermented soymilk by high production of 2, 3-butanedione and acetoin. *Food Microbiol.* 91:103540. doi: 10.1016/j.fm.2020.103540

Zhu, Y. Y., Thakur, K., Feng, J. Y., Cai, J. S., Zhang, J. G., Hu, F., et al. (2020). Riboflavin-overproducing lactobacilli for the enrichment of fermented soymilk: insights into improved nutritional and functional attributes. *Appl. Microbiol. Biotechnol.* 104, 5759–5772. doi: 10.1007/s00253-020-10649-1

Zommiti, M., Cambronel, M., Maillot, O., Barreau, M., Sebei, K., Feuilloley, M., et al. (2018). Evaluation of probiotic properties and safety of *Enterococcus faecium* isolated from artisanal Tunisian meat "Dried Ossban". *Front. Microbiol.* 9:1685. doi: 10.3389/fmicb.2018.01685

frontiers | Frontiers in Microbiology

TYPE Original Research
PUBLISHED 21 November 2023
DOI 10.3389/fmicb.2023.1267447

OPEN ACCESS

EDITED BY
Michela Verni,
Sapienza University of Rome, Italy

REVIEWED BY
Hong Mingsheng,
China West Normal University, China
Cao Rong,
Chinese Academy of Fishery Sciences, China

*CORRESPONDENCE
Yang Ning
✉ ningyang@caas.cn

RECEIVED 26 July 2023
ACCEPTED 23 October 2023
PUBLISHED 21 November 2023

CITATION
Wu X, Hu Y, Wang Q, Liu J, Fang S, Huang D, Pang X, Cao J, Gao Y and Ning Y (2023) Study on the correlation between the dominant microflora and the main flavor substances in the fermentation process of cigar tobacco leaves.
Front. Microbiol. 14:1267447.
doi: 10.3389/fmicb.2023.1267447

Study on the correlation between the dominant microflora and the main flavor substances in the fermentation process of cigar tobacco leaves

Xue Wu[1,2], Yanqi Hu[3], Qian Wang[1], Jian Liu[1], Song Fang[1], Dewen Huang[4], Xueli Pang[1], Jianmin Cao[1], Yumeng Gao[1,2] and Yang Ning[1]*

[1]Tobacco Research Institute, Chinese Academy of Agricultural Sciences, Qingdao, China, [2]Graduate School of Chinese Academy of Agricultural Sciences, Beijing, China, [3]Shandong China Tobacco Industry Limited Company, Jinan, China, [4]Hunan Tobacco Company Chenzhou Company, Chenzhou, China

The flavor of cigar tobacco leaf determines the quality of finished cigar tobacco, and the enhancement of flavor generally relies on microbial fermentation. In this paper, the correlation between the dominant microorganisms and the main flavor substances of cigar tobacco leaves during fermentation and the correlation between the two were investigated to reveal the correlation between microorganisms and flavor and the metabolic pathways of microorganisms affecting the flavor substances. During the fermentation process, the main flavors of cigar tobacco leaves were sweet, light and grassy, with hexanal, 2,6-dimethylpyridine, nonanal, phenylacetaldehyde, naphthalene, and methyl benzoate as the main constituents, and the key microorganisms *Haloferax mediterranei*, *Haloterrigena limicola*, *Candidatus Thorarchaeota archaeon SMTZ-45*, the genera *Methyloversatilis*, *Sphingomonas*, *Thauera*, *Pseudomonas*, *Penicillium*, and *Aspergillus*. Correlation analysis revealed that fungi were negatively correlated with the main aroma and inhibited the main flavor substances, while bacteria were positively correlated with Benzoic acid, methyl ester in the main flavor substances, which was conducive to the accumulation of green aroma. Functional analysis revealed that the dominant bacterial population was producing aroma by metabolizing glycoside hydrolases and glycosyltransferases, performing amino acid metabolism, carbohydrate metabolism and film transport metabolism. The present study showed that the bacterial and fungal dominant microorganisms during the fermentation of cigar tobacco were influencing the production and degradation of the main flavor substances through the enzyme metabolism by the occurrence of the Merad reaction.

KEYWORDS

cigar tobacco, macro-genome sequencing, gas chromatograph/sniffer, flavor substances, relative odor activity values, correlations

1 Introduction

In recent years, with the rapid development of China's economy, the consumer demand for medium–and high-end cigar cigarettes is gradually increasing (Yan et al., 2021a), and the sales volume of handmade cigars in China exceeds 20 million cigars in 2021 (Yan et al., 2021b). Medium- and high-end cigar cigarettes refer to handmade cigar cigarettes, whose production

process does not involve the addition of flavorings and spices and in which the volatile constituents of cigar tobacco leaves are directly originated from fermentation processes. The volatile components of cigar tobacco come directly from the fermentation process and the tobacco leaf itself (Gao et al., 2021). At present, the raw materials of cigar tobacco in China still have the problem that the main flavor is not clear and the aroma is not strong enough compared with the raw materials of Cuban cigar tobacco (Wang et al., 2020), therefore, the use of chemical means to analyze the main flavor qualitatively and quantitatively, and through microorganisms, enzymes, and some chemical reactions to enhance the flavor of cigar tobacco has become a hot spot of research (Zhao et al., 2007). It has been found that the growth and metabolism of microorganisms can cause the degradation or transformation of biomolecules such as lignin and proteins in tobacco, forming a series of volatile aroma substances, and at the same time reducing the green and heterogeneous gasses in tobacco, which will in turn enhance the quality of fermented tobacco (Su et al., 2011; Mo, 2017b). Tobacco leaves contain many microorganisms (Zhou et al., 2020) such as Bacillus, *Pseudomonas*, *Enterobacter*, *Sphingobacterium*, *Pantoea*, and *Methylobacterium* are the main genera of bacteria in tobacco leaves (Huang et al., 2010; Zhou et al., 2020). These bacteria degrade macromolecular organic matter in tobacco during fermentation. For example, *Pseudomonas* spp. can effectively degrade nicotine (Zhong et al., 2010), and *Bacillus* spp. can produce small aromatic substances by breaking down macromolecules (e.g., carotenoids; Maldonado-Robledo et al., 2003). Previous studies mainly focused on the changes of microbial community structure, the composition of volatile flavor substances and chemical substances during the fermentation of cigar tobacco leaves, and conducted some experiments on the addition of dominant microorganisms, but lacked the analysis of the main flavor and the study of the mechanism of microbial influence, which shows that it is crucial to carry out the study of the dominant microorganisms on the main flavor substances during the fermentation of cigar tobacco leaves.

The correlation between the pattern of change of dominant flora and flavor during cigar fermentation is the basis for the scientifically controllable design is cigar fermentation process. Due to the limitations of traditional isolation and culture techniques, only a small number of dominant flora can be isolated from a sample, even when a variety of media and isolation conditions are selected (Ye et al., 2021). In contrast, the combination of culture-free methods with macro-genome sequencing technology can overcome this shortcoming and detect the genomic DNA of all microscopic organisms in the samples (Shuai, 2018), which comprehensively reflects the true composition of their microbial communities. Detecting volatile metabolites in tobacco gas chromatography–mass spectrometry (GC–MS) as the most commonly used method (Cai et al., 2013; Zhang et al., 2013; Lin et al., 2014; Qin et al., 2021; Vu et al., 2021), but GC–MS/O can find the main flavor substances more accurately by taste, and the volatile compounds of lychee through the combination of GC–MS/O characterized and identified geraniol, linalool, and furanol as key aroma components of litchi (Feng et al., 2018). macro-genome sequencing technology can also systematically analyze the core microflora during fermentation and annotate the genes related to flavor substance formation. The microbiome and flavor formation-related genes of Sichuan bran vinegar were studied by macro-genome technology, and it was found that vinegar spirits possessed the basis for the formation of flavor substances through amino acid metabolism (Liu et al., 2022). Identified functional microorganisms in vinegar fermentation by correlation analysis between microbial communities and flavor metabolites (Huang et al., 2022).

In this study, we revealed the changes of microbial communities and main flavor substances during cigar fermentation by macro-genome sequencing and GC–MS/0, to understand the dominant microorganisms of cigar tobacco, and to analyze the correlation between the dominant microbial communities and the main flavor of cigar tobacco. We screened and analyzed the dominant microorganisms that have important effects on the quality and flavor of cigar tobacco leaves, with a view to producing de-stabilized microbial agents to improve the main flavor during the fermentation process of cigar tobacco leaves, and to enhance the characteristics and quality of domestic cigar tobacco leaves.

2 Materials and methods

2.1 Materials, reagents, and equipment

QX208 Cigar leaves were provided by the Tobacco Bureau of Chenzhou City, Hunan Province, and C7-C30 n-alkanes were purchased from Shanghai Sigma-Aldrich Trading Co. MS-H-Por solid-phase microextraction manual kit (Zhen Zheng Analytical Instruments Co., Ltd.), Agilent 78908B-5977A gas chromatography–mass spectrometry (Agilent, United States), 9,000 Olfactory Analyzer (Switzerland), and 57,348-U BVB/CAR/PDMS solid-phase microextraction fiber tip (50/30 micron), SUPERO, United States were used. DyNA Quant 200 Concentrometer, United States, Pharmacia Biotech Agarose Gel Electrophoresis, United States, Bio-Rad QuantiFluorTM-ST Blue Fluorescence Quantification System, United States, Promega GDS Gel Imaging System, United Kingdom METTLER TOLEDO Ice Maker, Japan, Sanyo PCR Instrument, United States, ABI.

2.2 Experimental methods

2.2.1 Experimental pre-treatment

Constant humidity and initial temperature are set at 70% and 32°C, respectively. In addition, after fermentation at constant temperature for 10 days, the temperature was raised by 2°C for a total of 80 days, and every 10 days was a fermentation stage from FA-FI to 9 fermentation stages. At the same time of each heating sampling, the four vertices and the center of the bag from the top to the bottom of the 300 g cigar leaves, fully mixed. Approximately 50 g of samples were placed in 50 mL sterile centrifuge tubes and vortex oscillated after addition of PBS buffer (PBS concentration and PH requirements: 1x PBS, PH 7.4); Microorganisms were allowed to fully shed from the surface of the object and accumulate in PBS buffer, the buffer was stored in a sterile centrifuge tube after filtration with a filter membrane and then stored at −80° C, and the dry ice transport sample was sent to Allwegene Tech. The company carries out the extraction and detection of microbiome DNA. Dry and crush 100 g of the sample and sift through 60 mesh. Add smoke (0.5 g; to 0.001 g), place 105 ppm phenylethyl acetate (internal standard) in a 25 mL headspace bottle, seal and set aside, and repeat each set three times.

2.2.2 HS-SPME-GC–MS/O analytical condition

HS-SPME analysis conditions: The temperature and heating equilibrium time of the solid-phase microextraction (SPME) manual device were 70°C and 30 min, respectively; in addition, the extraction was carried out with a 50/30 μm DVB/CAR/PDMS extraction head for 30 min.

GC–MS conditions: A DB-5MS quartz capillary column (30 m × 0.25 mm, 0.25 μm) was used. The high purity helium was used as the carrier gas, and the flow rate of the column was 1.6 mL/min (constant flow mode); the temperature of the injection port was 240°C; the non-split injection mode was used, and the injection volume was 2 μL. The initial temperature was 40°C, and the temperature was kept at 40°C for 2 min, and then it was increased to 220°C at a rate of 6°C/min. Finally, the temperature was increased to 280°C at 20°C/min for 10 min. The ion source used was an ionization source with an ionization voltage of 70 eV and an ion source temperature of 230°C, respectively. The transmission line temperature was 290°C. The scanning mode was full scan mode with a scanning range of 33–325 amu. Qualitative analysis was performed based on the total ion flow diagram, peak times, spectral libraries (NIST17 library), and retention indices. Phenethyl acetate internal standard was used for quantitative analysis.

The mass spectrometry quadrupole temperature was 150°C. The electron bombardment ion source, transmission line temperature (290°C), electron energy (70 eV) and scanning range were the same as the MS conditions. The shunt ratio of the olfactory port to the mass spectrometry terminal was 1:1, and the temperature of the olfactory port was 280°C. To avoid subjectivity and to record olfactory sensation characteristics and retention times, the GC–MS/O analysis was performed by five members of the same sample for olfactory description.

2.2.3 Macro-genome sequencing DNA extraction methods for cigar tobacco leaves

Extraction of microbial DNA reference E. Noah. N. A. Soil DNA Kit (Omega Bio-tek, Inc.,) [Omega E. Noah. N. A. Stool DNA Kit (Omega Bio-tek, Inc.,)]. The size and quality of extracted DNA were analyzed by electrophoresis on 1% agarose gel. The cigars that met the sequencing requirements were stored in a refrigerator at −80° C, and the unqualified samples were re-extracted. Hiseq libraries were constructed, library fragments were screened using 2% agarose gel, blocks of 400–450 BP fragments were excised for purification, then PCR enrichment was performed, and finally machine sequencing was performed on the Illumina Hiseq platform.

2.3 Data handling

2.3.1 Relative odor activity value

The relative odor activity value (ROAV) was used to assess the contribution of each volatile component to the flavor of cigar tobacco samples, following the calculation method of Liu et al. (2008), where ROAV>1 indicates that the component contributes the most to the flavor of the sample and is the key flavor component; 0.1 ≤ ROAV<1 indicates that the component can change the flavor of the sample; and ROAV<0.1 indicates that it has no significant effect on the flavor of the sample. ROAV<0.1 means that this component has no significant effect on the flavor of the sample. Within a certain range, the larger the ROAV, the greater the contribution of the substance to the overall flavor.

2.3.2 Analysis of macro-genomic data

Firstly, the original data were segmented, and the valid data were obtained by quality cutting. The reads of all samples were merged and assembled using the mosaic software MEGAHIT (or IDBA) based on the De-Brujin graph principle (Li et al., 2015, 2016), the De-Brujin graph was constructed according to the overlap relationship between the KMERS, and the Contigs above 800 BP were screened for statistical analysis and used for follow-up analysis. The ORF prediction of the stitched Contigs sequence was performed using Prodigal (Hyatt et al., 2010) software, the sequences were translated into amino acid sequences, and the non-redundant gene cataloge was obtained by CD-HIT software. The clean reads of each sample were compared with the non-redundant gene set (95% identity) by Bowtie2 software, statistical information on the abundance of genes in corresponding samples (Qin et al., 2010; Cotillard et al., 2013; Le et al., 2013; Villar et al., 2015; Zeller et al., 2015). The non-redundant genes were compared with KEGG, eggNOG and CAZy functional databases by Diamond Software, and the annotation of E < 1e-5 was selected to screen the proteins with the highest sequence similarity, so as to obtain the functional annotation information for each sequence alignment result, the alignment result with the highest score (one HSP > 60 bits) was selected for follow-up analysis (Bäckhed et al., 2015).

The data were processed by SPSS 27 software, the microbial data were analyzed by Allwegene Cloud Platform, and the Origin 2019 software was used to draw the grid map and correlation heatmap. The experimental results are presented as mean ± error.

3 Results

3.1 Dominant flavor analysis of cigar tobacco during the fermentation process

The aroma of cigar tobacco is produced by a combination of volatile substances, and those that can be detected by the human olfactory organs are unique to cigar tobacco. According to the GC-O olfactory intensity of the aromas and analyzed using the Origin heat map (Figure 1), the main aromas of cigar tobacco at all stages of fermentation are honey-like sweetness, cocoa sweetness, citrus-minty freshness, and grassy herbaceousness, supplemented by wood, spice (slightly spicy and peppery), floral, cocoa, and fruity aromas.

The level of odor intensity of olfactory perception does not indicate the degree of its contribution to the overall flavor of the sample, but also needs to be evaluated in conjunction with the threshold value of the flavor substances, which is different for different compounds. Some flavor substances, although their relative content is very low, contribute a lot to the overall flavor due to their low threshold value, and the compounds with a lower threshold value are more likely to be perceived by the olfactory organ when their relative content is certain. The odor thresholds of 18 volatile substances were found by GC–MS analysis of olfactory-perceived substances and by reviewing the aroma thresholds of volatile flavor substances that have been reported in books and related literature (Van Gemert, 2011; Table 1).

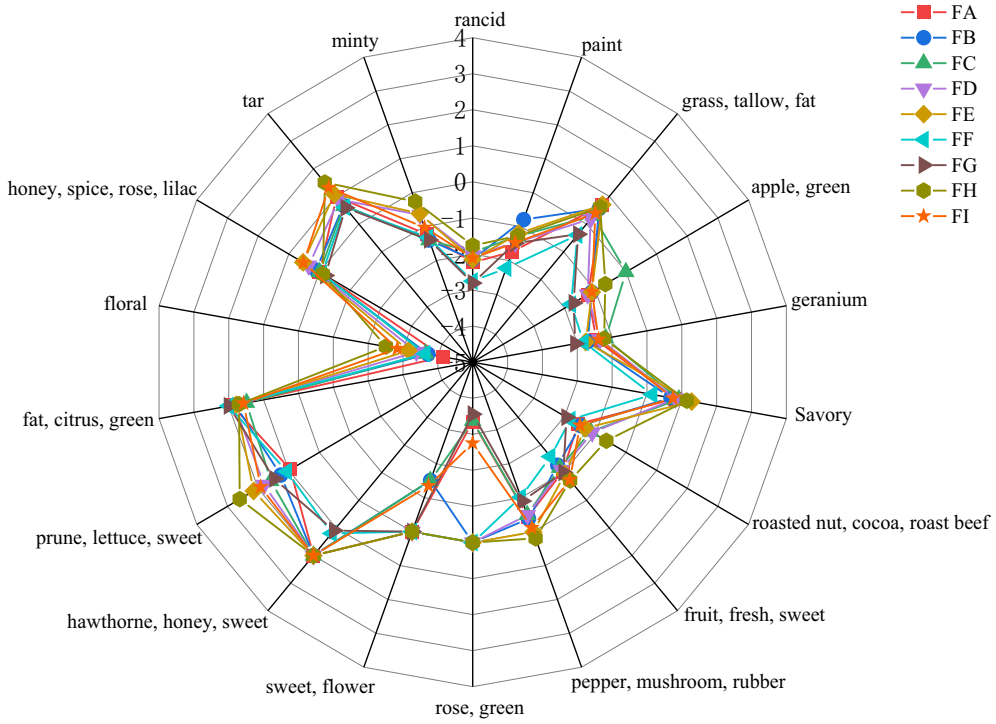

FIGURE 1
Analysis of smell results.

In this study, only the flavor substances for which thresholds could be found were analyzed. Phenylacetaldehyde was the flavor substance with the highest relative amount and low threshold value in the FA-E and FH-I fermentation stages, and nonanal was the flavor substance with the highest relative amount and low threshold value in the FF-FG fermentation stage; therefore, these two substances were defined as the standard flavor substances (Tstan = 100).

The ROAV value is an index that can quantify the contribution of volatile flavor components to the overall aroma of the sample, and the ROAV value was calculated according to 2.2, and the results are shown in Table 1. There were six flavor compounds with ROAV>1. Hexanal, 2,6-dimethylpyridine, nonanal, phenylglyoxal, naphthalene, and methyl benzoate were the main flavor compounds of the cigar tobacco, and the six aroma compounds were classified into floral, green flavor, cheesy flavor, and green flavor according to the aroma characteristics. The six aroma compounds are classified into five categories according to their aroma characteristics: floral, green flavor, cheesy, sweet, citrus, and caramel-nutty.

3.2 Study on dominant microflora during the fermentation of cigar tobacco leaves

3.2.1 Analysis of the dominant flora of the archaeal community in the fermentation process

Based on the abundance data of the species level of the Archaebacteria (biology) in cigar tobacco leaves at different fermentation stages were analyzed using heatmaps in the R language, as shown in Figure 2. There was no archaeal community on the surface of cigar tobacco leaves before fermentation, and the archaeal community appeared gradually after fermentation. The changes in the abundance of archaea were relatively large in the FB, FD, FG, and FI stages of fermentation, and the changes in the strains of archaea were mainly concentrated on the *Candidatus* species.

Differential analysis of the archaeal communities present on the surface of cigar tobacco leaves at different fermentation stages showed that the fermentation stages in which there were significant differences between species after cigar tobacco fermentation were mainly the FB, FD, FG, FH, and FI fermentation stages, with significant differences in the *Haloferax_mediterranei*, *Haloterrigena_limicola*, and *Candidatus_Thorarchaeota_archaeon_SMTZ-45* colonies (Figure 3).

Combined with the relative abundance and LDA score ≥ 2.5 at the species level in Figure 4, it can be seen that during the late fermentation *Haloferax-mediterranei*, *Haloterrigena-limicola*, *Candidatus-Thorarchaeota-archaeon-SMTZ-45* the most abundant archaeon in the colony and the key archaeon colony in the fermentation of cigar tobacco leaves.

3.2.2 Analysis of the dominant flora of the bacterial community in the fermentation process

Significance analysis of the bacterial community of cigar tobacco leaves in different fermentation stages was carried out as shown in Figure 5. The distribution shows that the bacterial community of the pre-fermentation samples differed significantly from that of the post-fermentation samples, and each fermentation stage occupied a different quadrant. The results showed that there were significant differences in the structure of the bacterial communities at different stages.

Based on the 97% similarity, all sample sequences were clustered, and based on the relative abundance information of all samples at the

TABLE 1 Aroma thresholds of volatile flavor substances in cigarillos during fermentation.

Retention time	Aroma	Substance	CAS	Threshold(medium-air; mg/Kg) Van Gemert (2011)	ROAV (mg/Kg)								
					FA	FB	FC	FD	FE	FF	FG	FH	FI
9.22	Rancid	Pyridine	110–86-1	2	0.006	0.007	0.011	0.009	0.007	0.002	0.002	0.017	0.008
10.06	Paint	Toluene	108–88-3	0.527	0.018	0.162	0.052	0.034	0.063	0.006	0.033	0.053	0.033
10.53	Grass, tallow, Fat	Hexanal	66–25-1	0.005	4.865	3.645	1.989	1.548	5.013	0.401	0.431	4.064	2.454
12	Apple, green	2-Hexenal, (E)-	6,728-26-3	0.11	0.057	0.076	0.000	0.056	0.078	0.016	0.020	0.214	0.077
12.63	Geranium	o-Xylene	95–47-6	0.450	0.035	0.020	0.065	0.045	0.017	0.015	0.009	0.058	0.041
12.88	Savory	Pyridine, 2,6-dimethyl-	108–48-5	0.003	6.477	4.828	8.274	6.626	19.23	1.421	0.000	13.874	5.612
13.66	Roasted nut, cocoa, roast beef	DIMETHYL PYRAZINE	108–50-9	0.718	0.027	0.033	0.071	0.079	0.047	0.016	0.011	0.230	0.032
13.92	Fruit, fresh, sweet	hexanoic acid methyl ester	106–70-7	0.07	0.091	0.054	0.067	0.080	0.112	0.026	0.097	0.193	0.185
15.54	Pepper, mushroom, rubber	5-Hepten-2-one, 6-methyl-	110–93-0	0.068	0.362	0.412	0.324	0.325	1.029	0.096	0.125	1.582	0.775
16.71	Rose, green	1-Hexanol, 2-ethyl-	104–76-7	25.482	0.000	0.000	0.000	0.000	0.000	0.000	0.000	0.000	0.002
17.07	Sweet, flower	Benzyl alcohol	100–51-6	2.5462	0.000	0.031	0.032	0.000	0.000	0.000	0.000	0.000	0.045
17.39	Hawthorne, honey, sweet	Benzeneacetaldehyde	122–78-1	0.0063	100	100	100	100	100	15.75	12.56	100	100
18.74	Prune, lettuce, herb, sweet	Benzoic acid, methyl ester	93–58-3	0.001	8.952	18.28	38.748	63.78	140.9	11.64	29.78	395.63	83.180
18.79	Fat, citrus, green	Nonanal	124–19-6	0.0011	80.397	65.59	30.849	69.68	60.54	100.0	100.0	50.910	37.333
19.91	Floral	Isophorone	1,125-21-9	200	0.000	0.000	0.000	0.000	0.001	0.000	0.000	0.003	0.001
20.07	Honey, spice, rose, lilac	Phenylethyl Alcohol	60–12-8	0.5642	0.000	1.298	0.000	2.269	3.435	0.819	0.646	0.768	3.321
21.16	Tar	Naphthalene	91–20-3	0.006	9.696	4.772	4.526	7.666	12.01	4.106	3.867	31.751	21.024
34.52	Minty	Hexadecanoic acid, methyl ester	112–39-0	>2	0.059	0.040	0.040	0.224	0.246	0.047	0.041	0.550	0.095

10.3389/fmicb.2023.1267447

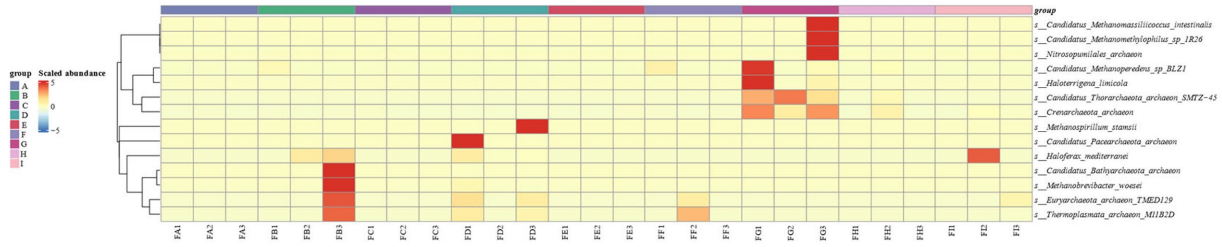

FIGURE 2
Heat map of archaebacterial species abundance clustering at the species level in different fermentation stages of cigar tobacco.

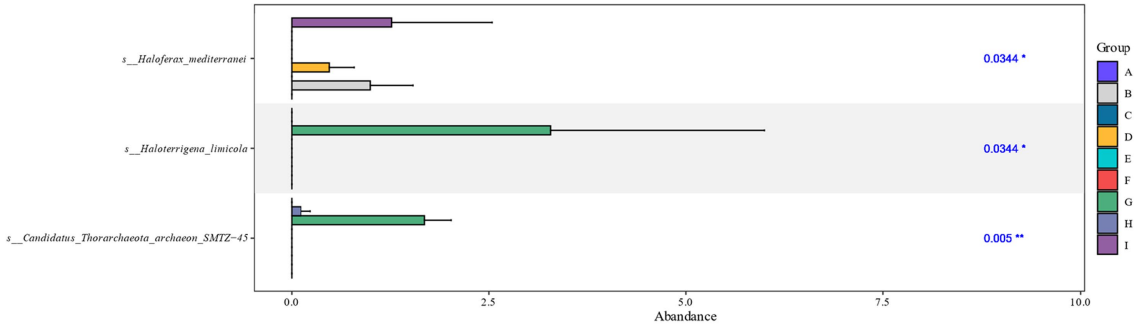

FIGURE 3
Kruskal-Wallis analysis of cigar tobacco at different fermentation stages based on species level. The horizontal coordinates of the bar graph indicate the relative abundance of a species in different subgroups, the vertical coordinates indicate the difference species, and different colors indicate different groups.

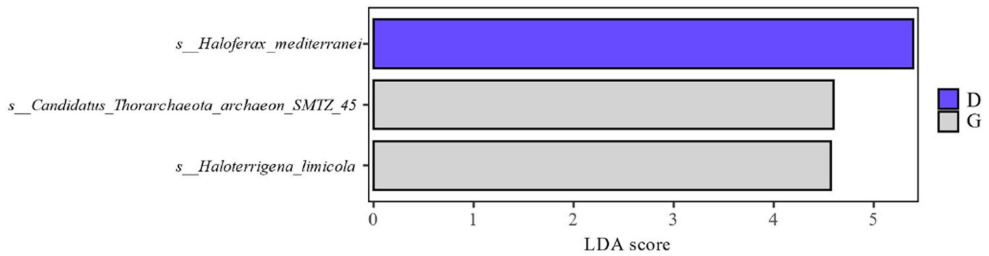

FIGURE 4
Distribution of LDA values of archaea at different levels during different fermentation stages of cigar tobacco leaves.

genus level and species level (the top 30 overall abundance species were taken here), the relative abundance of species at different levels was analyzed for variation, and the abundance share of bacterial communities was obviously different among the fermentation stages; the analysis of the results at the genus level in Figure 6 revealed that Serratia, *Methyloversatilis*, *Neisseria*, *Thauera*, *Sphingobacterium*, *Prevotella*, *Sodalis*, and *Pseudomonas* had high coefficients of variation, with *Methyloversatilis*, *Neisseria*, *Thauera*, *Prevotella* genus group of species showed a gradual increase in microorganisms with the extension of fermentation time. From the analysis of the results of the seven species levels in Figure 7, it was found that *Serratia_marcescens*, *Methyloversatilis_discipulorum*, *Sphingomonas_sp_TF3*, *Thauera_sp.*, *Neisseria_meningitidis*, *Serratia_ fonticola*, *Komagataeibacter_europaeus*, *Sphingomonas_echinoides*, and *s__Pseudomonas_aeruginosa* had high coefficients of variation, and all bacteria with high coefficients of variation were present in the high coefficients of variation except for *Komagataeibacter_europaeus*. *Komagataeibacter* europaeus is a gram-negative bacterium belonging to the genus *Komagataeibacter* of the family *Acetobacteraceae*, a common acetic acid bacterium capable of converting alcohols into acetic acid. *Komagataeibacter* europaeus is also capable of producing other beneficial metabolites such as polysaccharides and cellulases, which have potential applications.

From the analysis of LDA score ≥ 2.5 of the bacterial community at the species level of Figure 8, it can be seen that the genera *Pseudomonas*, *Methylorubrum*, *Sphingomonas*, *carotinifaciens*, and *Thauera* were the most abundant bacteria in the late fermentation stage of FG and FH fermentation. Combining the results of the relative abundance analyzes in Figures 6, 7 with the LDA score ≥ 2.5 at the

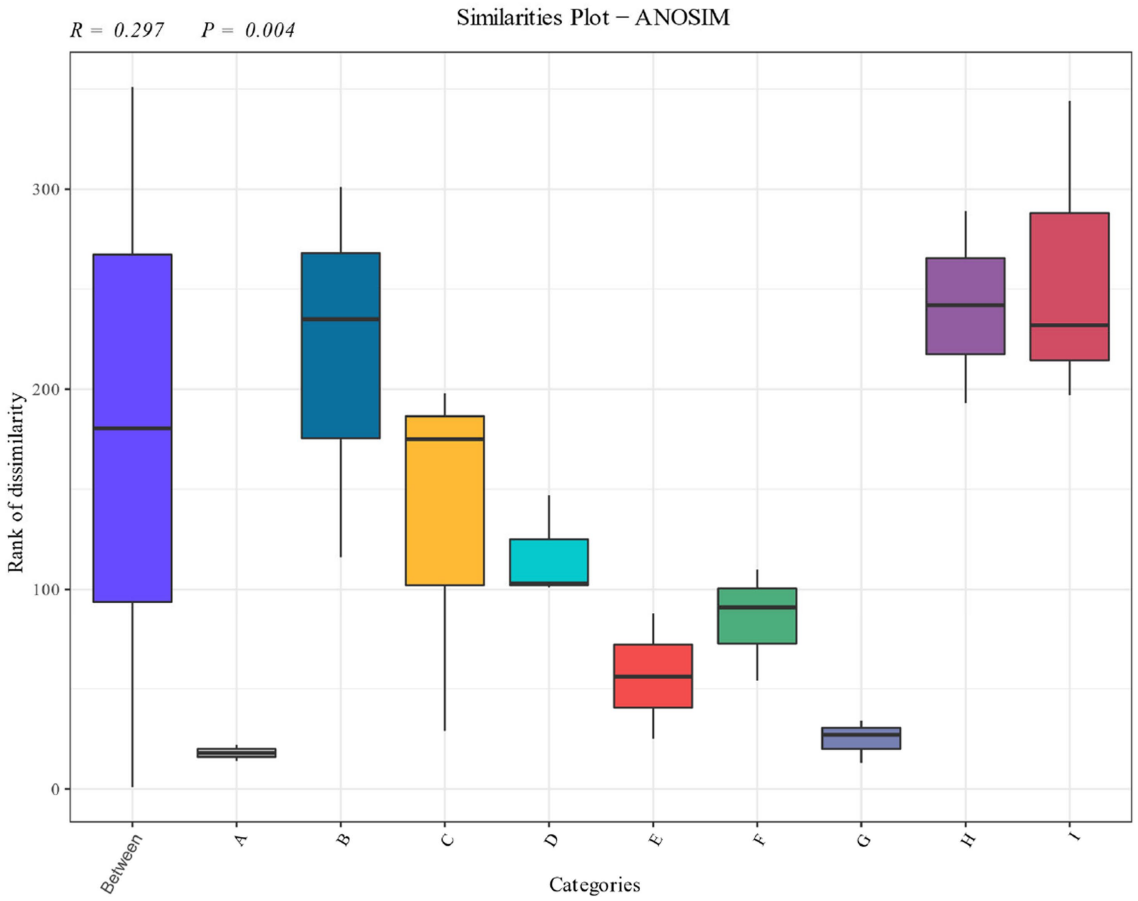

FIGURE 5
Anosim analysis of cigarillos at different fermentation stages based on species level. *R*-value is between (–1, 1), R-value is greater than 0, indicating significant difference between groups, and the confidence of statistical analysis is expressed by *p*-value, $p < 0.05$ indicates statistical significance.

species level in Figure 8, it can be seen that the genera *Methyloversatilis*, *Sphingomonas*, *Thauera* and *Pseudomonas* are the key bacterial colonies during the fermentation of cigar tobacco leaves.

3.2.3 Analysis of dominant flora of fungal communities during fermentation process

Anosim analysis of the fungal community at the species level during the fermentation of cigar tobacco is shown in Figure 9, which shows significant differences in the composition of the fungal community at the species level during the fermentation of cigar tobacco. As can be seen from the distributions, there were significant differences between the fungal communities of the samples before fermentation and the samples after fermentation, and the fungal communities in tobacco leaves at different stages of fermentation occupied different quadrants. The results showed that there were significant differences in the structure of fungal communities at different stages.

Based on the relative abundance of fungi at the species level (the top 30 species in terms of overall abundance were taken here) and the degree of variation of all the samples, it can be seen that the variation of the fungi *Diaporthe_helianthi* and *Diaporthe_ampelina* was more obvious (coefficient of variation >1) during the fermentation process, and the most abundant fungi were *Penicillium_steckii* and *Aspergillus_glaucus*, followed by *Aspergillus_cristatus* and *Diaporthe_helianthi*. *Penicillium_steckii* and *Aspergillus_glaucus*, followed by *Aspergillus_cristatus* and *Diaporthe_helianthi*, and the highest abundance was found in *Diaporthe_ampelina*, *Aspergillus_ampelina* and *Penicillium_glaucus* during fermentation. Genus types of fungi had higher relative abundance during the fermentation process (Figure 10).

LEfSe analysis as shown in Figure 11 showed that from the species level each fermentation stage fungal flora changed significantly during fermentation. At the species level LDA score ≥ 2.5, *Saitoella_complicata* in FC fermentation stage, *Penicillium_decumbens* in FF fermentation stage, *Aspergillus_glaucus* in FG fermentation stage, and *Trichoderma_atroviride* in FI fermentation stage were far higher than other fermentation stages, and the key fungal communities were mainly concentrated in the late fermentation stage, among which *Aspergillus_glaucus* was the most prominent in the FG fermentation stage. Combining the relative abundance, the degree of variability and the LDA scores, *Penicillium* spp. and *Aspergillus* spp. are the key fungal genera.

3.3 Correlation analysis between key flora and main flavor compounds

Through the studies in the previous two sections, the main microflora and the main flavor substances have been identified, and next, in this section, Pearson correlation analysis was used to further

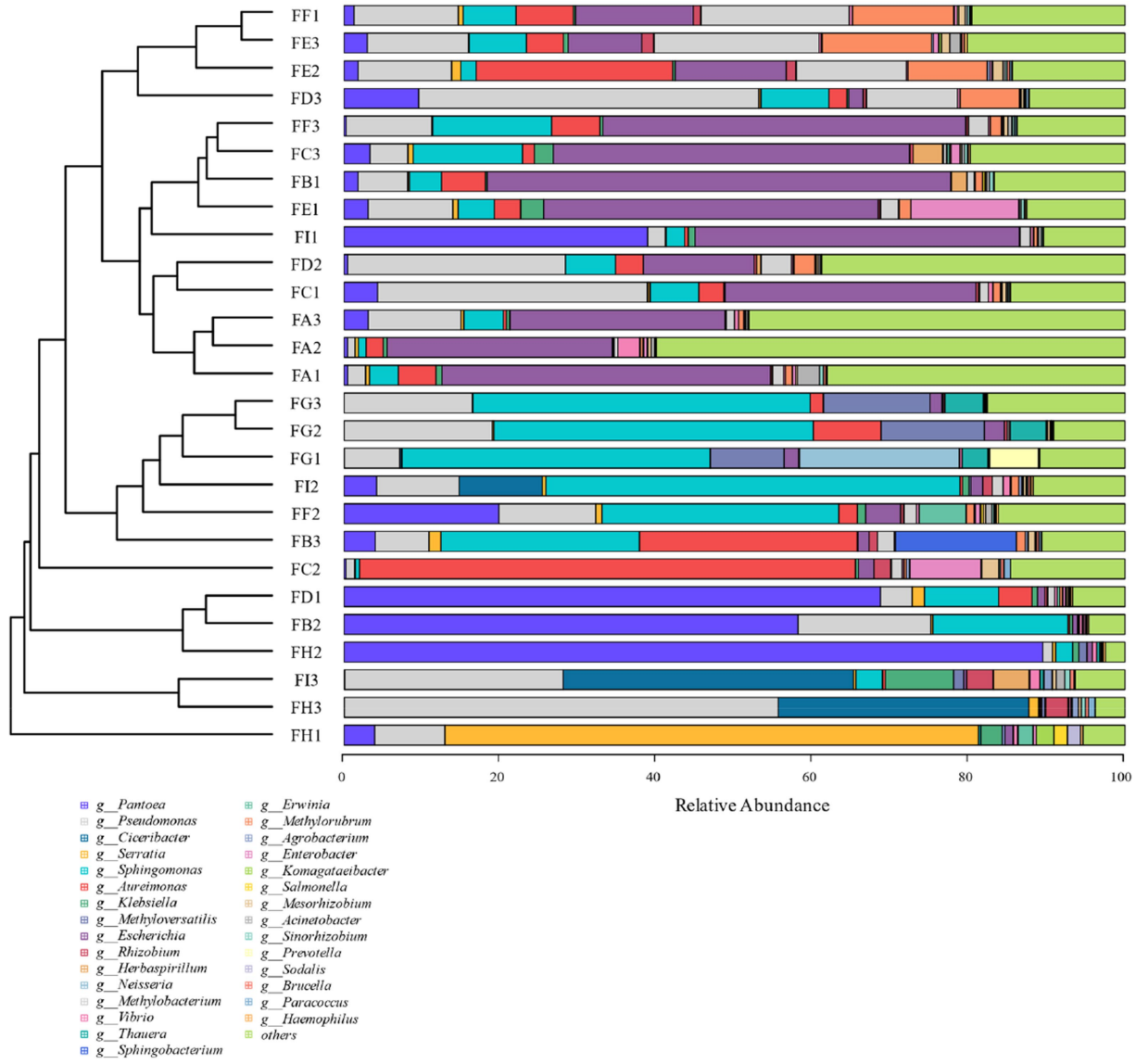

FIGURE 6
Cluster analysis of horizontal bacterial species of cigar tobacco genus at different fermentation stages.

study the correlation between the key bacterial genera and the main aroma substances at different fermentation stages of cigar tobacco leaves. The correlation heat map between key bacterial genera and main body flavor substances at different fermentation stages of cigar tobacco is shown in Figure 12. The effect of archaea on the main body flavor was not significant, the bacterial community *s__Pseudomonas_aeruginosa* showed a significant positive correlation with Benzoic acid, methyl ester (r2 = 0.685), and the fungal community *s__Penicillium_vulpinum* showed a significant positive correlation with Nonanal (r2 = 0.748). The bacterial community *s__Pseudomonas_aeruginosa* showed significant negative correlation with *Benzeneacetaldehyde* (r2 = −0.783), *s__Aspergillus_steynii*, *s__Aspergillus_terreus*, *s__Aspergillus_ sclerotialis* fungi of the genus *Aspergillus* had significant negative correlation (r2 > −0.7) with Hexanal, Pyridine, 2,6-dimethyl-, Benzoic acid, methyl ester, while *s__Aspergillus_ sclerotialis* showed a highly significant negative correlation with Naphthalene (r2 = −0.822). This suggests that *Aspergillus* spp. fungi inhibit the main aroma during fermentation, and *Aspergillus* spp. fungi in the FG fermentation stage affected the accumulation of green, floral, cheesy, and burnt-sweet aromas, while the high activity of the bacterium *Pseudomonas_aeruginosa* in the FG stage was favorable to the accumulation of green aroma, and at the same time inhibited the sweetness. In the FF fermentation stage, the increased activity of the fungus *Penicillium_vulpinum* favors the accumulation of citrus-like aromas.

3.4 Analysis of the functional contribution of dominant microorganisms in cigar tobacco leaves

By calculating the relative abundance of microorganisms in each metabolic pathway at the genus level, it is possible to demonstrate the functional contribution of the cigar tobacco fermentation flora to the KEGG and CAZy metabolic pathways. As shown in Figure 13 KEGG

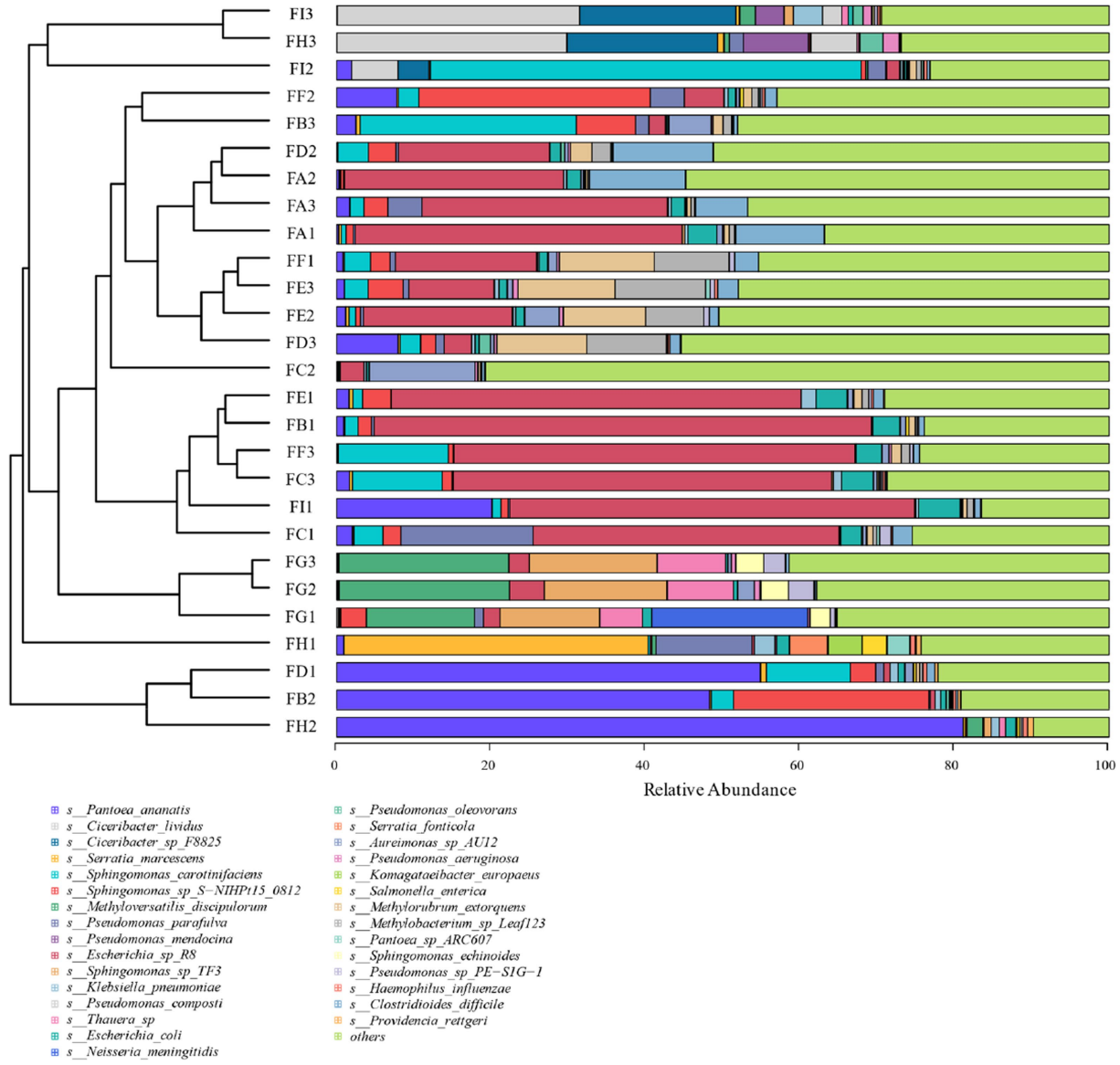

FIGURE 7
Cluster analysis of bacterial species at the level of cigar tobacco species at different fermentation stages.

7 major metabolic pathways, metabolism is the major biometabolic pathway during fermentation. Combined with the annotation results of the 6 major carbohydrate enzymes of the CAZy database in Figure 14, the metabolic enzymes of the genus were mainly dominated by GH: glycoside hydrolase and GT: glycosyltransferase. In addition, the KEGG 43 pathway metabolic pathway was found in Figure 15; amino acid metabolism, carbohydrate metabolism and film transport metabolic pathway were the main metabolic pathways in each fermentation stage of cigar tobacco. The main sources of aroma substances are carotenoid degradation products, Siberian degradation products, aromatic amino acid metabolites, and melanoidin products, which indicates that the main aroma of this paper comes from aromatic amino acid metabolites and melanoidin products, and that the metabolism of bacterial and fungal reproduction during the fermentation of cigar is mainly secreted by glycoside hydrolases and glycosyltransferases to degrade precursor substances.

4 Discussion

4.1 Major findings

Cigar tobacco is the tobacco with the most distinctive flavor profile, and the fermentation technology and microbial community contribute to the flavor of cigar tobacco leaves (Zheng et al., 2022). In this study, we found that the main flavor profile of cigar tobacco leaves after fermentation was honey-like sweetness, cocoa-flavored burnt-sweetness, citrus-mint-like freshness, and grass-like herbaceousness, and the main flavor substances were hexanal, 2,6-dimethylpyridine, nonanal, phenylglyoxal, naphthalene, and methyl benzoate. During fermentation, the key archaea *Haloferax_mediterranei*, *Haloterrigena_limicola*, *Candidatus_Thorarchaeota_archaeon_SMTZ-45*, and the key bacteria for the *Methyloversatilis* spp., *Sphingomonas* spp., *Thauera* spp., and *s__Pseudomonas* spp., and key fungi were *Penicillium* spp.

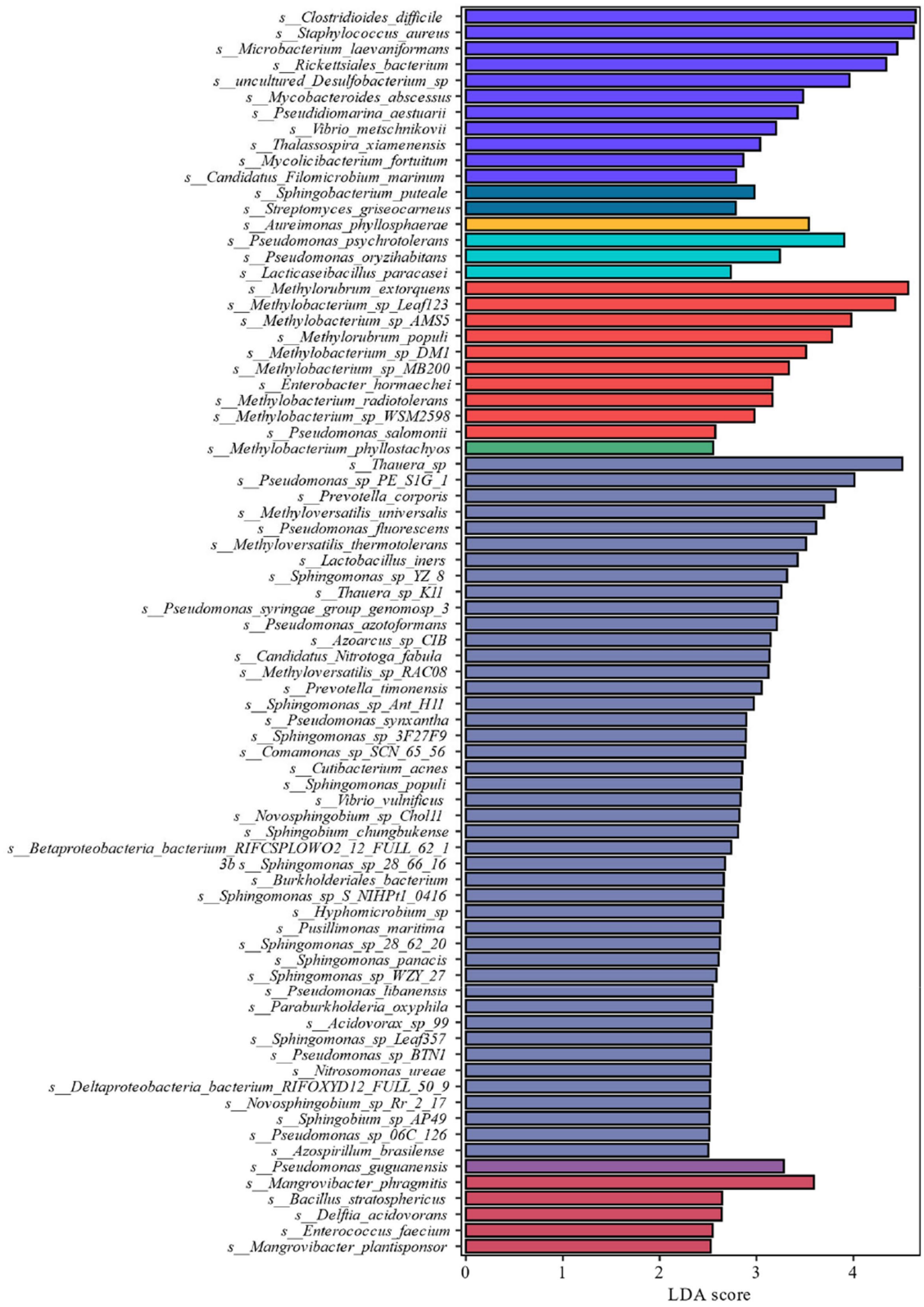

FIGURE 8
LDA value distribution of different species at different levels during different fermentation stages of cigar tobacco leaves.

and *Aspergillus* spp. Correlation analysis of the key colonies with the main flavor substances revealed that the key bacterial and fungal communities were significantly correlated with the main flavor substances, among which the fungi of *Aspergillus* spp. were mainly negatively correlated with Hexanal, Pyridine, 2,6-dimethyl-, Benzoic acid, methyl ester and Naphthalene in the main flavor substances.

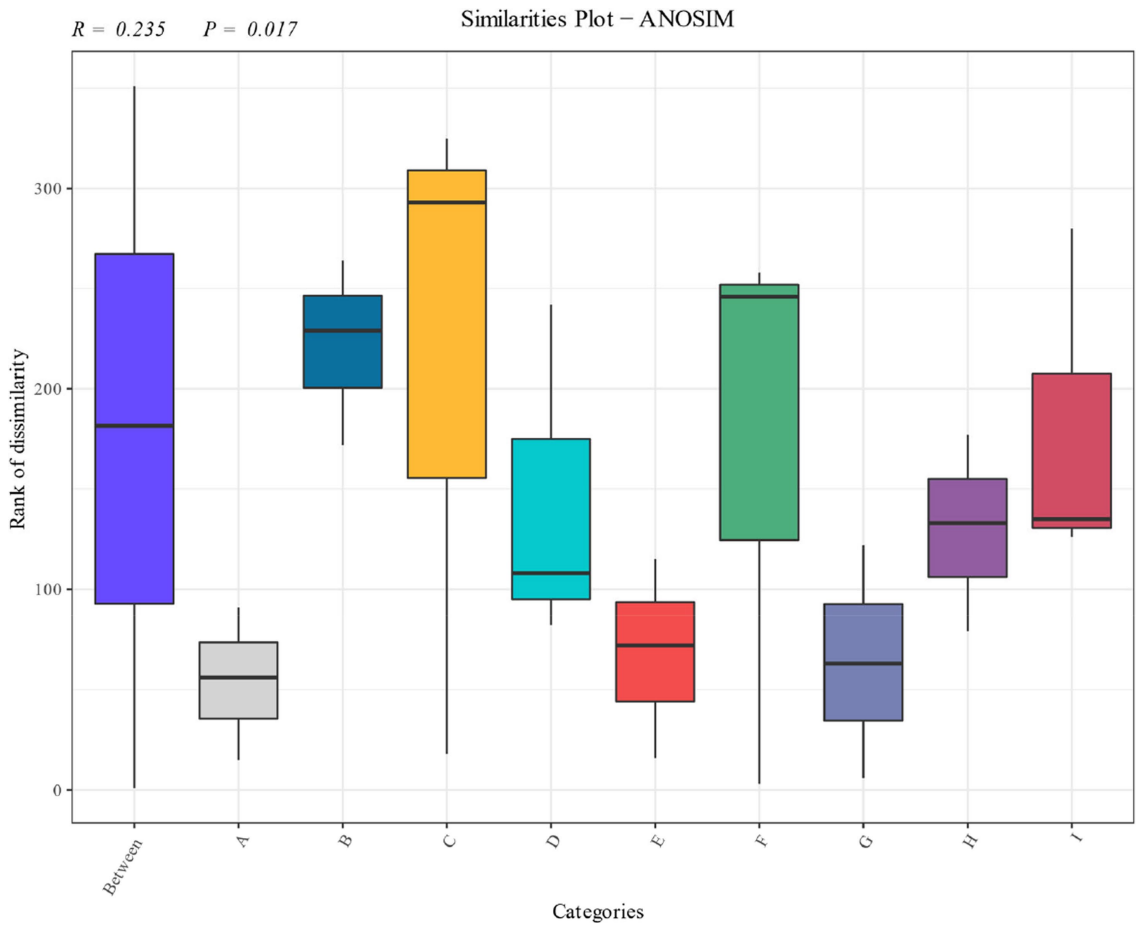

FIGURE 9
Anosim analysis of cigarillos at different fermentation stages based on species level. *R*-value is between (−1, 1), R-value is greater than 0, indicating significant difference between groups, and the confidence of statistical analysis is expressed by *p*-value, $p < 0.05$ indicates statistical significance.

Naphthalene was negatively correlated with the main aroma and inhibited the accumulation of green, floral, cheesy and caramelized aromas. *s__Pseudomonas_vulpinum* was positively correlated with Nonanal and favored the accumulation of citrus-like aromas. *s__Pseudomonas_aeruginosa* was positively correlated with Benzoic acid, methyl ester, and Naphthalene. aeruginosa was positively correlated with Benzoic acid, methyl ester and negatively correlated with Benzeneacetaldehyde, so that increased activity favored the accumulation of green aroma and inhibited the accumulation of sweet aroma. Functional analysis showed that the dominant bacteria secreted glycoside hydrolases and glycosyltransferases during metabolism, and the metabolic pathways of amino acid metabolism, carbohydrate metabolism and membrane transport were dominant, so the main aroma of this paper was derived from the metabolism of aromatic amino acids, and the products of Meladol.

4.2 Analysis of the correlation between microbes and flavor substances in cigar leaves

Currently, there is no systematic study on the mechanism of the influence of its own dominant microorganisms on flavor substances during the fermentation process of cigar tobacco (Evans et al., 2015), and the unique aroma substances are one of the criteria for evaluating the quality of tobacco and distinguishing the quality grade of tobacco, and the main aroma in the present study was the sweet, burnt-sweet, citrus-mint-like fresh and grassy aroma, supplemented by woody, spicy (slightly pungent pepper-like) aroma, floral, cocoa aroma and fruity aroma, which is similar to previous studies. When there is a slight decrease in total nitrogen, nicotine, starch and protein in the chemical composition (Mo, 2017a), it is actually the amino groups on proteins, peptides and amino acids that undergo a non-enzymatic reaction with the carbohydrate carbonyl group (Fu et al., 2019), which enhances the sweet, cocoa-like and milky powder-like aromas (Arsa and Theerakulkait, 2015; Abdelhedi et al., 2017; Lund and Ray, 2017) and also enhances the biological properties and antioxidant activity of milk proteins (Oh et al., 2013; Zhang et al., 2020). Increased clear flavor content is associated with the degradation of chemical components by microbial metabolic enzymes of tobacco leaves. In this study s__Sphingomonas_sp_TF3, *s__Aspergillus_nidulans* and *s__Diaporthe_helianthi* belonging to *Pseudomonas* and *Mycobacterium* spp. which proved to be dominant in roasted and cigarette tobacco studies (Han et al., 2016; Tyx et al., 2016; Chopyk et al., 2017; Smyth et al., 2017). Both can promote decomposition of organic matter (Hang et al.,

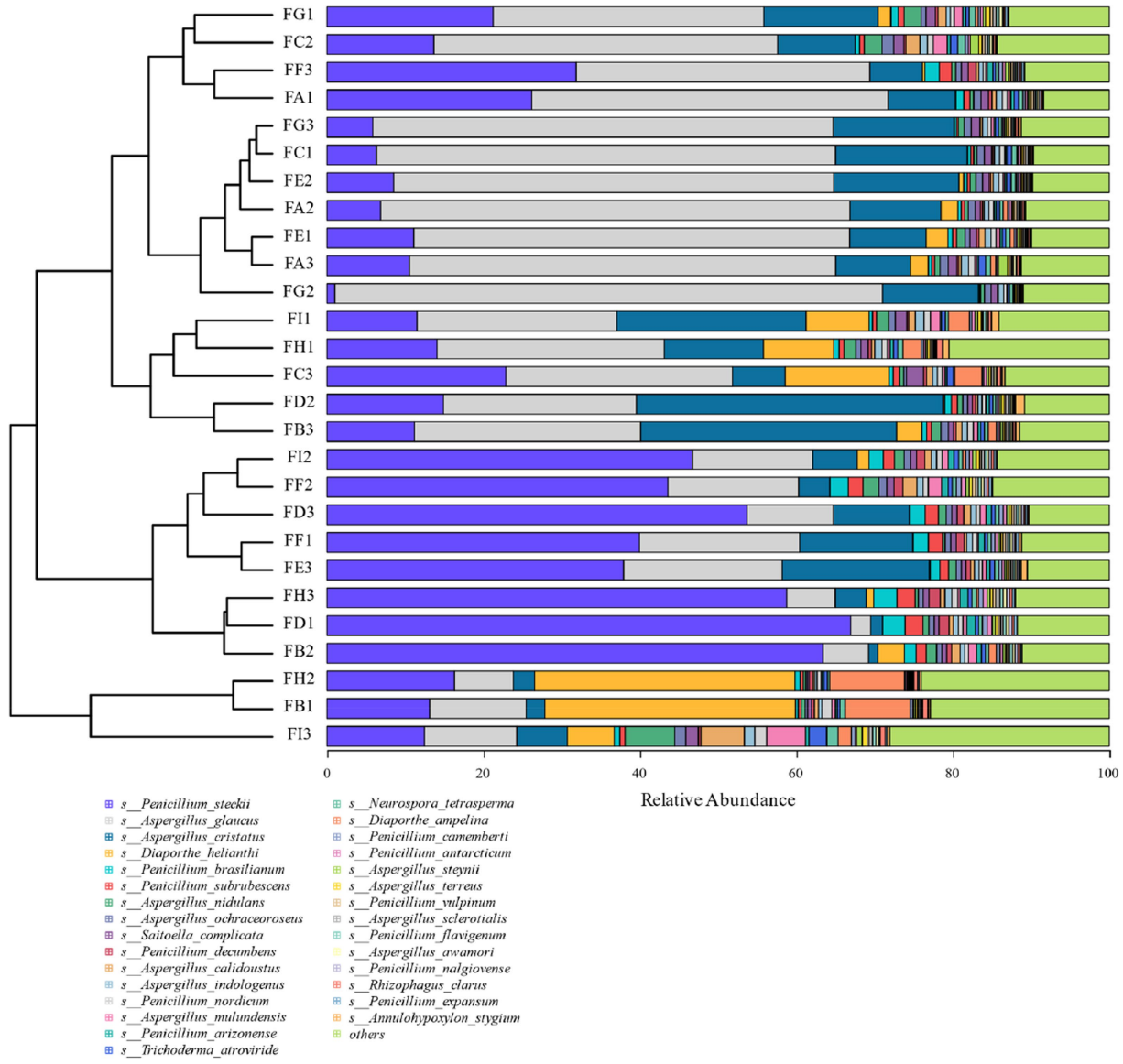

FIGURE 10
Cigar tobacco species level fungal species clustering analysis at different fermentation stages.

2018; Li et al., 2019; Zhang et al., 2019; Chen et al., 2020; Kong et al., 2023), and increased levels contribute to the degradation of tobacco chemicals (Liu et al., 2021). Bacteria of the genus *Pseudomonas* (Zhang Y. et al., 2018) in strains with pairs of degradation of methyl benzoate and the production of phenylacetaldehyde ability, and phenylacetaldehyde is formed by the degradation of precursors such as phenylalanine (Zhang Y. et al., 2018). Bacteria of the genus *Sphingomonas* (Liu et al., 2017; Hu et al., 2019) produce aldehydes, esters, and ketones during reproductive metabolism. Fungi of the genus Aspergillus (Victor et al., 2019) produce enzymes that convert fatty acids to Hexanal (hexanal), and lipids are first oxidized by lipoxygenase to form lipid hydroperoxides and then cleaved by hydrogen peroxide lyase to hexanal and other six-carbon aliphatic aromatic compounds. These aldehydes can be isomerized to trans-isomers and then reduced to hexanal (Yin et al., 2022), metabolism produces oxidases, aminotransferases, hydrolases and synthetases to synthesize and decompose Pyridine, 2,6-dimethyl-substances. Enzymes produced by *Penicillium vulpinum* catalyze the oxidative reaction of non-saturated fatty acids into the corresponding aldehydes, palmitoleic acid being the precursor substance of nonanal, and these odorant molecules may interact with nonanal, promoting its formation or altering its pathway of formation. This is consistent with the results of the functional analysis, mainly through two pathways analyzed for aroma production, on the one hand, microorganisms secreted enzymes to degrade amino acids and carbohydrates are two explained small molecules undergo a Merad reaction to produce aroma, and on the other hand, microorganisms directly produce aroma by utilizing and degrading aromatic amino acids, and in this paper, for the first time, we found that microorganisms can produce aroma substances by transporting genes through membranes. It is hypothesized that the process of aroma production may be in the fermentation process, microorganisms will secrete a thin film of biopolymers, covering the surface of cigar tobacco leaves to form a protective layer,

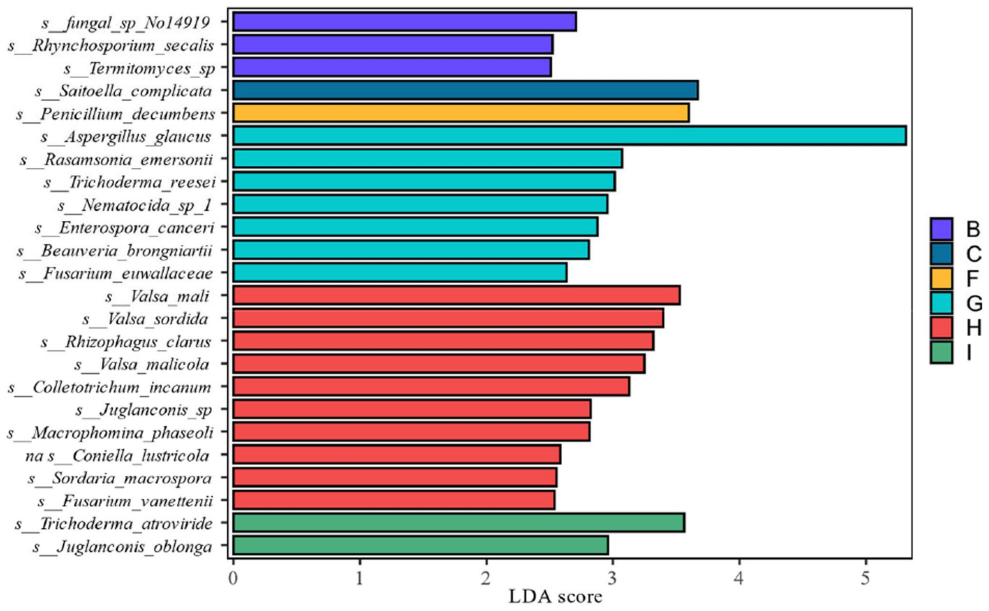

FIGURE 11
LDA value distribution of different in species different fermentation stages of cigar smoke.

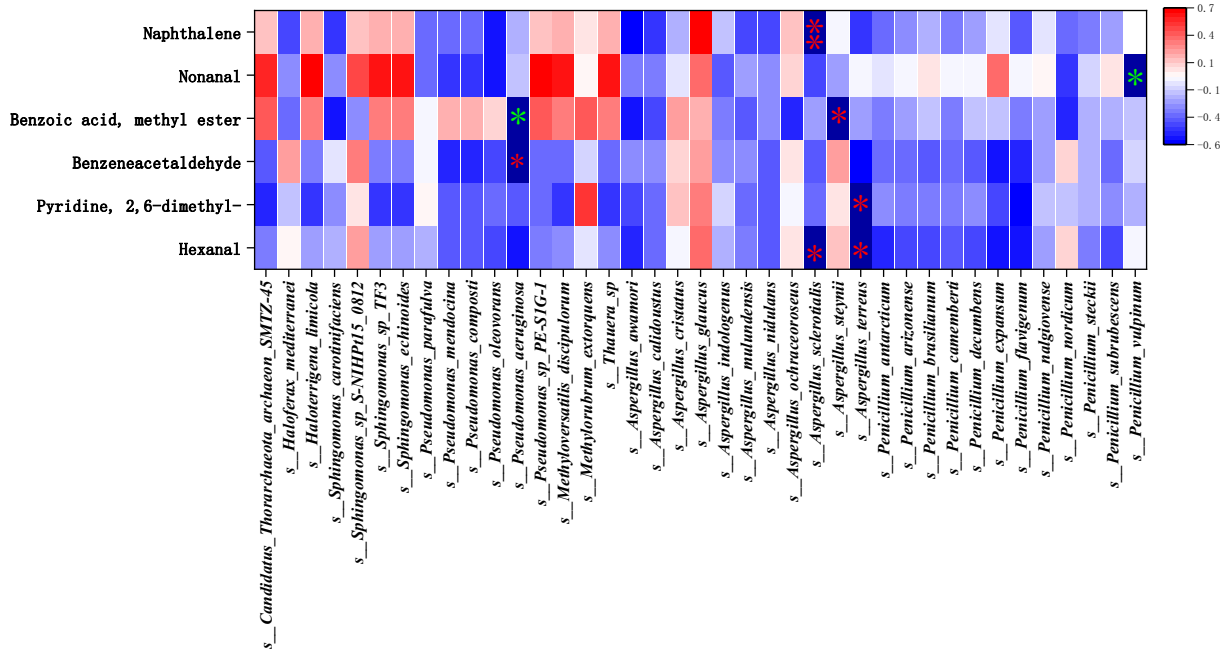

FIGURE 12
Correlation analysis between key microflora and main flavor substances. *is significant, ** is highly significant, green is positive correlation, red is negative correlation.

microorganisms in the fermentation process will produce genes that represent specific aroma substances, genes are transmitted to the surrounding microorganisms through the film, the microorganisms that receive the genes to synthesize the specific aroma substances, the synthesized aroma substances will be gradually released through the film onto the surface of the cigar leaf. Cigar tobacco leaf surface, the specific mechanism should be further studied to determine.

4.3 Future direction

The correlation between key microorganisms and the main flavor substances during the fermentation of cigar tobacco leaves was investigated to further reveal the specific contribution of microorganisms to the formation of odors and to provide a reference for the regulation of odor characteristics during the fermentation

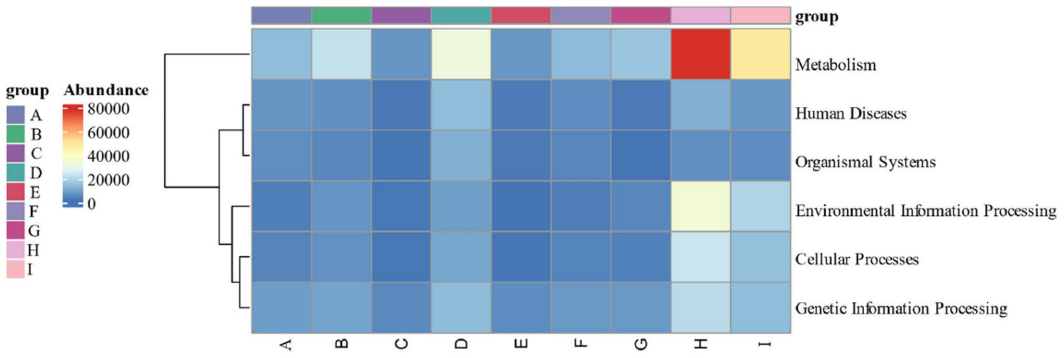

FIGURE 13
KEGG 7 major metabolic pathways.

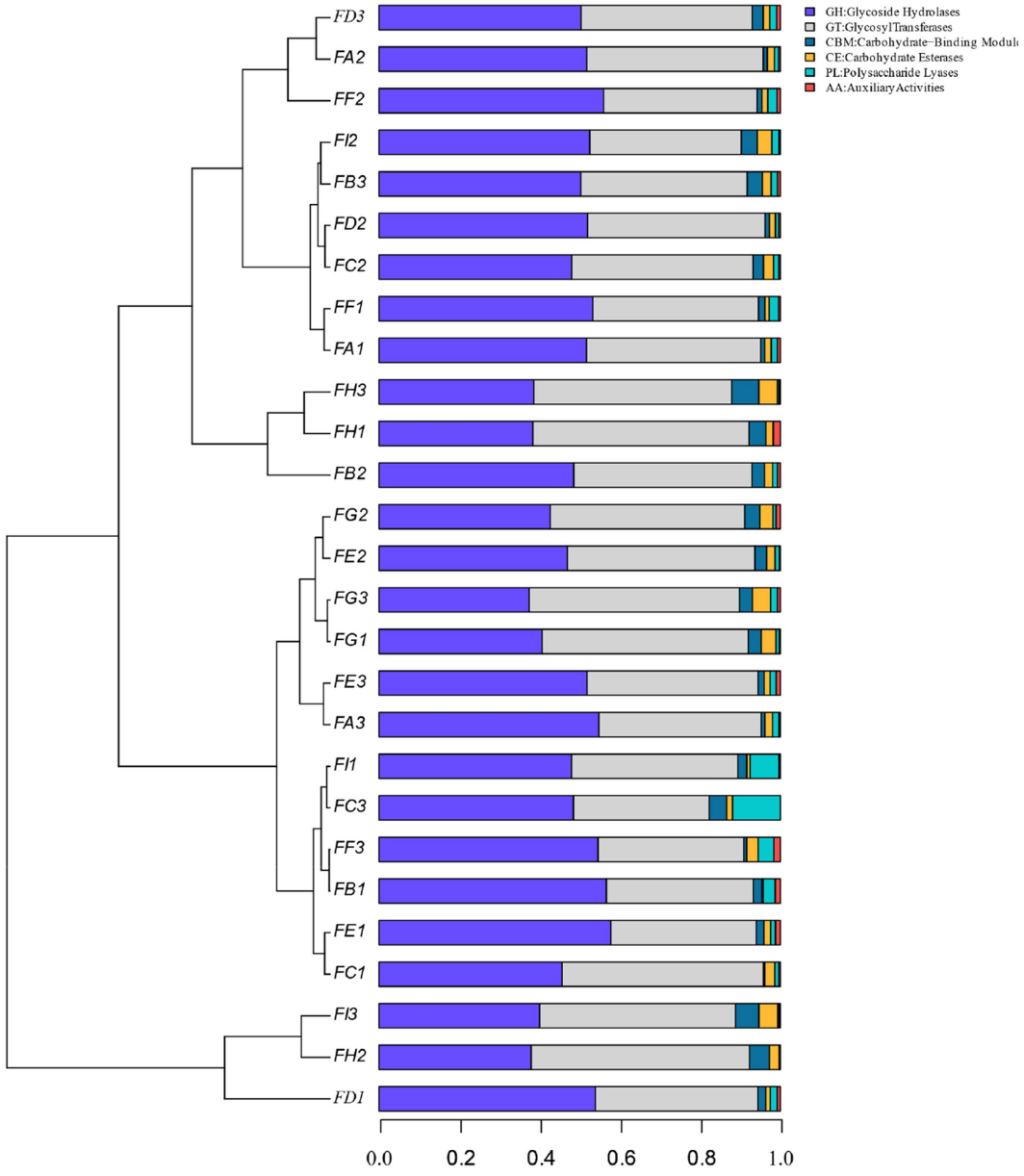

FIGURE 14
CAZy database of the 6 major carbohydrases.

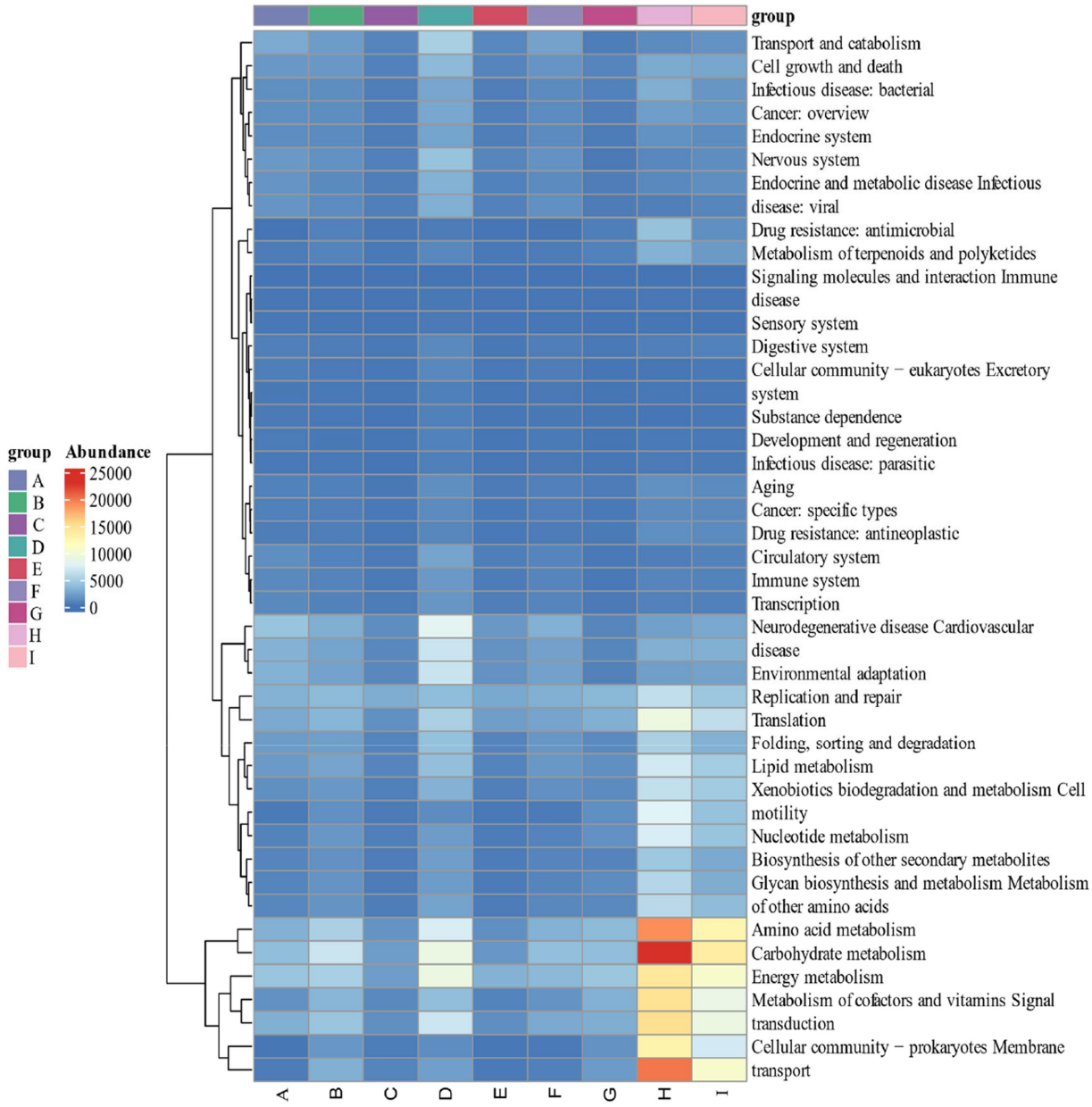

FIGURE 15
KEGG 43 pathway metabolic pathway.

process. The popularity of cigar cigarettes among consumers is inseparable from their unique flavor, therefore, it is increasingly important to develop fermentation strains that produce good flavor substances. Based on the present study, we can focus on the screening and development of flavor strains and the synergistic effect between the dominant strains and flavor strains, so as to develop new cigar leaf fermentation agents, which will promote the enhancement of the flavor of cigar and the standardization of the production of cigar tobacco.

Data availability statement

The original contributions presented in the study are included in the article/supplementary material, further inquiries can be directed to the corresponding author.

Author contributions

XW: Data curation, Software, Writing - original draft. YH: Conceptualization, Writing - review & editing. QW: Writing - review & editing. JL: Data curation, Software, Writing - review & editing. SF: Writing - review & editing. DH: Conceptualization, Writing - review & editing. XP: Software, Writing - review & editing. JC: Data curation, Writing - review & editing. YG: Data curation, Writing - review & editing. YN: Conceptualization, Writing - review & editing.

Funding

The author(s) declare financial support was received for the research, authorship, and/or publication of this article. The authors

would like to express their sincere thanks to the Science and Technology Innovation Program of Chinese Academy of Agricultural Sciences ASTIP-TRIC07, Chenzhou Tobacco Company Project (GB5C2021JS02), and the Science and Technology Program of Shandong Zhongtian Tobacco Industry Limited Liability Company (202201020) for the financial support of this study. The funders were not involved in the study design, analysis, interpretation of data, the writing of this article or the decision to submit it for publication.

Conflict of interest

YH was employed by Shandong China Tobacco Industry Limited Company and DH was employed by Chenzhou Tobacco Company.

The remaining authors declare that the research was conducted in the absence of any commercial or financial relationships that could be construed as a potential conflict of interest.

Publisher's note

All claims expressed in this article are solely those of the authors and do not necessarily represent those of their affiliated organizations, or those of the publisher, the editors and the reviewers. Any product that may be evaluated in this article, or claim that may be made by its manufacturer, is not guaranteed or endorsed by the publisher.

References

Abdelhedi, O., Mora, L., Jemil, I., Jridi, M., Toldra, F., Nasri, M., et al. (2017). Effect of ultrasound pretreatment and Maillard reaction on structure and antioxidant properties of ultrafiltrated smoothhound viscera proteins-sucrose conjugates. *Food Chem.* 230, 507–515. doi: 10.1016/j.foodchem.2017.03.053

Arsa, S., and Theerakulkait, C. (2015). Sensory aroma characteristics of alcalas hydrolyzed rice bran protein concentrate as affected by spray drying and sugar addition. *J. Food Sci. Technol.* 52, 5285–5291. doi: 10.1007/s13197-014-1610-5

Bäckhed, F., Roswall, J., Peng, Y., Feng, Q., Jia, H., Kovatcheva-Datchary, P., et al. (2015). Dynamics and stabilization of the human gut microbiome during the first year of life. *Cell Host Microbe* 17, 690–703. doi: 10.1016/j.chom.2015.04.004

Cai, K., Xiang, Z., Pan, W., Zhao, H., Ren, Z., Lei, B., et al. (2013). Identification and quantitation of glycosidically bound aroma compounds in three tobacco types by gas chromatography–mass spectrometry. *J. Chromatogr. A* 1311, 149–156. doi: 10.1016/j.chroma.2013.08.051

Chen, Y., Tian, W., Shao, Y., Li, Y.-J., Lin, L.-A., Zhang, Y.-J., et al. (2020). Miscanthus cultivation shapes rhizosphere microbial community structure and function as assessed by Illumina MiSeq sequencing combined with PICRUSt and FUNGUIld analyses. *Arch. Microbiol.* 202, 1157–1171. doi: 10.1007/s00203-020-01830-1

Chopyk, J., Chattopadhyay, S., Kulkarni, P., Smyth, E. M., Hittle, L. E., Paulson, J. N., et al. (2017). Temporal variations in cigarette tobacco bacterial community composition and tobacco-specific nitrosamine content are influenced by brand and storage conditions. *Front. Microbiol.* 8:358. doi: 10.3389/fmicb.2017.00358

Cotillard, A., Kennedy, S. P., Kong, L. C., Prifti, E., Pons, N., Le Chatelier, E., et al. (2013). Dietary intervention impact on gut microbial gene richness. *Nature* 500, 585–588. doi: 10.1038/nature12480

Evans, P. N., Parks, D. H., Chadwick, G. L., Robbins, S. J., Orphan, V. J., Golding, S. D., et al. (2015). Methane metabolism in the archaeal phylum Bathyarchaeota revealed by genome-centric metagenomics. *Science* 350, 434–438. doi: 10.1126/science.aac7745

Feng, S., Huang, M., Crane, J. H., and Wang, Y. (2018). Characterization of keyaroma-active compounds in lychee (*Litchi chinensis* Sonn.). *J. Food Drug Anal.* 26, 497–503. doi: 10.1016/j.jfda.2017.07.013

Fu, Y., Zhang, Y., Soladoye, O., and Aluko, R. (2019). Maillard reaction products derived from food protein-derived peptides: insights into flavor and bioactivity. *Crit. Rev. Food Sci. Nutr.* 60, 3429–3442. doi: 10.1080/10408398.2019.1691500

Gao, S., Gao, Y. Y., Fu, S. Z., Zhong, S. W., Deng, Y., Gao, J., et al. (2021). Comparative analysis of chemical composition of GH1 and GH2 cigarillos produced in Shifang and Liangshan production areas. *Processing of Agricultural Products* 70, 51–54. doi: 10.16693/j.cnki.1671-9646(X).2021.04.013

Han, J., Sanad, Y. M., Deck, J., Sutherland, J. B., Li, Z., Walters, M. J., et al. (2016). Bacterial populations associated with smokeless tobacco products. *Appl. Environ. Microbiol.* 82, 6273–6283. doi: 10.1128/AEM.01612-16

Hang, H., Xu, Q., Wang, W., Chen, Q., Wang, Y., and Li, X. (2018). Biodegradation of benzeneacetaldehyde by *Pseudomonas putida* ZWL73. *J. Environ. Sci.* 9, 272–278.

Hu, Y., Li, Q., Guo, W., Ai, L., and Tian, H. (2019). Dynamic changes in volatile compounds during the fermentation process of Chinese rice wine. *Food Chem.* 278, 492–501. doi: 10.1016/j.fochx.2023.100620

Huang, T., Lu, Z. M., Peng, M. Y., Liu, Z. F., Chai, L. J., Zhang, X. J., et al. (2022). Combined effects of fermentation starters and environmental factors on the microbial community assembly and flavor formation of Zhenjiang aromatic vinegar. *Food Res. Int.* 152:110900. doi: 10.1016/j.foodres.2021.110900

Huang, J., Yang, J., Duan, Y., Gu, W., Gong, X., Zhe, W., et al. (2010). Bacterial diversities on unaged and aging flue-cured tobacco leaves estimated by 16S rRNA sequence analysis. *Appl. Microbiol. Biotechnol.* 88, 553–562. doi: 10.1007/s00253-010-2763-4

Hyatt, D., Chen, G. L., Locascio, P. F., Land, M. L., Larimer, F. W., and Hauser, L. J. (2010). Prodigal: prokaryotic gene recognition and translation initiation site identification. *BMC Bioinformatics* 11:119. doi: 10.1186/1471-2105-11-119

Kong, G. H., Gu, X. J., Wu, J., Zheng, J. N., Huang, D. Q., Zhang, G. H., et al. (2023). Antiviral Isocoumarins from a cigar tobacco-derived endophytic fungus aspergillus oryzae. *Chem. Nat. Compd.* 59, 242–245. doi: 10.1007/s10600-023-03966-0

Le, C. E., Nielsen, T., Qin, J., Prifti, E., Hildebrand, F., Falony, G., et al. (2013). Richness of human gut microbiome correlates with metabolic markers. *Nature* 500, 541–546. doi: 10.1038/nature12506

Li, Y., Duan, Y., Zhang, Y., Wang, Y., and Zeng, W. (2019). Biodegradation of benzeneacetaldehyde by Pseudomonas sp. strain Y1. *J. Appl. Microbiol.* 126, 1173–1183.

Li, D., Liu, C. M., Luo, R., Sadakane, K., and Lam, T. W. (2015). MEGAHIT: an ultra-fast single-node solution for large and complex metagenomics assembly via succinct de Bruijn graph. *Bioinformatics* 31, 1674–1676. doi: 10.1093/bioinformatics/btv033

Li, D., Luo, R., Liu, C. M., Leung, C. M., Ting, H. F., Sadakane, K., et al. (2016). MEGAHIT v1. 0: a fast and scalable metagenome assembler driven by advanced methodologies and community practices. *Methods* 102, 3–11. doi: 10.1016/j.ymeth.2016.02.020

Lin, S., Zhang, J., Gao, Y., Zhang, X., Song, S., Long, Z., et al. (2014). Rapid and sensitive gas chromatography-triple quadrupole mass spectrometry method for the determination of organic acids in tobacco leaves. *Anal. Methods* 6, 5227–5235. doi: 10.1039/C4AY00688G

Liu, A., Wu, J., Wang, Y., et al. (2022). Analysis of microbiome and flavor-forming genes of Sichuan bran vinegar and vinegar spirits based on macro-genome sequencing. *Jiangsu Agric. J.* 38, 806–812.

Liu, F., Wu, Z., Zhang, X., Xi, G., Zhao, Z., Lai, M., et al. (2021). Community and metabolic functional analysis of microbial cigar tobacco in leaves during fermentation. *Microbiol. Open* 10:e1171. doi: 10.1002/mbo3.1171

Liu, D. Y., Zhou, G. H., and Xu, X. L. (2008). A new method for identifying key flavor compounds in foods: the "ROAV" method. *Food Sci.* 7, 370–374.

Liu, S., Bao, B., Ji, Y. J., Lin, S., Liu, S., Bao, Y. Q., et al. (2017). Analysis of changes in volatile flavor compounds during optimized fermentation of stinky Mandarin fish by electronic nose and SPME-GC-MS. (eds.) *2017 Proceedings of the 14th Annual Conference of the Chinese Society of Food Science and Technology and the 9th China-U.S. Food Industry High-Level Forum Abstracts*, 638–639.

Lund, M., and Ray, C. (2017). Control of Maillard reactions in foods: strategies and chemical mechanisms. *J. Agric. Food Chem.* 65, 4537–4552. doi: 10.1021/acs.jafc.7b00882

Maldonado-Robledo, G., Rodriguez-Bustamante, E., Sanchez-Contreras, A., Rodriguez-Sanoja, R., and Sanchez, S. (2003). Production of tobacco aroma from lutein. Specific role of the microorganisms involved in the process. *Appl. Microbiol. Biotechnol.* 62, 484–488. doi: 10.1007/s00253-003-1315-6

Mo, J. (2017a). *Study on the change rule of conventional chemical components and neutral gas substances during the fermentation of Maduro wrapper*. Zhengzhou: Henan Agricultural University

Mo, J. (2017b). *Study on the changes of conventional chemical and neutral aroma components during the fermentation of Maduro cigar wrapper leaves, Master's thesis*. Henan Agricultural University, Zhengzhou, China.

Oh, N., Lee, H., Lee, J., Joung, J., Lee, K., Kim, Y., et al. (2013). The dual effects of Maillard reaction and enzymatic hydrolysis on the antioxidant activity of milk proteins. *J. Dairy Sci.* 96, 4899–4911. doi: 10.3168/jds.2013-6613

Qin, J. J., Li, R. Q., Raes, J. J., Arumugam, M., Burgdorf, K. S., Manichanh, C., et al. (2010). A human gut microbial gene catalogue established by metagenomic sequencing. *Nature* 464, 59–65. doi: 10.1038/nature08821

Qin, G., Zhao, G., Ouyang, C., and Liu, J. (2021). Aroma components of tobacco powder from different producing areas based on gas chromatography ion mobility spectrometry. *Open Chem.* 19, 442–450. doi: 10.1515/chem-2020-0116

Shuai, R. (2018). *Research on macro genomic 16S rRNA fragment classification method based on integrated learning*. Harbin: Harbin Institute of Technology.

Smyth, E. M., Kulkarni, P., Claye, E., Stanfill, S., Tyx, R., Maddox, C., et al. (2017). Smokeless tobacco products harbor diverse bacterial microbiota that differ across products and brands. *Appl. Microbiol. Biotechnol.* 101, 5391–5403. doi: 10.1007/s00253-017-8282-9

Su, C., Gu, W., Zhe, W., Zhang, K. Q., Duan, Y., and Yang, J. (2011). Diversity and phylogeny of bacteria on Zimbabwe tobacco leaves estimated by 16S rRNA sequence analysis. *Appl. Microbiol. Biotechnol.* 92, 1033–1044. doi: 10.1007/s00253-011-3367-3

Tyx, R. E., Stanfill, S. B., Keong, L. M., Rivera, A. J., Satten, G. A., and Watson, C. H. (2016). Characterization of bacterial communities in selected smokeless tobacco products using 16S rDNA analysis. *PLoS One* 11:e0146939. doi: 10.1371/journal.pone.0146939

Van Gemert, L. J. (2011). *Odour thresholds compilations of odour threshold values in air, water and other media. 2nd Edn*. The Netherlands: Published by Oliemans Punter and Partners BV Zeist.

Victor, S., Travis, W., Renee, A., Alicia, M., and Marshall, L. (2019). Inhibition of Aflatoxin Formation in Aspergillus Species by Peanut (Arachis hypogaea) Seed Stilbenoids in the Course of Peanut–Fungus Interaction. *J. Agric. Food Chem.* 67, 6212–6221. doi: 10.1021/acs.jafc.9b01969

Villar, E., Farrant, G. K., Follows, M., Garczarek, L., Speich, S., Audic, S., et al. (2015). Ocean plankton. Environmental characteristics of Agulhas rings affect interocean plankton transport. *Science* 348:1261447. doi: 10.1126/science.1261447

Vu, A. T., Hassink, M. D., Taylor, K. M., McGuigan, M., Blasiole, A., Valentin-Blasini, L., et al. (2021). Volatile organic compounds in mainstream smoke of sixty domestic little cigar products. *Chem. Res. Toxicol.* 34, 704–712. doi: 10.1021/acs.chemrestox.0c00215

Wang, D., Liu, C. S., Xiang, H., Wang, J., Zhang, R. N., Tong, Y., et al. (2020). Overview of main cigar production areas and varietyresources at domestic and overseas. *Chin. Tobacco Sci.* 41, 93–98. doi: 10.13496/j.issn.1007-5119.2020.03.016

Yan, X. F., Wang, X., Kong, J. S., Lei, J. S., Qin, Y. Q., Anna, L. A., et al. (2021a). Analysis of national drying tobacco production and market changes in the past ten years. *China Tobacco Sci.* 42, 98–104. doi: 10.13496/j.issn.1007-5119.2021.02.015

Yan, X. F., Wang, Y. H., Lei, J. S., Zhou, J. L., Pan, Y., Hu, X., et al. (2021b). Exploration of domestic cigar classification and its practical application analysis. *Chin. Tob. Sci.* 27, 100–109. doi: 10.16472/j.chinatobacco.2021.T0029

Ye, C. W., Li, L., He, C., Li, D., Chen, L. -F., Fan, L., et al. (2021). Analysis of microbial community structure and diversity in cigar tobacco based on high-throughput sequencing. *Tobacco Sci. Technol.* 54, 1–9. doi: 10.16135/j.issn1002-0861.2020.0610

Yin, P., Kong, Y., Liu, P., Wang, J. J., Zhu, Y., Wang, G. M., et al. (2022). A critical review of key odorants in green tea: identification and biochemical formation pathway. *Trends Food Sci. Technol.* 129, 221–232. doi: 10.1016/j.tifs.2022.09.013

Zeller, G., Tap, J., Voigt, A. Y., Sunagawa, S., Kultima, J. R., Costea, P. I., et al. (2015). Potential of fecal microbiota for early-stage detection of colorectalcancer. *Mol. Syst. Biol.* 10:766. doi: 10.15252/msb.20145645

Zhang, Y., Liang, J., Li, L., Wang, Y., Zhang, X., and Li, X. (2018). Biodegradation of methyl benzoate by *Pseudomonas mendocina* NSYSU. *Int. J. Environ. Res. Public Health* 15:1915.

Zhang, R., Su, Q., Yang, C., and Chen, F. (2020). Effect of stacking fermentation time on quality of Wuzhishan cigar wrapper tobacco leaves. *Shandong Agric. Sci.* 52, 57–61. doi: 10.14083/j.issn.1001-4942.2020.04.010

Zhang, W.-H., Sun, R.-B., Xu, L., Liang, J.-N., and Zhou, J. (2019). Assessment of bacterial communities in cu-contaminated soil immobilized by a one-time application of micro−/nano-hydroxyapatite and phytoremediation for 3 years. *Chemosphere* 223, 240–249. doi: 10.1016/j.chemosphere.2019.02.049

Zhang, Y., Wang, X., Li, L., Li, W., Zhang, F., Du, T., et al. (2013). Simultaneous determination of 23 flavor additives in tobacco products using gas chromatography–triple quadrupole mass spectrometry. *J. Chromatogr. A* 1306, 72–79. doi: 10.1016/j.chroma.2013.07.059

Zhao, M., Wang, B., Li, F., Qiu, L., Li, F., Wang, S., et al. (2007). Analysis of bacterial communities on aging flue-cured tobacco leaves by 16S rDNA PCRDGGE technology. *Appl. Microbiol. Biotechnol.* 73, 1435–1440. doi: 10.1007/s00253-006-0625-x

Zheng, T., Zhang, Q., Wu, Q., Li, D., Wu, X., Li, P., et al. (2022). Effects of inoculation with Acinetobacter on fermentation of cigar tobacco leaves. *Front. Microbiol.* 13:911791. doi: 10.3389/fmicb.2022.911791

Zhong, W., Zhu, C., Shu, M., Sun, K., Zhao, L., Wang, C., et al. (2010). Degradation of nicotine in tobacco waste extract by newly isolated *Pseudomonas* sp. ZUTSKD. *Bioresour. Technol.* 101, 6935–6941. doi: 10.1016/j.biortech.2010.03.142

Zhou, J., Yu, L., Zhang, J., Zhang, X., Xue, Y., Liu, J., et al. (2020). Characterization of the core microbiome in tobacco leaves during aging. *Microbiol. Open* 9:e984. doi: 10.1002/mbo3.984

frontiers | Frontiers in Microbiology

TYPE Review
PUBLISHED 23 November 2023
DOI 10.3389/fmicb.2023.1250151

OPEN ACCESS

EDITED BY
Carlo Giuseppe Rizzello,
Sapienza University of Rome, Italy

REVIEWED BY
Roberto Pérez-Torrado,
Spanish National Research Council (CSIC), Spain
Jingwen Zhou,
Jiangnan University, China

*CORRESPONDENCE
Tianyou Yang
✉ yangtianyou2004@163.com

RECEIVED 29 June 2023
ACCEPTED 30 October 2023
PUBLISHED 23 November 2023

CITATION
Li L, Pan Y, Zhang S, Yang T, Li Z, Wang B, Sun H, Zhang M and Li X (2023) Quorum sensing: cell-to-cell communication in *Saccharomyces cerevisiae*. *Front. Microbiol.* 14:1250151. doi: 10.3389/fmicb.2023.1250151

Quorum sensing: cell-to-cell communication in *Saccharomyces cerevisiae*

Linbo Li[1], Yuru Pan[1], Shishuang Zhang[1], Tianyou Yang[1]*, Zhigang Li[1], Baoshi Wang[1], Haiyan Sun[2], Mingxia Zhang[1] and Xu Li[1]

[1]School of Life Sciences and Technology, Henan Institute of Science and Technology, Xinxiang, Henan, China, [2]Hainan Key Laboratory of Tropical Microbe Resources, Institute of Tropical Bioscience and Biotechnology, Chinese Academy of Tropical Agricultural Sciences, Haikou, Hainan, China

Quorum sensing (QS) is one of the most well-studied cell-to-cell communication mechanisms in microorganisms. This intercellular communication process in *Saccharomyces cerevisiae* began to attract more and more attention for researchers since 2006, and phenylethanol, tryptophol, and tyrosol have been proven to be the main quorum sensing molecules (QSMs) of *S. cerevisiae*. In this paper, the research history and hotspots of QS in *S. cerevisiae* are reviewed, in particular, the QS system of *S. cerevisiae* is introduced from the aspects of regulation mechanism of QSMs synthesis, influencing factors of QSMs production, and response mechanism of QSMs. Finally, the employment of QS in adaptation to stress, fermentation products increasing, and food preservation in *S. cerevisiae* was reviewed. This review will be useful for investigating the microbial interactions of *S. cerevisiae*, will be helpful for the fermentation process in which yeast participates, and will provide an important reference for future research on *S. cerevisiae* QS.

KEYWORDS

quorum sensing, quorum sensing molecules, quorum sensing system, response mechanism, *Saccharomyces cerevisiae*

1 Introduction

The cell-to-cell interactions that microorganisms use to communicate and coordinate their social behavior are crucial when they live in a community. Quorum sensing (QS) is a cell-to-cell signaling mechanism observed in microbe populations that is density-dependent (Efremenko et al., 2023). As the number of microbial cells reaches a critical level, it sends signals to neighboring microorganisms through signaling molecules called quorum sensing molecules (QSMs) that alter their behavior by regulating the expression of certain genes (Padder et al., 2018). The QSMs in microbial cells are related with the regulation of secondary metabolite production, symbiosis, bioluminescence, synthesis of antibiotics, regulation of nitrogen-fixing genes, pathogenesis, morphogenesis, competence, biofilm formation, etc (Chen et al., 2002; An et al., 2014). Historically, *Saccharomyces cerevisiae* has been used in food production and food processing for a long time, and it is generally used as a potential microbial cell factory for producing a variety of chemicals due to it being a very important type of strain. Research on QS of *S. cerevisiae* has been paid more and more attention since 2006, especially after the QSMs in *S. cerevisiae*, phenylethanol (Phe-OH) and tryptophol

(Try-OH), and tyrosol (Tyr-OH) were identified (Chen and Fink, 2006; Kebaara et al., 2008; Albuquerque and Casadevall, 2012).

In this review, we present research history, and hotspots of QS in *S. cerevisiae*, focusing particularly on the underlying mechanism of the QS system for *S. cerevisiae*. In addition, we also introduce the application of *S. cerevisiae* QS and QSMs in the food fermentation process. This review offers insights into density-dependent cell-to-cell communication of *S. cerevisiae*, which will be helpful for controlling the fermentation process in which *S. cerevisiae* is involved, such as beer brewing, wine making, and alcoholic fermentation.

2 Milestones and hotspots of QS research

2.1 Milestones of QS research

Quorum sensing (QS) is a process that links gene expression to the cell density of microbial populations (Albuquerque and Casadevall, 2012; Borea et al., 2018). During growth and reproduction, microbial populations secrete and release some specific signaling molecules due to the increase in cell density, and the concentration of their secreted signaling molecules can reach a threshold when the cell density reaches a certain level, and the signaling molecules then strongly induce synchronized gene expression by binding to their homologous receptor proteins, thus initiating or shutting down specific population biological behaviors (Turan et al., 2017; Franco et al., 2021; Tian et al., 2021). QS occurs widely in many different bacteria, as well as some fungi and yeast (Jagtap et al., 2020). QS was first identified and studied in bacteria, subsequently, fungal QS has been reported, and since 2006, QS in *S. cerevisiae* has attracted increasing attention.

In 1968, the behavior now identified as QS was discovered in the bioluminescent gram-negative bacterium *Photobacterium fischeri*, which exhibited bioluminescence upon reaching a high population density (Kempner and Hanson, 1968). In 1969, Lingappa et al. (1969) first reported the regulation of fungal QS, that is, filamentous growth of the human fungal pathogen *Candida albicans* depending on cell density. It was not until 1994 that Fuqua et al. (1994) named this density-dependent self-regulation phenomenon QS and defined the minimum behavioral unit needed to elicit certain bacterial behaviors at high cell densities as a "quorum" of bacteria. Since Chen and Fink (2006) first identified Phe-OH and Try-OH as active QSMs that induce filamentous growth in *S. cerevisiae* in 2006, QS in *S. cerevisiae* has attracted great attention. Subsequently, Smukalla et al. (2008) first proposed in 2008 that the flocculation of *S. cerevisiae* is regulated by QS. In 2013, Zupan et al. (2013) established an effective approach to study QS in yeast fermentation, which contributed to the separation, detection, and quantification of the potential QSMs Phe-OH, Try-OH, and Tyr-OH. Their work was followed in 2015 by Avbelj et al. (2015), which monitored the kinetics of QSM production and ARO genes expression in *S. cerevisiae* during wine fermentation, and initially confirmed correlations between peak production rates of the monitored QSMs Phe-OH, Try-OH, and Tyr-OH and peak expression of the genes responsible for their synthesis, i.e., *ARO8*, *ARO9*, and *ARO10*. Lenhart et al. (2019) studied the variation in the filamentous growth of an environmental strain of *S. cerevisiae* and its response to QSMs in 2019, and their research showed that the filamentous growth phenotype induced by QSMs was species-specific and only a few strains showed a response. In 2021, Huang and Reardon (2021a) demonstrated for the first time that adding yeast QSMs to reduce cell growth in *S. cerevisiae* could increase ethanol yield. In the same year, data from Najmi and Schneider (2021) suggested that yeast may use potential QS mechanisms to regulate ribosome biogenesis, particularly rRNA synthesis. Unlike other studies of morphological switching, this is the first QS mechanism to target a central metabolic process in yeast, providing a research basis for its potential therapeutic value. In 2022, Winters et al. (2022) proposed that Phe-OH induced filamentous growth could not be considered a QS mechanism because it did not meet the previously defined "physiological concentration" requirement. Still, Britton et al. (2023) challenged his view in the latest study. The study points out that the physiological concentrations reported by Winters et al. (2019) do not reflect the natural occurrence observed in a diffusion-limited fermentation environment using industrially relevant strains. Tian et al. (2023) studied the effect of the addition of QSMs on the fermentation of *S. cerevisiae*, and showed that the exogenous addition of Phe-OH promoted the accumulation of ethanol, which was similar to the results of Huang and Reardon (2021a) and provided basic data for using QSMs more than antibiotics in the prevention of contamination during the industrialized bioethanol production. QS has been observed in many microbial species, regulating the many diverse processes, including secretion of virulence factors, bioluminescence, cell adhesion and elongation, population density control, motility, biofilm formation, cell morphology and dimorphism, sporulation and antibiotic production (Miller and Bassler, 2001; Albuquerque and Casadevall, 2012; Wongsuk et al., 2016; Schuster et al., 2017; Padder et al., 2018; Gomez-Gil et al., 2019).

2.2 Hotspots of QS research

The importance of studying QS has received great attention, and since 1994, a good number of research publications on QS have been published. We searched the QS-related literature in the Web of Science (WOS) database and obtained 8,823 research articles, and used CiteSpace software (6.3. R3) to analyze their bibliometrics and visualization (Chen and Song, 2019). By keyword co-occurrence mapping, it was found that the main QS-related research topic has been quorum sensing, biofilm, quorum quenching, *Staphylococcus aureus*, *Pseudomonas aeruginosa*, farnesol, cystic fibrosis, cooperation, and multi-omics (**Figure 1A**). Bibliometric analysis allowed us to understand the global context of QS (Ashraf et al., 2021). The effect of the QS system on biofilm formation and regulation has been found, and research on quorum quenching is being undertaken and is a hotspot in related fields. At the same time, QS and disease prevention have always been the focus of researchers, and pathogenic bacteria, such as *S. aureus* and *P. aeruginosa*, are important biomaterials for QS research. Farnesol is one of the QSMs that is given much attention. With the development of multi-omics technology in recent years, an increasing number of omics technologies have been applied to QS research.

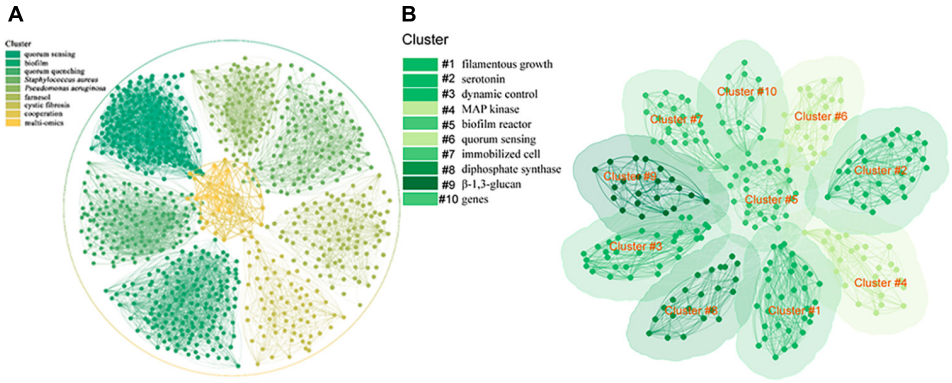

FIGURE 1
(A) Hotspots of QS research in microbiology **(B)** hotspots of QS research in *S. cerevisiae*.

To gain a clear view of QS in *S. cerevisiae*, we also used the search terms "*S. cerevisiae*" and "QS" to search the articles in the WOS database, retrieved 97 research articles, and analyzed their bibliometrics and performed visualization by CiteSpace software (Chen and Song, 2019). The keyword co-occurrence mapping showed that the main QS-related research topics for *S. cerevisiae* were filamentous growth, serotonin, dynamic control, MAP kinase, biofilm reactor, quorum sensing, immobilized cell, diphosphate synthase, β-1,3-glucan, and genes (**Figure 1B**). Filamentous growth has been shown to be a response to QS mechanisms in fungi through morphological transitions between single cells and pseudohyphae (Britton et al., 2023). Serotonin has been shown to be a compound produced during the metabolism of aromatic amino acids in *S. cerevisiae* and has an effect on yeast growth and cell morphology (Beatriz et al., 2018; Gonzalez, 2021). Dynamic control can be implemented either through a pathway dependent circuit or a pathway independent circuits (Yang et al., 2021; Xu et al., 2023). QS provides a pathway independent approach to autonomous dynamic control for the synthetic biology of microorganisms, where once critical signal concentrations are reached, population-wide cellular responses are initiated to influence gene expression to achieve simultaneous optimization of systems involving QS communication, cell growth competition, and cooperative production. This is more environmentally friendly and operable than chemical synthesis in industry (Dinh et al., 2020; Ge et al., 2020). The highly conserved mitogen-activated protein kinase (MAPK) signaling pathway is critical for eukaryotic cells to make appropriate adaptive responses to environmental changes (Gonzalez, 2021). Indeed, one of the best-known model systems for this signaling pathway is the response of haploid *S. cerevisiae* cells to mating pheromones, where QSMs stimulate yeast cell filamentous growth primarily via the MAPK pathway (Gomez-Gil et al., 2019; Seibel et al., 2021). Biofilm formation is one of the main regulatory mechanisms of QS. Phe-OH has a positive effect on biofilm formation of *S. cerevisiae* (Zhang et al., 2021b). As a barrier, biofilm can provide a stable internal environment for yeast cells to cope with the adverse environment such as ethanol stress and nutrient insufficiency (Tian et al., 2023). In the production of fuel ethanol, the conversion rate of repeated batch fermentation of *S. cerevisiae* in biofilm reactor is higher than that of free fermentation. In addition to a high yield of ethanol, a short fermentation cycle and excellent tolerance to ethanol were observed during this fermentation process (Yang et al., 2019; Zhang et al., 2021b). Immobilized cell technology is a new adsorption method developed based on microbial QS (Chen et al., 2020). After the cells are adsorbed on the carrier, a large number of cells grow, forming a dense bacterial community, and then showing QS (Yang et al., 2018). Utilizing immobilized cell technology can significantly improve the conversion of biomass, contributing to novel strategies to achieve the Sustainable Development Goals (Yang et al., 2019; Huang and Reardon, 2021b). Farnesol diphosphate synthetase is an important protein in the process of QSM farnesol synthesis. Using population density-regulated protein degradation system to dynamically regulate the expression level of related genes is a promising method for metabolic pathway control (Yang et al., 2021). β-1,3-glucan is the main component of fungal cell wall and is mainly responsible for regulating cell morphology endowing osmotic stability, and preventing stress in yeast (Mould and Hogan, 2021; Seibel et al., 2021). When QSMs accumulate to a certain threshold, they trigger synchronous gene expression by binding to their homologous receptor proteins, thus inducing QS (Britton et al., 2023; Efremenko et al., 2023). These data, when analyzed, showed that the available knowledge on the subject is still limited, and very little attention has been given to QS in *S. cerevisiae* and the mechanism of action of its QSMs, which has hindered the exploration of *S. cerevisiae* QS mechanism and the development of promising applications. Therefore, the study of QS in *S. cerevisiae* and the application of its QSMs in controlled fermentation have been the focus of attention in recent years.

3 QS system of *S. cerevisiae*

3.1 Regulation mechanism of QSMs synthesis in *S. cerevisiae*

In *S. cerevisiae*, the QSMs Phe-OH, Try-OH, and Tyr-OH are synthesized from the corresponding amino acids phenylalanine (Phe), tryptophan (Try) and tyrosine (Tyr) by transamination, decarboxylation and reduction via the Ehrlich pathway in a low-nitrogen environment (Tan and Prather, 2017; **Figure 2**). When

only aromatic amino acids are present as nitrogen sources, *GAP1* expression is induced, and the general amino acid permease Gap1p restores transport activity. In addition, the amino acid osmotic factor Ssy1p is a sensor via which cells detect extracellular aromatic amino acids as signals (Chen et al., 2016). Taking Phe as an example, Ssy1p first receives the Phe signal in a low nitrogen environment, which induces the expression of *GAP1* and the restoration of Gap1p activity. Gap1p transports Phe into the cell and participates in metabolic activity (Iraqui et al., 1999; Chen et al., 2017). In the Ehrlich pathway, Phe-OH is transaminated from Phe to the α-keto acid phenylpyruvate (PPA), which is decarboxylated to the higher aldehyde phenylacetaldehyde (PAA), which is then reduced to the higher alcohol Phe-OH by alcohol dehydrogenase (Etschmann et al., 2002). Via a similar mechanism, Try is transaminated to indole-3-pyruvate (IPA), followed by carboxylation to indole-3-acetaldehyde (IAA-ld), and then reduced to Try-OH (Chen and Fink, 2006; Avbelj et al., 2015). Tyr is transaminated to 4-hydroxyphenylpyruvate (4-HPPA), decarboxylated to 4-hydroxyphenylacetaldehyde (4-HPAA), and then reduced to Tyr-OH (Mas et al., 2014).

The transamination step in the Ehrlich pathway is catalyzed by the aromatic amino acid aminotransferase. There are two isoenzymes in *S. cerevisiae*, namely, aromatic amino acid aminotransferases I and II, both of which belong to the first family of aminotransferases and are encoded by the *ARO8* and *ARO9* genes, respectively, and have broad substrate specificity in the Ehrlich pathway. There are four known enzymes in *S. cerevisiae* that can catalyze the production of α-keto acids to higher aldehydes, which are encoded by *ARO10*, *PDC1*, *PDC5*, and *PDC6* (Brion et al., 2014; Choo et al., 2018). These enzymes participate in complex interactions with each other for processes such as activation, inhibition, and coordination. Among them, the PPA decarboxylase encoded by *ARO10* is the main enzyme involved in decarboxylation, and its broad substrate specificity has been confirmed by various genetic methods (Dickinson et al., 2003; Chen et al., 2017). The last step of the Ehrlich pathway for conversion to aromatic alcohols can be catalyzed by various alcohol dehydrogenases (Hazelwood et al., 2008). Six dehydrogenase genes are involved in the catalytic process in *S. cerevisiae*, including the five alcohol dehydrogenase genes *ADH1*, *ADH2*, *ADH3*, *ADH4*, and *ADH5* and the formaldehyde dehydrogenase gene *SFA1*. Any of these genes can individually catalyze the final step of the Ehrlich pathway, the dehydrogenation of aldehydes to form higher alcohols (Hazelwood et al., 2008).

As a crucial pathway to synthesize aromatic alcohols, regulation of the Ehrlich pathway is very important, however, the regulatory mechanism is not clear. With the development of bioinformatics and the study of the yeast response to aromatic alcohols, a few regulators that might be related to the Ehrlich pathway have been predicted. For example, Chen and Fink (2006) demonstrated that the transcription factor Aro80p controls the expression of Ehrlich pathway genes in response to aromatic amino acids (**Figure 2**). Aro80p, a member of the Zn2Cys6 protein family, was identified as a transcriptional activator for the induction of transaminase and decarboxylase genes by aromatic amino acids, which can activate the expression of the ARO9 and ARO10 genes by binding to ARO9 and ARO10 promoter binding sites (Iraqui et al., 1999; Lee and Hahn, 2013; Chen et al., 2017). Subsequently, Wuster and Babu (2010) predicted that Cat8p, Mig1p, Sip4p, Rgm1p, and Msn2p might be key transcriptional regulators controlling the differential expression of the genes affected by aromatic alcohols in their study of transcriptional control of the QS response in yeast. Cat8p is a zinc cluster protein as well as a regulator that represses the expression of the ADH2 gene in *S. cerevisiae* (Wang et al., 2017). Similarly, Mig1p is a transcription factor with two Cys2His2 zinc finger motifs, and it was reported that Mig1p regulates CAT8 and depends on the release of Mig1p from the promoter of CAT8 (Schüller, 2003). Furthermore, through multiple transcriptional network analysis methods, Wuster and Babu (2010) proposed that Cat8p and Mig1p participate in QS and might be important for aromatic alcohol-mediated communication. This was confirmed by Wang et al. (2017), who reported that a CAT8 overexpression strain and a MIG1 deletion strain could promote the expression of ARO9 and ARO10, and both could increase the production of Phe-OH. How CAT8 and MIG1 induce gene expression and whether they affect the performance of yeast have not yet been elucidated.

3.2 Factors influencing the production of QSMs in *S. cerevisiae*

The production of QSMs in *S. cerevisiae* depends on environmental factors, including cell density (Avbelj et al., 2015, 2016), nitrogen content (Chen and Fink, 2006), ethanol (Avbelj et al., 2015), and aerobic/anaerobic growth conditions (Avbelj et al., 2016; Jagtap et al., 2020; Franco et al., 2021). These factors contribute to the production of QSMs, which trigger phenotypic changes to promote morphological adaptations to new environmental conditions.

In *S. cerevisiae*, cell density regulates QSMs production. The production of QSMs per yeast cell is greater in yeast cells at high population density than in yeast cells at low population density (Zupan et al., 2013). When cells reach their specific quorum, the expression of *ARO9* and *ARO10* genes is upregulated, which stimulates the production of aromatic alcohols (Chen and Fink, 2006; Avbelj et al., 2015; **Figure 2**). Try-OH activates the transcription factor Aro80p and the expression of transaminase and decarboxylase genes, thus resulting in a positive feedback loop (Wuster and Babu, 2010; Jagtap et al., 2020). Nitrogen content in the medium affects QSMs production (Cullen and Sprague, 2001, 2012; Chen and Fink, 2006), as high concentrations of ammonium inhibit the expression of transaminases, decarboxylases, and dehydrogenases required for the synthesis of aromatic alcohols. It was reported that aromatic alcohol production peaked when the ammonium concentration was less than or equal to 50 μM and was significantly reduced at concentrations greater than 500 μM. The product ethanol during *S. cerevisiae* fermentation was also demonstrated to negatively influence the overall rate and onset time of aromatic alcohol synthesis and inhibit cell growth (Avbelj et al., 2015). However, it is unclear whether this reduction is related to the inhibition of aromatic alcohol synthesis or whether the cell density is not reaching the quorum due to ethanol inhibition. The study showed that when 2% ethanol was added to the medium, the cell growth of *S. cerevisiae* did not change, and the production kinetics of Try-OH and Tyr-OH were weakly inhibited compared with the control without ethanol. With the addition of 6% ethanol, there was a significant delay in peak production of all three

10.3389/fmicb.2023.1250151

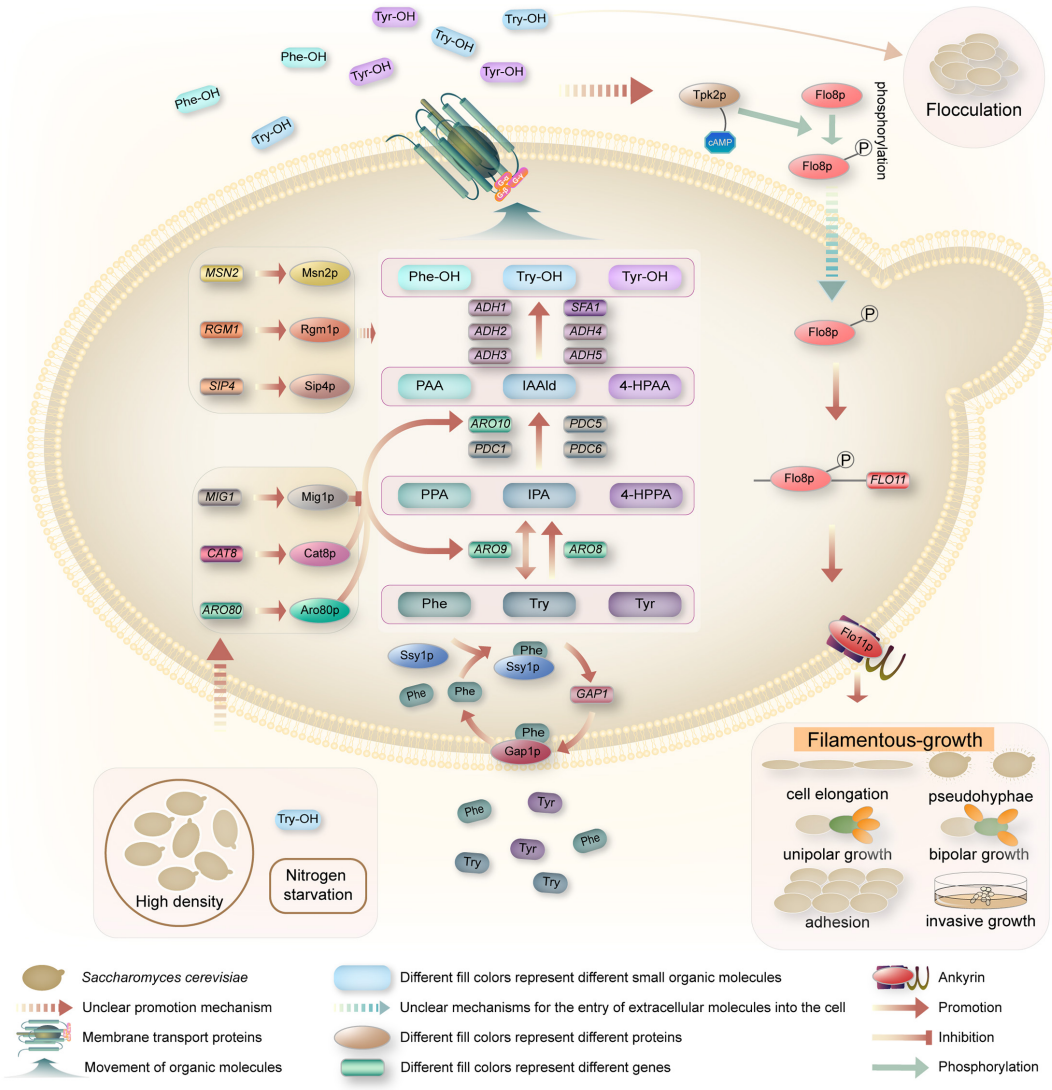

FIGURE 2
Schematic illustrations of quorum-sensing system in *S. cerevisiae*. When yeast cells reached quorum, the expression of *GAP1* and the recovery of Gap1p activity were induced by the amino acid osmotic factor Ssy1p, and the aromatic amino acids were transported into the cells. Phe, Try, and Tyr were transaminated to PPA, IPA, and 4-HPPA under the catalysis of aromatic amino acid transaminase encoded by *ARO8* and *ARO9* genes, respectively. These α-keto acids are then decarboxylated by *ARO10*, *PDC1*, *PDC5*, and *PDC6* encoded decarboxylase to produce PAA, IAA-ld, and 4-HPAA. These higher aldehydes are then reduced to Phe-OH, Try-OH, and Tyr-OH under dehydrogenase encoded by the dehydrogenase genes *ADH1*, *ADH2*, *ADH3*, *ADH4*, *ADH5*, and *SFA1*. Aromatic alcohols are transported outside the cell as QSMs by transporters, accumulating to a certain threshold and triggering QS phenotypes, i.e., flocculation or filamentous growth. Phe-OH and Try-OH affect the up-regulation of *FLO11* via the cAMP-dependent PKA subunit Tpk2p and the transcription factor Flo8p. Flo11p, the product of *FLO11*, is necessary for filamentous growth and is involved in cell elongation, pseudomycelium growth, unipolar growth, bipolar growth, cell adhesion, and invasive growth.

aromatic alcohols, most likely due to weak inhibition of cell growth. When 8% ethanol was added, the inhibitory effect on cell growth was enhanced, resulting in complete inhibition of Try-OH production, while the expression of the other two aromatic alcohols was delayed and only weakly expressed, possibly because the cell concentration did not exceed a specific threshold for initiating Try-OH production. When 12% ethanol was added, no cell growth was observed and no aromatic alcohols were produced. The report also showed that in all cases where ethanol was added, despite differences in cell growth curves, when the cell concentration reached $2 \times 10^7 \sim 3 \times 10^7$ cells/mL, $3 \times 10^7 \sim 4 \times 10^7$ cells/mL, and $2 \times 10^7 \sim 4 \times 10^7$ cells/mL, the production of Phe-OH, Try-OH, and Tyr-OH still began. These concentrations appear to represent the quorum for the synthesis of each of the three aromatic alcohols under the conditions of fermentation by this yeast (Avbelj et al., 2015). Aerobic/anaerobic conditions affect the production of aromatic alcohols, and alcohol dehydrogenase genes are upregulated under anaerobic conditions, which is beneficial for the production of aromatic alcohols by *S. cerevisiae*. Studies have shown that *S. cerevisiae* converts Phe to a mixture of 90% Phe-OH and 10% phenylacetate under aerobic conditions, while anaerobic conditions result in the almost complete conversion of Phe to Phe-OH (Vuralhan et al., 2003). Meanwhile, Avbelj et al. (2016) assert that *S. cerevisiae* produces higher concentrations of

aromatic alcohol when grows in anaerobic conditions than in aerobic conditions.

3.3 Response mechanism of QSMs in *S. cerevisiae*

To date, many studies have investigated the response mechanism of Phe-OH and Try-OH, while the response mechanism of Tyr-OH has rarely been reported. The sensing of Phe-OH and Try-OH relies on the cyclic adenosine monophosphate (cAMP)-dependent protein kinase A (PKA) subunit Tpk2 (**Figure 2**). It has been reported that the levels of cAMP are critical determinants of cellular filamentous growth (Mosch and Fink, 1997), regulate the activity of a family of protein kinases, referred to as PKA, and Tpk2, the catalytic subunit of PKA, promote filamentous growth (Pan and Heitman, 1999, 2002; Cullen and Sprague, 2012). Phosphorylation of Flo8p by Tpk2 leads to Flo8p activation (Pan and Heitman, 1999; Guo et al., 2000; Reynolds and Fink, 2001; Chen and Fink, 2006; Cullen and Sprague, 2012), and activated Flo8p, as a transcriptional activator, binds to regions of the *FLO11* promoter to promote gene expression (Pan and Heitman, 2002). Flo11p, a product of *FLO11*, is a glycosylated phosphatidylinositol (GPI)-anchored cell surface flocculating protein that is required for filamentous growth and is involved in pseudohyphal growth, invasive growth, unipolar growth, bipolar growth, cell elongation, and cellular adhesion (Smukalla et al., 2008; Avbelj et al., 2015; Winters et al., 2019).

Filamentous growth, which usually occurs under nutrient starvation, is thought to be a mechanism that allows cells to grow in their surroundings and forage for available nutrients (Jagtap et al., 2020) and is characterized by elongated cell morphology, unipolar budding, partial separation of mother and daughter cells, and substrate incursion (Gimeno et al., 1992). Depending on the cell type, filamentous growth in *S. cerevisiae* can be described as pseudohyphal or invasive growth. Filamentous growth in diploid cells has been described as pseudohyphal growth involving elongated cell morphology and alterations in budding patterns. A similar but separate response in haploid cells is known as haploid invasive growth, as these cells form filaments, which penetrate the agar (Cullen and Sprague, 2001, 2012). Preliminary studies by Chen and Fink (2006) have demonstrated that QSMs Phe-OH and Try-OH stimulated pseudohyphal growth under nitrogen-limited starvation conditions. Additionally, recent studies have investigated the effects of exogenous aromatic alcohols on the transformation of *S. cerevisiae* from the yeast cell form to a filamentous cell form. González et al. (2018) demonstrated that aromatic alcohols were able to affect invasive and pseudohyphal growth in a manner dependent on nutrient availability. However, Lenhart et al. (2019) demonstrated that the filamentous phenotypic response induced by Phe-OH and Try-OH in *S. cerevisiae* may be a strain-specific effect by using computational image analysis to quantify the production of pseudohyphae and assaying the diverse 100-genome collection of environmental isolates. Britton et al. (2023) then studied the native variation of yeast-to-filamentous phenotypic transition and its induction by Phe-OH in commercial brewing strains was investigated. The results showed that phenotypic switching was a general, highly variable response that occurred only in selected brewing strains. The results again confirmed that the filamentous phenotypic response induced by aromatic alcohol may be a strain specific effect. However, it is still necessary to accurately understand the internal molecular mechanisms and related metabolic pathways of QSMs in response to the differences in yeast filamentous growth phenotypes. As noted by Britton et al. (2023), it is possible that there are several reasons to explain the differences between commercially produced strains, such as that some strains may not be able to sense Phe-OH, or that some others may sense Phe-OH but not initiate the response, or that some strains may be unable to undergo filamentation. In addition, the author believes that it is necessary to study the effects of QS or QSMs on the taste, color, number of viable cells, ethanol production, physical and chemical properties, and nutrition and healthcare value of commercial brewing wine.

Flocculation is a social feature that depends on multiple cells cooperating simultaneously and a cooperative protection mechanism that protects cells from stressful environments, and the flocculation behavior of *S. cerevisiae* was shown to be related to Try-OH (Smukalla et al., 2008). Smukalla et al. (2008) found that adding the QSMs Try-OH could induce strong flocculation in the diploid strain *S. cerevisiae* EM93. In their study, the effects of Phe-OH, Try-OH, Tyr-OH, ethanol, butanol, and isoamyl alcohol on the flocculation behavior of EM93 were investigated, and it was found that this strain did not flocculate in nutrient-rich medium. This flocculation behavior is suggested by these authors to be a protective mechanism mediated by Try-OH, where mutual adhesion leads to the formation of flocs that prevent diffusion and thus provide physical protection for the innermost cells from harmful compounds in the external environment. Since flocculence requires a fairly large microbial population and Flo adhesin expression is only functional at higher population densities, it stands to reason that this particular adaptive feature, flocculation behavior in *S. cerevisiae*, occurs in cells exposed to Try-OH (Britton et al., 2020).

4 Biotechnological application of QS in *S. cerevisiae*

4.1 Adaptation to stress

Filamentous growth stimulated by *S. cerevisiae* QSMs is a foraging response that favors yeast survival under stressful conditions (Silva et al., 2007). Because both Flo8p and Mss11p are LisH domain-containing transcription factors and function as heterodimers to regulate *FLO11* gene expression (Su et al., 2009), improved the tolerance of yeast to butanol by increasing the expression of the filamentous growth response pathway transcription factor Mss11p. In addition, aromatic alcohols also stimulate other transcription factors, such as Mig1p and Cat8p, to regulate different stress responses so that high-density yeast fermentation based on QS could show strong tolerance and catalytic activity (Douglas et al., 2008). In addition, previous studies have shown that there is a relationship between QS and reactive oxygen species (ROS)-related metabolism in *S. cerevisiae*, where *ARO80* has been identified as the key gene regulating QS (Kang et al., 2021). This finding was confirmed by Kang et al. (2022),

who reported that deletion of the *ARO80* gene could decrease the oxidative tolerance of yeast cells and that adding exogenous QSMs contributed to increasing the oxidative tolerance of the mutant. Furthermore, the specific sensing of N-(3-oxododecanoyl)-L-homoserine lactone (C_{12}) from the opportunistic human pathogen *Pseudomonas aeruginosa* by *S. cerevisiae* activated its general stress response to reduce the damage caused by strong oxidative stress (Delago et al., 2021). Meanwhile, Ren et al. (2016) demonstrated that long-chain C_{12}-HSL, an N-acyl homoserine lactone (AHL) of bacterial QSMs, could increase the ethanol tolerance of *S. cerevisiae*.

Studies on ethanol tolerance by QS in *S. cerevisiae* have only been reported in recent years. A related investigation demonstrated that purified Tyr-OH (50 μM) exhibited protective effects against *S. cerevisiae* under 12% ethanol stress, and the fermentation capacity was significantly improved (Nath et al., 2021b). In addition, it has been reported that QS plays a certain role in the resistance to heavy metal stress. Nath et al. (2021a) conducted research on the effect of the QSMs Tyr-OH on heavy metal tolerance in *S. cerevisiae*. The tolerance to the heavy metals zinc (Zn^{2+}), manganese (Mn^{2+}), cobalt (Co^{2+}), and copper (Cu^{2+}) was determined in the presence or absence of Tyr-OH. They found that under the influence of Tyr-OH, the strain showed strong growth ability at the upper limit of heavy metal tolerance, was more adaptable to stressful environments, and had a protective effect. Compared with the use of physical and chemical means, it is more feasible and safe to use microbial QS system to face the stressed environment and enhance their own protection.

4.2 Increasing fermentation product formation

Phe-OH, Try-OH, and Tyr-OH, as QSMs, have been demonstrated to be synthesized and secreted by *S. cerevisiae* and have been used to improve fermentation products, including for enhancement of aroma in foods and drinks (Etschmann et al., 2002; Wang et al., 2011) and improvement of wine flavor and quality (Gonzalez-Marco et al., 2010). studied the antifungal activity mediated by Picha spp. QSMs Phe-OH and its effect on ethanol metabolism during the fermentation of sauce-flavor baijiu. Metabolome analysis and amplicon sequencing along with metatranscriptomic analysis demonstrated that Phe-OH can mediate antifungal mechanisms, including protein synthesis and DNA damage, and its role in food fermentation. The study can promote the niche establishment and growth of the functional yeast, the improvement of ethanol metabolism, and the enhancement of wine flavor (Zhang et al., 2021c). In addition, it has been also demonstrated that the QSM Try-OH has an effect on regulating ethanol fermentation in wine fermentation (José et al., 2018). At the same time, QSMs have also been shown to be associated with increased alcohol production from fermentation products. Some studies have provided evidence that the ethanol yield can be improved by adding yeast QSMs to reduce the cell growth of *S. cerevisiae* and observed that ethanol production can be up to 15% higher (Huang and Reardon, 2021a). Tian et al. (2023) not only determined the concentration of QSMs in *S. cerevisiae* but also investigated the effect of exogenous *S. cerevisiae* QSMs on the sole fermentation of *S. cerevisiae* and co-fermentation of *S. cerevisiae* with *Lactobacillus plantarum*. The results showed that the concentration of QSMs produced by *S. cerevisiae* increased with the increase in cell density, and only Phe-OH promoted the ethanol production of *S. cerevisiae*. The ethanol concentration of the sole fermentation of *S. cerevisiae* loaded with 120 mg/L Phe-OH reached 3.2 g/L in 9 h, which was 58.7% higher than that of the group without Phe-OH addition.

Luo et al. (2018) applied a novel adsorption method developed based on QS, biofilm immobilization, to rapidly enrich yeast, produce a large amount of biofilm, and achieve high levels of alcohol fermentation with an alcoholic strength of up to 15.3% (v/v). Huang and Reardon (2021b) immobilized *S. cerevisiae* in alginate and incorporated it into a two-column immobilized cell reactor system. In addition, the yeast QSM Phe-OH is added to increase ethanol production by restricting growth and diverting sugar to ethanol. Zhang et al. (2021a) used acetic acid as a signaling molecule to initiate a QS system to promote the production of 2,3-butanediol in *S. cerevisiae* W141. The results showed that the yield of 2,3-butanediol was proportional to the cell density, and when 1.5 g/L acetic acid was added during the fermentation process, the yield of 2,3-BD was the highest, reaching 3.01 ± 0.04 g/L.

Moreover, the QS system is used as a tool in metabolic engineering. Recently, the design, construction, and implementation of QS circuits for the programmed control of bacterial phenotypes and metabolic pathways have attracted much attention (Ge et al., 2020). Williams et al. (2015) constructed a gene switch that automatically triggered expression at high population density in *S. cerevisiae* and used this strategy to increase the production of para-hydroxybenzoic acid produced by the shikimate pathway. Yang et al. (2021) used a QS-mediated protein degradation system to increase α-farnesene production in *S. cerevisiae*. First, they integrated a plant hormone cytokinin system with the endogenous yeast Ypd1-Skn7 signal transduction pathway and designed QS-regulated protein degradation circuits for dynamic metabolic pathway control in *S. cerevisiae*. Then, based on this control method, they constructed an auxin-induced protein degradation system and applied this circuit to control the degradation of Erg9 to produce α-farnesene, and the titer of α-farnesene increased by 80%. In addition, the QS system of yeast has also been applied in the field of sewage treatment, and biofilm augmentation in yeast-based microbial fuel cells. These results demonstrate the feasibility of novel strategies to achieve sustainability goals in biomass conversions.

4.3 Food preservation

Phe-OH, Try-OH, and Tyr-OH can be used as antioxidants, antimicrobials, and disinfectants (Cueva et al., 2012). These aromatic alcohols have been used as biotechnological tools in the food industry, fragrances, and cosmetics due to their antimicrobial and oxidative protection properties (Gonzalez-Marco et al., 2010; Lu et al., 2016). The most common way to prevent spoilage in the food industry is the use of chemical preservatives. However, the use of chemicals not only is harmful to the environment and leads to unnecessary residues in food but also is bad for health. In this regard, Phe-OH produced by yeast can be advantageously applied in food as a natural preservative.

Liu et al. (2014) found that the yeast *K. apiculata* strain 34-9 acted as an antagonist with biological control activity against postharvest diseases of citrus fruit because the strain could produce Phe-OH, which could influence filamentous growth, adhesion, and biofilm formation and biological control efficiency. Likewise, Phe-OH produced by *Pichia anomala* was shown to inhibit spore germination, growth, toxin production, and gene expression in *Aspergillus flavus* (Hua et al., 2014; Chang et al., 2015). Huang et al. (2020) studied the antifungal effects of the QSMs Phe-OH against the food spoilage molds *Penicillium expansum* and *Penicillium nordicum*. The results showed that Phe-OH inhibited the conidial germination and growth of the two molds in a non-lethal, reversible, and concentration-dependent manner, but unlike other antifungal agents, phenethyl alcohol did not damage the conidial cell membrane. Compared with the chemical synthesis method, the biosynthesis method of Phe-OH, Try-OH, and Tyr-OH is more environmentally friendly and feasible to achieve green sustainable development.

5 Conclusion

In this review, we first introduced the definition of QS and selected the main research milestones for QS from 1968 to 2023, especially those for *S. cerevisiae* since 2006. This helped us recognize the research history and understand the important events in QS research. The research articles on the QS of *S. cerevisiae* in the last two decades are indexed in WOS and were visually analyzed based on CiteSpace software. The statistical results provide an important reference for future research. In this paper, the QS system of *S. cerevisiae* was discussed, with emphasis on the regulation mechanism of QSMs synthesis, the influencing factors of QSMs production, and the response mechanism of QSMs. The importance of understanding the mechanisms will help evaluate the cellular interactions of *S. cerevisiae* in terms of the effects on QS signal producers and receivers. Finally, the biotechnological application of QS in *S. cerevisiae* is introduced, mainly in the aspects of adaptation to stress, increasing the formation of fermentation products, and food preservation. If anything, reviewing the QS and QSMs in *S. cerevisiae* will be useful for investigating microbial interactions and controlling industrial fermentation processes such as brewing and food production.

At present, the research on QS of microorganisms including yeast is still in the initial stage, and there are still many problems to be solved. For example, in commercial brewing, it is necessary to discuss the role of QS of yeast in mixed fermentation and its influence on enhancing flavor substances or nutrients, so as to improve the ecological niche of brewing wine. In the field of biofuels, it is necessary to explore the influence of QS systems on microbial fermentation to produce fuel ethanol, fuel cells, etc., in order to improve the rate of energy self-sufficiency. In the field of biological control, the QS system is used to increase the effect of biological control, strengthen biological remediation, improve environmental protection, and realize the new strategy of sustainable development. In the field of medicine and health, the effects of QS systems as a new tool on food spoilage, fungal infection, clinical environment, and disease treatment were discussed. Putting all together, it will be of great significance to continue researching and developing the application of QS systems.

Author contributions

LL, YP, and SZ carried out the original literature screening under the supervision of ZL, TY, and MZ. YP drafted the manuscript with inputs from LL, SZ, and TY. All authors contributed to the article, edited, revised and approved the final version of the manuscript.

Funding

This research was supported by the Science and Technology Program of Henan Province (222102110122), the Open Project Program of Key Laboratory of Feed Biotechnology, the Ministry of Agriculture and Rural Affairs of the People's Republic of China (No. SUN01) Innovative Research Team (in Science and Technology) in University of Henan Province (22IRTSHN025), and China Agriculture Research System of Finance and Agriculture Ministry (CARS-11-HNSHY).

Conflict of interest

The authors declare that the research was conducted in the absence of any commercial or financial relationships that could be construed as a potential conflict of interest.

Publisher's note

All claims expressed in this article are solely those of the authors and do not necessarily represent those of their affiliated organizations, or those of the publisher, the editors and the reviewers. Any product that may be evaluated in this article, or claim that may be made by its manufacturer, is not guaranteed or endorsed by the publisher.

References

Albuquerque, P., and Casadevall, A. (2012). Quorum sensing in fungi–a review. *Med. Mycol.* 50, 337–345. doi: 10.3109/13693786.2011.652201

An, J. H., Goo, E., Kim, H., Seo, Y.-S., and Hwang, I. (2014). Bacterial quorum sensing and metabolic slowing in a cooperative population. *PNAS* 111, 14912–14917. doi: 10.1073/pnas.1412431111

Ashraf, S. A., Siddiqui, A. J., Elkhalifa, A. E. O., Khan, M. I., Patel, M., Alreshidi, M., et al. (2021). Innovations in nanoscience for the sustainable development of food and agriculture with implications on health and environment. *Sci. Total Environ.* 768:144990. doi: 10.1016/j.scitotenv.2021.144990

Avbelj, M., Zupan, J., Kranjc, L., and Raspor, P. (2015). Quorum-sensing kinetics in *Saccharomyces cerevisiae*: A symphony of aro genes and aromatic alcohols. *J. Agric. Food Chem.* 63, 8544–8550. doi: 10.1021/acs.jafc.5b03400

Avbelj, M., Zupan, J., and Raspor, P. (2016). Quorum-sensing in yeast and its potential in wine making. *Appl. Microbiol. Biotechnol.* 100, 7841–7852. doi: 10.1007/s00253-016-7758-3

Beatriz, G., Jennifer, V., María-Jesús, T., Albert, M., and Gemma, B. (2018). Aromatic amino acid-derived compounds induce morphological changes and modulate the cell growth of wine yeast species. *Front. Microbiol.* 9:670. doi: 10.3389/fmicb.2018.00670

Borea, L., Naddeo, V., Belgiorno, V., and Choo, K. H. (2018). Control of quorum sensing signals and emerging contaminants in electrochemical membrane bioreactors. *Bioresour. Technol.* 269, 89–95. doi: 10.1016/j.biortech.2018.08.041

Brion, C., Ambroset, C., Delobel, P., Sanchez, I., and Blondin, B. (2014). Deciphering regulatory variation of THI genes in alcoholic fermentation indicate an impact of Thi3p on *PDC1* expression. *BMC Genomics* 15:1085. doi: 10.1186/1471-2164-15-1085

Britton, S., Rogers, L., White, J., Neven, H., and Maskell, D. (2023). Disparity in pseudohyphal morphogenic switching response to the quorum sensing molecule 2-phenylethanol in commercial brewing strains of *Saccharomyces cerevisiae*. *FEMS Microbes* 4, 1–8. doi: 10.1093/femsmc/xtad002

Britton, S. J., Neven, H., and Maskell, D. L. (2020). Microbial small-talk: Does quorum sensing play a role in beer fermentation? *J. Am. Soc. Brew Chem.* 79, 231–239. doi: 10.1080/03610470.2020.1843928

Chang, P. K., Hua, S. S., Sarreal, S. B., and Li, R. W. (2015). Suppression of aflatoxin biosynthesis in *Aspergillus flavus* by 2-phenylethanol is associated with stimulated growth and decreased degradation of branched-chain amino acids. *Toxins* 7, 3887–3902. doi: 10.3390/toxins7103887

Chen, C., and Song, M. (2019). Visualizing a field of research: A methodology of systematic scientometric reviews. *PLoS One* 14:e0223994. doi: 10.1371/journal.pone.0223994

Chen, H., and Fink, G. R. (2006). Feedback control of morphogenesis in fungi by aromatic alcohols. *Genes Dev.* 20, 1150–1161. doi: 10.1101/gad.1411806

Chen, T., Zhu, J., Liu, D., Chen, Y., and Ying, H. (2020). Research progress in immobilized fermentation based on quorum sensing. *Chin. J. Bioprocess Eng.* 18, 170–176. doi: 10.3969/j.issn.1672-3678.2020.02.005

Chen, X., Schauder, S., Potier, N., Van Dorsselaer, A., Pelczer, I., Bassler, B. L., et al. (2002). Structural identification of a bacterial quorum-sensing signal containing boron. *Nature* 415, 545–549. doi: 10.1038/415545a

Chen, X., Wang, Z., Guo, X., Liu, S., and He, X. (2017). Regulation of general amino acid permeases Gap1p. GATA transcription factors Gln3p and Gat1p on 2-phenylethanol biosynthesis via Ehrlich pathway. *J. Biotechnol.* 242, 83–91. doi: 10.1016/j.jbiotec.2016.11.028

Chen, X., Wang, Z., and He, X. (2016). Advances in biosynthesis of 2-phenylethanol by yeasts. *Chin. J. Biotech.* 32, 1151–1163. doi: 10.13345/j.cjb.150539

Choo, J. H., Han, C., Lee, D. W., Sim, G. H., Moon, H. Y., Kim, J. Y., et al. (2018). Molecular and functional characterization of two pyruvate decarboxylase genes. PDC1 and PDC5, in the thermotolerant yeast *Kluyveromyces marxianus*. *Appl. Microbiol. Biotechnol.* 102, 3723–3737. doi: 10.1007/s00253-018-8862-3

Cueva, C., Mingo, S., Munoz-Gonzalez, I., Bustos, I., Requena, T., del Campo, R., et al. (2012). Antibacterial activity of wine phenolic compounds and oenological extracts against potential respiratory pathogens. *Lett. Appl. Microbiol.* 54, 557–563. doi: 10.1111/j.1472-765X.2012.03248.x

Cullen, P. J., and Sprague, G. (2001). Glucose depletion causes haploid invasive growth in yeast. *PNAS* 97, 13619–13624. doi: 10.1073/pnas.240345197

Cullen, P. J., and Sprague, G. F. Jr. (2012). The regulation of filamentous growth in yeast. *Genetics* 190, 23–49. doi: 10.1534/genetics.111.127456

Delago, A., Gregor, R., Dubinsky, L., Dandela, R., Hendler, A., Krief, P., et al. (2021). A bacterial quorum sensing molecule elicits a general stress response in *Saccharomyces cerevisiae*. *Front Microbiol.* 12:632658. doi: 10.3389/fmicb.2021.632658

Dickinson, J. R., Salgado, L. E., and Hewlins, M. J. (2003). The catabolism of amino acids to long chain and complex alcohols in *Saccharomyces cerevisiae*. *J Biol Chem* 278, 8028–8034. doi: 10.1074/jbc.M211914200

Dinh, C. V., Chen, X., and Prather, K. L. J. (2020). Development of a Quorum-Sensing Based Circuit for Control of Coculture Population Composition in a Naringenin Production System. *ACS Synthetic Biol.* 9, 590–597. doi: 10.1021/acssynbio.9b00451

Douglas, L. M., Li, L., Yang, Y., and Dranginis, A. M. (2008). Expression and characterization of the flocculin Flo11/Muc1, a *Saccharomyces cerevisiae* mannoprotein with homotypic properties of adhesion. *Eukary. Cell* 6, 2214–2221. doi: 10.1128/EC.00284-06

Efremenko, E., Senko, O., Stepanov, N., Aslanli, A., Maslova, O., and Lyagin, I. (2023). Quorum sensing as a trigger that improves characteristics of microbial biocatalysts. *Microorganisms* 11:1395. doi: 10.3390/microorganisms11061395

Etschmann, M. M., Bluemke, W., Sell, D., and Schrader, J. (2002). Biotechnological production of 2-phenylethanol. *Appl. Microbiol. Biotechnol.* 59, 1–8. doi: 10.1007/s00253-002-0992-x

Franco, A., Gacto, M., Gómez-Gil, E., Madrid, M., Vicente-Soler, J., Vázquez-Marín, B., et al. (2021). "Quorum sensing: A major regulator of fungal development," in *Developmental Biology in Prokaryotes and Lower Eukaryotes*, eds T. G. Villa and T. de Miguel Bouzas (Cham: Springer International Publishing).

Fuqua, W. C., Winans, S. C., and Greenberg, E. P. (1994). Quorum sensing in bacteria: the LuxR-LuxI family of cell density-responsive transcriptional regulators. *J. Bacteriol.* 176, 269–275. doi: 10.1128/jb.176.2.269-275.1994

Ge, C., Sheng, H., Chen, X., Shen, X., Sun, X., Yan, Y., et al. (2020). Quorum sensing system used as a tool in metabolic engineering. *Biotechnol. J.* 15, e1900360. doi: 10.1002/biot.201900360

Gimeno, C. J., Ljungdahl, P. O., Styles, C. A., and Fink, G. R. (1992). Unipolar cell divisions in the yeast *S. cerevisiae* lead to filamentous growth: Regulation by starvation and RAS. *Cell* 68, 1077–1090. doi: 10.1016/0092-8674(92)90079-R

Gomez-Gil, E., Franco, A., Madrid, M., Vazquez-Marin, B., Gacto, M., Fernandez-Breis, J., et al. (2019). Quorum sensing and stress-activated MAPK signaling repress yeast to hypha transition in the fission yeast *Schizosaccharomyces japonicus*. *PLoS Genet.* 15:e1008192. doi: 10.1371/journal.pgen.1008192

González, B., Vázquez, J., Morcillo-Parra, M. Á., Mas, A., Torija, M. J., and Beltran, G. (2018). The production of aromatic alcohols in non-Saccharomyces wine yeast is modulated by nutrient availability. *Food Microbiol.* 74, 64–74. doi: 10.1016/j.fm.2018.03.003

Gonzalez, R. (2021). Mechanisms involved in interspecific communication between wine yeasts. *Foods* 10:1734.

Gonzalez-Marco, A., Jimenez-Moreno, N., and Ancin-Azpilicueta, C. (2010). Influence of nutrients addition to nonlimited-in-nitrogen must on wine volatile composition. *J. Food Sci.* 75, S206–S211. doi: 10.1111/j.1750-3841.2010.01578.x

Guo, B., Styles, C. A., Feng, Q., and Fink, G. R. (2000). A *Saccharomyces* gene family involved in invasive growth, cell–cell adhesion, and mating. *PNAS* 97, 12158–12163. doi: 10.1073/pnas.220420397

Hazelwood, L. A., Daran, J. M., van Maris, A. J., Pronk, J. T., and Dickinson, J. R. (2008). The Ehrlich pathway for fusel alcohol production: a century of research on *Saccharomyces cerevisiae* metabolism. *Appl. Environ. Microbiol.* 74, 2259–2266. doi: 10.1128/AEM.02625-07

Hua, S. S., Beck, J. J., Sarreal, S. B., and Gee, W. (2014). The major volatile compound 2-phenylethanol from the biocontrol yeast, *Pichia anomala*, inhibits growth and expression of aflatoxin biosynthetic genes of *Aspergillus flavus*. *Mycotoxin Res.* 30, 71–78. doi: 10.1007/s12550-014-0189-z

Huang, C., Qian, Y., Viana, T., Siegumfeldt, H., Arneborg, N., Larsen, N., et al. (2020). The quorum-sensing molecule 2-phenylethanol impaired conidial germination, hyphal membrane integrity and growth of *Penicillium expansum* and *Penicillium nordicum*. *J. Appl. Microbiol.* 129, 278–286. doi: 10.1111/jam.14621

Huang, X. F., and Reardon, K. F. (2021a). Quorum-sensing molecules increase ethanol yield from *Saccharomyces cerevisiae*. *FEMS Yeast Res.* 21:8. doi: 10.1093/femsyr/foab056

Huang, X. F., and Reardon, K. F. (2021b). Strategies to achieve high productivity, high conversion, and high yield in yeast fermentation of algal biomass hydrolysate. *Eng. Life Sci.* 22, 119–131. doi: 10.1002/elsc.202100095

Iraqui, I., Vissers, S., Bernard, F., Craene, J., Boles, E., Urrestarazu, A., et al. (1999). Amino acid signaling in *Saccharomyces cerevisiae*: A permease-like sensor of external amino acids and f-box protein Grr1p are required for transcriptional induction of the *AGP1* gene, which encodes a broad-specificity amino acid permease. *Mol. Cell Biol.* 19, 989–1001. doi: 10.1128/MCB.19.2.989

Jagtap, S. S., Bedekar, A. A., and Rao, C. V. (2020). *Quorum sensing in yeast*. Washington, DC: American Chemical Society.

José, M., Valera, ángeles, M., Morcillo-Parra, Izabela, Zagórska, et al. (2018). Effects of melatonin and tryptophol addition on fermentations carried out by Saccharomyces cerevisiae and non-Saccharomyces yeast species under different nitrogen conditions. *Int J Food Microbiol.* 289, 174–181.

Kang, X., Gao, Z. H., Zheng, L. J., Zhang, X. R., and Li, H. (2021). Regulation of Lactobacillus plantarum on the reactive oxygen species related metabolisms of *Saccharomyces cerevisiae*. *Lwt-Food Sci. Technol.* 147:111492. doi: 10.1016/j.lwt.2021.111492

Kang, X., Zhang, J. X., Xu, Y. L., Zhang, X. R., Cui, F. X., and Li, H. (2022). Knocking-out *ARO80* promotes the intracellular ROS accumulation through weakening MAPK pathway of *Saccharomyces cerevisiae*. *Chem. Eng. Sci.* 252:117507. doi: 10.1016/j.ces.2022.117507

Kebaara, B. W., Langford, M. L., Navarathna, D. H. M. L. P., Dumitru, R., Nickerson, K. W., and Atkin, A. L. (2008). *Candida albicans* Tup1 Is Involved in Farnesol-Mediated Inhibition of Filamentous-Growth Induction. *Eukaryotic Cell* 7, 980–987. doi: 10.1128/EC.00357-07

Kempner, E. S., and Hanson, F. E. (1968). Aspects of light production by *Photobacterium fischeri*. *J. Bacteriol.* 95, 975–979. doi: 10.1128/jb.95.3.975-979.1968

Lee, K., and Hahn, J. S. (2013). Interplay of Aro80 and GATA activators in regulation of genes for catabolism of aromatic amino acids in Saccharomyces cerevisiae. *Mol. Microbiol.* 88, 1120–1134. doi: 10.1111/mmi.12246

Lenhart, B. A., Meeks, B., and Murphy, H. A. (2019). Variation in filamentous growth and response to quorum-sensing compounds in environmental isolates of *Saccharomyces cerevisiae*. *G3: Genes Genomes Genet.* 9, 1533–1544. doi: 10.1534/g3.119.400080

Lingappa, B. T., Prasad, M., Lingappa, Y., Hunt, D. F., and Biemann, K. (1969). Phenethyl alcohol and tryptophol: autoantibiotics produced by the fungus *Candida albicans*. *Science* 163, 192–194. doi: 10.1126/science.163.3863.192

Liu, P., Fang, J., Chen, K., Long, C.-A., and Cheng, Y. (2014). Phenylethanol promotes adhesion and biofilm formation of the antagonistic yeast *Kloeckera apiculata* for the control of blue mold on citrus. *FEMS Yeast Res.* 14, 536–546. doi: 10.1111/1567-1364.12139

Lu, X., Wang, Y., Zong, H., Ji, H., Zhuge, B., and Dong, Z. (2016). Bioconversion of L-phenylalanine to 2-phenylethanol by the novel stress-tolerant yeast *Candida glycerinogenes* WL2002-5. *Bioengineered* 7, 418–423. doi: 10.1080/21655979.2016.1171437

Luo, H., Liu, Q., Chen, Y., Sun, Z., Li, Y., and Xu, W. (2018). Production of fuel ethanol by immobilized yeast based on microbial cluster effect. *Chin. J. Bioprocess. Eng.* 16, 35–40. doi: 10.3969/j.issn.1672-3678.2018.03.005

Mas, A., Guillamon, J. M., Torija, M. J., Beltran, G., Cerezo, A. B., Troncoso, A. M., et al. (2014). Bioactive compounds derived from the yeast metabolism of aromatic amino acids during alcoholic fermentation. *Biomed. Res. Int.* 2014:898045. doi: 10.1155/2014/898045

Miller, M. B., and Bassler, B. L. (2001). Quorum sensing in bacteria. *Annu. Rev. Microbiol.* 55, 165–199. doi: 10.1146/annurev.micro.55.1.165

Mosch, H. U., and Fink, G. R. (1997). Dissection of filamentous growth by transposon mutagenesis in *Saccharomyces cerevisiae*. *Genetics* 145, 671–684. doi: 10.1093/genetics/145.3.671

Mould, D. L., and Hogan, D. A. (2021). Intraspecies heterogeneity in microbial interactions. *Curr. Opin. Microbiol.* 62, 14–20. doi: 10.1016/j.mib.2021.04.003

Najmi, S. M., and Schneider, D. A. (2021). Quorum sensing regulates rRNA synthesis in Saccharomyces cerevisiae. *Gene* 776:145442. doi: 10.1016/j.gene.2021.145442

Nath, B. J., Das, K. K., Talukdar, R., and Sarma, H. K. (2021a). Tyrosols retrieved from traditionally brewed yeasts assist in tolerance against heavy metals and promote the growth of cells. *FEMS Microbiol. Lett.* 368, fnab152. doi: 10.1093/femsle/fnab152

Nath, B. J., Mishra, A. K., and Sarma, H. K. (2021b). Assessment of quorum sensing effects of tyrosol on fermentative performance by chief ethnic fermentative yeasts from northeast India. *J. Appl. Microbiol.* 131, 728–742. doi: 10.1111/jam.14908

Padder, S. A., Prasad, R., and Shah, A. H. (2018). Quorum sensing: A less known mode of communication among fungi. *Microbiol. Res.* 210, 51–58. doi: 10.1016/j.micres.2018.03.007

Pan, X., and Heitman, J. (1999). Cyclic AMP-dependent protein kinase regulates pseudohyphal differentiation in *Saccharomyces cerevisiae*. *Mol. Cell Biol.* 19, 4874–4887. doi: 10.1128/MCB.19.7.4874

Pan, X., and Heitman, J. (2002). Protein kinase A operates a molecular switch that governs yeast pseudohyphal differentiation. *Mol. Cell Biol.* 22, 3981–3993.

Ren, G., Ma, A., Liu, W., Zhuang, X., and Zhuang, G. (2016). Bacterial signals *N*-acyl homoserine lactones induce the changes of morphology and ethanol tolerance in *Saccharomyces cerevisiae*. *AMB Express* 6:117. doi: 10.1186/s13568-016-0292-y

Reynolds, T. B., and Fink, G. (2001). Bakers' yeast, a model for fungal biofilm formation. *Science* 291, 878–881. doi: 10.1126/science.291.5505.878

Schüller, H.-J. (2003). Transcriptional control of nonfermentative metabolism in the yeast Saccharomyces cerevisiae. *Curr. Genet.* 43, 139–160. doi: 10.1007/s00294-003-0381-8

Schuster, M., Sexton, D. J., and Hense, B. A. (2017). Why quorum sensing controls private goods. *Front. Microbiol.* 8:885. doi: 10.3389/fmicb.2017.00885

Seibel, K., Schmalhaus, R., Haensel, M., and Weiland, F. (2021). Molecular basis and regulation of flocculation in Saccharomyces cerevisiae and Saccharomyces pastorianus–a review. *BrewingScience* 74, 39–50.

Silva, P. C., Horii, J., Miranda, V. S., Brunetto, H., and Ceccato-Antonini, S. (2007). Characterization of industrial strains of *Saccharomyces cerevisiae* exhibiting filamentous growth induced by alcohols and nutrient deprivation. *World J. Microbiol. Biotechnol.* 23, 697–704. doi: 10.1007/s11274-006-9287-1

Smukalla, S., Caldara, M., Pochet, N., Beauvais, A., Guadagnini, S., Yan, C., et al. (2008). *FLO1* is a variable green beard gene that drives biofilm-like cooperation in budding yeast. *Cell* 135, 726–737. doi: 10.1016/j.cell.2008.09.037

Su, C., Li, Y., Lu, Y., and Chen, J. (2009). Mss11, a transcriptional activator, is required for hyphal development in *Candida albicans*. *Eukaryotic Cell* 8, 1780–1791. doi: 10.1128/EC.00190-09

Tan, S. Z., and Prather, K. L. (2017). Dynamic pathway regulation: recent advances and methods of construction. *Curr. Opin. Chem. Biol.* 41, 28–35. doi: 10.1016/j.cbpa.2017.10.004

Tian, J., Lin, Y., Su, X., Tan, H., Gan, C., and Ragauskas, A. (2023). Effects of Saccharomyces cerevisiae quorum sensing signal molecules on ethanol production in bioethanol fermentation process. *Microbiol. Res.* 271:127367. doi: 10.1016/j.micres.2023.127367

Tian, X., Ding, H., Ke, W., and Wang, L. (2021). Quorum sensing in fungal species. *Annu. Rev. Microbiol.* 75, 449–469. doi: 10.1146/annurev-micro-060321-045510

Turan, N. B., Chormey, D. S., Buyukpinar, C., Engin, G. O., and Bakirdere, S. (2017). Quorum sensing: Little talks for an effective bacterial coordination. *TrAC Trends Anal. Chem.* 91, 1–11. doi: 10.1016/j.trac.2017.03.007

Vuralhan, Z., Morais, M. A., Tai, S. L., Piper, M. D., and Pronk, J. T. (2003). Identification and characterization of phenylpyruvate decarboxylase genes in *Saccharomyces cerevisiae*. *Appl. Environ. Microbiol.* 69, 4534–4541. doi: 10.1128/AEM.69.8.4534-4541.2003

Wang, H., Dong, Q., Guan, A., Meng, C., Shi, X., and Guo, Y. (2011). Synergistic inhibition effect of 2-phenylethanol and ethanol on bioproduction of natural 2-phenylethanol by *Saccharomyces cerevisiae* and process enhancement. *J. Biosci. Bioeng.* 112, 26–31. doi: 10.1016/j.jbiosc.2011.03.006

Wang, Z., Bai, X., Guo, X., and He, X. (2017). Regulation of crucial enzymes and transcription factors on 2-phenylethanol biosynthesis via Ehrlich pathway in Saccharomyces cerevisiae. *J. Ind. Microbiol. Biotechnol.* 44, 129–139. doi: 10.1007/s10295-016-1852-5

Williams, T. C., Averesch, N. J. H., Winter, G., Plan, M. R., Vickers, C. E., Nielsen, L. K., et al. (2015). Quorum-sensing linked RNA interference for dynamic metabolic pathway control in *Saccharomyces cerevisiae*. *Metab. Eng.* 29, 124–134. doi: 10.1016/j.ymben.2015.03.008

Winters, M., Arneborg, N., Appels, R., and Howell, K. (2019). Can community-based signalling behaviour in *Saccharomyces cerevisiae* be called quorum sensing? A critical review of the literature. *FEMS Yeast Res.* 19, foz046. doi: 10.1093/femsyr/foz046

Winters, M., Aru, V., Howell, K., and Arneborg, N. (2022). *Saccharomyces cerevisiae* does not undergo a quorum sensing-dependent switch of budding pattern. *Sci. Rep.* 12:8738. doi: 10.1038/s41598-022-12308-z

Wongsuk, T., Pumeesat, P., and Luplertlop, N. (2016). Fungal quorum sensing molecules: Role in fungal morphogenesis and pathogenicity. *J. Basic Microbiol.* 56, 440–447. doi: 10.1002/jobm.201500759

Wuster, A., and Babu, M. M. (2010). Transcriptional control of the quorum sensing response in yeast. *Mol. Biosyst.* 6, 134–141. doi: 10.1039/b913579k

Xu, M., Sun, M., Meng, X., Zhang, W., Shen, Y., and Liu, W. (2023). Engineering pheromone-mediated quorum sensing with enhanced response output increases fucosyllactose production in *Saccharomyces cerevisiae*. *ACS Synthet. Biol.* 12, 238–248. doi: 10.1021/acssynbio.2c00507

Yang, L., Zheng, C., and Chen, Y. (2018). FLO genes family and transcription factor MIG1 regulate *Saccharomyces cerevisiae* biofilm formation during immobilized fermentation. *Front. Microbiol.* 9:1860. doi: 10.3389/fmicb.2018.01860

Yang, L., Zheng, C., Chen, Y., Shi, X., Ying, Z., and Ying, H. (2019). Nitric oxide increases biofilm formation in *Saccharomyces cerevisiae* by activating the transcriptional factor Mac1p and thereby regulating the transmembrane protein Ctr1. *Biotechnol. Biofuels* 12, 1–15.

Yang, X., Liu, J., Zhang, J., Shen, Y., Qi, Q., Bao, X., et al. (2021). Quorum sensing-mediated protein degradation for dynamic metabolic pathway control in *Saccharomyces cerevisiae*. *Metab. Eng.* 64, 85–94. doi: 10.1016/j.ymben.2021.01.010

Zhang, C., Tong, T., and Ge, J. (2021a). Acetic acid acting as a signal molecule in quorum sensing system enhances production of 2,3-butanediol in *Saccharomyces cerevisiae*. *Prep. Biochem. Biotechnol.* 52, 487–497. doi: 10.21203/rs.3.rs-238949/v1

Zhang, D., Wang, F., Yu, Y., Ding, S., Chen, T., Sun, W., et al. (2021b). Effect of quorum-sensing molecule 2-phenylethanol and ARO genes on *Saccharomyces cerevisiae* biofilm. *Appl. Microbiol. Biotechnol.* 105, 3635–3648. doi: 10.1007/s00253-021-11280-4

Zhang, H., Du, H., and Xu, Y. (2021c). Volatile organic compounds mediated antifungal activity of Pichia and its effect on the metabolic profiles of fermentation communities. *Appl. Environ. Microbiol.* 87, e2992–e2920.

Zupan, J., Avbelj, M., Butinar, B., Kosel, J., Sergan, M., and Raspor, P. (2013). Monitoring of quorum-sensing molecules during minifermentation studies in wine yeast. *J. Agric. Food Chem.* 61, 2496–2505. doi: 10.1021/jf3051363

frontiers | Frontiers in Microbiology

TYPE Original Research
PUBLISHED 12 December 2023
DOI 10.3389/fmicb.2023.1287802

OPEN ACCESS

EDITED BY
Sylvester Holt,
University of Copenhagen, Denmark

REVIEWED BY
Yushun Gong,
Hunan Agricultural University, China
Yanchun Shao,
Huazhong Agricultural University, China
Dileep Kumar,
University of Szeged, Hungary

*CORRESPONDENCE
Chang-song Chen
✉ fjnkycys@163.com

RECEIVED 02 September 2023
ACCEPTED 27 November 2023
PUBLISHED 12 December 2023

CITATION
Wang X-p, Shan R-y, Li Z-l, Kong X-r, Hou R-t, Wu H-n and Chen C-s (2023) Metabolic improvements of novel microbial fermentation on black tea by *Eurotium cristatum*. *Front. Microbiol.* 14:1287802. doi: 10.3389/fmicb.2023.1287802

Metabolic improvements of novel microbial fermentation on black tea by *Eurotium cristatum*

Xiu-ping Wang[1], Rui-yang Shan[1], Zhao-long Li[2], Xiang-rui Kong[1], Ruo-ting Hou[1], Hui-ni Wu[1] and Chang-song Chen[1]*

[1]Tea Research Institute, Fujian Academy of Agricultural Sciences, Fuzhou, China, [2]Institute of Animal Husbandry and Veterinary Medicine, Fujian Academy of Agricultural Sciences, Fuzhou, China

Due to its traditional fermentation, there are obvious limits on the quality improvements in black tea. However, microbial fermentation can provide an abundance of metabolites and improve the flavor of tea. The "golden flower" fungi are widely used in the microbial fermentation of tea and has unique uses in healthcare. To further explore the improvements in black tea quality achieved via microbial fermentation, we used widely targeted metabolomics and metagenomics analyses to investigate the changes in and effects of metabolites and other microorganisms during the interaction between the "golden flower" fungi and black tea. Five key flavor metabolites were detected, the levels of catechin, epigallocatechin gallate, (–)-epicatechin gallate were decreased by different degrees after the inoculation of the "golden flower" fungus, whereas the levels of caffeine and (+)-gallocatechin increased. Botryosphaeriaceae, Botryosphaeriales, Dothideomycetes, Aspergillaceae, Trichocomaceae, and Lecanoromycetes play a positive role in the black tea fermentation process after inoculation with the "golden flower" fungi. D-Ribose can prevent hypoxia-induced apoptosis in cardiac cells, and it shows a strong correlation with Botryosphaeriaceae and Botryosphaeriales. The interaction between microorganisms and metabolites is manifested in tryptophan metabolism, starch and sucrose metabolism, and amino sugar and nucleotide sugar metabolism. In conclusion, the changes in metabolites observed during the fermentation of black tea by "golden flower" fungi are beneficial to human health. This conclusion extends the knowledge of the interaction between the "golden flower" fungi and black tea, and it provides important information for improving the quality of black tea.

KEYWORDS

***Eurotium cristatum*, black tea, fermentation, microorganisms, metabolites, interactions**

1 Introduction

Black tea is commonly produced in China, India, Kenya, Sri Lanka, and other countries. It plays a significant role in boosting regional economic growth and battling poverty. Black tea consumption comprises 78% of the world's tea consumption (Takashi and Isao, 2003; Azapagic et al., 2016; Niranjan et al., 2022). The color and taste of tea mainly depend mainly on non-volatile compounds, such as polyphenols, amino acids, and caffeine, and bioalgae (Zhen, 2002). Catechins accounts for approximately 80 per cent of the total polyphenols; the

catechins can be further divided into (+)-gallocatechin, (−)-epigallocatechin, (+)-catechin, (−)-epicatechin, (−)-epigallocatechin-3-gallate, (−)-gallocatechin gallate, (−)-epicatechin-3-gallate, and catechin gallate (Fang et al., 2021). Theanine constitutes around 50% of the total amino acids present. Caffeine is the major purine alkaloid present in tea. These characteristic compounds are responsible for the unique flavors of tea (Zhen, 2002). The fermentation process has a significant impact on the flavor and quality of black tea products. The primary fermentation process of black tea is endogenous enzymatic oxidation; therefore, there is not much capacity for quality improvement, particularly in terms of health benefits and slimming properties (Bancirova, 2010). Microbial fermentation of tea is more important for attaining high-quality flavor and health benefits than endogenous fermentation of black tea. The microbial fermentation process generates large amounts of polyphenol oxidase, cellulase, and pectinase, which considerably enhance the health benefits, esthetic appeal, and weight reduction of tea (Tang et al., 2022; Zhang et al., 2022). The expansion of the black tea processing chain using microbial flora is, therefore, essential to enhancing the quality of black tea.

The production of Fu-brick tea and other dark teas relies heavily on the "golden flower" fungi. The "golden flower" fungi were identified as *Eurotium cristatum* (Du et al., 2019), they can metabolize and transform phenolic compounds such as catechins in tea. Being among the primary components of tea, these metabolites have no effects on normal cells while having antimutagenic, anticancer, and tumor cell-inhibitory effects (Oguni et al., 1988; Mukhtar et al., 1992; Katiyar et al., 1993; Lea et al., 1993; Du et al., 2019). Therefore, these metabolites are beneficial to the health of the human body. According to some studies, adding the "golden flower" fungi to finished black tea after fermentation can raise theophylline levels and enhance the black tea's quality (Yu et al., 2015). This study confirms the potential of the "golden flower" fungi to improve the growth and processing of black tea products. Unfortunately, the precise molecular mechanism underlying the interaction between the "golden flower" fungi and black tea has not been investigated. To enhance the flavor and health benefits of black tea and to encourage the growth of the black tea industry, it is important to investigate the changes in the microbial population occurring during the interaction between the "golden flower" fungi and black tea.

Various symbiotic bacteria, including *Bacillus* bacteria, must work together with the "golden flower" fungi for the fermentation of tea (Xiang et al., 2022). Determining the symbiotic functional microorganisms involved in fermentation by the "golden flower" fungi is, therefore, essential for improving this process and ensuring a consistent output of metabolites. The community composition and organization of the aforementioned symbiotic bacteria are no longer a mystery because of the widespread use of macrogenetic sequencing techniques (Huang et al., 2019). The composition and function of the secondary metabolites are also frequently investigated using high-throughput next-generation sequencing technologies (Huang et al., 2019; Fan et al., 2021). With the help of these two techniques, we can clarify the corresponding relationship between functional microorganisms and functional metabolites in the interaction between the "golden flower" fungi and black tea. The joint analysis of the metagenome and the metabolome can establish the logical relationships among microbes, metabolites, and phenotypes. The research into how various microorganisms affect the secondary metabolites of tea has been severely constrained by the absence of such studies, which hinders the promotion and advancement of the fermentation process using the "golden flower" fungi.

In order to investigate the changes, effects, and interactions of microorganisms and metabolites during black tea fermentation after the addition of the "golden flower" fungi, this study selected finished black tea, inoculated it with the fungus, and used widely targeted metabolomics and metagenomic analysis techniques. By utilizing the "golden flower" fungi, this study enhances the quality, flavor, and health benefits of black tea. It also contributes favorably to the advancement of deep processing technology for black tea and the expansion of tea goods.

2 Materials and methods

2.1 Sample collection

The fresh leaves processed into black tea used in this research were from "Fuxuan," a new variety of high-quality tea tree bred by the Fujian Provincial Academy of Agricultural Sciences. The "golden flower" fungi were isolated and obtained from Anhua dark tea. The pre-*E. cristatum* samples refer to untreated black tea, while the post-*E. cristatum* samples are black tea samples that were irradiated with two rounds of food-grade cobalt-60 radiation and then inoculated with the "golden flower" fungi at a concentration of 10^{8-9} pfu/mL. The samples were cultured at a temperature of 26°C and a relative humidity of 50% for 5 days, followed by low-temperature drying. Both groups of samples underwent comprehensive targeted metabolomic profiling and metagenomic sequencing.

2.2 Total antioxidant capacity assay

Take 20 mg of freeze-dried samples, add 100 microliters of frozen PBS solution, thoroughly crush the pulp, release antioxidant, centrifuge approximately 12,000× *g* for 5 min at 4°C, and take up the supernatant. The antioxidant capacity was measured by using the Total Antioxidant Capacity Assay Kit with the FRAP method (Beyotime Biotechnology, S0116).

2.3 Widely targeted metabolomics analysis

The freeze-dried samples were crushed with a mixer mill for 30 s at 60 Hz. After precisely weighing 10 mg aliquots of individual samples, 500 µL of extract solution (methanol/water = 3:1, precooled at −40°C, containing internal standard) was added. After 30 s of vortex mixing, the samples were centrifuged at 12,000 rpm (RCF = 13,800× *g*, *R* = 8.6 cm) for 15 min at 4°C. After the supernatant was carefully filtered through a 0.22 µm microporous membrane, the samples were analyzed by Allwegene Company (Beijing). The mobile phase A was 0.1% formic acid in water, and the mobile phase B was acetonitrile. The column temperature was set to 40°C. The autosampler temperature was set to 4°C, and the injection volume was 2 µL. A Sciex QTrap 6,500+ (Sciex Technologies) was applied for assay development. Typical ion source parameters were as follows: ion spray

voltage, +5,500/−4,500 V, curtain gas: 35 psi, temperature: 400°C, ion source gas 1, 60 psi; ion source gas 2, 60 psi; DP, ±100 V.

2.4 Metabolome data processing and analysis

SCIEX Analyst Workstation Software (Version 1.6.3) was employed for MRM data acquisition and processing. MS raw data (.wiff) files were converted to the .txt format using msConvert. The R program and database were applied for peak detection and annotation (Smith et al., 2006; Kuhl et al., 2012; Zhang et al., 2015). In the ion chromatogram, the target compounds showed symmetrical chromatographic peaks, and the chromatographic separation of the target compounds was well achieved. After data processing, orthogonal partial least squares-discriminant analysis (OPLS-DA) and principal component analysis were performed on metabolite data before and after inoculation, and the results were visualized by scatter plots (Mi et al., 2019; Yang et al., 2020). Differentially accumulated metabolites (DAMs) between the pre-*E. cristatum* and post-*E. cristatum* groups were determined according to *t*-test value of $p < 0.05$ and VIP >1. Lastly, the KEGG pathway database was used to enrich the metabolic pathways of DAMs, and R was used to visualize the results.

TABLE 1 The total antioxidant capacity in post-*E. cristatum* and pre-*E. cristatum* samples.

	Pre-*E. cristatum* (μmol/mL)	Post-*E. cristatum* (μmol/mL)	Log_2 fold change (Pre-*E. cristatum* vs. Post-*E. cristatum*)	*p*-value
Total antioxidant capacity	0.46 ±0.005	0.59 ±0.004	−0.35	0.00001***

2.5 DNA extraction and metagenomics analysis

The total DNA of the tea samples was extracted using the CTAB/SDS method. The purity and quality of the genomic DNA were checked on 1% agarose gels, and the DNA concentration was precisely quantified using a Qubit fluorometer. DNA sequencing libraries were deep-sequenced on the Illumina Novaseq PE150 platform at Allwegene Company (Beijing). The quality of the raw data was assessed using fastp (Chen et al., 2018), and then these high-quality reads were assembled to contigs using MEGAHIT (Li et al., 2015)(parameters: kmer_min = 47, kmer_max = 97, step = 10).[1] Open reading frames (ORFs) in contigs were identified using Prodigal (Hyatt et al., 2010).[2] A nonredundant gene catalog was constructed using CD-HIT (Fu et al., 2012).[3]

2.6 Metagenomics data processing and analysis

The taxonomic annotation was conducted using Diamond[4] (Buchfink et al., 2015) against the Kyoto Encyclopedia of Genes and Genomes database[5] with an e-value cutoff of 1×10^{-5}. The annotation of antibiotic resistance genes was conducted using Diamond[6] (Buchfink et al., 2015) against the CARD database[7] with an e-value cutoff of 1×10^{-5}. To generate bar plots illustrating the composition of dominant species at various taxonomic levels in each sample, the R language was utilized. LEfSe analysis was conducted to identify biomarkers across groups. KEGG metabolic pathways were analyzed to detect the distinctions and changes in the functional genes of metabolic pathways and in the protein

1 https://github.com/voutcn/megahit, version 1.1.2
2 https://github.com/hyattpd/prodigal/wiki
3 http://www.bioinformatics.org/cd-hit/, version 4.6.1
4 http://www.diamondsearch.org/index.php, version 0.8.35
5 http://www.genome.jp/keeg/, version 94.2
6 http://www.diamondsearch.org/index.php, version 0.8.35
7 https://card.mcmaster.ca/home, version 3.0.9

TABLE 2 The differences in the contents of 10 flavor-related metabolites in post-*E. cristatum* and pre-*E. cristatum* samples.

Name	Formula	Pre-*E.cristatum*	Post-*E.cristatum*	Log_2 Fold Change (Pre-*E.cristatum* vs. Post-*E. cristatum*)	*p*-Value
Epigallocatechin gallate	$C_{22}H_{18}O_{11}$	4.677± 0.70	2.200± 0.21	1.09	0.004**
(−)-Epicatechin gallate	$C_{22}H_{18}O_{10}$	15.510± 0.62	8.890± 0.64	0.80	0.0002***
Catechin	$C_{15}H_{14}O_6$	0.222± 0.05	0.132± 0.02	0.75	0.048*
(+)-Gallocatechin	$C_{15}H_{14}O_7$	0.005± 0.00	0.183± 0.16	−5.20	0.117
Caffeine	$C_8H_{10}N_4O_2$	416.258± 11.76	542.496± 22.90	−0.38	0.001***
Theanine	$C_7H_{14}N_2O_3$	/	/		
(−)-Epicatechin	$C_{15}H_{14}O_6$	/	/		
Epigallocatechin	$C_{15}H_{14}O_7$	/	/		
Gallocatechin gallate	$C_{22}H_{18}O_{11}$	/	/		
Catechin gallate	$C_{22}H_{18}O_{10}$	/	/		

functions of bacterial communities among different groups. Combining the abundance information for unigenes, the relative abundance of antibiotic resistance genes (ARGs) was calculated for significant differential analysis. Canonical correlation and correlation analyses were used to analyze the correlation between signature microorganism communities and these detected metabolites.

3 Results

3.1 Total antioxidant capacity assay

We tested the antioxidant properties of the black tea before and after inoculation with the "golden flower" fungi in order to evaluate the tea's chemical characteristics (Table 1). Antioxidant capacity increased from 0.46 to 0.59 μmol/mL after inoculation.

3.2 Quantitative analysis of flavor-related metabolites

In order to assess the flavor changes in black tea after inoculation with the "golden flower" fungi, quantitative analysis was performed on 10 key flavor metabolites: caffeine, theanine, (−)-epicatechin, (−)-epicatechin gallate, epigallocatechin gallate, catechin, epigallocatechina, gallocatechina, gallocatechine gallate, and catechine gallate. Among these metabolites, five were detected in black tea before and after inoculation (Table 2). Specifically, the content of

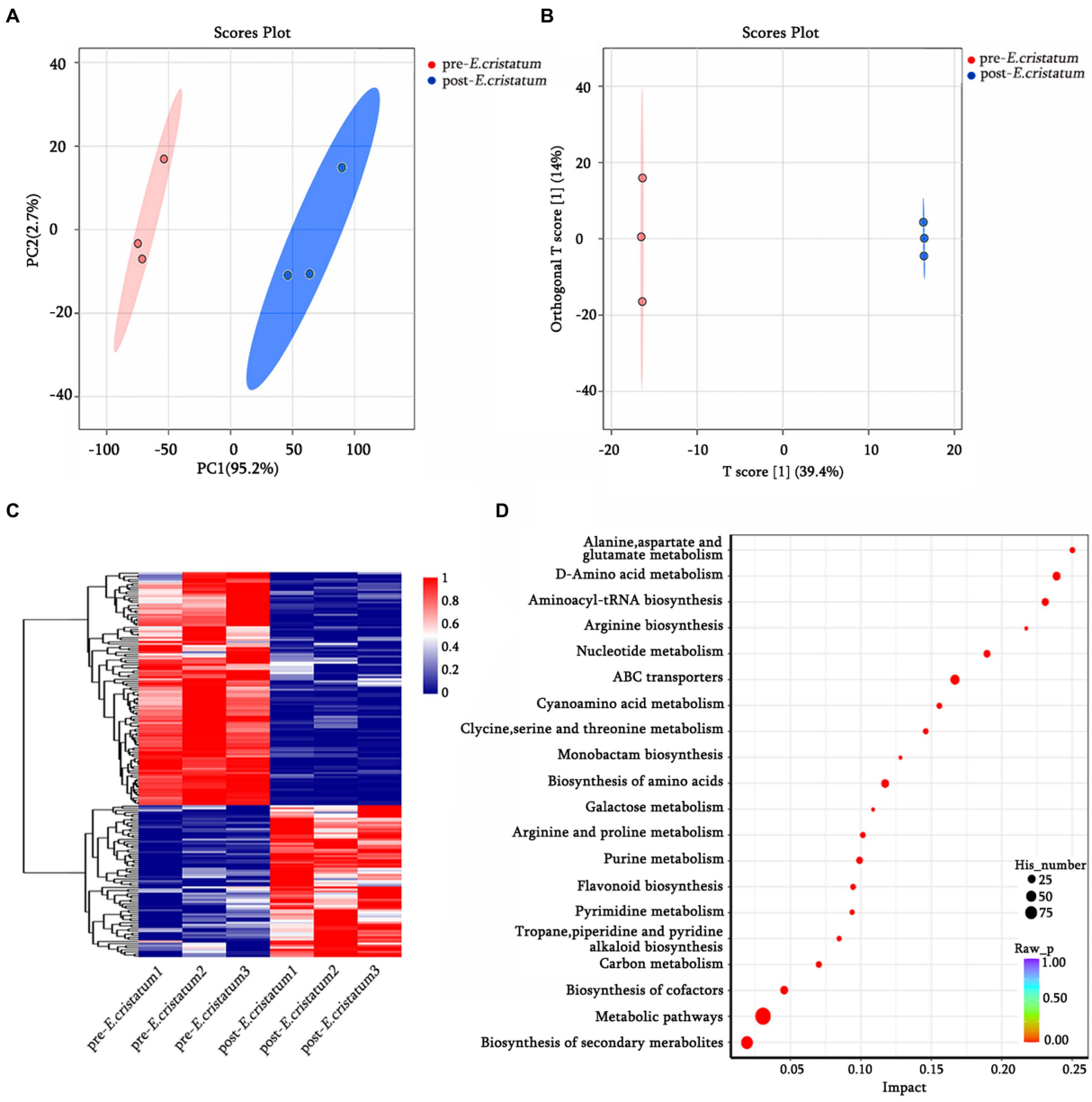

FIGURE 1
The qualitative and functional analyses of metabolome data for pre-*E. cristatum* and post-*E. cristatum* samples. **(A)** The scatter plot of PCA scores of pre-*E. cristatum* and post-*E. cristatum* samples. **(B)** The OPLS-DA model of pre-*E. cristatum* and post-*E. cristatum* samples. **(C)** The DAM clustering heat map comparing samples. **(D)** The top 20 KEGG pathways identified in the enrichment analysis of DAMs.

catechin, epigallocatechin gallate, (−)-epicatechin gallate were decreased by different degrees after the inoculation of the "golden flower" fungus. In contrast, the content of (+)-gallocatechin and caffeine increased after inoculation.

3.3 Metabolic characteristics of tea samples

The data we obtained by conducting comprehensive targeted metabolomic analysis on black tea samples before and after inoculation with the "golden flower" fungi were further subjected to a series of multivariate pattern recognition analyses. Principal component analysis (PCA) revealed the first component of the two groups of tea leaves (Figure 1A) with an R^2X value of 95.2%, indicating good discrimination between the two groups. Orthogonal partial least squares discriminant analysis (OPLS-DA) showed significant differences between the two types of tea (Figure 1B), with scores from both groups falling within the 95% confidence interval. Through KEGG annotation, a total of 156 metabolites were identified (Figure 1C). Within the KEGG annotation, the 156 differentially regulated metabolites were mapped to 80 pathways (Figure 1D), with the majority enriched in metabolic pathways, the biosynthesis of secondary metabolites, ABC transporters, D-amino-acid metabolism, and other material metabolic processes.

3.4 Composition of bacterial and fungal communities in pre-*E. cristatum* and post-*E. cristatum* samples

After obtaining the data, we annotated the species at different classification levels in the black tea samples and analyzed the changes in the species composition before and after inoculation with the "golden flower" fungi. The annotation of the bacterial species showed that, at the class level (Figure 2A), the proportions of Flavobacteriia and Deltaproteobacteria decreased significantly from 47 and 38 to 1% after inoculation with the "golden flower" fungi. The proportion of Gammaproteobacteria, in contrast, increased dramatically from 5 to 89%, making them the dominant bacteria. At the genus level (Figure 2C), *Chryseobacterium* and *Corallococcus* showed significant decreases after inoculation with the "golden flower" fungi, decreasing from 46 and 40% to 2 and 13%, respectively. The proportion of *Pseudomonas*, however, increased after inoculation with the "golden flower" fungi. The annotation of the fungal species showed that, at the class level (Figure 2B), Eurotiomycetes strains were present at the highest proportions both before and after inoculation with the "golden flower" fungi, with the post-inoculation proportion increasing to 96%. At the genus level (Figure 2D), *Aspergillus* strains were present at the highest proportions both before and after inoculation, with the post-inoculation proportion increasing to 86%.

3.5 Screening analysis of signature microorganisms and differential gene analysis

LefSe analysis was performed to identify signature bacteria and fungi and further analyze the microbial community. Sphingobacteriaceae, Sphingobacteriales, and Bacteroidia were identified as characteristic bacterial communities after inoculation (Figure 3A), whereas Aspergillaceae, Trichocomaceae, and Lecanoromycetes were the characteristic fungal communities after inoculation (Figure 3B). Chloroplast, Cyanobacteriia, and Cyanobacteria were the characteristic bacterial communities before

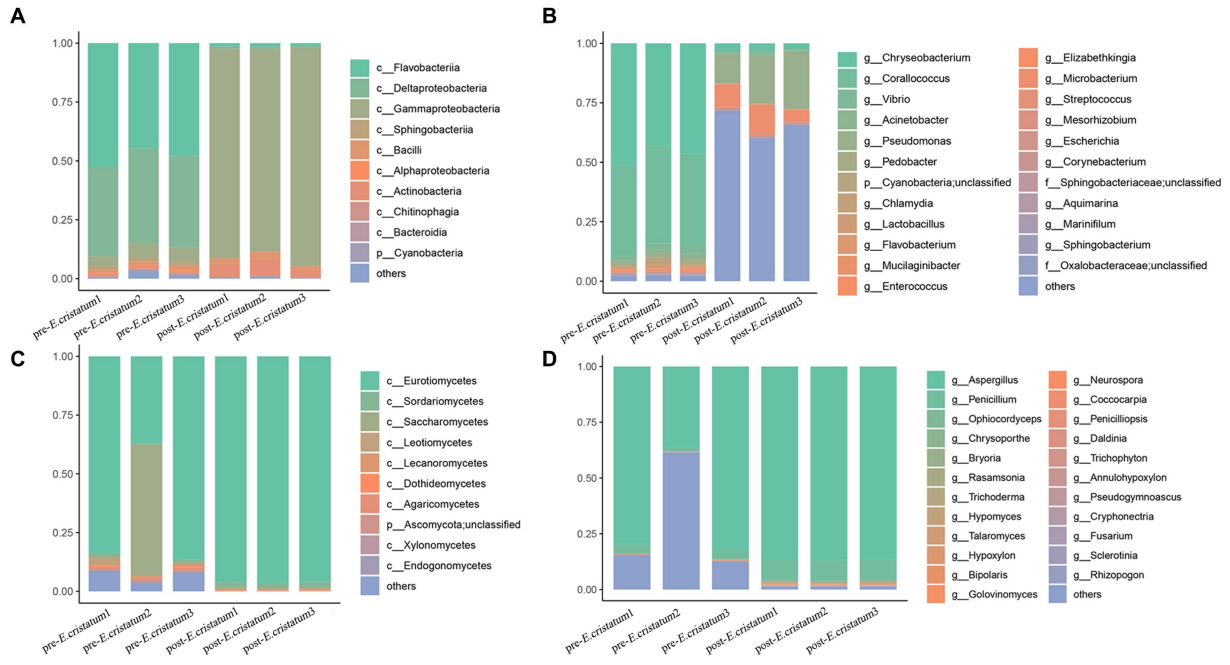

FIGURE 2
The diverse species composition of pre-*E. cristatum* and post-*E. cristatum* samples. **(A)** The species composition at the bacterial class level. **(B)** The species composition at the fungal class level. **(C)** The species composition at the bacterial genus level. **(D)** The species composition at the fungus genus level.

inoculation (Figure 3A), whereas Botryosphaeriaceae, Botryosphaeriales, and Dothideomycetes were the characteristic fungal communities before inoculation (Figure 3B). After inoculation with the "golden flower" fungi, the specific fermentation environment of black tea became unfavorable for the survival of the pre-inoculation signature microorganisms, leading to their disappearance.

Based on KEGG annotation, the differences in the functional genes of the microbial community in black tea samples before and after inoculation with the "golden flower" fungi are demonstrated (Figure 3C). After inoculation with the "golden flower" fungi, the abundance of many KEGG pathways increased, including tryptophan metabolism, starch and sucrose metabolism, and amino sugar and nucleotide sugar metabolism. Analysis of the significantly differentially expressed antibiotic resistance genes (Figure 3D) showed that most of the resistance genes, such as *abaQ* and bicyclomycin-multidrug efflux protein_bcr, were significantly increased in black tea after inoculation with the "golden flower" fungi.

3.6 Comprehensive analysis of microorganisms and metabolites

The canonical correlation analysis of the effects of signature microorganisms was performed on the distribution of metabolites before and after the inoculation with the "golden flower" fungi (Figure 4). Sphingobacteriaceae, Sphingobacteriales, Bacteroidia, Bacteroidota, Cyanobacteriia, and Cyanobacteria had a negative impact on the fermentation of black tea after inoculation with the "golden flower" fungi, with Bacteroidota playing the most significant role (Figure 4A). Additionally, Botryosphaeriaceae, Botryosphaeriales, Dothideomycetes,

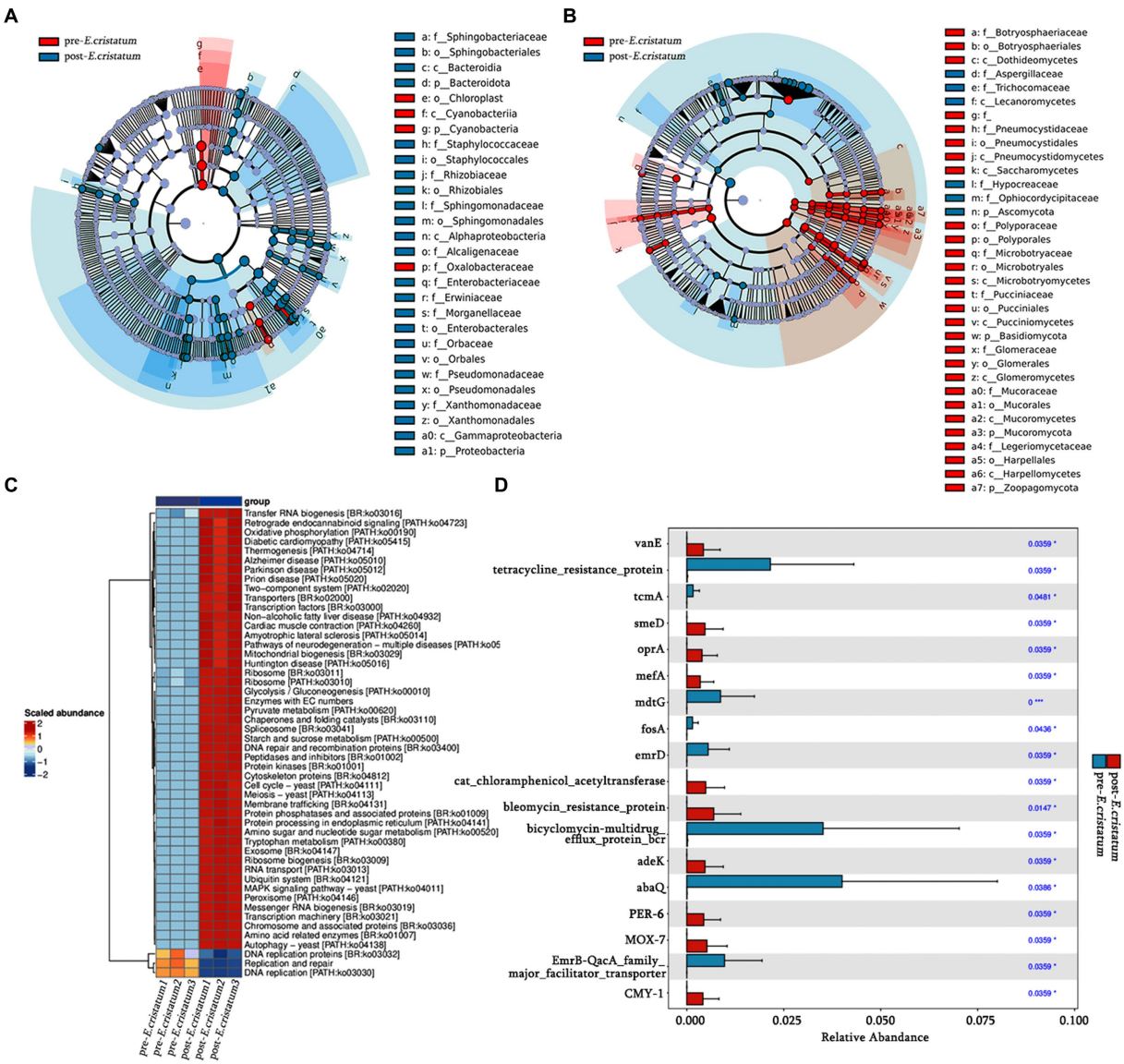

FIGURE 3
The signature microorganisms and bacterial pathway annotations. **(A)** Characteristic bacterial LEfSe analysis. **(B)** Characteristic fungal LEfSe analysis. **(C)** KEGG pathways enriched in bacteria. **(D)** Histogram of significantly different resistance genes.

Aspergillaceae, Trichocomaceae, and Lecanoromycetes had a positive impact on the fermentation of black tea after inoculation (Figure 4B). The changes in five flavor metabolites may be associated with these microbial communities, with fungi such as Botryosphaeriaceae, Botryosphaeriales, Dothideomycetes, Aspergillaceae, Trichocomaceae, and Lecanoromycetes assisting in fermentation by the "golden flower" fungi. Correlation analysis (Supplementary Table S1) revealed that D-ribose was the metabolite most strongly correlated with Botryosphaeriaceae and Botryosphaeriales; 2-picolinic acid was the metabolite most strongly correlated with Dothideomycetes; L-arginine was the metabolite most strongly correlated with Aspergillaceae and Trichocomaceae; D-sorbitol was the metabolite most strongly correlated with Lecanoromycetes.

On the basis of KEGG annotation (Figure 5), the abundance of tryptophan metabolism, starch and sucrose metabolism, and amino sugar and nucleotide sugar metabolism pathways increased. Metabolite enrichment analysis of these pathways revealed 9 DAMs. In tryptophan metabolism, 3 DAMs, namely, indoleacetate, kynurenate, and picolinate, were upregulated, while 1 DAM, formylanthranilate, was downregulated. In starch and sucrose metabolism, 2 DAMs, namely, maltose and D-glucose-6P, were upregulated. In amino sugar and nucleotide sugar metabolism, 3 DAMs, namely, alpha-D-glucose, galactose-1-P, and D-arabinose, were downregulated.

4 Conclusion

As distinctive microorganisms, fungi such as those in the Botryosphaeriaceae, Botryosphaeriales, Dothideomycetes, Aspergillaceae, Trichocomaceae, and Lecanoromycetes families may be used for the fermentation of black tea. D-Ribose, 2-picolinic acid, L-arginine, and D-sorbitol are metabolites that have strong relationships with particular bacteria. The "golden flower" fungi have long been regarded as one of the most significant microbial constituents in tea, but the beneficial symbiotic bacteria and metabolites that are connected to them also invite additional research to uncover the causal linkages among the various biota engaged in tea fermentation. Enhancing black tea quality and streamlining the production process can be accomplished by determining the microbial succession and interaction of metabolites that affect the biochemical composition of black tea.

5 Discussion

Fermented microorganisms and metabolites give tea many beneficial qualities (Zhen, 2002; Tang et al., 2022), but few studies have explored the mechanisms of the effect of "golden flower" tea on black tea. In this study, widely targeted metabolomics revealed significant changes in the metabolites; five of these are key flavor metabolites closely linked to the taste and effect of tea. Furthermore, metagenomic analysis techniques revealed fluctuations in microbial clusters; 6 types of fungi are characteristic microorganisms because of their great changes.

The functions of tea-related compounds are diverse, and most research has focused on the functional contributions of metabolites (Someya et al., 2002; Wu et al., 2023). Quantitative analysis of 7 flavor metabolites has been explored in other research (Wu et al., 2023), and proved that these flavor metabolites have an important role to play in the taste and health effects of Fu-brick tea. Compared with this study, there have been changes in the levels of caffeine and gallocatechin after black tea's inoculation with "golden flower" fungi (Table 1). Gallocatechin has antioxidant functions and protective effects against diseases such as cancer and heart disease (Someya et al., 2002). Caffeine relaxes smooth muscle of the bronchi, making it of value for the treatment of asthma and the bronchospasm of chronic bronchitis (Lin et al., 2022). In addition, the various metabolites were predominantly enriched in metabolic pathways, secondary metabolite production, ABC transporters, D-amino acid metabolism, and other material metabolic activities after the inoculation with the "golden flower" fungi. Theanine, caffeine, and catechins, which are the secondary metabolites found in tea, are significant contributors to the distinctive flavors of tea (Fang et al., 2021). A potential target for regulating immunity and infection is amino acid metabolism (Tomé, 2021).

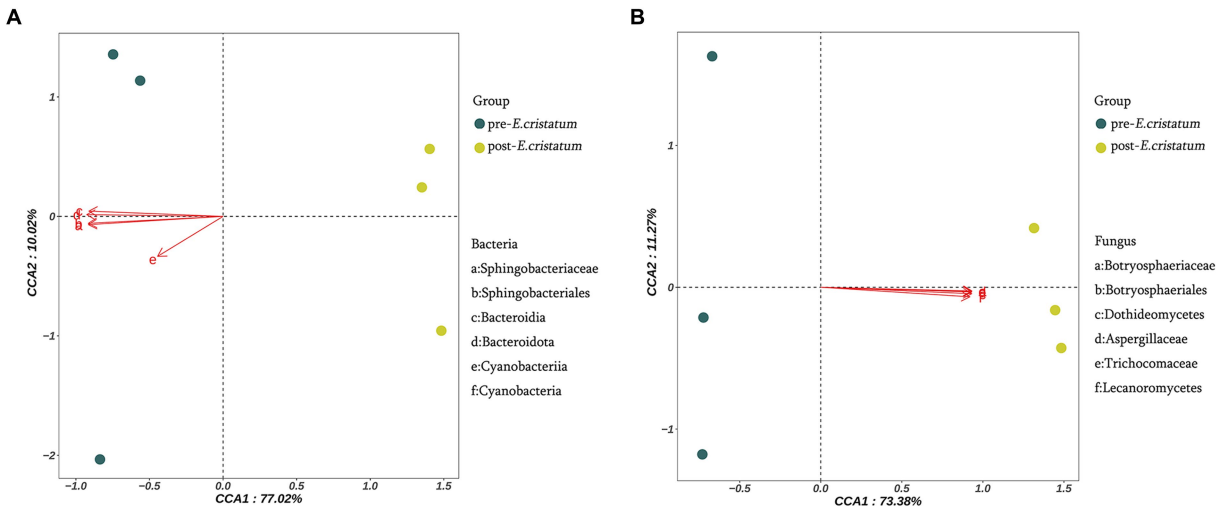

FIGURE 4
Canonical correlation analysis of microorganisms and metabolites. **(A)** Canonical correlation analysis of signature bacterial communities and metabolites. **(B)** Canonical correlation analysis of signature fungal communities and metabolites.

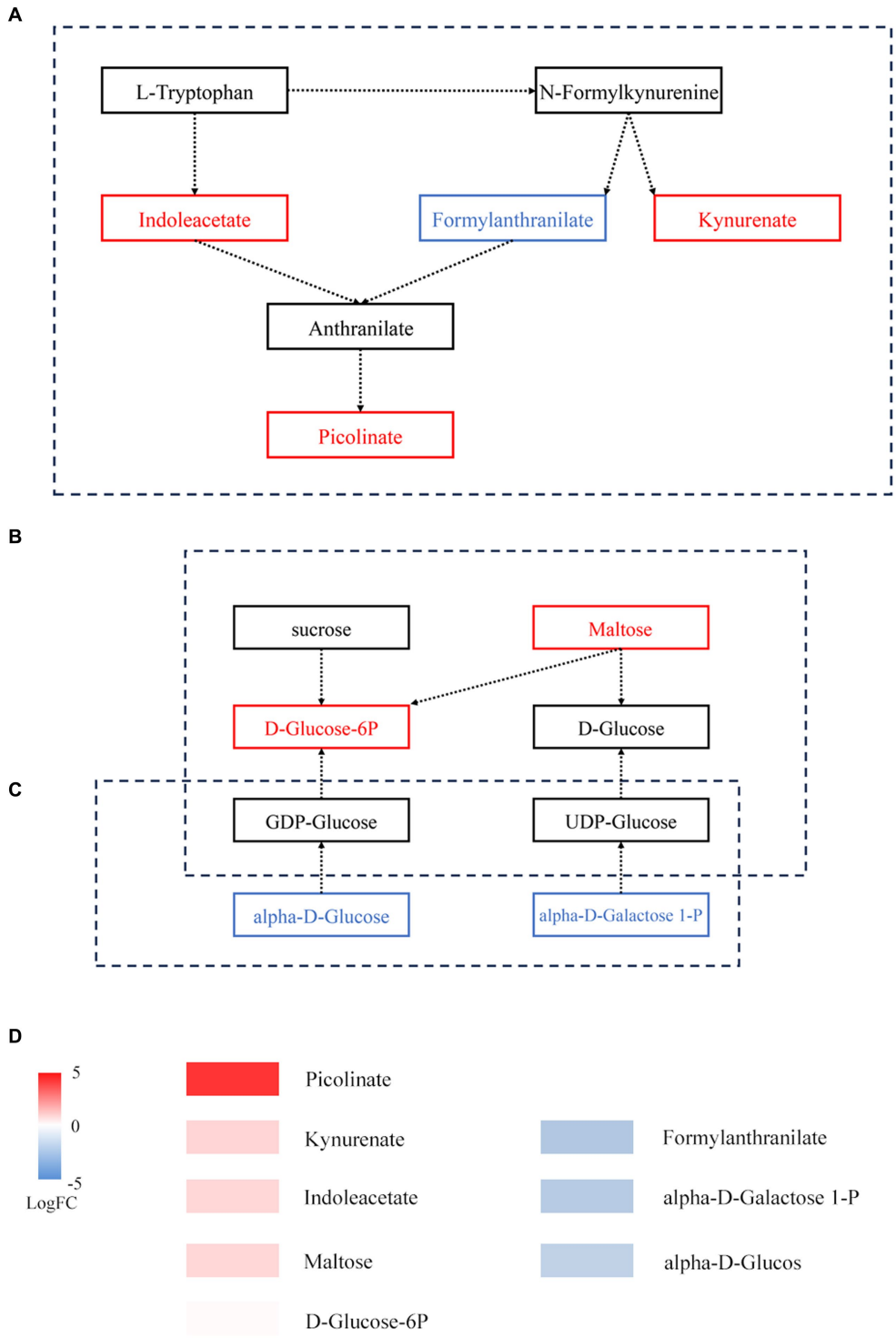

FIGURE 5
Metabolic pathways of DAMs before and after fermentation. **(A)** Tryptophan metabolism. **(B)** Starch and sucrose metabolism. **(C)** Amino sugar and nucleotide sugar metabolism. The box represents metabolites; red represents upregulated metabolites, while blue represents downregulated metabolites. **(D)** Expression of DAMs involved in panels **(A–C)**.

Our observations were largely supported by earlier research linking the "golden flower" fungi to the biochemical makeup of tea. For example, few studies on Fu-brick tea have explored the alteration of microbial communities in the fermentation process (Xiang et al., 2022). In the current study, after the inoculation of black tea with "golden flower" fungi, the trend of changes in the contents of Eurotiomycetes and Dothideomycetes is consistent with the trend of change after the fermentation of Fu-brick tea (Xiang et al., 2022), Eurotiomycetes gradually becomes the dominant class, while the content of Dothideomycetes significantly decreases. The microbial composition of black tea changes after inoculation. For example, there is a decrease in Flavobacteriia and Deltaproteobacteria, and an

increase in *Penicillium*, Lecanoromycetes, and Gammaproteobacteries. Some *Penicillium* spp. can produce l-asparaginase, and this enzyme is being employed for acute lymphoblastic leukemia and lymphosarcoma therapies (De Carvalho et al., 2021). Lecanoromycetes can be consumed as a herbal supplement, as well as being a component of tea and foods (Xu et al., 2018; Song et al., 2022). Gammaproteobacteria, one of the important microorganisms in the fermentation process, is a signature microorganism in Fu-brick tea. These changes play a key role in the health-related qualities of black tea. After inoculation with "golden flower" fungi, the specific fermentation environment of black tea is not conducive to the survival of microorganisms such as Flavobacteriia and Deltaproteobacteria and causes their reduction or disappearance.

There is a strong link between certain metabolites, such D-ribose, and specific bacteria. In hypoxic cardiac cells, D-ribose has been demonstrated to inhibit apoptosis (Caretti et al., 2013). L-arginine administration over an extended period was shown to ameliorate cardiovascular disease symptoms (Boger, 2014). Within a specific range, D-sorbitol can improve the body's absorption of vitamin B (Herbert et al., 1959). Tryptophan metabolism, starch and sucrose metabolism, and amino sugar and nucleotide sugar metabolism all depend on the interplay of microbes and metabolic byproducts. The entire immunological homeostasis depends heavily on tryptophan metabolism (Le Floc'h et al., 2011). The products of amino sugar and nucleotide sugar metabolism can enter starch and sucrose metabolism (Figure 5C). In starch and sucrose metabolism, D-glucose-6P is produced from starch under the catalysis of beta-fructofuranosidase, and the significant increase in D-glucose-6P and maltose may be caused by the accelerated rate at which starch is degraded. A variety of fungi play a role in promoting fermentation by the "golden flower" fungi in black tea (Figure 4B). These compounds may serve as a source of energy during fermentation by the "golden flower" fungi. Additionally, we also analyzed the expression of antibiotic resistance genes; *abaQ*, sodium chloride, certain antibiotics, and multidrug resistance genes can yield antibacterial and antiviral effects (Clark et al., 1998; Pérez-Varela et al., 2018; Kato et al., 2019; Baron et al., 2020).

Artificial inoculation with "golden flower" fungi is a new approach to improving tea products. Studies have shown that adding "golden flower" fungi to finished black tea can increase the level of theophylline (Yu et al., 2015). However, these studies mainly focused mainly on the taste and sensory qualities of tea. In this study, we focused not only on metabolic changes, but also on the appearance of the fungus and bacteria, thus providing a comprehensive understanding of the molecular mechanisms in the fermentation process. Furthermore, our research explored the common roles of metabolites and microorganisms. It is critical to find any microbes and metabolites that could support the growth of the "golden flower" fungi and develop black tea. However, the further effects of dominant strains and distinctive metabolites on black tea are still unclear. Future research on these prevalent strains and metabolites may help expand the black tea industry.

Data availability statement

The original contributions presented in the study are included in the article/Supplementary material, further inquiries can be directed to the corresponding author.

Author contributions

X-pW: Data curation, Writing – original draft. R-yS: Methodology, Resources, Writing – original draft. Z-lL: Methodology, Writing – original draft. X-rK: Data curation, Software, Writing – original draft. R-tH: Writing – original draft. H-nW: Writing – original draft. C-sC: Writing – review & editing.

Funding

The author(s) declare financial support was received for the research, authorship, and/or publication of this article. This research was supported by the Ministry of Agriculture and Rural Affairs of P. R. China (CARS-19), "5511" Collaborative Innovation Project for agricultural high-quality development and transcendence (XTCXGC2021004), Fujian public welfare projects (2021R1029003, 2022R1029003, and 2023R1027005).

Acknowledgments

We are thankful for the funding of the project and for the technical support of Allwegene.

Conflict of interest

The authors declare that the research was conducted in the absence of any commercial or financial relationships that could be construed as a potential conflict of interest.

Publisher's note

Supplementary material

The Supplementary material for this article can be found online at: https://www.frontiersin.org/articles/10.3389/fmicb.2023.1287802/full#supplementary-material

References

Azapagic, A., Bore, J., Cheserek, B., Kamunya, S., and Elbehri, A. (2016). The global warming potential of production and consumption of Kenyan tea. *J. Clean. Prod.* 112, 4031–4040. doi: 10.1016/j.jclepro.2015.07.029

Bancirova, M. (2010). Comparison of the antioxidant capacity and the antimicrobial activity of black and green tea. *Food Res. Int.* 43, 1379–1382. doi: 10.1016/j.foodres.2010.04.020

Baron, T. H., DiMaio, C. J., Wang, A. Y., and Morgan, K. A. (2020). American gastroenterological association clinical practice update: management of pancreatic necrosis. *Gastroenterology* 158, 67–75. doi: 10.1053/j.gastro.2019.07.064

Boger, R. H. (2014). The pharmacodynamics of L-arginin. *J Nutr* 137, 1650S–1655S. doi: 10.1093/jn/137.6.1650S

Buchfink, B., Xie, C., and Huson, D. H. (2015). Fast and sensitive protein alignment using DIAMOND. *Nat. Methods* 12, 59–60. doi: 10.1038/nmeth.3176

Caretti, A., Bianciardi, P., Marini, M., Abruzzo, P. M., Bolotta, A., Terruzzi, C., et al. (2013). Supplementation of creatine and ribose prevents apoptosis and right ventricle hypertrophy in hypoxic hearts. *Curr. Pharm. Des.* 19, 6873–6879. doi: 10.2174/13816128193913127114218

Chen, S.-F., Zhou, Y.-Q., Chen, Y.-R., and Gu, J. (2018). fastp: an ultra-fast all-in-one FASTQ preprocessor. *Bioinformatics* 34, i884–i890. doi: 10.1093/bioinformatics/bty560

Clark, K. J., Grant, P. G., Sarr, A. B., Belakere, J. R., Swaggerty, C. L., Phillips, T. D., et al. (1998). An in vitro study of theaflavins extracted from black tea to neutralize bovine rotavirus and bovine coronavirus infections. *Vet. Microbiol.* 63, 147–157. doi: 10.1016/S0378-1135(98)00242-9

De Carvalho, A. C., Junior, O. C. Y., De Camillis, R. L., de Medeiros, L. S., and Veiga, T. A. M. (2021). *Penicillium* genus as a source for anti-leukemia compounds: an overview from 1984 to 2020. *Leuk. Lymphoma* 62, 2079–2093. doi: 10.1080/10428194.2021.1897804

Du, H.-P., Wang, Q., and Yang, X.-B. (2019). Fu brick tea alleviates chronic kidney disease of rats with high fat diet consumption through attenuating insulin resistance in skeletal muscle. *Agric. Food Chem* 67, 2839–2847. doi: 10.1021/acs.jafc.8b06927

Fan, F.-Y., Huang, C.-S., Tong, Y.-L., Guo, H.-W., Zhou, S.-J., Ye, J.-H., et al. (2021). Widely targeted metabolomics analysis of white peony teas with different storage time and association with sensory attributes. *Food Chem.* 362:130257. doi: 10.1016/j.foodchem.2021.130257

Fang, K.-X., Xia, Z.-Q., Li, H.-J., Jiang, X.-H., Qin, D.-D., Wang, Q.-S., et al. (2021). Genome-wide association analysis identified molecular markers associated with important tea flavor-related metabolites. *Hortic Res* 8:42. doi: 10.1038/s41438-021-00477-3

Fu, L.-M., Niu, B.-F., Zhu, Z.-W., Wu, S.-T., and Li, W.-Z. (2012). CD-HIT: accelerated for clustering the next-generation sequencing data. *Bioinformatics* 28, 3150–3152. doi: 10.1093/bioinformatics/bts565

Herbert, V., Bierfass, M., Wasserman, L. R., Estren, S., and Brody, E. (1959). Effect of D-sorbitol on absorption of vitamin B12 by human subjects able to produce intrinsic factor. *Am. J. Clin. Nutr.* 7, 325–327. doi: 10.1093/ajcn/7.3.325

Huang, F. J., Zheng, X. J., Ma, X.-H., Jiang, R.-Q., Zhou, W.-Y., Zhou, S.-P., et al. (2019). Theabrownin from Pu-erh tea attenuates hypercholesterolemia via modulation of gut microbiota and bile acid metabolism. *Nat. Commun.* 10:4971. doi: 10.1038/s41467-019-12896-x

Hyatt, D., Chen, G.-L., Locascio, P. F., Land, M. L., Larimer, F. W., and Hauser, L. J. (2010). Prodigal: prokaryotic gene recognition and translation initiation site identification. *BMC Bioinformatics* 11:119. doi: 10.1186/1471-2105-11-119

Katiyar, S. K., Agarwal, R., Zaim, M. T., and Mukhtar, H. (1993). Protection against *N*-nitrosodiethylamine and benzo[*a*]pyrene-induced forestomach and lung tumorigenesis in A/J mice by green tea. *Carcinogenesis* 14, 849–855. doi: 10.1093/carcin/14.5.849

Kato, M., Ota, H., Okuda, M., Kikuchi, S., Satoh, K., Shimoyama, T., et al. (2019). Guidelines for the management of *Helicobacter pylori* infection in Japan: 2016 revised edition. *Helicobacter* 24:e12597. doi: 10.1111/hel.12597

Kuhl, C., Tautenhahn, R., Böttcher, C., Larson, T. R., and Neumann, S. (2012). CAMERA: an integrated strategy for compound spectra extraction and annotation of liquid chromatography/mass spectrometry data sets. *Anal. Chem.* 84, 283–289. doi: 10.1021/ac202450g

Le Floc'h, N., Otten, W., and Merlot, E. (2011). Tryptophan metabolism, from nutrition to potential therapeutic applications. *Amino Acids* 41, 1195–1205. doi: 10.1007/s00726-010-0752-7

Lea, M.-A., Xiao, Q., Sadhukhan, A. K., Cottle, S., Wang, Z.-Y., and Yang, C.-S. (1993). Inhibitory effects of tea extracts and (−)-epigallocatechin gallate on DNA synthesis and proliferation of hepatoma and erythroleukemia cells. *Cancer Lett.* 68, 231–236. doi: 10.1016/0304-3835(93)90151-X

Li, D.-H., Liu, C.-M., Luo, R.-B., Sadakane, K., and Lam, T. W. (2015). MEGAHIT: an ultra-fast single-node solution for large and complex metagenomics assembly via succinct de Bruijn graph. *Bioinformatics* 31, 1674–1676. doi: 10.1093/bioinformatics/btv033

Lin, F., Zhu, Y., Liang, H., Li, D., Jing, D., Liu, H., et al. (2022). Association of coffee and tea consumption with the risk of asthma: a prospective cohort study from the UK biobank. *Nutrients* 14:4039. doi: 10.3390/nu14194039

Mi, J.-X., Zhang, Y.-N., Lai, Z.-H., Li, W.-S., Zhou, L.-F., and Zhong, F.-J. (2019). Principal component analysis based on nuclear norm minimization. *Neural Netw.* 118, 1–16. doi: 10.1016/j.neunet.2019.05.020

Mukhtar, H. M., Wang, Z.-Y., Katiyar, S. K., and Agarwal, R. (1992). Tea components: antimutagenic and anticarcinogenic effects. *Prev. Med.* 21, 351–360. doi: 10.1016/0091-7435(92)90042-G

Niranjan, H. K., Kumari, B., Raghav, Y. S., Mishra, P., Khatib, A. M. G. A., Abotaleb, M., et al. (2022). Modeling and forecasting of tea production in India. *J. Animal Plant Sci.* 32, 1598–1604. doi: 10.36899/JAPS.2022.6.0569

Oguni, I., Nasu, K., Yamamoto, S., and Nomura, T. (1988). On the antitumor activity of fresh green tea leaf. *Agric. Biol. Chem.* 52, 1879–1880. doi: 10.1080/00021369.1988.10868935

Pérez-Varela, M., Corral, J., Aranda, J., and Barbé, J. (2018). Functional characterization of AbaQ, a novel efflux pump mediating quinolone resistance in *Acinetobacter baumannii*. *Antimicrob. Agents Chemother.* 62:e00906-18. doi: 10.1128/aac.00906-18

Smith, C. A., Want, E. J., O'Maille, G., Abagyan, R., and Siuzdak, G. (2006). XCMS: processing mass spectrometry data for metabolite profiling using nonlinear peak alignment, matching, and identification. *Anal. Chem.* 78, 779–787. doi: 10.1021/ac051437y

Someya, S., Yoshiki, Y., and Okubo, K. (2002). Antioxidant compounds from bananas (*Musa Cavendish*). *Food Chem.* 79, 351–354. doi: 10.1016/S0308-8146(02)00186-3

Song, H., Kim, K. T., Park, S. Y., Lee, G. W., Choi, J., Jeon, J., et al. (2022). A comparative genomic analysis of lichen-forming fungi reveals new insights into fungal lifestyles. *Sci. Rep.* 12:10724. doi: 10.1038/s41598-022-14340-5

Takashi, T., and Isao, K. (2003). Oxidation of tea catechins: chemical structures and reaction mechanism. *Food Sci. Technol. Res.* 9, 128–133. doi: 10.3136/fstr.9.128

Tang, Y., Chen, B., Huang, X., He, X., Yi, J., Zhao, H., et al. (2022). Fu brick tea alleviates high fat induced non-alcoholic fatty liver disease by remodeling the gut microbiota and liver metabolism. *Front. Nutr.* 9:62323. doi: 10.3389/fnut.2022.1062323

Tomé, D. (2021). Amino acid metabolism and signalling pathways: potential targets in the control of infection and immunity. *Nutr. Diabetes* 11:20. doi: 10.1038/s41387-021-00164-1

Wu, H., Zhao, H.-H., Ding, J., Wang, Y.-H., Hou, J., and Yang, L. (2023). Metabolites and microbial characteristics of Fu brick tea after natural fermentation, 114775. *LWT* 181. doi: 10.1016/j.lwt.2023.114775

Xiang, M.-C., Chu, J., Cai, W.-J., Ma, H.-K., Zhu, W.-J., Zhang, X.-L., et al. (2022). Microbial succession and interactions during the manufacture of Fu brick tea. *Front. Microbiol.* 13, 1664–302X. doi: 10.3389/fmicb.2022

Xu, M.-N., Heidmarsson, S., Thorsteinsdottir, M., Kreuzer, M., Hawkins, J., Omarsdottir, S., et al. (2018). Authentication of Iceland Moss (*Cetraria islandica*) by UPLC-QToF-MS chemical profiling and DNA barcoding. *Food Chem.* 245, 989–996. doi: 10.1016/j.foodchem.2017.11.073

Yang, Q., Tian, G.-L., Qin, J.-W., Wu, B.-Q., Tan, L., Xu, L., et al. (2020). Coupling bootstrap with synergy self-organizing map-based orthogonal partial least squares discriminant analysis: stable metabolic biomarker selection for inherited metabolic diseases. *Talanta* 219:121370. doi: 10.1016/j.talanta.2020.121370

Yu, F., Huang, Y.-J., Yao, Y.-N., Xiong, G.-X., and Huang, Y.-Y. (2015). Effects of different materials on the qualities of *Eurotium cristatum* tea. *Chin. Agricult. Sci. Bull.* 31, 222–226. doi: 10.11924/j.issn.1000-6850.casb14120125

Zhang, B., Ren, D.-Y., Zhao, A.-Q., Shao, H.-J., Li, T., Niu, P.-F., et al. (2022). *Eurotium cristatum* exhibited anti-colitis effects via modulating gut microbiota-dependent tryptophan metabolism. *Agric. Food Chem.* 70, 16164–16175. doi: 10.1021/acs.jafc.2c05464

Zhang, Z.-M., Tong, X., Peng, Y., Ma, P., Zhang, M.-J., Lu, H.-M., et al. (2015). Multiscale peak detection in wavelet space. *Analyst* 140, 7955–7964. doi: 10.1039/C5AN01816A

Zhen, Y.-S. (2002). *Tea – bioactivity and therapeutic potential*. London: CRC Press.

Frontiers in Microbiology

Explores the habitable world and the potential of microbial life

The largest and most cited microbiology journal which advances our understanding of the role microbes play in addressing global challenges such as healthcare, food security, and climate change.

Discover the latest Research Topics

See more →

Frontiers

Avenue du Tribunal-Fédéral 34
1005 Lausanne, Switzerland
frontiersin.org

Contact us

+41 (0)21 510 17 00
frontiersin.org/about/contact